



**HAL**  
open science

## Epigenetic studies of plasmodium falciparum pre-erythrocytic stages

Gigliola Zanghi

► **To cite this version:**

Gigliola Zanghi. Epigenetic studies of plasmodium falciparum pre-erythrocytic stages. Parasitology. Université Pierre et Marie Curie - Paris VI, 2016. English. NNT : 2016PA066733 . tel-01942167

**HAL Id: tel-01942167**

**<https://theses.hal.science/tel-01942167>**

Submitted on 3 Dec 2018

**HAL** is a multi-disciplinary open access archive for the deposit and dissemination of scientific research documents, whether they are published or not. The documents may come from teaching and research institutions in France or abroad, or from public or private research centers.

L'archive ouverte pluridisciplinaire **HAL**, est destinée au dépôt et à la diffusion de documents scientifiques de niveau recherche, publiés ou non, émanant des établissements d'enseignement et de recherche français ou étrangers, des laboratoires publics ou privés.

# Université Pierre et Marie Curie

Ecole doctorale Complexité du vivant

*Paludisme: identification et validation pré-clinique de nouvelles cibles thérapeutiques*

*Biologie des interactions hôte-parasite*

## **Epigenetic studies of *Plasmodium falciparum* pre-erythrocytic stages**

Par **Gigliola Zanghì**

Thèse de doctorat de Parasitologie

Dirigée par Dominique Mazier & Artur Scherf

Présentée et soutenue publiquement le 1<sup>er</sup> Décembre 2016

Devant un jury composé de:

Pr. Guennadi SEZONOV	Président du jury
Pr. Maria M. MOTA	Rapporteur
Dr. Stéphanie BLANDIN	Rapporteur
Pr. Till VOSS	Examineur
Pr. Laurent RÉNIA	Examineur
Dr. Rogerio AMINO	Examineur
Pr. Dominique MAZIER	Directeur de thèse
Pr. Artur SCHERF	Co-Directeur de thèse



*Per aspera ad astra*

Marco Tullio Cicerone



## ACKNOWLEDGEMENTS

My deepest acknowledgement goes to Dominique and Artur, who provided me the opportunity to develop my scientific knowledge during this 3 years-journey. Thank you Dominique for having supported me throughout this PhD. Thank you Artur for your invaluable contribution. And thank you both for mentoring me and pushing me towards the development of my scientific thinking.

I would like to thank all the members of my PhD Jury, who accepted to evaluate and discuss this project, regardless of their busy agendas, bringing their priceless scientific value into this work.

Furthermore, I would like to thank to both Dominique's and Artur's teams for accepting me as a member, making me feel comfortable in a friendly work environment. A special thanks goes to Shruthi for all the scientific and nonscientific help she provided, supporting during the last past year of my PhD. Shruthi, your students will be really lucky! Thank you Rosaura, Catherine and Olivier, for all the scientific discussions where you showed your contagious passion for research. Shuai, Claudia and Henriette, thank you for having shared so many professional moments, encouraging me to positively pursue this project's goals. Thank you Roger, Daniel, Giulia, Selma and Anna, for all the funny and crazy moments in the lab, that allowed softening so many stressful moments. And, finally thanks Julien, Anne, Kiki, Patty, Sebastian, Jess, Letizia, Clementine, Mallaury, Quang and all the past and present members of both teams, with whom I had the pleasure to work with.

Thank you to all my friends, with a particular thank you, to my first colleague, and then friend Lidia, for all the suggestions and support during these 3 years. Thank you to my brother, who encouraged me to follow my dreams. Thanks to my boyfriend, Salvo, for having supported me and for having accompanied me through this hard period. Salvo, without you none of this would not make sense. Thanks to my father, who passed me the love for research. Daddy, even if you are no longer here, I hope I made you proud.

A special and deep thank you goes to my mother, who was always there for me, no matter my mood. Mommy, without you none of this would have been possible.

Thank you all of you again for this outstanding PhD time.

Giglio



## TABLE OF CONTENTS

ACKNOWLEDGEMENTS.....	4
TABLE OF CONTENTS.....	6
LIST OF FIGURES .....	10
LIST OF TABLES .....	12
SUMMARY.....	17
INTRODUCTION.....	19
<b>1. Introduction to Malaria.....</b>	<b>21</b>
<b>1.1 Malaria Epidemiology.....</b>	<b>21</b>
1.1.1 Malaria Disease.....	22
1.1.2 Chronicity of Malaria Infection.....	24
<b>1.2 Current Situation and Challenges of Malaria Control.....</b>	<b>24</b>
1.2.1 Drug Treatments.....	25
1.2.2 Vaccine Candidates in Development .....	26
1.2.2.1 Subunit Vaccines.....	26
1.2.2.2 Live Attenuated Parasite Vaccines.....	29
<b>2. Etiologic Agent and <i>Plasmodium</i> Biology.....</b>	<b>31</b>
<b>2.1 <i>Plasmodium</i> Life Cycle.....</b>	<b>33</b>
<b>2.2 Parasite development in the mosquito.....</b>	<b>35</b>
2.2.1 <i>Plasmodium</i> Sporozoites .....	36
<b>2.3 Infection of the Mammalian Host.....</b>	<b>37</b>
2.3.1 Skin Stage.....	37
2.3.2 Liver Stage .....	39
2.3.2.1 Arrest in the Sinusoid.....	39
2.3.2.2 Sinusoid Traversal.....	40
2.3.2.3 Invasion of Hepatocytes .....	41
2.3.3 Exo-erythrocytic Merozoite Formation and Release .....	41
2.3.4 Blood Stage .....	42
<b>3. Genome organization and gene expression in <i>P. falciparum</i>.....</b>	<b>44</b>
<b>3.1 <i>P. falciparum</i> Chromosome Organization and Structure.....</b>	<b>44</b>
<b>3.2 Chromatin and its Regulation in <i>P. falciparum</i>.....</b>	<b>46</b>
<b>3.3 Transcription and Post-transcriptional Gene Regulation .....</b>	<b>49</b>
<b>4. Epigenetic Regulation in <i>P. falciparum</i>.....</b>	<b>51</b>
<b>4.1 Histone Modifications and their Writers and Eraser .....</b>	<b>51</b>
4.1.1 Mechanisms of Histone Modifications .....	53
4.1.1.1 Acetylation .....	53
4.1.1.2 Deacetylation.....	53
4.1.1.3 Lysine methylation.....	53

4.1.1.4 Lysine Demethylation .....	54
4.1.2 <i>P. falciparum</i> Hetrochromatin Protien 1 (PfHP1) and other histone modifications readers .....	58
<b>4.2 Nuclear Organization</b> .....	59
<b>4.3 Epigenetic Control of Sexual Commitment</b> .....	60
<b>4.4 Epigenetic Control of Hypnozoites</b> .....	61
<b>5. Biology and Regulation of <i>P. falciparum</i> Erythrocyte Membrain Protein 1 (PfEMP1)</b> .....	63
<b>5.1 PfEMP1 function</b> .....	64
<b>5.2 PfEMP1/<i>var</i> gene organization ans structure</b> .....	64
<b>5.3 Classification of adhesive domains in PfEMP1</b> .....	66
5.3.1 Type 3 PfEMP1 .....	68
5.3.2 DC4-Type PfEMP1 .....	68
5.3.3 DC5-Type PfEMP1 .....	68
5.3.4 DC8- and DC13-Type PfEMP1 .....	68
5.3.5 <i>var</i> 2CSA-Type PfEMP1 .....	69
<b>5.4 <i>var</i> gene Transcription and its Regulation</b> .....	69
<b>OBJECTIVES</b> .....	73
<b>RESULTS</b> .....	75
<b>ARTICLE 1</b> .....	77
<i>Plasmodium falciparum</i> full life cycle and <i>Plasmodium ovale</i> liver stages in humanized mice .....	77
<b>ARTICLE 2</b> .....	80
<i>Plasmodium falciparum</i> PfSET7: enzymatic characterization and cellular localization of a novel protein methyltransferase in sporozoite, liver and erythrocytic stage parasites.....	80
<b>ARTICLE 3</b> .....	83
A SMYD-type methyltransferase PfSET6 associates with a subset of gene loci of <i>Plasmodium falciparum</i> and forms multiple cytoplasmic foci during asexual, sexual blood stage and sporozoite stage .....	83
<b>ARTICLE 4</b> .....	128
Analysis of the epigenetic landscape of <i>Plasmodium falciparum</i> reveals expression of a clonally variant PfEMP1 member on the surface of sporozoites .....	128
<b>DISCUSSION</b> .....	153
<b>1. Genome-wide ChIP-seq analysis of <i>P. falciparum</i> sporozoites</b> .....	155
1.1 <i>P. falciparum</i> sporozoites epigenome .....	156
1.2 Clonally variant gene regulation .....	157
<b>2 <i>var</i><sup>sporo</sup> expression in <i>P. falciparum</i> sporozoites</b> .....	159
2.1 Adhesive properties of sporozoites and PfEMP1 .....	159
2.2 Immunogenic properties.....	161

<b>3. PfEMP1 protein expression in <i>P. falciparum</i> liver stage</b> .....	161
<b>CONCLUSION &amp; PERSPECTIVES</b> .....	163
<b>BIBLIOGRAPHY</b> .....	165
<b>ANNEXES</b> .....	183
<b>ARTICLE 5</b> .....	185
In Vitro Analysis of the Interaction between Atovaquone and Proguanil against Liver Stage Malaria Parasites .....	185



## LIST OF FIGURES

Figure 1 : <b>Malaria incidence rates 2000 – 2015.</b> .....	22
Figure 2 <b> Malaria candidate vaccine.</b> .....	27
Figure 3: <b>Evolutionary tree of Apicomplexa.</b> .....	31
Figure 4: <b>Morphology of the apicomplexan parasite</b> .....	32
Figure 5 : <b><i>Plasmodium</i> spp. life cycle.</b> .....	34
Figure 6 : <b><i>Plasmodium</i> in the mosquito vector.</b> .....	35
Figure 7: <b>The morphology of the <i>Plasmodium</i> sporozoite.</b> .....	37
Figure 8: <b>Representation of motile sporozoites injected into the skin.</b> .....	38
Figure 9: <b>Liver infection by <i>Plasmodium</i> sporozoites.</b> .....	40
Figure 10 : <b>Dynamics of the parasite membrane during the late liver phase</b> .....	42
Figure 11: <b><i>P. falciparum</i> asexual blood stages in the human host.</b> .....	43
Figure 12. <b><i>P. falciparum</i> chromosome organization</b> .....	45
Figure 13. <b>Nucleosome structure with the four canonical histones (H3, H4, H2A, and H2B) in <i>P. falciparum</i>.</b> .....	47
Figure 14: <b>Histone H3 post-translational modifications.)</b> .....	52
Figure 15: <b>Nuclear architecture of <i>P. falciparum</i> ring stages.</b> .....	60
Figure 16: <b>Model for variegated expression of AP2-G.</b> .....	61
Figure 17. <b>PfEMP1 trafficking to the surface of IE.</b> .....	63
Figure 18 : <b>Genomic organization and nuclear position of <i>var</i> genes</b> .....	66
Figure 19 : <b>Chromosomal organization of <i>Plasmodium falciparum var</i> genes and <i>P. falciparum</i> erythrocyte membrane protein 1 (PfEMP1) domain architecture</b> .....	67
Figure 20 : <b>Schematic presentation of histone H3 silent or active marks.</b> .....	70



## LIST OF TABLES

Table 1: Features of different subtelomeric repeat elements in <i>P. falciparum</i> .....	46
Table 2: List of histone modifications identified in <i>P. falciparum</i> blood stages. P.....	48
Table 3: Translation, Decay and Repression regulators in <i>Plasmodium spp.</i> .....	50
Table 4 : Predicted and verified histone mark writers and eraser in <i>P. falciparum</i> .....	55
Tableau 5: Predicted and verified histone mark readers in <i>P. falciparum</i> .....	57



## ABBREVIATION

ACT	Artemisinin-based Combination Therapy
AMA1	Apical Membrane Antigen-1
ApiAP2	Apicomplexan Aptela 2
ATS	Acidic Terminal Domain
BBB	Blood Brain Barrier
CD	Chromodomain
ChIP	Chromatin Immunoprecipitation
CIDR	Cysteine-rich Interdomain Regions
CSA	Chondroitin Sulphate A
CSD	Chromo Shadow Domain
CSP	Circumsporozoite Protein
CT	Cell Traversal
CV	Central Venule
DARC	Duffy Antigen/Chemokine Receptor
DBL	Duffy Binding Like
DMSO	Dimethyl Sulfoxide
EC	Endothelial Cells
ECM	Extracellular Matrix
EEF	Exoerythrocytic Form
EPCR	Endothelial Protein C Receptor
EXP1	Exported Protein 1
FISH	Fluorescence In Situ Hybridization
G6PD	glucose-6-phosphate dehydrogenase
GAPs	Genetically Attenuated Parasites
H3K9me3	Trimethyl Histone H3 Lysine 9
HATs	Histone Acetyltransferases
HDACs	Histone Deacetylases
HDMEC	Human Skin and Dermal Microvascular Endothelial Cells
HKMTs	Histone Lysine Methyltransferases
IDC	Intra-Erythrocytic Developmental Cycle
IFA	Immunofluorescence Assay
IFN $\gamma$	Interferon $\gamma$
IMC	Inner Membrane Complex
iRBCs	infected Red Blood Cells
JHDM	Jumonji-C Histone Demethylase
K13	Kelch Protein 13
KC	Kupffer Cells
LSD1	Lysine-Specific Demethylase
ME	Multiple Epitope
MJ	Moving Junction
MSP1	Merozoite Surface Protein-1
NGOs	Non-Governmental Organizations

PAM	Pregnancy-Associated Malaria
PBEs	Puf-Binding Elements
PERCs	Perinuclear Repression Center
PfBDP	<i>P. falciparum</i> Bromodomain-Containing Protein
PfEMP1	<i>P. falciparum</i> Erythrocyte Membrane Protein 1
PfHP1	<i>P. falciparum</i> Heterochromatin Protein 1
PfRH5	<i>P. falciparum</i> Reticulocyte-Binding Protein Homologue 5
PfSir2	<i>P. falciparum</i> , Sirtuin2 Proteins
PM	Peritrophic Matrix
PTMs	Post-Translational Modifications
Puf	Pumilio and fem-3 binding factor homolog
PV	Parasitophorous Vacuole
PVM	Parasitophorous Vacuole Membrane
RAS	Radiation-Attenuated Salivary Gland Sporozoites
RDT	Rapid Diagnostic Test
SAM	S-(5'-Adenosyl)-L-methionine
SET	Su(var)3-9 and 'Enhancer of zeste' Trithorax
SM	Severe Malaria
TAREs	Telomere Associated Repetitive Elements
TAS	Telomere-Associated Sequences
TBV	Transmission-Blocking Vaccine
TLP	TRAP-Like Proteins
TRAP	Thrombospondin-Related Adhesive Protein
ups	upstream promoter sequence
VSGs	Variant Surface Glycoproteins
WHO	World Malaria Report 2015



## SUMMARY

Epigenetic mechanisms control key processes during *Plasmodium falciparum* blood stage development such as antigenic variation, malaria pathogenesis and sexual commitment. In addition, in some *Plasmodium* species, dormant malaria liver stages appear to be influenced by epigenetic components. However, the epigenetic landscape has not been reported for the pre-erythrocytic sporozoite and liver stages.

To characterize epigenetic regulation in sporozoites, we tested the major epigenetic regulators *P. falciparum* Heterochromatin Protein 1 (PfHP1) and the histone lysine methyltransferases (PfSET6 and PfSET7) in *P. falciparum* sporozoites. Given the difficulty to obtain sufficient material from infected mosquitoes, I first developed a chromatin immunoprecipitation (ChIP) method that allows working with low parasite numbers. This technique allowed me to obtain reliable genome-wide occupancy data for repressive heterochromatin and active euchromatin marks. Notably, I discovered an unprecedented mechanism of silencing in sporozoites, where in a stage specific manner, several hundreds of genes encoding parasite proteins that are exported to the surface are transcriptionally repressed. This is based on an expansion of facultative heterochromatin boundaries in sporozoites. Moreover, I demonstrate that a single member of the polymorphic *var* gene family, which encodes the blood stage virulence factor PfEMP1 (called *var*<sup>sporo</sup> PfEMP1 in this study), is expressed at the surface of sporozoites. This is in contrast to blood stages where PfEMP1 is transported to the erythrocyte surface and participates in cytoadhesion.

Overall, my findings give rise to new and important biological questions including what are the factors that regulate heterochromatin boundaries and what is the function of an important virulence-associated surface antigen in pre-erythrocytic stages. Given that the mechanism of sporozoite homing to the liver remains unknown, my findings point to a putative function of this adhesion molecule during sporozoite migration in mosquitoes and humans. Moreover, the expression of a highly polymorphic and strain-specific antigen on the surface of sporozoites might provide a molecular explanation for the observation that the protective immune response induced by attenuated sporozoites used for vaccine development is strain-specific.



# INTRODUCTION



# 1. Introduction to Malaria

Malaria has affected humans for more than 4,000 years. This disease takes its name from the Italian phrase, *mal' aria* or «bad air». Malaria is caused by infection with *Plasmodium*, a protozoan parasite belonging to the Apicomplexan phylum that is transmitted by female *Anopheles* mosquitoes. Our understanding of malaria pathology began in 1880 with the discovery of the parasite in the blood of malaria patients by Alphonse Laveran. In 1898, the Italian malariologists Giovanni Battista Grassi, Amico Bignami, Giuseppe Bastianelli, Angelo Celli, Camillo Golgi and Ettore Marchiafava, demonstrated that human malaria was transmitted by Anopheline mosquitoes. It was 50 years later, in 1948 that Henry Shortt and Cyril Garnham discovered that malaria parasites develop in the liver before entering the blood stream, and in 1982 Wojciech Krotoski showed the presence of dormant stages in the liver, identifying the final stage in the life cycle of the parasite.

## 1.1 Malaria Epidemiology

Malaria has been recognized as a severe and life-threatening illness, and is still one of the major infective diseases affecting humans worldwide. Although more than 100 *Plasmodium* species exist, only five of them cause malaria in humans (*Plasmodium falciparum*, *Plasmodium vivax*, *Plasmodium ovale*, *Plasmodium malariae* and *Plasmodium knowlesi*, a zoonotic parasite).

*P. falciparum* is most prevalent in the African continent and is the deadliest of the *Plasmodium* species, causing 75% of total deaths annually. *P. falciparum* is responsible for severe malaria (SM), including cerebral malaria, which can be fatal if not treated. *P. vivax* has the widest geographical distribution: it is mainly spread over South and South-East Asia and American countries and 35% of the world's population is at risk of infection. *P. ovale* is present in West Africa, Philippines, eastern Indonesia and Papua New Guinea. *P. malariae* is spread throughout sub-Saharan Africa, South-East Asia, Indonesia, western Pacific islands and in some areas of the Amazon Basin of South America. *P. knowlesi* is commonly found in South-East Asia; while this parasite primarily causes malaria in macaques, it also infect humans and accounts for up to 70% of malaria cases in certain areas of South Asia.

Notably, between 2000 and 2015 there was an 18% reduction in the number of malaria cases and a decline of 48% in the number of malaria-related deaths. In 2000, there were an estimated 262 million malaria cases leading to 839 000 deaths (World Malaria Report 2015, WHO), which reduced to 216 million cases and ~500000 deaths in 2015. Despite the large reduction, most cases occurred in the African region (88%), followed by South-East Asia (10%) and the Eastern Mediterranean Region (2%) (Figure 1). 90% of all malaria-related deaths occurred in Africa, 78% of which were of children aged less than 5 years.

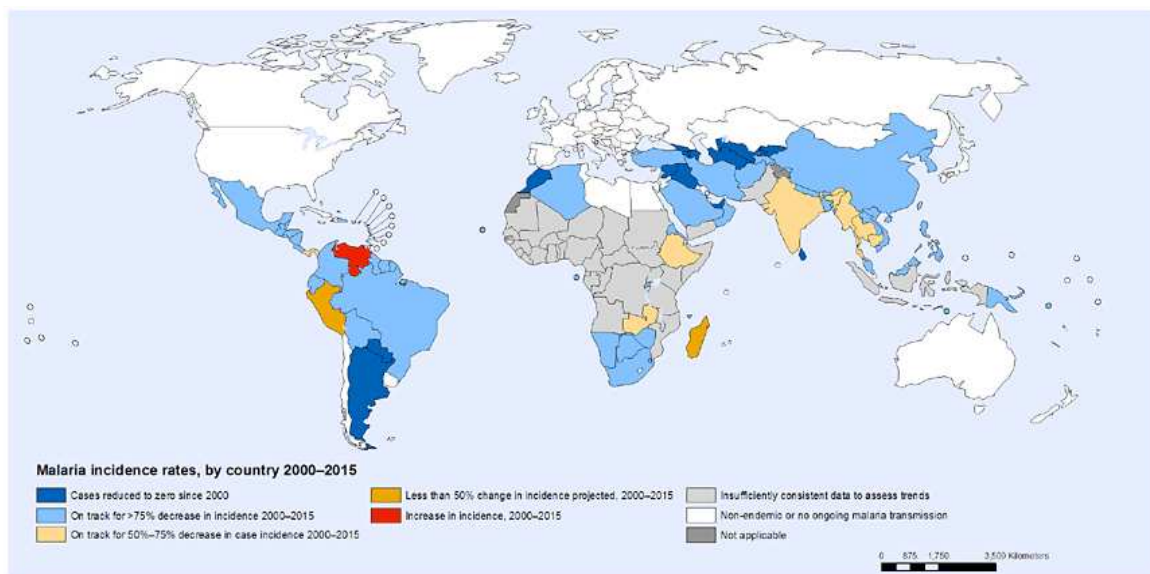


Figure 1 :Malaria incidence rates 2000 – 2015. (from the World Malaria Report 2015)

Significant progress in battling malaria has been made in the past years, such as the complete eradication of malaria in Sri Lanka in 2016; but still, a child dies every minute in Africa making malaria one of the most important problems of public health in the world. Indeed, in 2016, the World Health Organization (WHO) postponed the objective to eradicate malaria to 2030. A lot of work remains to be done, with a need for cohesion between scientific discoveries in laboratories and field application, handled by Non-Governmental Organizations (NGOs) and the Health Ministry of every endemic country.

### 1.1.1 Malaria Disease

Malaria is a febrile illness with a wide range of clinical symptoms, from flu-like, such as fever, chills, headache, sweats, fatigue, nausea and vomiting, to severe malaria with seizures, coma and multiple organ failure. Malaria symptoms appear in periodic cycles and the time between each episode depends on the species. *P. falciparum*, *P. vivax* and *P. ovale*

are characterized by a fever with 48 hour periodicity, called tertian fever, while for *P. malariae*, a quartan fever (72 h periodicity) is evident. The severity of the disease is also linked to the species: only *P. falciparum* can cause severe malaria and if not treated in time becomes lethal. The three main complications caused by *P. falciparum* are: cerebral malaria, severe anaemia and respiratory acidosis. Other complications include hypoglycaemia, pulmonary oedema, circulatory collapse, abnormal haemorrhage and disseminated intravascular coagulation with consequent haemoglobinuria.

Patients with cerebral malaria show high parasite levels and parasite-induced pigmentation in the brain microcirculation, due to necrosis and alterations in the endothelium of cerebral vessels. The parasite breaches the blood brain barrier (BBB), a membrane that strictly regulates brain circulation by inhibiting the passage of microorganisms and other toxic exogenic substances into the brain. When infected red blood cells (iRBCs) adhere to endothelial cells in the brain microvasculature, they compromise the integrity of the BBB, causing increased permeability (Wassmer et al., 2006). This allows the influx of foreign substances that activate the microglia cells to release pro-inflammatory cytokines, damaging astrocytes and glial cells that are crucial for BBB maintenance (Medana and Turner, 2006).

The host response plays a key role in modulating the severity of the disease; indeed, the risk of developing severe malaria is maximal in children and pregnant woman. For instance, children do not have a fully developed immune response, increasing their susceptibility to cerebral malaria and severe anaemia. Pregnant women are also more prone to develop severe malaria and can develop a specific form of malaria called pregnancy-associated malaria (PAM), with complications for the mother and foetus. PAM results from the binding of iRBCs to the placental intervillous space, interfering with the transmission of nutrients to the foetus causing low birth weight, stillbirth or spontaneous abortion. Travellers from countries that are not malaria-endemic are also prone to developing severe malaria, due to the absence of immune memory to protect against malaria.

People living in endemic countries develop an acquired immune response with age, reducing the risk of severe complications. Naturally acquired immunity to *P. falciparum* protects millions of people who are routinely exposed to parasite infection from severe malaria. This type of acquired immunity is lost if the individual moves away from the endemic country for long periods of time, and if re-exposed, the person's immune system will respond in a naïve manner to parasite infection. However, cellular and molecular mechanisms

of naturally acquired immunity against malaria are ill defined. Sero-epidemiological studies consistently suggest that acquired immunity is primarily mediated by antibodies and is directed against the pathogenic asexual blood stages, but we need to consider the immune response against sporozoites and exo-erythrocytic stage that may contribute to protection (Offeddu et al., 2012).

*P. vivax* infection remains uncomplicated but can induce more severe paroxysms (fever, sweats and chills), and higher pro-inflammatory cytokine levels. The host response is activated more strongly in *P. vivax* than *P. falciparum* infections: this mechanism controls parasitaemia and prevents organ failure and severe malaria (Hemmer et al., 2006).

### 1.1.2 Chronicity of Malaria Infection

Similar to other parasitic infections, human malaria is a chronic disease. Even if individuals in endemic countries develop a state of protection that prevents the occurrence of clinical symptoms, low-grade parasitemia can be found in more than half of the adults protected against the disease. Longitudinal studies have shown that these patients will develop a patent parasitemia at one point or another in their lifetime. The advantage to the parasite from this chronic status is evident: it provides a parasite reservoir, which is essential when there is no transmission (considering that *Plasmodium* infections are seasonal), since it allows the parasite to lie in wait for the mosquito vector population to re-establish itself in the breeding season. *P. falciparum* maintains the chronicity of infection through antigenic variation, *i.e.*, by altering the expression of surface proteins recognized by the host immunity, the parasite is able to escape the host immune response. The host immune response to *P. falciparum* infection is largely dependent on the recognition of the immunodominant and clonally variant surface molecule called PfEMP1 (*P. falciparum* erythrocyte membrane protein 1) on the iRBC surface (Leech et al., 1984) (more details in Section 5).

## 1.2 Current Situation and Challenges of Malaria Control

In light of growing antimalarial drug resistance, better strategies to control malaria need to be developed. Indeed, a combination of vector control, diagnostics, chemotherapy and

effective vaccines will ensure continued reduction in the number of malaria cases and eventually lead to global malaria eradication.

### 1.2.1 Drug Treatments

Malaria is curable if diagnosed and treated in time, but unfortunately the treatment is not accessible to everybody worldwide. The treatment is species-specific and takes into account pre-existing parasite resistance in certain malaria-endemic areas. Malaria can be diagnosed by microscopy or rapid diagnostic test (RDT), which is mandatory before the administration of treatment. After diagnosis, the primary aim of intervention is to eliminate parasitemia, thus preventing the progression towards severe malaria. Moreover, immediate treatment reduces the possibility of transmission via mosquito bites. Importantly, the risk of developing antimalarial resistance increases when the treatment is not correct and when an inaccurate posology (doses and days of treatment) is prescribed.

Drug resistance has emerged to most effective antimalarials, beginning with the first antimalarial drug, quinine. While the resistance to quinine appeared 278 years after drug introduction, the resistance to new medicaments such as chloroquine (structural analog of quinine), proguanil and atovaquone appeared much faster (1-15 years; e.g., atovaquone resistance emerged in less than a year after its market introduction (Cottrell et al., 2014) Due to the lack of new drugs on the market and the emergence of drug resistance, the new therapeutic strategy to treat malaria is a combination/cocktail of different drugs such as malarone that is composed of atovaquone and proguanil. The combination of molecules with different modes of action and different targets decreases the risk of parasite resistance.

Today the firstline treatment recommended by the WHO for uncomplicated malaria caused by *P. falciparum* is artemisinin-based combination therapy (ACT). Artemisinin is derived from *Artemisia annua*, which is a common herb that is spread worldwide and is used by Chinese herbalists in the treatment of malaria. The active antimalarial substance from *A. annua* was isolated by Youyou Tu in 1972, who was awarded the Nobel Prize for Physiology/Medicine in 2015. However, *P. falciparum* strains with reduced susceptibility to artemisinin have appeared and spread in South-East Asia (Ashley et al., 2014). Multiple studies established that artemisinin resistance is associated with slow parasite clearance in patients and increased survival of early ring stage parasites *in vitro*. Moreover, parasite transcriptional profiles reflected induction of an “unfolded protein response” and decelerated

parasite development, and elevated parasite phosphatidylinositol-3-kinase activity (Fairhurst, 2015). Mutations in the parasite's kelch protein 13 (K13) gene have been linked to artemisinin resistance (Huang et al., 2015). K13 mutations that confer artemisinin resistance are widespread in South East Asia; others are present at low frequency in Africa but are not yet associated with resistance (Fairhurst, 2015). In Africa, ACT treatment for *P. falciparum* is still efficient but multidrug resistance might soon emerge evidencing the need for the development of new drugs.

*P. vivax* infections are treated with cloroquine in areas where this drug remains effective and in combination with primaquine to eliminate the dormant stages responsible for *P. vivax* relapses. Unfortunately, primaquine cannot be widely administrated due to its lethal effect on people with glucose-6-phosphate dehydrogenase (G6PD) deficiency. Instead, ACTs are used against *P. vivax* in areas where chloroquine resistance has been identified.

## 1.2.2 Vaccine Candidates in Development

Research and development of malaria vaccines as definitive solutions to eliminate malaria are ongoing, but still no fully efficient vaccine exists. Significant progress towards a malaria vaccine, specifically for *P. falciparum*, has been made in the past years, with numerous candidates in clinical trials. The possible targets for vaccines are surface antigens expressed in each of the parasite development phases in the human host (i.e. pre-erythrocytic, erythrocytic and sexual; Figure 2 and discussed in section 1.2.2.1), with the aim to effectively disrupt the parasite lifecycle, thus, preventing transmission, infection, and illness. A multi-stage vaccine targeting two or more of these phases is likely needed to achieve malaria eradication and sterile protection. In addition to subunit formulations, a second approach for vaccine development involves whole attenuated parasites. Both of these are discussed below.

### 1.2.2.1 Subunit Vaccines

Targeting the **pre-erythrocytic stage** of the parasite's life cycle remains appealing because the vaccine will block the pathogen during the initial, obligatory and asymptomatic phase, preventing clinical symptoms and transmission. The most advanced malaria vaccine candidate is RTS,S/AS01 (Mosquirix®, GSK), a recombinant protein comprised of portions of *P. falciparum* circumsporozoite protein (CSP), the major surface antigen of mosquito-derived sporozoites (Figure 2), co-expressed with the hepatitis B virus surface antigen and

formulated with AS01 adjuvant. For this vaccine, Phase III clinical trial has been recently completed, showing only moderate efficacy (RTS,S Clinical Trials Partnership 2015). Latest results demonstrated that vaccination with RTS/S, followed by a boost dose administered 18 months after the primary schedule, reduced the number of cases of clinical malaria by 36% in children aged 5-17 months and by 26% in infants aged 6-12 weeks at the end of the study, but it present a decreased of efficacy over time in both groups.

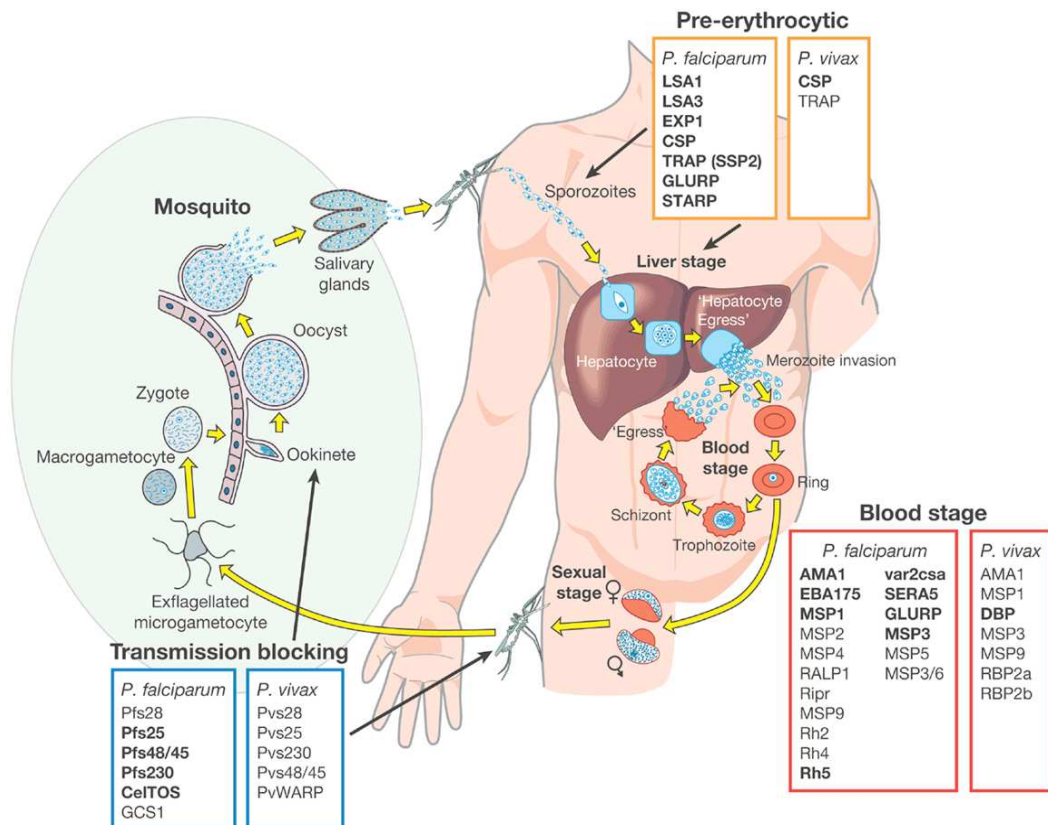


Figure 2 **Malaria candidate vaccine.** All the candidate antigens are superimposed on *Plasmodium* life cycle (Barry and Arnott, 2014)

Another candidate is the adenoviral vectored vaccine ME-TRAP, a multiple epitope (ME) string, consisting of T and B cell epitopes from pre-erythrocytic *P. falciparum* antigens, fused to the thrombospondin-related adhesive protein (TRAP; Figure 2) (Dudareva et al., 2009). Recent studies demonstrated the safety and high immunogenicity of ME-TRAP, which induces elevated T cell response (Kimani et al., 2014; Ogwang et al., 2013). A phase 2a efficacy study using controlled human malaria infections with sporozoites resulted in sterile protection in of 21% and delays in patency of 36% (Ewer et al., 2013). Further clinical trials

to assess safety and immunogenicity in children and infants and protective efficacy in the field need to be done.

Interesting approaches have been utilized for the development of a vaccine against the **erythrocytic stage** of the parasite, which could be administered in addition to or in combination with the partially effective pre-erythrocytic vaccine. Among the antigens expressed in the parasite blood stage, efforts in vaccine research have focused on merozoite surface protein-1 (MSP1) (Holder, 2009) and apical membrane antigen-1 (AMA1) (Figure 2) (Remarque et al., 2008). Vaccines targeting these blood-stage antigens showed a robust safety profile, they are well tolerated and stimulate strong humoral and cellular immune response. Nevertheless, these vaccines do not protect malaria-naïve individuals, as shown for the vaccine encoding *P. falciparum* CSP and AMA1 (Tamminga et al., 2013). One possible explanation is that these antigens are polymorphic: MSP1 is essentially dimorphic (Takala and Plowe, 2009), while *P. falciparum* AMA1 is highly polymorphic (Remarque et al., 2008).

Another strong vaccine candidate identified is *P. falciparum* reticulocyte-binding protein homologue 5 (PfRH5; Figure 2). Full-length PfRH5 is highly susceptible to antibodies, representing a significant target of acquired human immunity (Douglas et al., 2011). Experiments in non-human primate models of malaria show protective efficacy of PfRH5 vaccines (Drew and Beeson, 2015).

*Anopheles* mosquitoes represent a possible target for a transmission-blocking vaccine (TBV). Parasite antigens expressed on **gametocytes or mosquito stages** (see Section 2 for parasite life cycle) can be used to induce the production of antibodies in the human host, which circulate in the blood and can be ingested during the mosquito blood meal. Antibodies target surface membrane proteins on sexual/sporogonic stages or mosquito midgut antigens (Sauerwein and Bousema, 2015). A substantial number of targets have been identified and tested in preclinical studies over the past decades: lead vaccine candidates include pre-fertilization proteins Pfs48/45 (Rener et al., 1983; Vermeulen et al., 1985) and Pfs230 (Quakyi et al., 1987) and post fertilization antigen Pfs25 critical for parasite recognition and attachment to the mosquito midgut (Vermeulen et al., 1985). Monoclonal and polyclonal antibodies directed against Pfs25 conjugated with a detoxified form of exotoxin A from *Pseudomonas aeruginosa* is being tested in a phase1a clinical trial in Mali (Shimp et al., 2013).

Despite the progress toward a *P. falciparum* vaccine, *P. vivax* vaccine research requires additional investigation. The identification and characterization of novel *P. vivax* antigens for all stages of the lifecycle and mechanisms involved in infection relapse need to be elucidated. Currently, only two vaccine candidates are in advanced stages of clinical testing. The first is a recombinant protein called *P. vivax* malaria protein 001 (VMP001) that induced protective immunity in *Aotus nancymae* monkeys (Yadava et al., 2014). The second candidate targets the peculiarity of *P. vivax* to invade reticulocytes. It is a viral vectored vaccine based on the interaction of the parasite's Duffy antigen/chemokine receptor (DARC) (Wertheimer and Barnwell, 1989) and is currently in phase Ia clinical trials (Chitnis and Sharma, 2008).

### 1.2.2.2 Live Attenuated Parasite Vaccines

The limited efficacy of subunit vaccines in clinical trials has provided the rationale for whole organism approaches, especially for pre-erythrocytic malaria vaccine development. Three different approaches have been recently developed: radiation attenuated sporozoites, genetically attenuated parasites, and sporozoite inoculation under chloroquine prophylaxis.

In 1967, Nussenzweig and collaborators demonstrated that immunizing mice with **radiation-attenuated salivary gland sporozoites** (RAS) of the mouse malaria parasite *Plasmodium berghei* induced sterilizing protection against a wild-type sporozoite challenge (Nussenzweig et al., 1967). RAS arrest occurred during liver stage development but the precise point of arrest is heterogeneous. Immunization with RAS parasites has been efficient in both human (Clyde, 1990; Hoffman et al., 2002) and non-human primates (Hafalla et al., 2006). However, there are some caveats to RAS inoculation. For instance, a too high radiation dose arrests parasite development too early (Silvie et al., 2002), resulting in low protection (Hoffman et al., 2002), whereas insufficient radiation allows complete liver stage development of some of the parasites, leading to breakthrough blood stage infections. The second important disadvantage is the high dose of injected sporozoites necessary to achieve complete long-lasting protection. Interestingly, clinical trials with RAS indicated that while intradermal or subcutaneous routes of immunization were not effective, the intravenous route resulted in up to 100% protection (Seder et al., 2013).

The **genetically attenuated parasites** (GAPs) are able to infect hepatocytes but do not complete development, due to knockout of target genes specifically involved in liver stage

development. Genetic ablation experiments in rodent malaria parasites yielded numerous GAPs (Annoura et al., 2012; Mueller et al., 2005a, 2005b; van Dijk et al., 2005) and recently *P. falciparum* GAPs have been produced and tested in humans. Many studies have been done on the *Plasmodium* 6-Cys proteins, which have critical roles throughout parasite development. Immunization with the rodent *P. berghei* p36p(-) and *P. yoelii* p52(-)/p36(-) sporozoites resulted in protective immunity against subsequent challenge with infectious wild-type sporozoites (van Dijk et al., 2005). However, injection into humans showed incomplete attenuation (Spring et al., 2013). Overall, studies suggest that the best GAP vaccination strategy will consist of a parasite that arrests very late in liver stage development without causing a blood stage infection.

A third strategy consists of sporozoite inoculation under chloroquine prophylaxis. In 2009, it was observed that such a strategy confers more effective protection against a homologous challenge with *P. falciparum* malaria than does RAS immunization (Roestenberg et al., 2009). Intact sporozoites under chloroquine treatment develop into a first generation of blood-stage parasites (Yayon et al., 1983) presenting to the host's immune system a broader array of pre-erythrocytic and erythrocytic stage antigens. Immunity was associated with parasite-specific production of interferon  $\gamma$  (IFN $\gamma$ ) and interleukin 2 by pluripotent effector memory cells *in vitro* (Roestenberg et al., 2009) and a sustained *P. falciparum*-specific T-cell IFN $\gamma$  recall response that persisted over years, conferring sterile protection (Roestenberg et al., 2009). Other studies demonstrated that sporozoite exposure under drug cover (pyrimethamine, azithromycin and chloroquine) leads to potent protection compared to RAS.

The inefficient development of neutralizing antibodies against malaria after vaccination has been partially attributed to the genetic diversity of many *P. falciparum* proteins and the parasite's ability to clonally vary the proteins on the surface of iRBCs, such as the PfEMP1 family. Therefore, the design of optimal vaccines should be accompanied by better characterization of cellular and molecular mechanisms of naturally acquired immunity against malaria (Bull and Abdi, 2016)

## 2. Etiologic Agent and *Plasmodium* Biology

The etiologic agent of malaria is *Plasmodium spp.* *Plasmodium* belongs to Apicomplexa, a large phylum of parasitic protists within the eukaryotic kingdom Alveolata. The parasites of this phylum responsible for severe disease in humans and animals include *Plasmodium*, *Toxoplasma*, *Cryptosporidium*, *Eimeria*, *Babesia*, and *Theileria*, showed in the genealogical tree of Figure 3. Apicomplexans have a complex life cycle that involves asexual and sexual development within different hosts. The complexity of the cycle has an impact on the transcriptomic and proteomic repertoires of the parasite, which is needed to regulate gene expression during development and morphological and physiological changes.

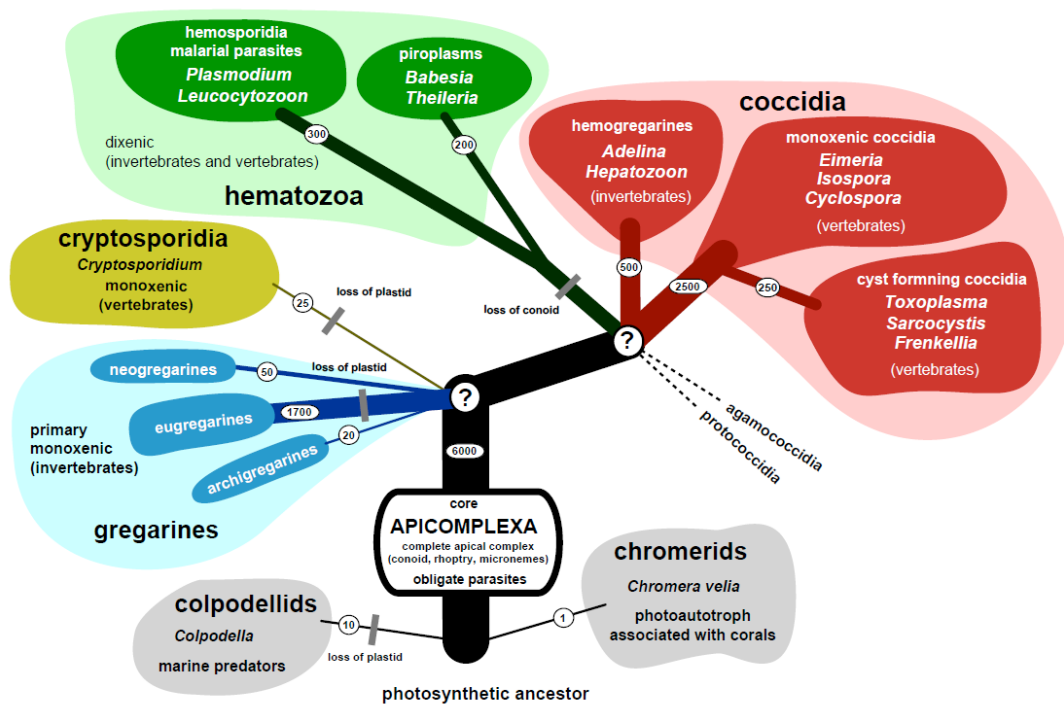


Figure 3: **Evolutionary tree of Apicomplexa.** The principal parasitic groups are gregarines (in blue), hematozoa (in green) and coccidia (in red). (Vlachou et al., 2006)

Apicomplexans are obligate intracellular parasitic protists with an apical complex structure consisting of apical organelles; of note, most of them possess a unique organelle called the apicoplast, a plant-derived non-photosynthetic plastid, which is essential for growth. All members of this phylum have infectious stages, the zoites, which are characterized by a particular polarized shape and unique intracellular structure including

specialized secretory organelles located in the apical region: rhoptries, micronemes and dense granules (Figure 4).

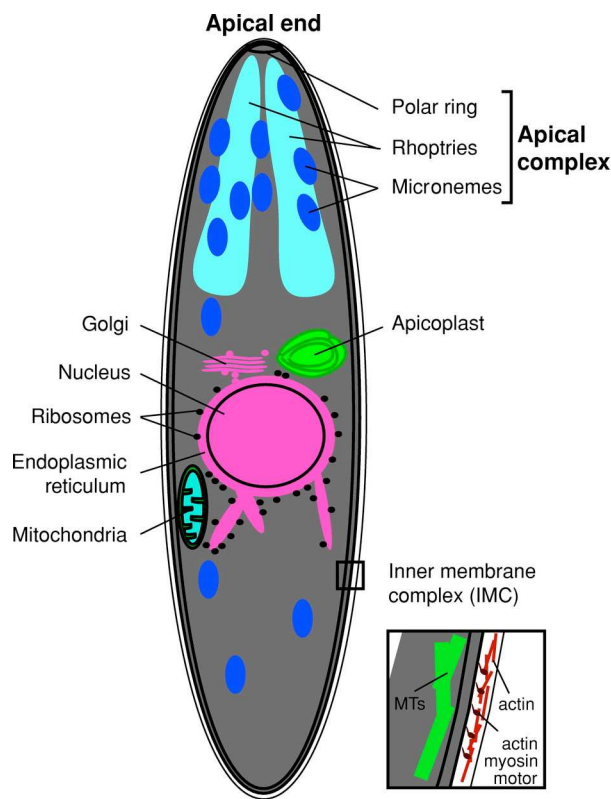


Figure 4: **Morphology of the Apicomplexan parasite** through schematic representation of a *Plasmodium* sporozoite showing some of its organelles and subcellular structures (Kappe et al., 2004).

Rhoptries and micronemes are associated with the anterior end, while dense granules are often in the posterior end or spread out through the cytoplasm (Figure 4). Their motility is powered by the glideosome, a macromolecular complex consisting of adhesive proteins that are released apically and translocated to the posterior pole of the parasite by the action of an actomyosin system anchored in the inner membrane complex (IMC) of the parasite (Figure 4) (Keeley and Soldati, 2004). The IMC is characterized by the presence of cortical alveoli, flattened vesicles packed into a continuous layer supporting the membrane, typically forming a flexible pellicle and essential for motility and invasion processes (Morrissette and Sibley, 2002). The most important Apicomplexan parasites infecting humans belong to the *Plasmodium* genus.

## 2.1 *Plasmodium* Life Cycle

*Plasmodium spp.* life cycle is extraordinarily complex: this protozoan parasite has a two-host life cycle that involves invertebrates (Anopheles mosquitoes) and vertebrates. Malaria parasites replicate by asexual multiplication twice in the mammalian host, within hepatocytes and red blood cells, and once sexually in mosquitoes, within the midgut (Figure 5). The parasite is transmitted by the bite of an infected mosquito that injects thousand of sporozoites into the mammalian host during its blood meal. This migratory form passes through the skin to reach the blood circulation, arriving in the liver via a branch of the portal vein or hepatic artery (Baldacci and Ménard, 2004; Kappe et al., 2004; Mota and Rodriguez, 2004).

Once in the liver, the sporozoite transmigrates through different hepatocytes before productively infecting one of them. In the “final” hepatocyte, the sporozoite develops within a specific compartment surrounded by a membrane, the so-called parasitophorous vacuole (PV), and undergoes a morphological transformation (which involves sporozoite activation and the formation of the transformation bulb) (Kaiser et al., 2003), resulting in the first hepatic form which can exponentially and asymptotically replicate via mitosis to reach a maximum of 10000 daughter cells or merozoites within a single schizont. Notably, for 2 of the five species infecting humans (*P. vivax* and *P. ovale*) and 3 species infecting Macaca (*P. cynomolgi*, *P. simiovale* and *P. fieldi*) a subset of intra-hepatocytic sporozoites remain in a uni-nucleated quiescent state called hypnozoites that at some point is able to activate and produce thousands of merozoites. The modes of hypnozoite commitment and activation remain unknown. Once the liver schizont is fully mature, the merozoites egress from the liver into the blood stream where they are able to invade and infect red blood cells, thus starting the symptomatic phase of *Plasmodium* infection. Within the red blood cells, the merozoite asexually multiplies using mitosis to generate new daughter merozoites that infect other erythrocytes. This cycle can perpetuate for long periods of time. In parallel, some merozoites (1-2%) can undergo sexual commitment to produce sexual forms, the gametocytes.

Male and female gametocytes are transmitted to healthy mosquitoes during its blood meal. Due to the reduction of temperature inside the mosquito midgut (from 37 to 25°C), the male gametocyte exflagellates to produce 8 male gametes that can fertilize the female gamete generated from the female gametocyte. The resulting diploid zygote meiotically replicates

into the ookinete, a motile form capable of traversing the midgut epithelium of the mosquito, attaching to the inner midgut wall, and differentiating into an oocyst. Each oocyst develops into thousands of sporozoites, which migrate to the mosquito salivary gland and are stored there for several days, ready to be injected into the vertebrate host during the next blood meal. In the next sub-sections, each stage is discussed in more detail.

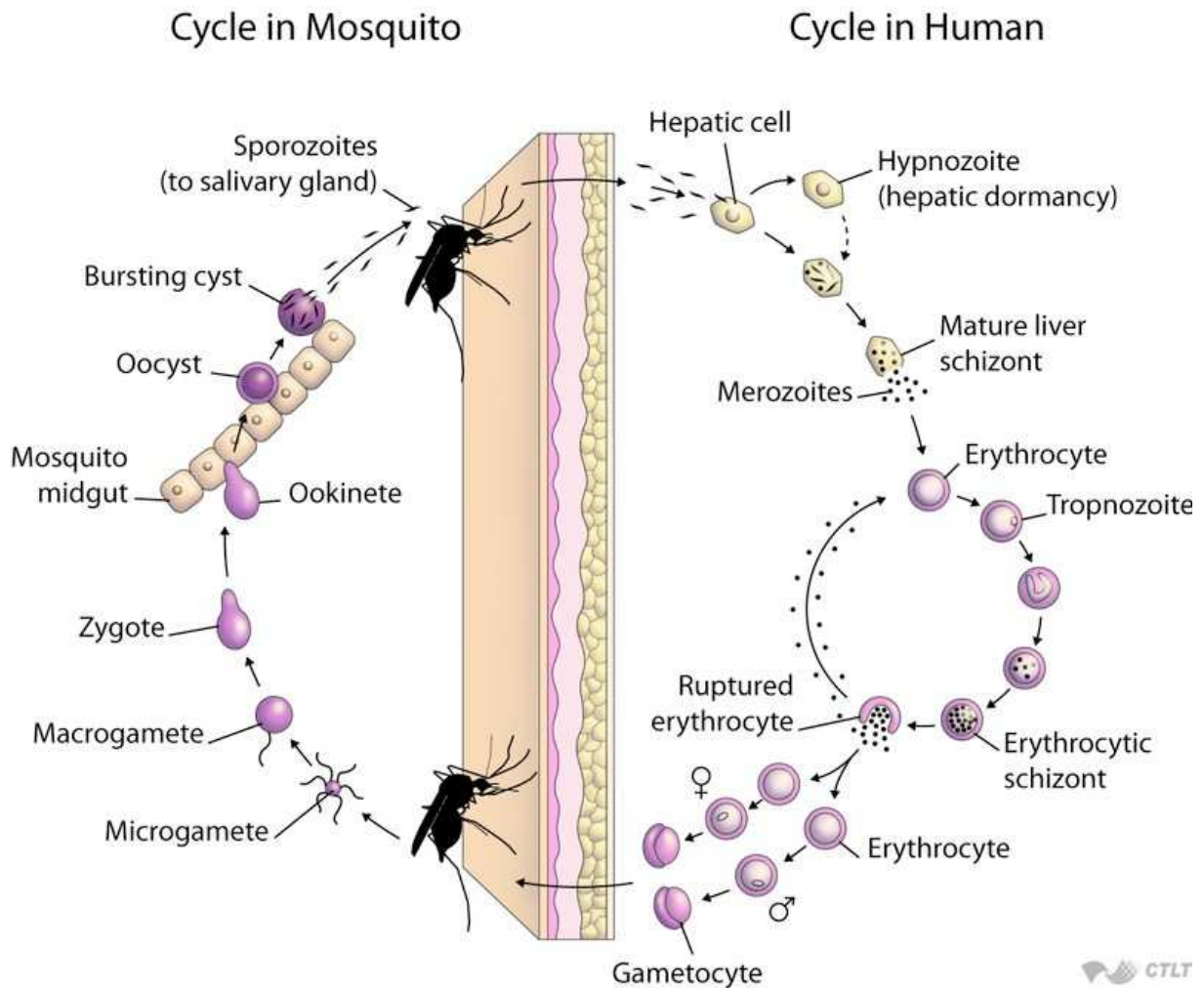


Figure 5 : *Plasmodium* spp. life cycle. *Plasmodium* development involves different stages in the mosquito vector and the mammalian host (© Johns Hopkins Bloomberg School of Public Health)

## 2.2 Parasite development in the mosquito

The parasite journey in the mosquito begins with the ingestion of infected blood in the mosquito midgut lumen, as shown in Figure 6. *Plasmodium* female and male gametocytes mature into gametes. Each male gametocyte by a process called exflagellation, generates eight haploid motile gametes. Exflagellation occurs principally due to temperature decrease and pH changes as well as through exposure to xanthurenic acid in the insect midgut (Billker et al., 1998). Next, male and female gamete fusion results in the formation of a zygote, which differentiates into a motile invasive stage called ookinete. The ookinete penetrates the peritrophic matrix (PM) and the mosquito midgut epithelium, passing from the apical to the basal surface, where it transforms into a young oocyst. Ookinete laminin, the major component of the basal lamina, is essential to traverse the epithelium and for oocyst development. Of note, at this stage, the parasite has to deal with the mosquito immune response for the first time, which is responsible for the high parasite mortality observed during ookinete-oocyst transition. Indeed, this phase represents the first bottleneck in the *Plasmodium* life cycle.

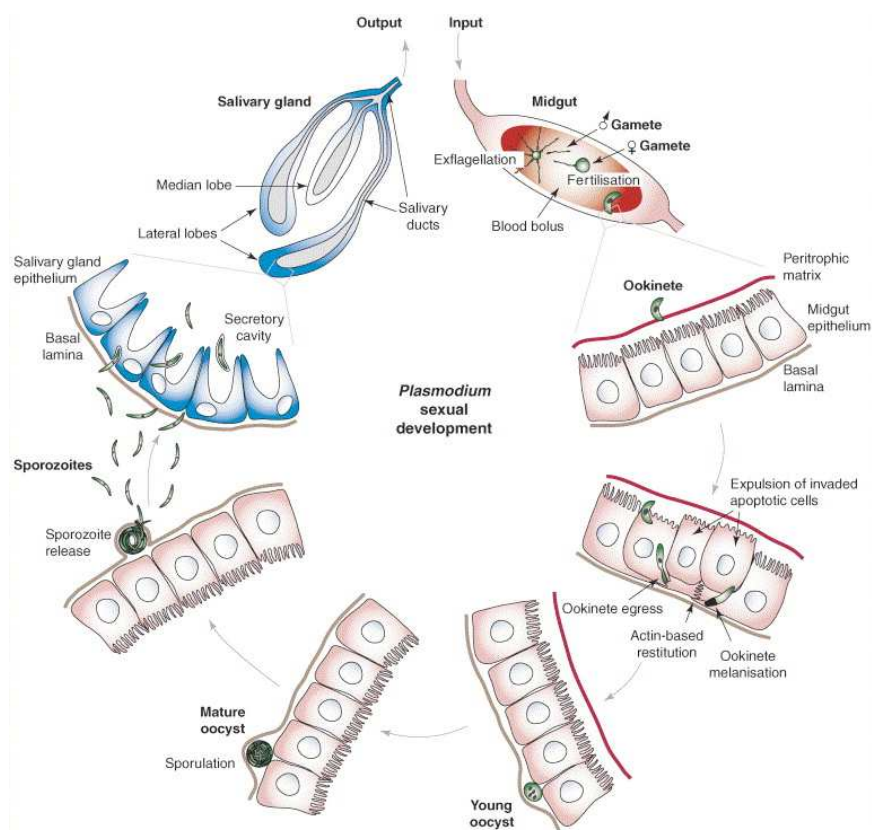


Figure 6 : *Plasmodium* in the mosquito vector. *Plasmodium* development lasts for approximately three weeks (Vlachou et al., 2006).

*Anopheles* mosquitoes respond to *Plasmodium* infection with an epithelial response and with an innate immune memory response. On the other hand, *P. falciparum* through a highly polymorphic antigen Pfs47 evades two well-defined anti-plasmodial responses mediated by the complement-like system: parasite killing/melanization and lysis without melanization (Garver et al., 2009).

Successful transition depends on parasite motility and its ability to recognize and traverse the midgut epithelial barrier, and escape from the mosquito humoral and local immune response (Vlachou et al., 2006). The oocyst develops extracellularly, producing and releasing thousands of sporozoites into the haemolymph of the mosquito. The sporozoites traverse different barriers, interact with receptors of host cells and escape from the mosquito immune response, before arriving in the salivary gland. Successful sporozoites invade salivary glands: they traverse cells within vacuoles before reaching the secretory cavity of the salivary gland by crossing the apical membrane (Pimenta et al., 1994). Intriguingly, sporozoites form large bundles of parasites arranged in parallel arrays inside the salivary gland ducts, ready to be ejected into the mammalian host during their blood meal. Additionally, in the salivary gland, sporozoites undergo a maturation step, which is associated with the up-regulation of a specific subset of genes (UIS genes) at the mRNA level (Matuschewski et al., 2002b).

Mosquitoes probing the skin of the vertebrate host to reach a blood vessel inject saliva containing vasodilators, anticoagulants and *Plasmodium* sporozoites. Sporozoite transmission during a mosquito bite represents the second bottleneck in the *Plasmodium* life cycle. Despite salivary glands containing hundreds of thousands of sporozoites, only few of them (between 10 and 200) are injected during each blood feeding (Frischknecht et al., 2004; Ponnudurai et al., 1991; Rosenberg et al., 1990).

### **2.2.1 *Plasmodium* Sporozoites**

Sporozoites represent the transmission stage between the mosquito and the mammalian host. Upon release from the oocyst, thousands of sporozoites migrate through different mosquito cells and membranes to finally colonize the salivary glands, where they can be stored for several days. Additionally, in the mammalian host, the sporozoites migrate through the skin and blood circulation towards the liver (Prudêncio and Mota, 2007), where they replicate to produce thousands of infectious merozoites. To optimally move, the

sporozoite (represented in figure 7), is an elongated polarized cell, 10-15  $\mu\text{m}$  long and 1  $\mu\text{m}$  in diameter. The cell is enveloped in a triple pellicle made by the plasma membrane and the underlying IMC, with the shape of the sporozoite maintained by microtubules. Sporozoites contain two sets of secretory organelles, the rhoptries and the micronemes. The rhoptries are large, paired, pear-shaped organelles filled with proteins and phospholipids. The micronemes are small vesicles with a neck-like extension. Microneme proteins are typically involved in gliding motility, adhesion to substrates and host cell recognition, while rhoptry proteins are implicated in entry into the host cell and parasitophorous vacuole formation (Baum et al., 2006, p. 200; Counihan et al., 2013; Santos et al., 2009).

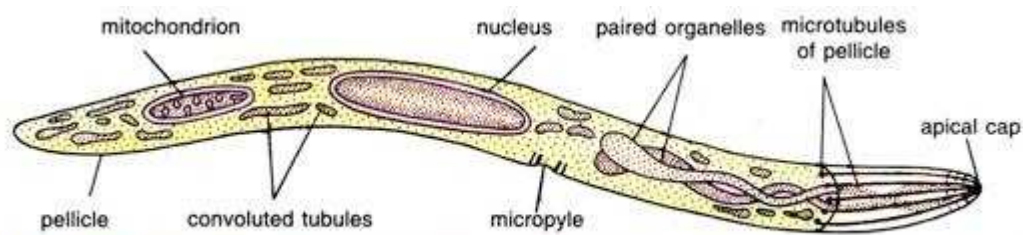


Figure 7: **The morphology of the *Plasmodium* sporozoite.** The anterior cell pole contains the apical complex comprising two rhoptries and large number of micronemes. Another unique organelle is the inner membrane complex, which is associated with a set of microtubules. (Garnham et al., 1963)

## 2.3 Infection of the Mammalian Host

Sporozoites injected in the mammalian dermis travel from the site of mosquito bite in the skin to the liver, where they enter and develop inside hepatocytes. They multiply and differentiate into the parasite form called merozoite, which reaches the blood circulation to infect erythrocytes, causing the symptoms of the disease.

### 2.3.1 Skin Stage

Sporozoites glide in the skin with a speed of  $\sim 1\text{-}2 \mu\text{m/s}$  displaying a tortuous and random three-dimensional movement pattern for more than one hour (Ménard et al., 2013; Sidjanski and Vanderberg, 1997). Many sporozoites remain in the skin for hours, with the pattern of sporozoite exit from the injection site resembling a slow trickle (Yamauchi et al., 2007). Sporozoites, as they glide into the dermis, contact and traverse either endothelial cells of blood vessels to enter the blood stream, the main route used to reach the liver, or

endothelial cells of the lymphatic system (Figure 8). Sporozoites that enter the lymphatic circulation stop at the draining lymph node where they are degraded by dendritic cells (da Silva et al., 2012).

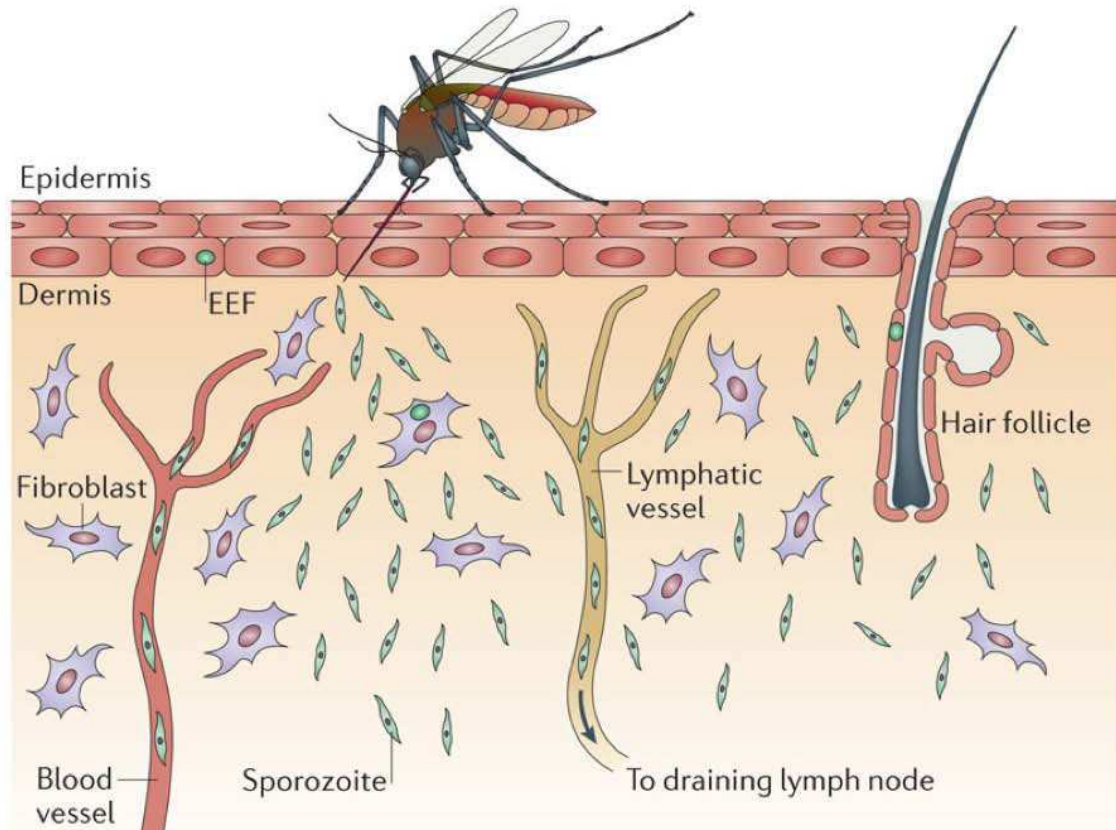


Figure 8: **Representation of motile sporozoites injected into the skin.** *Plasmodium* sporozoites can pursue different routes, leaving the bite site via blood or lymphatic vessels, or remaining in the skin (Ménard et al., 2013)

Although the liver is the principal (if not only) target organ for sporozoite differentiation into merozoites, extra-hepatic parasite development has been reported. Studies in *P. berghei* have shown that some sporozoites initiate development into exoerythrocytic forms in the lymph node (Amino et al., 2006) or the dermis (Gueirard et al., 2010), constituting a potential secondary reservoir; but the relevance of these rare events still need to be established. Other studies using *P. berghei* and *P. yoelii* suggested that some sporozoites can persist in association with hair follicles (Figure 8), an immuno-privileged site of the mammalian body, leading to the hypothesis that sporozoites may become quiescent when associated with hair follicles, thus providing a source of relapses, similar to *P. vivax* hypnozoites in the liver (Cogswell, 1992; Gueirard et al., 2010).

### 2.3.2 Liver Stage

The liver represents the first target site where sporozoites can develop and multiply. As shown in Figure 9a, the basic unit of the liver parenchyma is the lobule; this structure is surrounded by connective tissues forming six portal fields. Each portal field contains one branch each of the portal venule, the hepatic arteriole and the bile ductule. The arterial and portal blood merge entering the liver lobule, pass inside sinusoids, along cords of hepatocytes, and leave via the central vein (Frevert, 2004). The liver sinusoid wall, represented in Figure 9b, is composed of specialized endothelial cells containing small fenestrae (Wisse et al., 1985) and Kupffer cells (KC), resident macrophages of the liver responsible for the removal of degraded and/or foreign molecules from the blood. This conformation allows exchange between the blood and fluids in the perisinusoidal space (space of Disse) located between the sinusoid cellular wall and the hepatocytes. In the space of Disse reside stellate cells, which are fat-storing cells and the main producers of the liver extracellular matrix (ECM). Sporozoites (represented in red in Figure 8b) infect the liver in three steps: (1) arrest in the sinusoid, (2) passage through sinusoidal cells, and (3) invasion of hepatocytes.

#### 2.3.2.1 Arrest in the Sinusoid

The tropism of the sporozoite for the liver is mainly due to the surface antigen Circumsporozoite Protein or CSP, (Frevert et al., 1993). CSP is essential for sporozoite development in oocysts (Wang et al., 2005), and is involved in various processes

A second antigen, TRAP (thrombospondin-related adhesive protein) present in the micronemes and secreted upon cell contact also participates in sporozoite homing into the liver. Loss-of-function mutations in the two adhesive motifs specifically decrease sporozoite invasion but do not affect gliding and adhesion to cells (Matuschewski et al., 2002a).

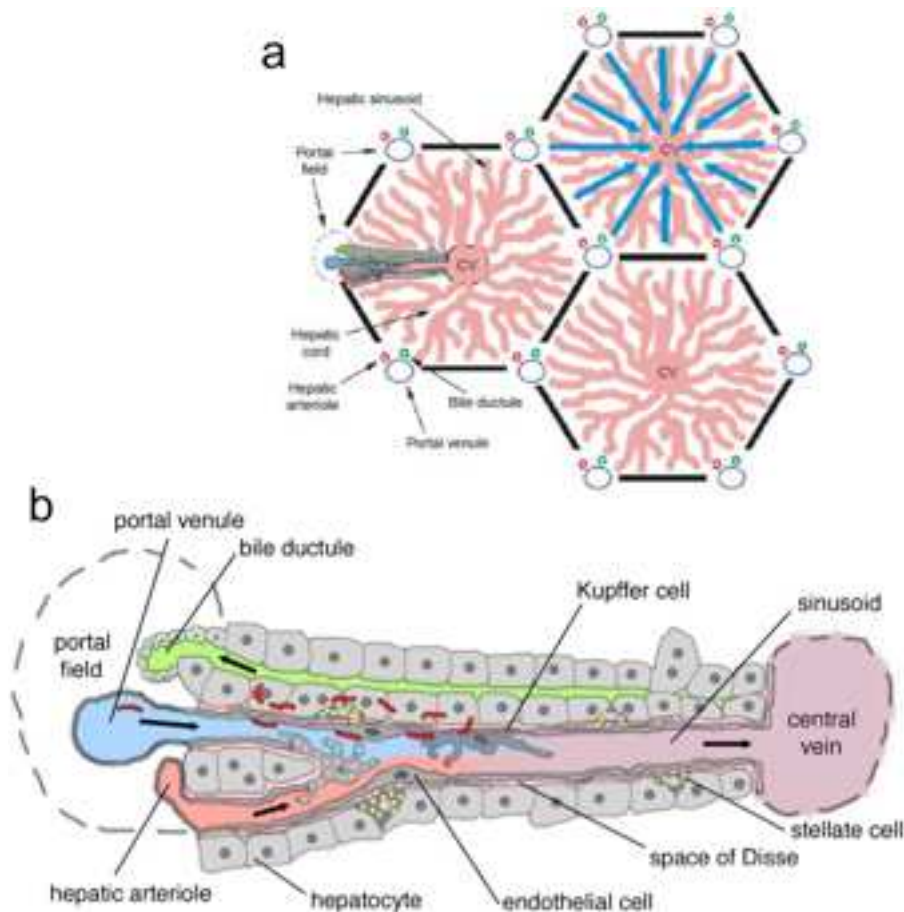


Figure 9: **Liver infection by *Plasmodium* sporozoites.** (a) The hepatic lobule represents the liver unit. The portal venous and arterial blood supplies enter the liver lobule at the portal field, merge after entering the sinusoid, flow along cords of hepatocytes, and exit the lobule at the central vein (CV). (Frevert, 2004) (b) Dynamics of *Plasmodium* liver infection. Liver sinusoids are lined with fenestrated endothelia and Kupffer cells. They are separated from hepatocytes by the space of Disse where stellate cells localize. In red the sporozoite enters through the portal vein or the hepatic artery into the sinusoid where it subsequently glides along it to finally encounter a Kupffer cell. After migration across the sinusoidal cells, sporozoites gain access to the underlying hepatocytes. (Frevert et al., 2005).

### 2.3.2.2 Sinusoid Traversal

The parasite glides along the sinusoid, frequently moving against the bloodstream, until it recognizes select chondroitin and heparan sulfate proteoglycans on the surface of Kupffer cells (KCs) via CSP (Pradel et al., 2002). Frevert and collaborators proposed the gateway model hypothesizing that, sporozoites translocate across the sinusoidal barrier exclusively through KCs inside a non-fusogenic PV. In keeping with this, it has been observed that sporozoites can migrate through cells (Mota and Rodriguez, 2001), with genetic studies in *P. berghei* identifying several parasite factors involved in the process of cell traversal (CT). However, recent intravital imaging studies demonstrated that KCs do not constitute a mandatory gateway for *Plasmodium* sporozoites (Tavares et al., 2013). The

authors showed that sporozoites can cross the liver sinusoidal barrier by multiple mechanisms, most of which are associated with cell traversal activity through endothelial cells (EC) and/or Kupffer cells. However, CT-deficient mutants still maintain a residual capacity to cross sinusoidal barriers (Ishino et al., 2005; Kariu et al., 2006), and the mechanisms used might correspond to either a paracellular pathway, as suggested for *Toxoplasma* tachyzoite transmigration (Barragan et al., 2005) or a transcellular pathway, through the formation of channels inside EC, like those generated by extravasating leukocytes (Carman and Springer, 2004) or through manipulating the fenestrations of liver sinusoidal EC (Warren et al., 2007). Finally, the sporozoite crosses the space of Disse to continue its path to the liver parenchyma where it encounters hepatocytes.

### **2.3.2.3 Invasion of Hepatocytes**

The sporozoite transmigrates through several hepatocytes before homing in on its final niche hepatocyte. Here, it switches to productive invasion and differentiates into an exoerythrocytic form (EEF). A sequence of steps occurs during productive invasion: initially, a “distant” attachment is mediated by proteins secreted by micronemes. The rhoptry proteins are then secreted to form the moving junction (MJ), followed by engagement of the parasite actin-myosin motor, leading to parasite internalization. The parasite forms a parasitophorous vacuole (PV) (Besteiro et al., 2011), enclosed in a membrane (PVM), where its development takes place. Inside the vacuole the parasite is protected from the host immune response and can undergo schizogonic development. At this stage, the parasite nucleus divides multiple times with a concomitant syncytial organisation without cell segmentation. After 2 days or 6-7 days respectively for rodent and primate parasites, the schizont is mature and full of merozoites.

### **2.3.3 Exo-erythrocytic Merozoite Formation and Release**

Formation of individual liver stage merozoites begins when the parasite plasma membrane invaginates to demarcate individual merozoites with a single haploid nucleus and the necessary organelles (Figure 10). The PVM then breaks down, releases merozoites and PV contents into the host cell cytoplasm, in turn activating host cell mitochondrial disintegration and inhibiting host cell protein biosynthesis. The host cell now detaches.

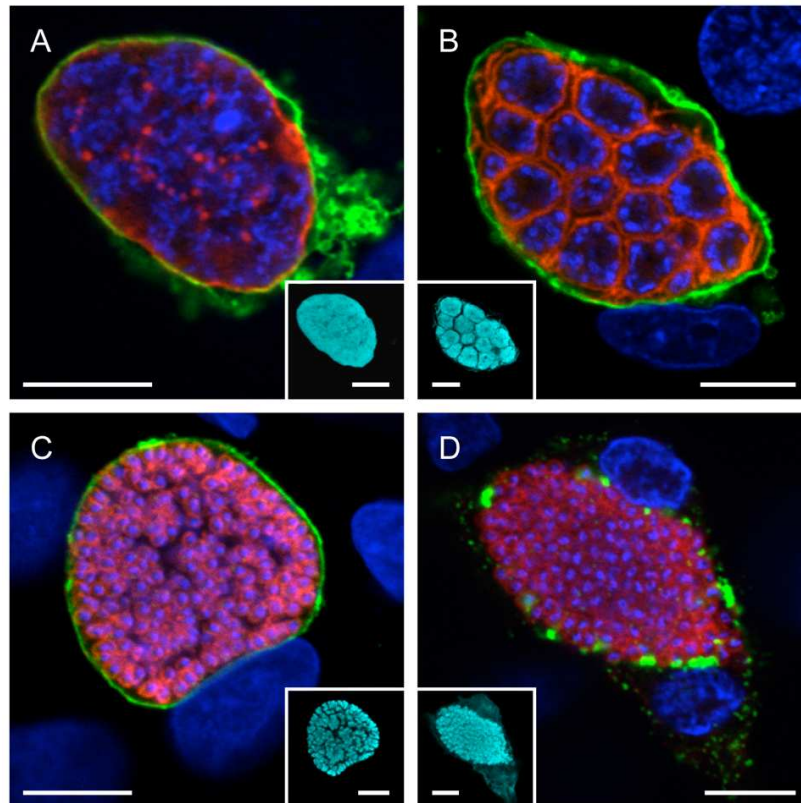


Figure 10 : **Dynamics of the parasite membrane during the late liver phase.** HepG2 cells infected with *P. berghei* at different time points after infection. While the PM (anti-MSP1 in red) surrounded the parasite as a whole during the late schizont stage (A), it began to invaginate around groups of nuclei (DAPI in blue) during cytomere formation (B). It eventually surround individual merozoites both before (C) and after (D) PVM (anti-exported protein 1 (anti-EXP1 in green)). (Graewe et al., 2012)

At this point, the merozoites, large bags of hepatocyte membrane containing dozens of merozoites are shuttled out of the liver unharmed, by passing the highly phagocytic Kupffer cells, and travel to the lungs where they are arrested. During passage to the lung, the intact host cell membrane of the merozoite is used by the parasite as protection from the host immune system. After several hours, the hepatocyte-derived merozoite membrane disintegrates and releases merozoites into the pulmonary bloodstream, which can then infect erythrocytes (Baer et al., 2007).

#### 2.3.4 Blood Stage

Blood stage invasion begins with the interaction between a merozoite and the erythrocyte surface, which is an active and rapid process (<60 s) (Cowman and Crabb, 2006). Once internalized, the parasite resides in a sealed compartment, the PV, distinct from the erythrocyte cytosol, as is observed in the liver stage (Figure 11). To survive and multiply within the RBC, the parasite modifies the host cell cytoplasm and cell surface

morphologically and physiologically. These include, hemoglobin uptake, gaseous exchange, cytoadherence to the peripheral circulation to provide an optimum environment for parasite growth (i.e., high levels of carbon dioxide and low levels of oxygen), and avoiding splenic clearance, etc. In the case of *P. falciparum*, parasite-derived proteins such as the *Plasmodium falciparum* erythrocyte membrane protein 1 (PfEMP1), are trafficked to the surface of the iRBC and enable the parasite to cytoadhere to endothelial and other intravascular cells (more details in Section 5). This property is maintained by a sophisticated system of antigenic variation with programmed switching of surface antigens to evade the immune system and allows for chronic infection of the host (Discussed in section 5) (Guizetti and Scherf, 2013).

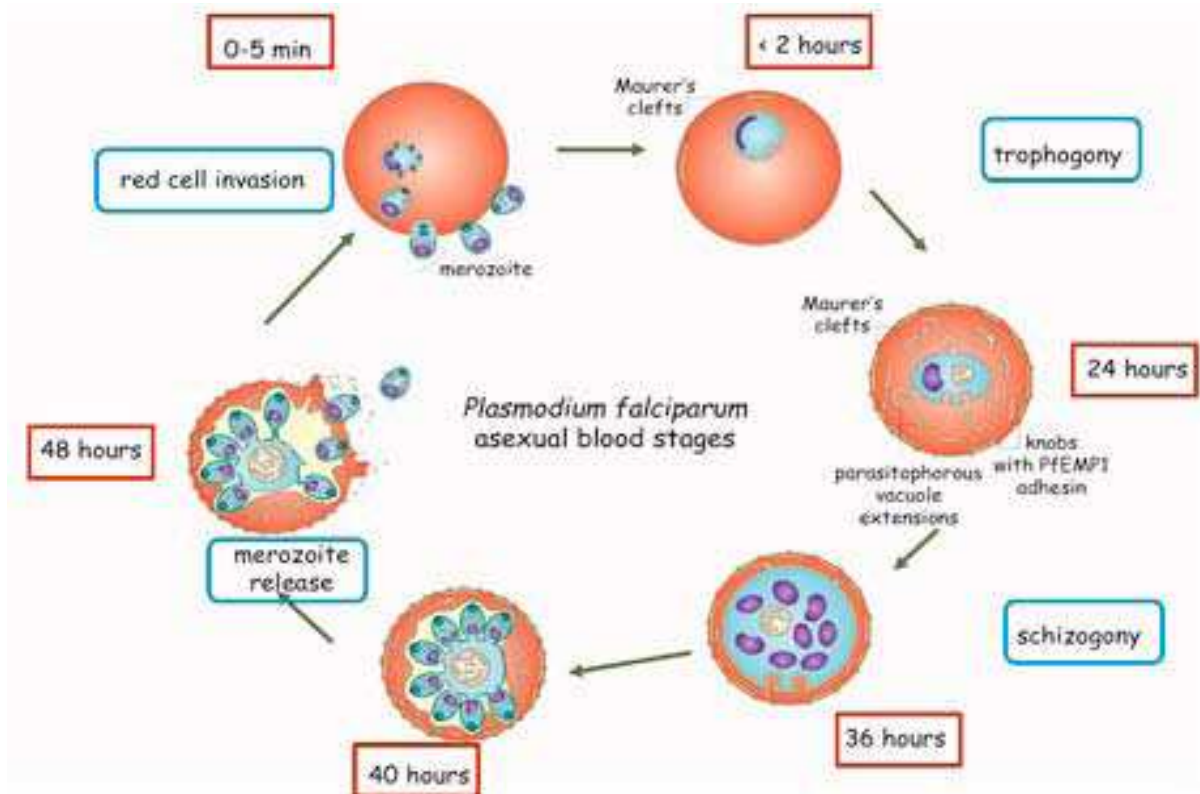


Figure 11: *P. falciparum* asexual blood stages in the human host (Maier et al., 2009).

### 3. Genome organization and gene expression in *P. falciparum*

Given its remarkable life cycle (as discussed in Section 2) and its capability to colonize numerous host and insect cells, the *Plasmodium spp.* parasite needs to respond quickly to diverse and hostile environments, and persist in the host until transmission is achieved. Studies to understand how the parasite adapts, survives and propagates under varied growth environments revealed that it differentially regulates gene expression during its life cycle (Bozdech et al., 2003; Le Roch et al., 2003), at the transcriptomic and proteomic levels. This regulation is orchestrated by several mechanisms, including epigenetic, transcriptional, post-transcriptional and translational regulation. Due to the absence of most specialized eukaryotic transcription factors in the *Plasmodium* genome (Gardner et al., 2002a), the epigenetic machinery has an important role in gene expression regulation. Indeed, to date, the only known *Plasmodium spp.* DNA-binding transcriptional regulators belong to the 27-member Apicomplexan Aptela 2 or ApiAP2 family (Painter et al., 2011). While some ApiAP2 proteins are expressed in a stage-specific manner, a subset of them are expressed throughout the four stages of the intraerythrocytic cycle (ring, trophozoite, early schizont and late schizont stage). The predicted DNA-binding AP2 domain is ~60 aa in size and can be found alone, or in tandem with one or two additional AP2 domains. These domains bind with high specificity to unique DNA motifs, which are typically found in the upstream promoter regions of distinct sets of genes.

#### 3.1 *P. falciparum* Chromosome Organization and Structure

The sequencing of the *P. falciparum* genome performed in 2002 revealed that the nuclear genome has 5,300 protein-encoding genes (Gardner et al., 2002a); the most recent annotation contains 5700 protein-coding genes and select groups of non-coding genes. In addition, it has two organellar genomes, the mitochondrial genome of 6 kb and the non-photosynthetic plant derived apicoplast genome of 35 kb.

The highly AT-rich nuclear haploid genome of *P. falciparum* is 23.0 Mb in size and organized into 14 linear chromosomes (Gardner et al., 2002b). The chromosomes have a size

ranging from 0.643 Mb for chromosome 1 to 3.29 Mb for chromosome 14. Each chromosome is compartmentalized, containing conserved regions in its central domain where the housekeeping genes are located, and polymorphic regions at its telomeric ends where highly variable gene families cluster (Scherf et al., 2008a). Chromosomes ends are made of tandem telomeric repeats (GGGTT(T/C)A), followed by an array of noncoding and coding DNA elements, the so-called telomere-associated sequences (TAS), in the subtelomeric regions (Figure 12). The terminal tract of *P. falciparum* telomeric DNA is assembled into a non-nucleosomal chromatin structure, the telosome (Figueiredo et al., 2000) that can contribute to epigenetic regulation. Moreover, the non-coding regions of TAS are composed of a mosaic of six different blocks of repetitive sequences that are located between the telomere and the coding region of TAS; these elements are called “telomere associated repetitive elements” (TAREs) and span 20-40 kb (Table 1) (Figueiredo et al., 2000; Scherf et al., 2001). TARE6, also known as rep20 based on the minimal repeat unit, is responsible for chromosome-end size polymorphism. Notably, adjacent to the non-coding TAREs are located member of multi-gene families such as *var*, *rif* and *stevor*.

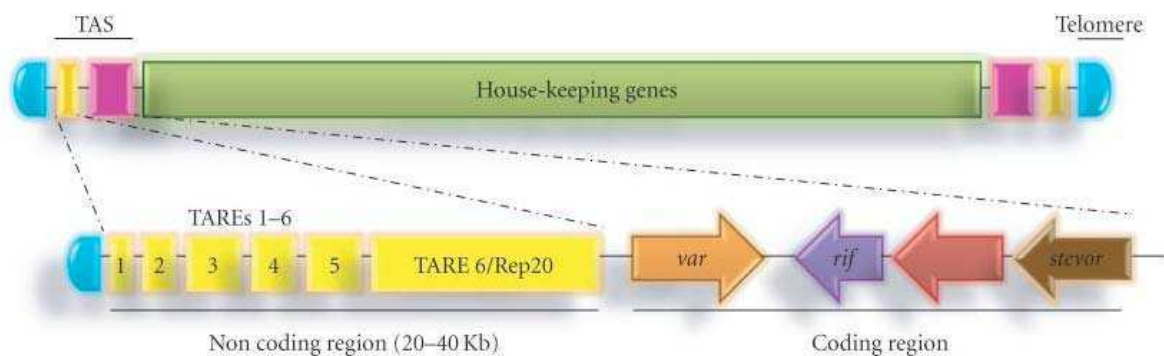


Figure 12: ***P. falciparum* chromosome organization.** The *P. falciparum* haploid nuclear genome is organized into 14 linear chromosomes. Each chromosome is composed of an internal region in which housekeeping genes are located, and a chromosome end that displays a higher-order DNA organization. Downstream of telomeres resides at highly polymorphic TAS composed of a noncoding and a coding region. The noncoding region contains six TAREs, which are always positioned in the same order but are of variable length (Hernandez-Rivas et al., 2010)

The telomeres play a major role in nuclear architecture. Telomeres have been shown to form clusters and to anchor chromosomes to the nuclear periphery, forming distinct nuclear compartments (J. J. Lopez-Rubio et al., 2009). These nuclear domains have an important role in epigenetic gene regulation, as proteins essential for telomeric silencing are found to be concentrated at the telomeres and/or subtelomeric regions.

Table 1: Features of different subtelomeric repeat elements in *P. falciparum*

<i>Name</i>	<i>Size</i>	<i>Sequence Features</i>
<b>TARE1</b>	0.9-1.9 kb	Tandem repeats of 7bp. Polymorphic within and between the chromosomes
<b>TARE2</b>	1.6 kb	135 bp degenerate sequence repeated 12 times, interspersed by two distinct 21 bp sequences
<b>TARE3</b>	2.1-2.8 kb	3-4 consecutive elements of 700 bp
<b>TARE4</b>	0.7-2 kb	Highly degenerated, short repeats with interspersed non repetitive sequence of 230 bp
<b>TARE5</b>	1.4-2 kb	Moderately degenerated tandem repeats 12 bp
<b>TARE6</b>	8.4-21 kb	Degenerate sequence of 21 bp

### 3.2 Chromatin and its Regulation in *P. falciparum*

In *Plasmodium spp.*, chromatin is organized as in other eukaryotic organisms, into fundamental units of ~147 bp of DNA wrapped around an histone octamer; these units are called nucleosomes and serve as binding sites for transcription factors to regulate gene expression (Cary et al., 1994).

The *P. falciparum* genome encodes four canonical histones required to assemble the nucleosome (H2A, H2B, H3 and H4) and four histone variants (H2A.Z, H2Bv, H3.3 and CenH3); however it lacks a gene encoding for histone H1, the linker histone (Miao et al., 2006). This partially explains the lack of higher order compaction of nuclear DNA in *P. falciparum*. Histones H3 and H4 contain N-terminal tails that are sites of post-translational modifications (PTMs), covalent alterations of specific amino acid residues that involve addition or removal of chemical groups mediated by specific enzymes. By mass-spectrometry, PTMs such as acetylation and methylation have been identified in *Plasmodium* Histone H3 and H4 at different positions (Figure 12) (Cui and Miao, 2010). These are summarized in Table 2.

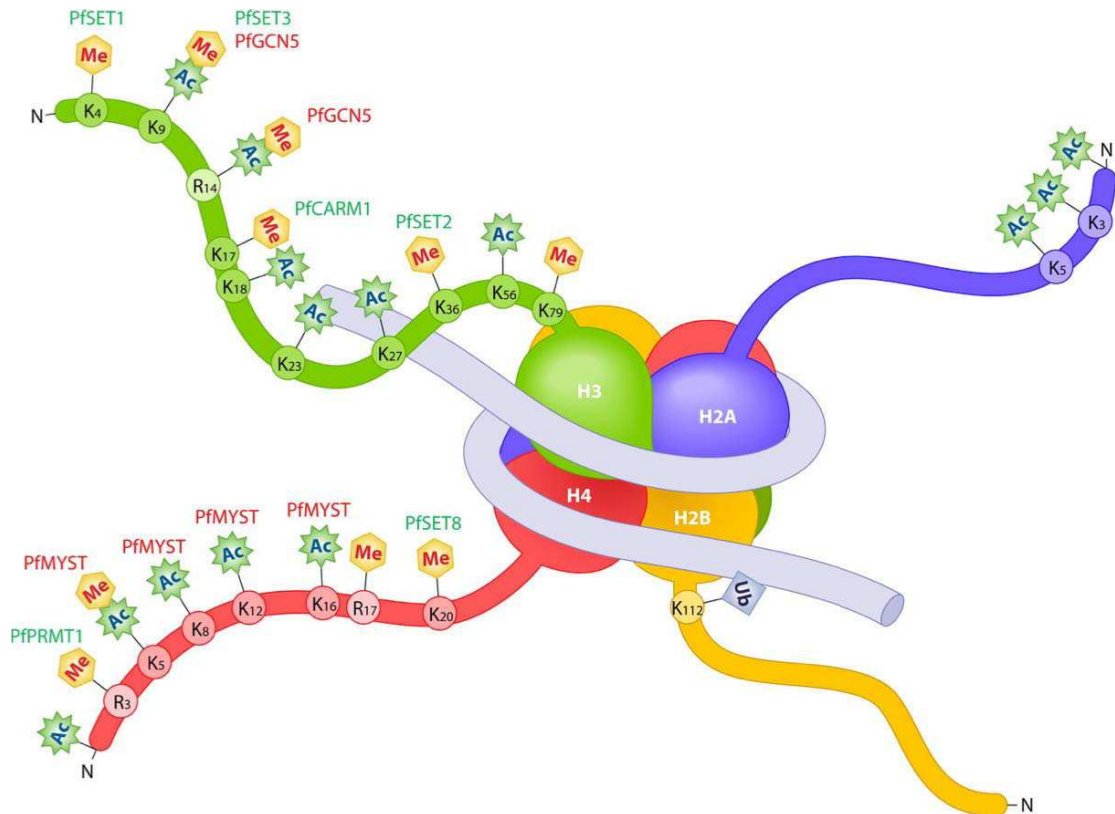


Figure 13. Nucleosome structure with the four canonical histones (H3, H4, H2A, and H2B) in *P. falciparum*. Covalent PTMs (methylation [Me], acetylation [Ac], and ubiquitination [Ub]) and enzymes catalyzing the addition of the PTMs (PfGCN5, PfSET1, PfSET2, PfCARM1, PfPRMT1, PfMYST, and PfSET8)(Cui and Miao, 2010)

PTMs are reversible and alter the chromatin structure (*cis* effects), thus regulating gene expression. Maintenance of PTMs is mediated by a variety of “writer and eraser” proteins such as methyltransferases, demethylases, acetylases and deacetylases (discussed in Section 4), which serve as a marking system to recruit specialized reader proteins such as heterochromatin protein 1 (PfHP1) and bromodomain protein 1 to the site of the modification (*trans* effects) (Doerig et al., 2015a) (discussed in Section 4). Specific combinations of *cis* and *trans* effects create distinct biological signals, termed as the “histone code”, which dictates particular cellular outcomes (Strahl and Allis, 2000). Histone modifications identified so far in *P. falciparum* are listed in Table 2.

Table 2: List of histone modifications identified in *P. falciparum* blood stages. PTM = Post-Translational Modification (Cui and Miao, 2010; Saraf et al., 2016a)

<i>PTM</i>	<i>H2A</i>	<i>H2A.Z</i>	<i>H2B</i>	<i>H2B.Z</i>	<i>H3</i>	<i>H3.3</i>	<i>CenH3</i>	<i>H4</i>
<b>K<sup>ac</sup></b>	N-term	N-term	N-term		K9	K9	K23 <sup>nc</sup>	N-term
	K3	K11	K3		K14	K14	K26 <sup>nc</sup>	K5
	K5	K15	K8		K18	K18	K60 <sup>a,nc</sup>	K8
		K19	K13		K27	K23		K12
		K25	K14		K56	K27		K16
		K28	K18					
<b>ST<sup>ac</sup></b>		K30	K35 <sup>c</sup>					
		K35	K64 <sup>nc</sup>					K67 <sup>a,nc</sup>
	T101 <sup>a</sup>		S24	T30 <sup>nc</sup>	T107	T11		S47 <sup>a</sup>
			S28 <sup>a</sup>	S54		S86		
<b>me<sup>1</sup></b>			S50 <sup>nc</sup>					
			T61 <sup>nc</sup>					
	K75				K4	K4		K5
<b>me<sup>2</sup></b>					K14	R17		K12
					R17			K20
								K91 <sup>a</sup>
								R3
<b>me<sup>3</sup></b>								R17
			K64		K4	K4		K67
					K115			K20
<b>Fo</b>					R17	R17		R3
			K35		K4	K4		K20
			K49		K9			
			K64		K36			
					K79			
<b>Oh</b>					K115			
	K20	R115	R25	R29	K14	K36	R108	R45
	K41 <sup>nc</sup>		K49	K53	K27	R42 <sup>b</sup>		
	R42		K64	R95	K36	K53		
					R42 <sup>b</sup>	R72		
					R53	R116 <sup>b</sup>		
					R72			
				R83				
<b>Ubq</b>					R116 <sup>b</sup>			
	P48	Y77	Y32	K53	Y54	K53		D68
	Y50	H138	K35	D64	K79	Y99		Y72
	Y57	K139	K38	D67 <sup>nc</sup>	D106	D106		K77
<b>Phs</b>					H113	H113		D85
					K115	K115		
					P121 <sup>b</sup>	P121 <sup>b</sup>		
<b>Cr</b>								
<b>Cr</b>			S56 <sup>a</sup>		Y78 <sup>nc</sup>			
			T85					
<b>Cr</b>			S49 <sup>a</sup>		K115 <sup>a</sup>	K115		

### 3.3 Transcription and Post-transcriptional Gene Regulation

Gene expression in *Plasmodium spp.* is regulated at multiple levels. During sexual blood stages, ~4600 of the 5700 *P. falciparum* genes are transcribed in a cyclical manner, such that every mRNA peaks at only one time point of the RBC life cycle. Importantly, mRNAs belonging to a functional group are co-transcribed, usually when their protein function is required. This has led to researchers proposing a “just-in-time” transcription model to explain gene expression in asexual blood stages. This is regulated by epigenetic mechanisms including histone PTMs, histone variants, nucleosome occupancy and potentially DNA modifications, as well as transcription factors of the ApiAP2 family and potentially other DNA-binding proteins (Kirchner et al., 2016a).

Once a transcript has been made and transported to the cytoplasm, it can take several routes: production of protein, temporal translational repression or mRNA decay (reviewed in (Vembar et al., 2016). While immediate protein production is the primary outcome of gene expression, for 30% of *P. falciparum* genes a delay between peak mRNA and protein levels has been reported in asexual blood stages. This has led researchers to propose a second “just-in-time translation” strategy utilized by the parasite to coordinate protein expression (Foth et al., 2011; Roch et al., 2004). Post-transcriptional and translational regulatory mechanisms may involve several RNA-binding proteins and other parasite-specific proteins that are yet to be characterized (Table 3) (Gardner et al., 2002a; Vembar et al., 2016). In blood stage parasites, recently an RNA-binding protein called Alba was discovered as being involved in regulating the timing of translation of a number of merozoite invasion transcripts (Vembar et al., 2015).

Adding further complexity to gene regulation processes are the highly prevalent translational repression mechanisms found in gamétocytes and sporozoites. In *P. falciparum* PfPuf1 and PfPuf2 two members of Puf (Pumilio and fem-3 binding factor homolog) family, were shown to be differentially expressed in gametocytes, Subsequent analysis demonstrated an essential role for PfPuf2 in repressing gametocytogenesis, in particular male differentiation (Miao et al., 2010), and translational repression via binding to Puf-binding elements (PBEs) in the 5' and 3'UTRs of its target mRNAs (Miao et al., 2013). In sporozoites, global translational repression is achieved by phosphorylation of the translation initiation factor, eIF2a. Overall, gene regulation remains a much studied topic in *Plasmodium* research.

Table 3: Translation, Decay and Repression regulators in *Plasmodium spp.*

Process	Molecular player	<i>Plasmodium spp.</i>	Lifecycle stage	Properties	Reference
Translation	eIF2 $\alpha$ Kinases: IK1, IK2, PK4	<i>P. falciparum</i> <i>P. berghei</i>	IDC Sporozoites Gametocytes	IK1 is primarily transcribed in asexual blood stages, IK2 in sporozoites and PK4 during the IDC and in gametocytes; IK1 and IK2 are not essential to parasite growth (all stages of development) whereas the PK4 gene cannot be deleted in blood stages	(Zhang et al., 2010)49
	PfDZ50	<i>P. falciparum</i>	IDC	DDX6/Dhh1 RNA helicase and homolog activities of PfDZ50 have been demonstrated in vitro as has its ability to bind to PefIF4E and repress translation	(García-of Martínez et al., 2004)
	PfAlba1	<i>P. falciparum</i>	IDC	PfAlba1 is essential to blood stage development; The in vivo RNA interactome of PfAlba1 consists of >105 mRNAs, including mRNAs encoding erythrocyte invasion proteins such as Rap1, AMA1, RhopH3 and CDPK1	(Baum et al., 2009; Chêne et al., 2012)
mRNA decay	PfCaf1	<i>P. falciparum</i>	IDC	Deadenylase subunit of the CCR4-NOT complex; Of the 1031 mRNAs that are misregulated upon PfCaf1 depletion, mRNAs encoding erythrocyte egress and invasion proteins are over-represented	(Peeters et al., 2015)49
	RNA exosome (RRP6, DIS3)	<i>P. falciparum</i>	IDC	PfRRP6 and PfDIS3 coimmunoprecipitate with the exosome and localize to the nucleus and cytoplasm, respectively, of ring stage parasites	(Zhang et al., 2014)49
Traslational Repression	PbDOZI-CITH Complex	<i>P. berghei</i>	Female gametocytes	PbDOZI and PbCITH localize to the cytoplasm in P-granule-like structures with the PbDOZI-CITH complex and Le Roch, composed of 11 proteins; Targets include 730 mRNAs, several of which are repressed in sexual stages and translated only in zygote and ookinets	(Balu et al., 2011; Bunnik and Le Roch, 2015; Peccarelli and Kebaara, 2014)49
	Puf2	<i>P. falciparum</i> <i>P. berghei</i> <i>P. yoelii</i>	Gametocytes Sporozoites	PfPuf2 binds the Puf-binding element in the 5' and 3' UTR of two mRNAs, Pfs25 and Pfs28, in gametocytes and translationally represses them; PbPuf2 and PyPuf2 translationally regulate the UIS mRNAs in sporozoites	(Miao et al., 2010, 2013)49
	Bruno/CELF	<i>P. falciparum</i> <i>P. berghei</i>	IDC, Female gametocytes	PfCELF1 localizes to punctate structures in the cytoplasm; ~1100 mRNA targets of PfCELF1 have been identified using vitro RNA-binding assays; PbCELF2 associates with the DOZI-CITH complex	(Balu et al., 2011)49
	Alba1, 2 and 3	<i>P. berghei</i> <i>P. falciparum</i>	Female gametocytes, IDC	PbAlba1, 2 and 3 associate with the DOZI-CITH complex; PfAlba1, 2 and 3 bind to RNA in vitro; The cytoplasmic localization of PfAlba1 and 2 in trophozoites and schizonts is punctate and reminiscent of P granules	(Balu et al., 2011; Baum et al., 2009)49

## 4. Epigenetic Regulation in *P. falciparum*

“Epigenetics” describes the heritable changes in gene activity, that occur independent of changes in DNA sequence and are established through reversible chromatin and/or DNA modifications. In *P. falciparum* blood stage parasites, epigenetic mechanisms regulate not only antigenic variation but also the clonally variant expression of proteins involved in RBC invasion, solute transport and sexual commitment. Epigenetic changes in gene expression are commonly orchestrated by dynamic alteration of chromatin structure by reversible post-translational modifications (PTMs) of histones. Moreover, PTMs are recognised by effectors that can oligomerize and condense nucleosomal arrays (e.g. heterochromatin protein 1 (HP1)), re-organise local chromatin structure (e.g. SWI/SNF-family remodellers) or place/remove other histone modifications (e.g. methyltransferases (HKMTs), demethylases, acetyltransferases or deacetylases (HDACs such as Sirtuins) (Figure 14; Tables 4 and 5) (Bannister and Kouzarides, 2011). Chromatin-modifying enzymes cooperate in a complex mechanism with genetic elements such as the promoter, intron and other *cis*-acting DNA elements to facilitate or inhibit gene expression. Histone modifications also effectuate spatial gene regulation by creating specific nuclear sub-compartments that are critical for default silencing and monoallelic expression.

### 4.1 Histone Modifications and their Writers and Eraser

Histone PTMs are extremely important to create the histone code, acting directly on the interaction between nucleosomes and DNA, or indirectly recruiting non-histone proteins that act on the chromatin (Kouzarides, 2007). Direct interaction affects chromatin ultrastructure: for example, histone lysine acetylation has the potential to unfold chromatin by neutralizing the basic charge of lysine (Table 4). Indirectly, these modification recruit protein readers that stabilize chromatin and/or provide scaffolds for binding of the transcription, replication or DNA repair machinery (Table 5).

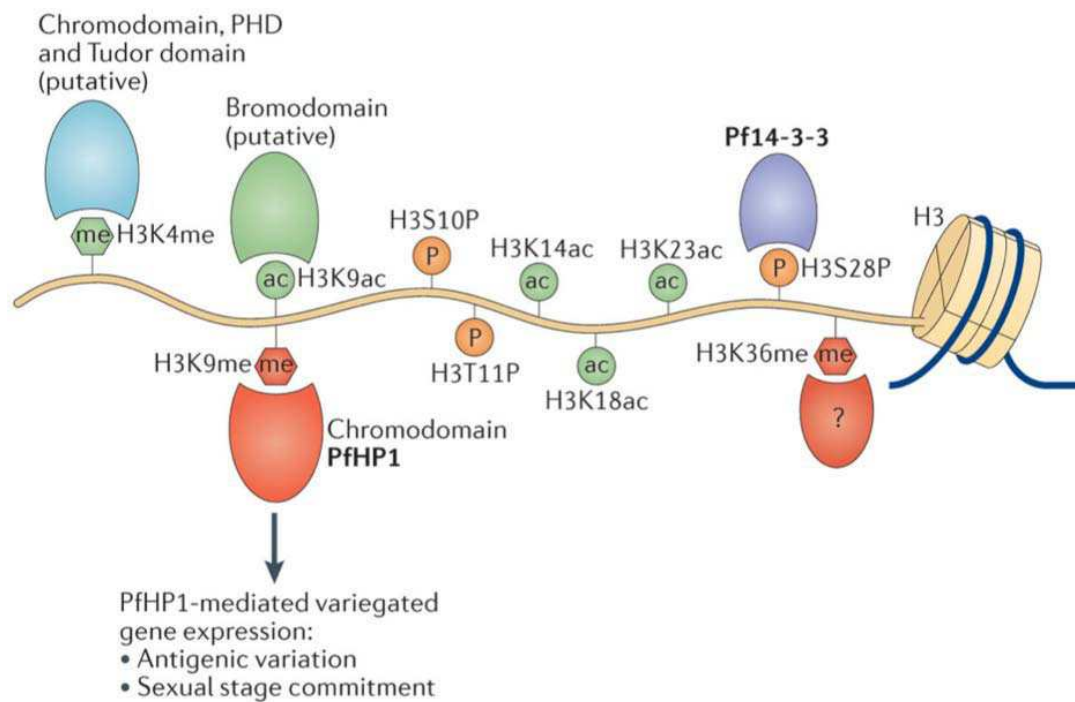


Figure 14: **Histone H3 post-translational modifications.** Post-translational modifications (PTMs) and their writers and readers observed in the amino-terminal region of histone H3 of *Plasmodium falciparum* — including methylation (me; on lysine 4 (K4), K9 and K36), acetylation (ac; on K9, K14, K18 and K23) and phosphorylation (P; on serine 10 (S10), threonine 11 (T11) and S28). Silencing marks are coloured in red, and marks linked to active and poised genes are in green. (Doerig et al., 2015b)

Several PTMs have been detected in the histones of malaria parasites (as described in Section 3, Table 2); however, in most cases, their role in the parasite life cycle is largely unexplored. The PTMs best characterized in *Plasmodium spp.* are acetylation and methylation and to some extent, phosphorylation (Table 2). Reversible protein acetylation and methylation co-regulate many functions. For instance, monocistronic stage-specific transcription is linked to histone methylation and acetylation, whereas clonally variant gene expression, particularly in the case of virulence gene families, correlates with a default silencing mechanism mediated by histone methylation. Moreover, recent proteomic studies showed lysine acetylation of 230 cytoplasmic and nuclear proteins, including protein kinases and histones, in *P. falciparum* blood stages. Nevertheless, given their abundance and essentiality, histones provide the best example to study the biological role for protein acetylation and methylation in *Plasmodium spp.*

#### 4.1.1 Mechanisms of Histone Modifications

The principal modifications of histones can be grouped in different classes; some of their writers are described below.

##### 4.1.1.1 Acetylation

These modifications have been associated mainly with transcriptional activation. The resulting relaxed chromatin facilitates RNA polymerase binding and mRNA transcription. Histone Acetyltransferases (HATs) are the enzymes that add an acetyl group from an acetyl-coA donor onto histone tails. Generally, HATs modify more than one lysine to obtain a cumulative effect, although some HATs can be more specific (Table 4).

##### 4.1.1.2 Deacetylation

The removal of an acetyl group is mediated by histone deacetylases (HDACs). This modification is required when the cell needs to recover the positive charge of lysine to compact chromatin and block transcription. In *P. falciparum*, Sirtuin2 proteins, PfSir2A and PfSir2B, function as histone deacetylases, and associate with telomeres and ~50 kb subtelomeric regions that include *var* genes (Table 4). The knockout of PfSir2A causes de-repression of a subset of *var* genes of the upstream promoter sequence (ups) A and B subtypes (discussed in Section 5), as well as some members of another clonally variant gene family the *rifins* (Merrick and Duraisingh, 2007). Inactivation of PfSir2B results in derepression of the upsC *var* subfamily (Tonkin et al., 2009). The de-repression is likely due to the inability to replace the activation mark (acetylation) with the repressive mark (trimethylation).

##### 4.1.1.3 Lysine methylation

All methylated forms of lysine are cationic at physiological pH. With the addition of methyl groups, the hydrophobicity of the lysine increases, and its capacity to donate hydrogen decreases. Different methylation states confer diverse physicochemical properties to lysine, with diverse readouts mediated by specific effector molecules. Lysine methylation has been associated with both activating and repressing action. In *P. falciparum*, various histone modification (e.g. H3K4me3, H3K9ac) correlate with transcriptional activity, whereas the

generally repressing trimethyl histone H3 lysine 9 (H3K9me3) has been found associated only with clonally variant genes in blood stage parasites and telomeric regions (discussed in Section 5). Importantly, H3K9me3 is not involved in general transcriptional repression in *P. falciparum* as it is in other eukaryotic organisms. Moreover, H3K9me3 and the other modification H3K9me1/me2 regulate the monoallelic expression of the *var* gene family.

The methylation of the histone H3 is mediated by a class of proteins called histone lysine methyltransferase (HKMTs; Table 4); compared to acetyltransferases, these proteins have enormous specificity. The *Plasmodium* genome encodes 10 SET-domain-containing HKMTs: PfSET6 and PfSET10 are predicted to possess H3K4 specificity, while PfSET3 is predicted to possess H3K9-specific methylation activity. The importance of histone methylation in the parasite life cycle has been demonstrated by studies in which the treatment with inhibitors of HKMTs inhibited parasite growth and development (Malmquist et al., 2012). This inhibition of parasite growth was rapid and irreversible. Moreover, the role of HKMTs has been extended to other stages of the *Plasmodium* life cycle. For instance, treatment of quiescent stages with HKMTs inhibitors supports the hypothesis that epigenetic mechanisms may control hypnozoite commitment and/or activation (discussed in Section 4.5 below) (Doerig et al., 2015b).

#### 4.1.1.4 Lysine Demethylation

The *P. falciparum* genome encodes for three histone demethylase orthologues of the lysine-specific demethylase (LSD1) and the Jumonji-C histone demethylase (JHDM) families (Volz et al., 2010) (Table 4). Knockout of PfLSD1 showed a similar phenotype to PfSir2A knockout for *var* gene repression (Comeaux and Duraisingh, unpublished data).

Table 4 : Predicted and verified histone mark writers and eraser in *P. falciparum*

<i>Modification</i>	<i>Gene family</i>	<i>Protein Gene ID</i>	<i>Validated enzymatic activity?</i>	<i>Inhibitor Compound Series</i>
DNA Methylation	m5C Mtase	PfDNMT2 PF3D7_0727300		
Histone Acetylation	GNAT	PfGCN5 PF3D7_0823300	(Fan 2004)	Curcumin (Cui et al., 2007) Anacardic acid (Cui et al., 2008)
	GNAT	PF3D7_0109500		
	GNAT	PF3D7_1437000		
	GNAT	PF3D7_1003300		
	GNAT	PF3D7_1323300		
	GNAT	PF3D7_0805400		
	GNAT-related	PF3D7_1227800		
	MYST	PfMYST PF3D7_1118600		
	MYST	PF3D7_0809500		
	HAT1	PF3D7_0416400		
Histone Deacetylation	Class I	PfHDAC1 PF3D7_0925700	(Patel 2009)	Apicidin (Chaal et al., 2010; Darkin-Rattray et al., 1996)
				Hydroxamates (Andrews et al., 2008; Patel et al., 2009)
	Class II	PfHDAC2 PF3D7_1472200		Apicidin (Chaal et al., 2010; Darkin-Rattray et al., 1996)
				Hydroxamates (Andrews et al., 2008; Patel et al., 2009)
	Class II	PfHDAC3 PF3D7_1008000		FR235222 (in <i>T. gondii</i> ) (Bougdoor et al., 2009)
	Class III	Sir2A PF3D7_1328800	(Merrick and Duraisingh, 2007)	Nicotinamide (Prusty et al., 2008)
				Surfactin

				(Andrews et al., 2012)
	Class III	Sir2B		
		PF3D7_1451400		
Histone lysine Methylation	SET	PfSET1		BIX-01294?
		PF3D7_0629700		(Malmquist et al., 2012)
	SET	PfSET2	(Cui et al., 2008)	
		PF3D7_1322100		
Histone lysine Methylation	SET	PfSET3		
		PF3D7_0827800		
	SET	PfSET4		BIX-01294?
		PF3D7_0910000		(Malmquist et al., 2012)
	SET	PfSET5		
		PF3D7_1214200		
	SET	PfSET6		BIX-01294?
		PF3D7_1355300		(Malmquist et al., 2012)
	SET	PfSET7		
		PF3D7_1115200		
	SET	PfSET8	(Cui et al., 2008)	
		PF3D7_0403900		
	SET	PfSET9		
		PF3D7_0508100		
	SET	PfSET10	(Jennifer C. Volz et al., 2012)	BIX-01294?
		PF3D7_1221000		(Malmquist et al., 2012)
Histone arginine Methylation	Class I	PfRMT1	(Fan et al., 2009)	Sinefungin
	(asymmetric)	PF3D7_1426200		(Fan et al., 2009)
	Putative Class I	PfRMT4/		
	(asymmetric)	PfCARM1		
		PF3D7_0811500		
	Class II	PfRMT5		
	(symetric)	PF3D7_1361000		
Histone Demethylation	LSD	PfLSD1		
		PF3D7_1211600		
	JmJC	PfJmJC1		
		PF3D7_0809900		
	JmJC	PfJmJC2		
		PF3D7_0602800		
Histone Phosphorylation	many potential	many potential		

Table 5: Predicted and verified histone mark readers in *P. falciparum*

<i>Modification</i>	<i>Domain Family</i>	<i>Protein/ Gene ID</i>	<i>Validated binding</i>
Histone Acetylation	Bromodomain	PfGCN5	
		PF3D7_0823300	
		PfSET1	
		PF3D7_0629700	
		PF3D7_0110500	
		PF3D7_1033700	
		PF3D7_1212900	
		PF3D7_1234100	
		PF3D7_1475600	
		Histone Methylation	Chromodomain
PF3D7_1220900			
PfCHD1			
PF3D7_1023900			
PF3D7_1140700			
	Chromodomain-like	PfMYST	
		PF3D7_1118600	
	Tudor domain	PfTSN	
		PF3D7_1136300	
	PhD domain	PfSET1	
		PF3D7_0629700	
		PfSET2	
		PF3D7_1322100	
		PfSET10	
		PF3D7_1221000	
PfLSD1			
PF3D7_1211600			
PfISWI			
PF3D7_0624600			
PF3D7_1433400			
PF3D7_1008100			
PF3D7_1310300			
PF3D7_1475400			
PF3D7_0310200			
PF3D7_1141800			
PF3D7_1360700			
PF3D7_1460100			
Histone Phosphorylation	14-3-3	PF14-3-3I	(Dastidar et al., 2012)
		PF3D7_0818200	
		PF14-3-3II	
		PF3D7_1362100	

#### 4.1.2 *P. falciparum* Heterochromatin Protein 1 (PfHP1) and other histone modifications readers

*P. falciparum* heterochromatin protein 1 (PfHP1) is the first identified *Plasmodium* protein that displays features of histone-mark recognition and translation of the histone code into biological processes in malaria parasites. Analysis of the amino-acid sequence of PfHP1 revealed the presence of the two characteristic HP1 domains: a chromodomain (CD) and a chromo shadow domain (CSD). The CD domain enables PfHP1 to bind specifically to H3K9me2 and H3K9me3 while the function of the CSD domain is to enable protein dimerization (Pérez-Toledo et al., 2009). In *P. falciparum* blood stages, it was shown that PfHP1 is a major component of heterochromatin in perinuclear chromosome clusters. Furthermore, ChIP-on-chip studies showed that PfHP1 localized to subtelomeric regions as well as to silent members of the *var* gene family, and interacts poorly with telomeric repeats. Notably, and as expected, PfHP1 has the same genome-wide distribution as PfH3K9me3, the mark which it recognizes (Flueck et al., 2009a; J.-J. Lopez-Rubio et al., 2009).

In mammals, the HP1 family is composed of three variants ( $\alpha$ ,  $\beta$  and  $\gamma$ ), encoded by three different genes (Jones et al., 2001). These proteins play different roles: HP1  $\alpha$  and  $\beta$  participate in heterochromatin formation, while HP1  $\gamma$  participates in euchromatin formation. The *P. falciparum* genome contains a single *hpl* gene, and the encoded PfHP1 protein is able to dimerize with a potential role in heterochromatin formation and maintenance. Functional analysis of PfHP1 obtained from conditional protein knockdown studies showed that the protein is necessary for the heritable silencing of heterochromatin-associated genes, in particular the maintenance of monoallelic expression of clonally variant genes: 52 out of 60 members of the *var* gene family were upregulated as were several members of the *rif* family (see Section 5 for more details). Moreover, the PfHP1 mutant exhibited an altered G1/S transition phase during mitotic blood stage proliferation and increased sexual commitment (i.e., gametocyte production increased by >25-fold) by regulating the expression of the gametocyte-specific ApiAP2 transcription factor, AP2-G (discussed in Section 4.4) (Brancucci et al., 2014). These data, taken together, highlights the major pathway for epigenetic inheritance in *P. falciparum* that is represented by H3K9me3/PfHP1-dependent gene regulation.

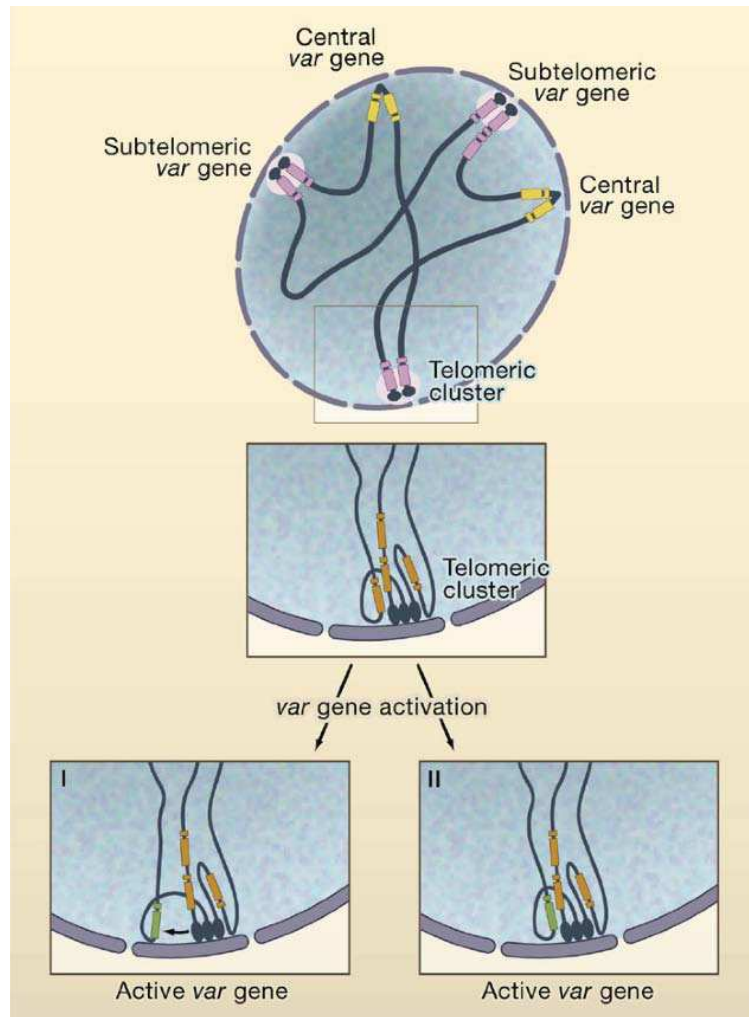
*P. falciparum* has seven predicted bromodomain proteins that can potentially bind to acetylated histones (Josling et al., 2012). Of these, the parasite-specific chromatin association factor, bromodomain protein (PfBDP1), is the only one that is characterized. PfBDP1 directly interacts with histone H3, in particular H3K9ac, as well as a member of the ApiAP2 family and another bromodomain-containing protein (PfBDP2). Studies of PfBDP1 genome-wide occupancy localized it primarily to transcription start sites, consistent with a function in regulating promoter activity and RNA Polymerase II recruitment. PfBDP1 knockdown resulted in growth inhibition, possibly due to the down-regulation of a wide range of invasion related genes in schizonts and a resulting defect in erythrocyte invasion (Josling et al., 2015).

Proteins containing 14-3-3 domains are predicted to bind phosphoserines of histones (Dastidar et al., 2012). Three putative 14-3-3 proteins are predicted in *P. falciparum*, two of which are highly expressed in asexual stages. The alignment of Pf14-3-3I and Pf14-3-3II shows conservation of residues necessary for the interaction with phosphorylated proteins or peptides, as well as the residues responsible for dimerization. Pf14-3-3I preferentially binds to histone H3 phosphorylated on Ser28 *in vitro*, independent of neighbouring modified residues. However, the *in vivo* functions of the Pf14-3-3 proteins are not known.

## 4.2 Nuclear Organization

In addition to a nucleolar compartment, a distinct architectural component of *P. falciparum* nuclei is formed by 4-7 perinuclear telomeric clusters: all *P. falciparum* telomeres and subtelomeric *var* genes cluster at the nuclear periphery by an unknown mechanism. Surprisingly, central chromosomal *var* genes co-localise also to these telomeric clusters (J.-J. Lopez-Rubio et al., 2009; Ralph and Scherf, 2005) (See Section 5 for more details). A repeat region within the intron of central *var* genes appears to recruit episomes to the nuclear periphery (Zhang et al., 2011). This intronic region interacts with a protein complex consisting of actin and a member of the ApiAP2 family. Importantly, the nuclear architecture is a requirement for default silencing of *var* genes (See Section 5 for more details). Indeed antibodies able to recognize silencing marks like H3K9me3 are enriched in the perinuclear telomeric clusters supporting the concept of Perinuclear Repressive Centers (PERCs) (J.-J. Lopez-Rubio et al., 2009) (Figure 15). Moreover, combining RNA-Fluorescence In Situ

Hybridization with DNA-FISH showed that the activation of any *var* gene involves its nuclear repositioning into a peripheral region compatible with transcription, the so-called *var* active site.



site.

Figure 15: **Nuclear architecture of *P. falciparum* ring stages.** Subnuclear localization has been implicated in *var* gene regulation. Silenced subtelomeric and central *var* genes associate with telomeric clusters at the nuclear periphery (Scherf et al., 2008b).

### 4.3 Epigenetic Control of Sexual Commitment

The ApiAP2 transcription factor, AP2-G, was recently described as the master regulator of sexual commitment (Sinha et al., 2014). AP2-G binds to a short eight nucleotide

palindrome sequence located upstream of known gametocyte-specific genes and its disruption leads to loss of mature gametocytes. Intriguingly, AP2-G is subject to epigenetic regulation, possibly in a manner similar to *var* genes (See Section 5 for more details). The presence of H3K9me3 in the promoter and gene body of AP2-G, and subsequent PfHP1 binding, leads to AP2-G repression and low levels of gametocyte production. However, when the epigenetic machinery is dysregulated, as in the case of PfHP1 knockdown, there is AP2-G activation and increased production of gametocytes (Brancucci et al., 2014). In this case, the activation marks H3K9ac and H3K4me3 allow the transcription of AP2-G (Figure 16).

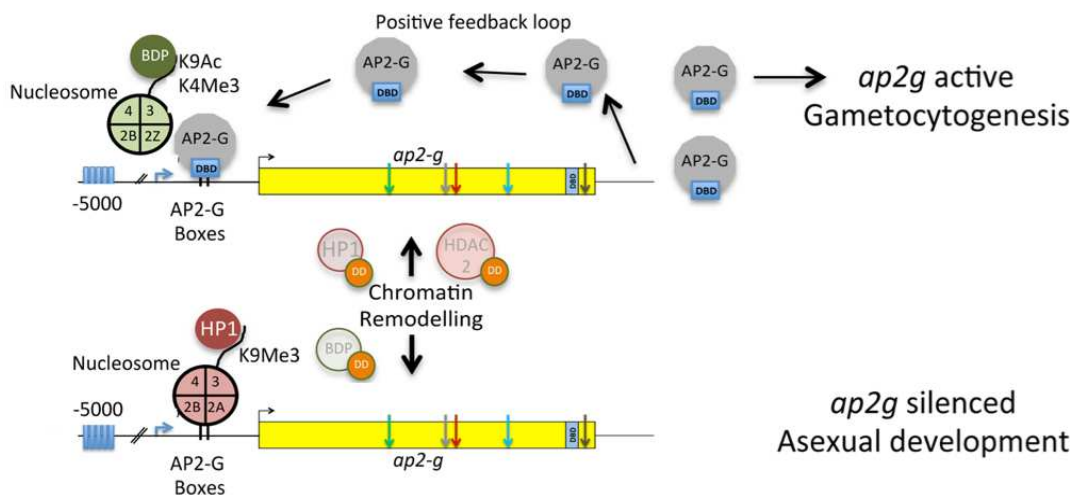


Figure 16: **Model for variegated expression of AP2-G.** The model predicts that the gene is epigenetically silenced by facultative heterochromatin. This state is unstable allowing low frequency activation leading to two distinct activation states of AP2-G in blood stages (Kirchner et al., 2016b).

#### 4.4 Epigenetic Control of Hypnozoites

Recent work using inhibitors of histone methyltransferases in blood stages (Malmquist et al., 2012) showed an effect *in vitro* on dormant liver stages of *P. cynomolgi* (simian model of *P. vivax* for its capacity to form hypnozoites). At specific concentrations, a small molecule inhibitor called BIX-01294 reactivated *P. cynomolgi* hypnozoites, suggesting strongly that histone methylation may control genes involved in the maintenance of dormancy (Dembélé et al., 2014). As observed for clonally variant gene expression during blood stage development and the transcription factor AP2-G that controls sexual commitment, histone PTMs and

epigenetics may be the underlying mechanism to maintain hypnozoite dormancy (Kafsack et al., 2014).

## 5. Biology and Regulation of *P. falciparum* Erythrocyte Membrane Protein 1 (PfEMP1)

The variant surface antigen *P. falciparum* erythrocyte membrane protein 1 (PfEMP1) constitutes a family of high molecular weight (>200 kDa) proteins that are strain-specific and exported by the parasite to the iRBC surface for display within electron-dense surface protrusions called knobs (Figure 17) (Contreras et al., 1988; Langreth et al., 1979; Leech et al., 1984). This protein family is implicated in two main functions that correlate with severity of *P. falciparum* infection. The first is their immunoregulatory activities on host immune cells and the second is their adhesion properties to different host receptors (Howard et al., 1988). Indeed, only ring stage parasites can be detected in the peripheral circulation of infected individuals, because iRBCs older than 18 h are sequestered in the post-capillary venules of various tissues and organs (Miller, 1969). This pathophysiological feature can have important consequences for the outcome of *Plasmodium* infection, especially when sequestration occurs in organs such as the brain or placenta.

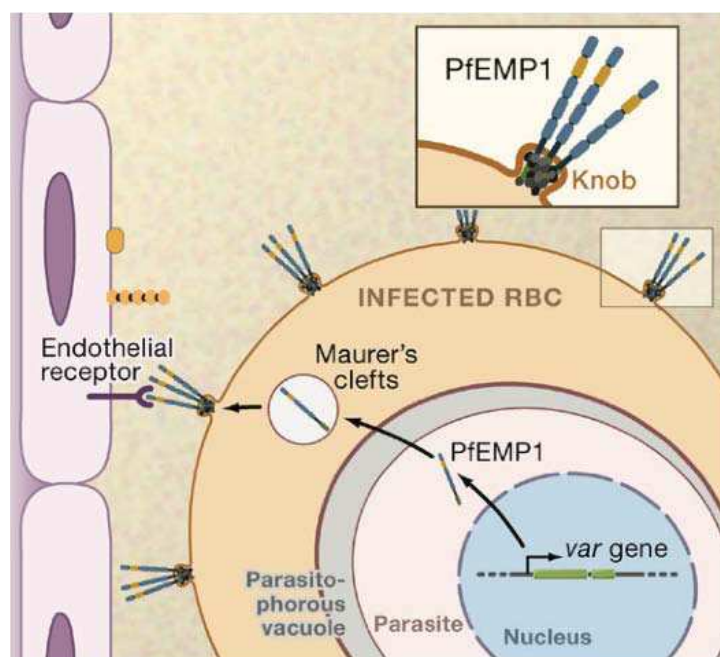


Figure 17. **PfEMP1 trafficking to the surface of IE.** PfEMP1 is exported via vesicle-like structures (Maurer's clefts) to the plasma membrane of the infected red blood cell and associates with a parasite-derived electron-dense protrusion called the knob on the host erythrocyte surface. PfEMP1 mediates adhesion of infected erythrocytes to receptors on endothelial cells and other host cells (Scherf et al., 2008b).

## 5.1 PfEMP1 function

The primary function of PfEMP1 proteins is to mediate iRBC sequestration to the host receptors vascular endothelium (Baruch et al., 1996). This characteristic sets PfEMP1 proteins apart from other variant surface antigen families such as the variant surface glycoproteins or VSGs of trypanosomes whose primary function is to avoid clearance by the humoral immune system and delay the acquisition of protective anti-trypanosome antibodies. Several studies have shown that different PfEMP1 proteins can bind to host receptors such as CD36, TSP, ICAM-1, VCAM-1, E-selectin, CSA, P-selectin,  $\alpha\beta3$  and PECAM-1/CD31. The best studied are the binding to CD36, which is implicated in IE adhesion associated with uncomplicated malaria, binding to ICAM-1 (CD54), which is implicated in cerebral malaria, and the binding of a specific PfEMP1 var2CSA to chondroitin sulphate A (CSA; discussed below), which is implicated in pregnancy-associated malaria (Salanti et al., 2004, 2003).

PfEMP1 proteins are also implicated in rosette formation, i.e., the binding of multiple uninfected erythrocytes to an iRBC; this is another adhesion phenotype that involves the semi-conserved N-terminal head structure of PfEMP1 and carbohydrates on the erythrocyte surface (Chen et al., 2000, 1998; Rowe et al., 1997). While rosetting is PfEMP1-dependent in *P. falciparum*, other *Plasmodium spp.*, in particular *P. vivax*, also exhibit this phenomenon, in a non-EMP1 dependent manner. *P. falciparum* rosettes have been associated with severe disease and studies have shown that the treatment with rosetting inhibitory antibodies can prevent severe malaria (Carlson et al., 1990; Kun et al., 1998; Rowe et al., 1995; Treutiger et al., 1992). More recently two other surface proteins of the clonally variant Rifin and Stevor families were shown to be involved in rosette formation (Goel et al., 2015; Niang et al., 2014).

## 5.2 PfEMP1/var gene organization and structure

PfEMP1 proteins are encoded by the *var* multigene family (Baruch et al., 1995; Smith et al., 1995; Su et al., 1995)(Baruch et al 1995, Smith et al 1995, Su et al 1995), whose expression is modulated by a sophisticated system of mutual exclusiveness, so-called monoallelic expression to bring about clonal antigenic variation. In the haploid *P. falciparum*

genome there are around 60 *var* genes distributed either in sub-telomeric clusters of chromosomes 1-13 or within internal clusters of chromosomes 4, 7, 8 and 12 (Figure 18). A total of 36 *var* genes are located in subtelomeric regions and the remaining 24 *var* genes are clustered in central regions as 5 tandem arrays of three to seven *var* genes distributed over 4 chromosomes. Each chromosome subtelomeric region contains one to three *var* genes followed by groups of *rif*, *stevor* and other gene families, primarily encoding exported proteins.

The *var* genes can be divided into five distinct groups based on the 5' promoter regions (i.e., Upstream promoter sequence or Ups): UpsA, UpsB, UpsC, UpsD and UpsE. They can be further divided into three groups in function of their chromosome position: UpsD and UpsC are located centrally in the chromosomes, UpsB are either central or subtelomeric arranged in tandem with other UpsB or UpsC and transcribed away from the telomere, whereas UpsA and UpsE are subtelomeric and are transcribed towards the telomere in a direction opposite to UpsB *var*. The *var* open reading frame is between 6 and 13 kb long and contains two exons (Figure 18). Exon 1 encodes for the N-terminal extracellular part of the protein and exon 2 encodes for a short trans-membrane domain and the intracellular C-terminal segment (acidic terminal domain or ATS), that anchors PfEMP1 at knobs (Figure 17) (Su et al., 1995).

PfEMP1 are modular proteins: the amino acid sequence encoded by exon 1 can be divided into Duffy-binding-like (DBL) domains, varying from 2-10 per PfEMP1 molecule, and cysteine-rich interdomain regions (CIDR) (Baruch et al., 1997). The DBL domains are further classified into three structural subdomains: those with a mixed helix-sheet structure (S1) or those composed of distinct helix bundles (S2 and S3). All PfEMP1 subfamilies except for var2CSA have a N-terminal head structure composed of a semi-conserved DBL $\alpha$  domain and a CIDR domain (Gardner et al., 2002a). The head structure is followed by a second, and different, DBL-CIDR pair in most PfEMP1 proteins.

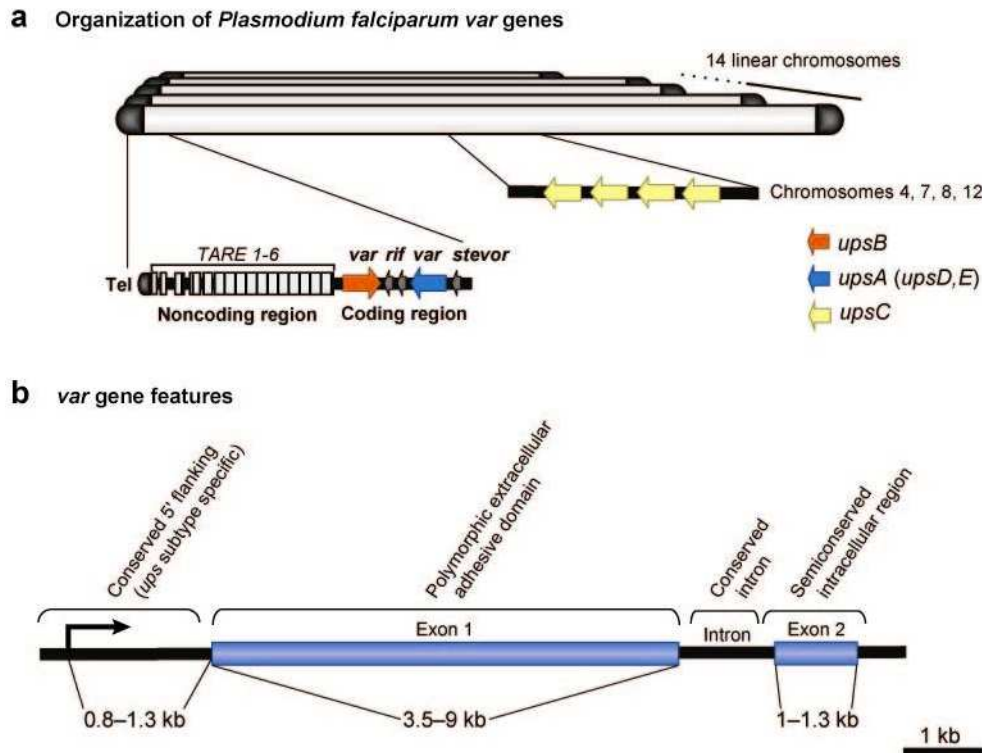


Figure 18 : **Genomic organization and nuclear position of var genes.** (a) Subtelomeric regions of all 14 linear chromosomes have noncoding repeats of variable size (*TARE 1–6*) (telomere-associated repeat elements) located next to telomere repeats (b) Common features of the *var* gene family (Scherf et al., 2008a).

Crystal structures of single CIDR $\alpha$  and DBL domains have shown that the extracellular part of PfEMP1 proteins is composed of  $\alpha$ -helical bundles connected by flexible and highly variable loops. This is the scaffold on which sequence variation takes place. In the absence of a full-length crystal structure, X-ray spectroscopy analysis of full-length recombinant PfEMP1 shows an elongated and zigzag-shaped rigid molecule with a length of approximately 20-30 nm. In contrast, the full-length extracellular domain of var2CSA adopts a more compact globular shape, likely mediated by tighter inter-domain interactions. This high-order structure of the proteins should facilitate their interaction with their cognate receptor.

### 5.3 Classification of adhesive domains in PfEMP1

It is now well established that the CIDR and DBL domains of PfEMP1 possess adhesive properties. The CIDR domain binds to CD36 whereas DBL domains interact with ICAM-1, CSA and CR1. The CIDR domains are divided based on their sequence into three

groups ( $\alpha$ ,  $\beta$  and  $\gamma$ ) and the DBL domains into five groups ( $\alpha$ ,  $\beta$ ,  $\gamma$ ,  $\delta$  and  $\epsilon$ ); sequence classification of DBL and CIDR domains can be predictive of binding properties (Figure). Along the PfEMP1 proteins the number of DBL and CIDR domains is variable, but the domain architecture is not random, with preferential tandem domain associations such as DBL $\alpha$ CIDR $\alpha$ , DBL $\delta$ CIDR $\beta$  and DBL $\beta$ C2, etc. These associations have a functional significance for PfEMP1 folding, transport and/or binding activity. Notably, the binding phenotype determines tissue tropism, which contributes to parasite survival, transmission and disease outcome.

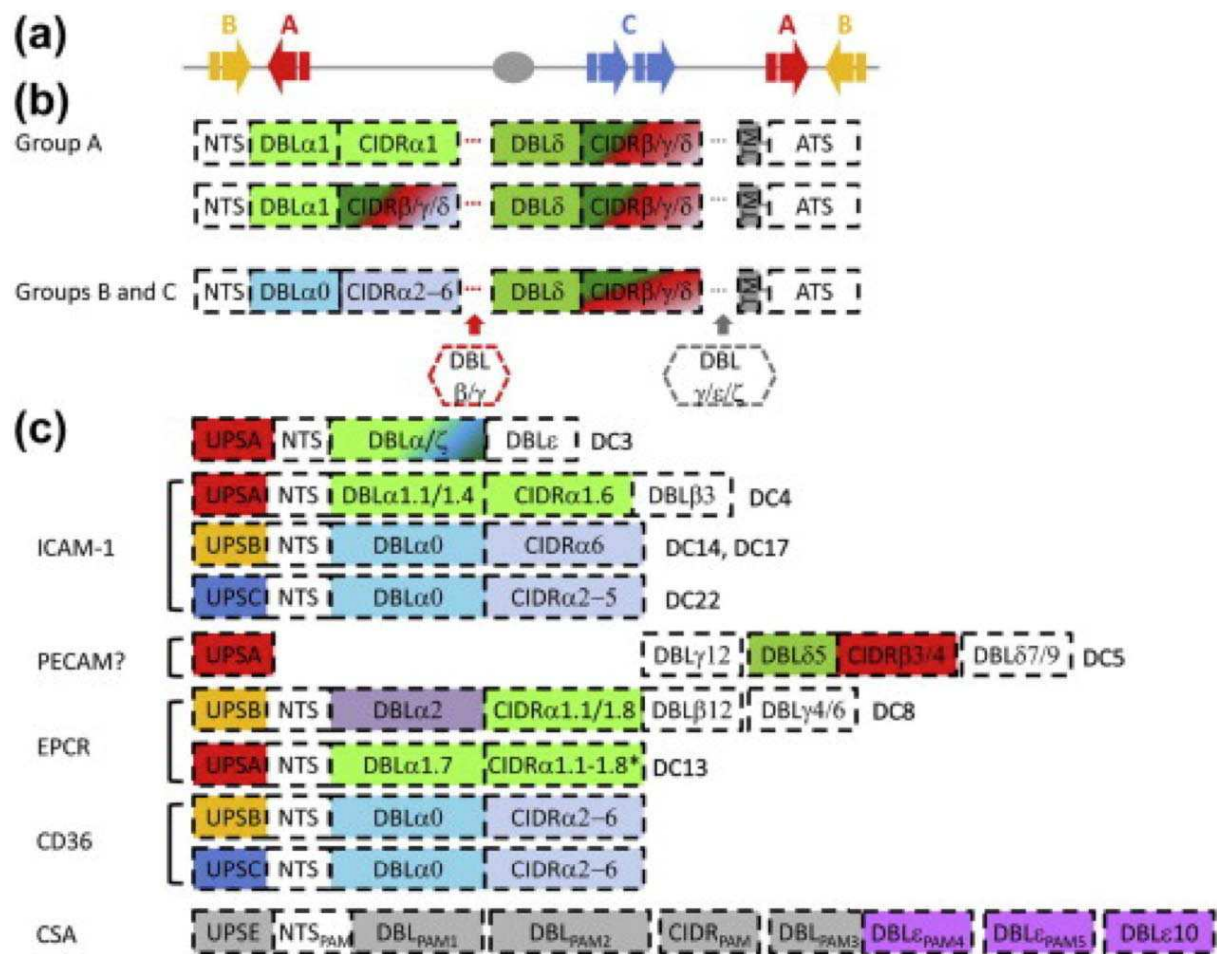


Figure 19 : **Chromosomal organization of *Plasmodium falciparum* var genes and *P. falciparum* erythrocyte membrane protein 1 (PfEMP1) domain architecture.** (a) Subtelomeric location of Group A and B var genes in all chromosomes, with transcription in opposite directions. Group C var genes are found in central chromosomal regions. (b) Different PfEMP1 domains, Duffy-binding-like (DBL) and cysteine-rich interdomain region (CIDR) domains. PfEMP1 groups B and C predominantly have a four-domain structure, whereas mainly Group A have additional DBL. (c) Tandem domain arrangements are linked to different known adhesion phenotypes. (Hviid and Jensen, 2015)

### 5.3.1 Type 3 PfEMP1

This subfamily of PfEMP1 proteins is composed of the smallest proteins, which contain only two extracellular domains, an N-terminal DBL $\alpha$ /DBL $\xi$  domain and a C-terminal DBL $\epsilon$  domain (Gardner et al., 2002b). The DBL $\xi$  - DBL $\epsilon$  sequence together forms the DC3 domain that is characteristic of this subfamily. The function and the receptor specificity of this family remain unknown and field studies showed that only a minority of *P. falciparum*-exposed individuals express this group of PfEMP1.

### 5.3.2 DC4-Type PfEMP1

This subfamily of PfEMP1 is characterized by the DC4 cassette, which is composed of three domains (DBL $\alpha$ /CIDR $\alpha$ /DBL $\beta$ ) and a CIDR $\alpha$  domain similar to the endothelial protein C receptor (EPCR). This PfEMP1 group mediates binding to ICAM-1 (CD54), but not to thrombospondin receptor CD36, and is associated with uncomplicated malaria (Bengtsson et al., 2013). However, it was shown that transcription of *var* genes encoding for DC4 PfEMP1 is higher in patients with cerebral malaria than in patients with severe disease, suggesting that DC4 may mediate iRBC adhesion in the pathogenesis of cerebral malaria (Lavstsen et al., 2012).

### 5.3.3 DC5-Type PfEMP1

The DC5 cassette is composed of a DBL $\gamma$ /DBL $\delta$ /CIDR $\beta$ /DBL $\beta$  structure (Rask et al., 2010). This subfamily is expressed in children with severe malaria and exhibits adhesion properties towards PECAM-1 (CD31), which is expressed by endothelial cells, monocytes, platelets and granulocytes (Baruch et al., 1996).

### 5.3.4 DC8- and DC13-Type PfEMP1

DC8 is constituted of four domains (DBL $\alpha$ /CIDR $\alpha$ /DBL $\beta$ /DBL $\gamma$ ) and DC13 contains two domains (DBL $\alpha$ /CIDR $\alpha$ ). These two subfamilies are the most prevalent in individuals infected by *P. falciparum* and bind to the endothelial protein C receptor (EPCR) (Turner et al., 2013), a transmembrane glycoprotein homologous to CD1/major histocompatibility complex molecules that is expressed on several cell types including the endothelium of many tissues.

### 5.3.5 var2CSA-Type PfEMP1

The var2CSA subfamily is composed of PfEMP1s that possess seven unusually structured extracellular domains that occur in tandem. These include three N-terminal DBL<sub>PAM</sub> domains followed by three DBL<sub>ε</sub> domains with a CIDR<sub>PAM</sub> between the second and the third DBL<sub>PAM</sub> domain. The var2CSA-type PfEMP1 proteins lack the typical N-terminal head structure present in all the other PfEMP1s and bind to chondroitin sulphate A (CSA) (Salanti et al., 2004, 2003), playing a central role in the pathogenesis of placental malaria (Fried and Duffy, 1996). The tropism of CSA-adhering iRBCs for the placenta is related to the particular sulphation pattern of CSA in the intervillous space (PfEMP1 review) and its high density (Rieger et al., 2015).

## 5.4 var gene Transcription and its Regulation

*var* genes encoding *P. falciparum* erythrocyte membrane protein 1 (PfEMP1), are part of the three multigene families identified in *P. falciparum* that undergo antigenic variation; the two other families are *rif* encoding the Rifin proteins and the *stevor* (Subtelomeric Variant Open Reading Frame) genes encoding the Stevor proteins. Amongst these, *var* gene regulation is the best studied. *var* gene transcription is strictly regulated by a process called monoallelic expression, wherein in any given cell, a single *var* gene is transcribed in ring stages with the other 59 *var* genes maintained in a transcriptionally silent state. Multiple layers of epigenetic and genetic regulation mediate silencing, activation and poising of the single *var* gene and potentially allowing switching to a different *var* gene. The first evidence for epigenetic regulation came from knockout studies of the histone deacetylase PfSir2, which resulted in the de-repression of several *var* genes (Freitas-Junior et al., 2005). Subsequent analyses of the distribution of histone PTMs – activating marks such as H3K9Ac and H3K4me2/3 and repressive marks such as H3K9me3 – strongly indicated that the promoters and exon 1 of the active *var* gene is associated with H3K9Ac and to a lesser extent H3K4me2/3, while the same regions of the silent *var* genes were enriched for H3K9me3, (J.-J. Lopez-Rubio et al., 2009; Lopez-Rubio et al., 2007). Moreover, in mature stages, when *var* transcription is absent, the active *var* continues to be depleted for the repressive marks; instead, it is now enriched for H3K4me3 relative to H3K9Ac (Figure 20). Whether the same mechanism applies to the *rif* and *stevor* genes is still not fully established.

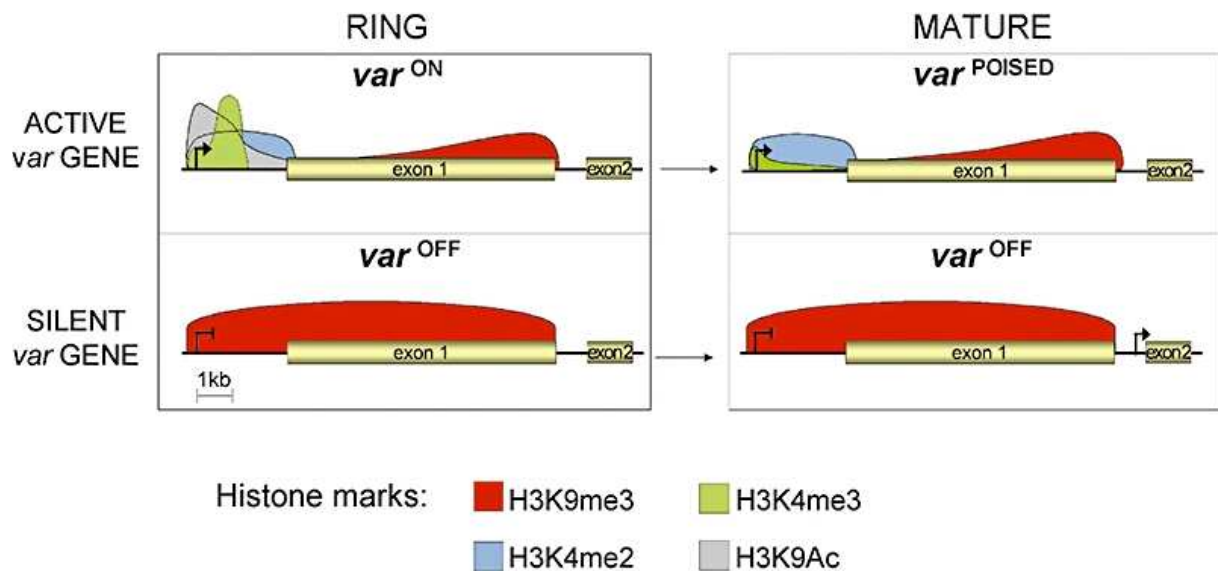


Figure 20 : **Schematic presentation of histone H3 silent or active marks.** The repressive H3K9me3 in *var2csa* activation is dynamically removed in the transcription start site upon gene activation and is restored upon repression. Histone H3K4me3 and H3K9ac are linked to active *var* genes peak in chromatin associated with 5' flanking *var* region. (Lopez-Rubio et al., 2007)

Furthermore, genome wide occupancy studies of the H3K9me3 reader PfHP1 demonstrated that this protein plays an essential role in establishing the default-silencing pathway for *var* genes. PfHP1 establishes facultative heterochromatin at silent *var* loci by binding to H3K9me3 and as discussed in Section 4, depletion of PfHP1 disrupts this heterochromatin structure, thereby allowing the transcription of several *var* genes simultaneously. However, several points of *var* epigenetic regulation are not well-understood: the histone methyltransferase responsible for laying the h3K9me3 mark, the mechanism by which PfHP1 boundaries are regulated, the machinery that allows for *var* gene switching, etc.

Besides epigenetic factors, nuclear spatial organization and genetic elements also play a role in *var* monoallelic expression. With regards to the former, it was observed that while all silent *var* genes localize to telomeric clusters or PERCs (see Section 4), the active *var* gene occupies a position within the nuclear periphery that is adjacent to but distinct from the PERCs (Figure 15) With regards to the latter, studies of the promoter region of different *var* sub-types indicated the presence of one or more essential motifs that regulate monoallelic expression. Moreover, the intron appears to mediate *var* silencing, possibly via transcription

of the bidirectional promoter that is present in select introns and the resulting non-coding intronic RNAs (Amit-Avraham et al., 2015; Vembar et al., 2014). Exonucleases also showed activity in controlling transcription of multiple *var* gene by mediating the degradation of nascent *var* transcripts, so-called cryptic RNAs (Zhang et al., 2014). Recent studies shed light on the role of non-coding RNAs of the 15-member RNA of Unknown function 6 (RUF-6) family in *P. falciparum*, which encodes non-coding RNAs with high GC-content (GC-rich ncRNA or GC-elements), on *var* gene activation. The GC-rich ncRNA localized to the *var* expression site in the nucleus in *trans* and notably, the overexpression of distinct GC-rich elements resulted in activation of specific subsets of *var* genes (Guizetti et al., 2016). Overall, *var* gene regulation involves multiple layers, and many questions still remain unanswered.



## OBJECTIVES

Epigenetic regulation has been recognized to play a central role in gene expression in *P. falciparum*. It lies at the heart of gene expression in *P. falciparum* blood stages: by regulating access of the transcriptional machinery to chromatin via post-translational modifications (PTMs) of histones, nucleosome occupancy and global architecture, epigenetic mechanisms orchestrate monoallelic expression of the clonally variant gene families responsible for the major virulence properties of *P. falciparum*. In addition, recent studies showed that small molecule inhibitors of histone modifying enzymes not only kill all parasite stages, but also reactivate hypnozoites, the liver quiescent forms, of *P. cynomolgi* (a simian model of *P. vivax*). These results strongly suggest that the epigenetic machinery is conserved in all stages of the *Plasmodium* life cycle and can be exploited to accomplish unique, thus far unknown, functions in pre-erythrocytic stages.

**The objective of this thesis is to systematically analyze the major repressive machinery composed of histone H3K9me3 and HP1 in pre-erythrocytic stages of malaria parasites.**

To answer to this question, I first characterize the distribution of the epigenetic mark H3K9me3, and its potential writers and readers, in sporozoites and liver stage schizonts of *P. falciparum* and *P. ovale*. I then focus on the role of H3K9me3 and its reader in *P. falciparum* sporozoite biology.

### **Distribution of H3K9me3/PfHP1 distribution in pre-erythrocytic stages**

Working with a humanized mouse malaria model, I analyzed the presence of histone H3K9me3 and HP1 in sporozoites and liver stage schizonts obtained from *P. falciparum* and *P. ovale* infection (**Article 1**); I then analyzed the distribution of two potential histone H3K9me3 writers, the histone methyltransferases PfSET6 and PfSET7, in *P. falciparum* pre-erythrocytic stages (**Article 2 and Article 3**);

### **Epigenetic regulation of gene expression in *P. falciparum* sporozoites**

To better characterize the role of H3K9me3/PfHP1 in *P. falciparum* pre-erythrocytic stages, I performed an epigenomic analysis of sporozoites and analyzed the genome-wide distribution of histone H3K9me3, PfHP1 and the activating histone modification, H3K9Ac (**Article 4**).



# RESULTS



## ARTICLE 1

### ***Plasmodium falciparum* full life cycle and *Plasmodium ovale* liver stages in humanized mice**

Soulard, Bosson-Vanga, Lorthiois, Roucher, Franetich, **Zanghì**, et al, **Nature Communications, 2015**

The liver stage is an intriguing phase of the *Plasmodium* life cycle and given its low parasite load, it is an ideal target for elimination. Unfortunately, human *Plasmodium spp.* present strict host cell specificity and hence, *in vivo* models for liver stage development are limited. So far, *P. falciparum*, *P. vivax* and *P. ovale* liver stages have been studied using *in vitro* primary cell culture or in select cases in primates *in vivo*. Recently, immunodeficient mice simultaneously engrafted with human hepatocytes and human red blood cells have been generated, so-called humanized mice. In this study, we used these mice to study *P. falciparum* infection and found that the parasites completed the mammalian life cycle, from sporozoite inoculation to gametocyte production and mosquito transmission. Moreover, the humanized mice sustain the maturation of *P. ovale* in the liver with the appearance of hypnozoites and evidence of delayed schizogony. This study indicated that a humanized model can be used to study *Plasmodium* liver stage biology and immunology, with a specific focus on hypnozoite commitment, maintenance and activation.

**My contribution to this work involved sporozoite production starting with clinical isolates of *P. ovale* obtained from hospitalized patients. I used infected patient blood to transmit the parasite to the mosquitoes and reared the mosquitoes in the insectarium to produce mature sporozoites. Moreover, I performed immunofluorescence assays performed to characterize liver stage development of *P. falciparum* and *P. ovale* parasites and analyzed HP1 distribution in these stages. Of note, the anti-PfHP1 antibodies efficiently recognize the *P. ovale* HP1 protein, providing a tool to study *P. ovale* hypnozoites.**



ARTICLE

Received 12 Nov 2014 | Accepted 29 May 2015 | Published 24 Jul 2015

DOI: 10.1038/ncomms8690

OPEN

# *Plasmodium falciparum* full life cycle and *Plasmodium ovale* liver stages in humanized mice

Valérie Soulard<sup>1,2,3</sup>, Henriette Bosson-Vanga<sup>1,2,3,4,\*</sup>, Audrey Lorthiois<sup>1,2,3,\*†</sup>, Clémentine Roucher<sup>1,2,3</sup>, Jean- François Franetich<sup>1,2,3</sup>, Gigliola Zanghi<sup>1,2,3</sup>, Mallaury Bordessoulles<sup>1,2,3</sup>, Maurel Tefit<sup>1,2,3</sup>, Marc Thellier<sup>5</sup>, Serban Morosan<sup>6</sup>, Gilles Le Naour<sup>7</sup>, Frédérique Capron<sup>7</sup>, Hiroshi Suemizu<sup>8</sup>, Georges Snounou<sup>1,2,3</sup>, Alicia Moreno-Sabater<sup>1,2,3,\*</sup> & Dominique Mazier<sup>1,2,3,5,\*</sup>

Experimental studies of *Plasmodium* parasites that infect humans are restricted by their host specificity. Humanized mice offer a means to overcome this and further provide the opportunity to observe the parasites *in vivo*. Here we improve on previous protocols to achieve efficient double engraftment of TK-NOG mice by human primary hepatocytes and red blood cells. Thus, we obtain the complete hepatic development of *P. falciparum*, the transition to the erythrocytic stages, their subsequent multiplication, and the appearance of mature gametocytes over an extended period of observation. Furthermore, using sporozoites derived from two *P. ovale*-infected patients, we show that human hepatocytes engrafted in TK-NOG mice sustain maturation of the liver stages, and the presence of late-developing schizonts indicate the eventual activation of quiescent parasites. Thus, TK-NOG mice are highly suited for *in vivo* observations on the *Plasmodium* species of humans.

<sup>1</sup>Sorbonne Universités, UPMC Univ Paris 06, CR7, Centre d'Immunologie et des Maladies Infectieuses (CIMI-Paris), 91 Bd de l'hôpital, F-75013 Paris, France. <sup>2</sup>INSERM, U1135, CIMI-PARIS, 91 Bd de l'hôpital, F-75013 Paris, France. <sup>3</sup>CNRS, ERL 8255, CIMI-PARIS, 91 Bd de l'hôpital, F-75013 Paris, France. <sup>4</sup>Université FHB, UFR SPB, Département de Parasitologie-Mycologie, BP V 34 Abidjan, Ivory Coast. <sup>5</sup>AP-HP, Groupe Hospitalier Pitié-Salpêtrière, Service Parasitologie-Mycologie, Centre National de Référence du Paludisme, 83 Bd de l'hôpital, F-75013 Paris, France. <sup>6</sup>UPMC Univ. Paris 06, INSERM, UMS28, 105 Bd de l'hôpital, F-75013 Paris, France. <sup>7</sup>AP-HP, UPMC Univ. Paris 06, Groupe Hospitalier Pitié-Salpêtrière, Service d'anatomie et cytologie pathologiques, 83 Bd de l'hôpital, F-75013 Paris, France. <sup>8</sup>Central Institute for Experimental Animal, Kawasaki, Kanegawa, Japan. \* These authors contributed equally to this work. † Present address: INSERM U1016, CNRS UMRS 8104, Institut Cochin, F-75014 Paris, France. Correspondence and requests for materials should be addressed to V.S. (email: valerie.soulard@upmc.fr).

Malaria remains a major cause of death and morbidity worldwide<sup>1</sup>, with infections by *Plasmodium falciparum* accounting for the majority of malaria mortality, though the less virulent *P. vivax*, and probably *P. ovale*, also contribute significantly to morbidity.

*Plasmodium* sporozoites injected by an infected mosquito migrate to the liver and initiate the hepatic stage of the parasite life cycle by invading hepatocytes within which they multiply and differentiate into schizonts containing thousands of hepatic merozoites. These merozoites are subsequently released into the blood where they initiate the erythrocytic stage by invading and replicating within red blood cells (RBCs). Some of these asexual blood parasites differentiate into gametocytes that will ensure parasite transmission to the mosquito vector. *P. vivax* and *P. ovale* show a slightly different life cycle within the mammalian host, as some sporozoites once in the liver do not develop immediately into schizonts, but remain at an uninucleate stage, in a quiescent form named hypnozoite, before resuming hepatic development on the impulse of still unknown factors, causing relapses weeks, months or even years after the primary infection<sup>2</sup>.

The search for novel or improved means to control malaria, whether chemotherapeutic or immunoprophylactic, is dependent on the availability of practical experimental models for preclinical investigations. Investigations on the parasite species that infect humans are hampered by the strict specificity to the host's cells. *In vivo* models have been limited to infections of selected species of South American primates, that are now increasingly restricted by ethical and cost considerations. At present, routine *in vitro* cultivation is only available for the blood stages of *P. falciparum*, and that of the liver stages of this parasite is best obtained using primary human hepatocytes alone or in coculture<sup>3–5</sup>, though hepatic development in HCO4 cell lines has been reported albeit with much lower levels of infection<sup>6,7</sup>. Cultivation of the *P. vivax* liver stages is equally well sustained when human primary hepatocytes or a HepG2 cell line are used<sup>8,9</sup>.

In general, *Plasmodium* hepatic stage cultures are limited to 5–10 days of cultivation, though recent advances have extended this to a month or so<sup>3,4</sup>. Consequently, our knowledge of the biology and immunology of the malarial liver stages is limited and fragmentary, and is minimal for the hypnozoites. The major interest in these hepatic forms is that they represent the initial obligatory phase of the life cycle of *Plasmodium* in the human host. During this pre-erythrocytic phase the parasites are present in very low numbers and generally develop over a short period (5–14 days). This makes them an ideal target for parasite elimination<sup>10</sup>.

Immunodeficient mice engrafted with human cells, offer a cost-effective and easily manipulated laboratory model to study human-restricted pathogens *in vivo*<sup>11</sup>. To date, such mice engrafted with human hepatocytes (hHEP) or human RBCs (hRBC) have been shown to sustain *P. falciparum* hepatic development and the multiplication of the blood stages<sup>12–17</sup>. Efficient liver humanization relies simultaneously on an immunodeficiency in the host to facilitate xenotransplantation and on the selective elimination of endogenous murine hepatocytes to make room for the transplanted human hepatocytes to repopulate the liver. In this manner, *P. falciparum* liver stage maturation was first observed in homozygous Alb-UpA SCID mice<sup>13,14</sup>, where expression of the hepatotoxic urokinase plasminogen activator (UpA) transgene under the albumin promoter leads to a constitutive loss of endogenous hepatocytes. Thus, UpA-SCID mice are best engrafted at very young age (3–4 weeks) but given their low level of immunodeficiency additional treatment to deplete NK

cells and macrophages is required<sup>13</sup>. Recently, mice deficient for fumarylacetoacetate hydrolase (FAH<sup>-/-</sup>) with the broader immunodeficient Rag2<sup>-/-</sup> IL2Rγ<sup>-/-</sup> background (FRG) were also used for liver humanization<sup>18</sup>. The FAH<sup>-/-</sup> mice suffer from an acute liver failure that can be rescued by providing NTBC (2-(2-nitro-4-trifluoromethylbenzoyl)-1,3-cyclohexanedione) at regular intervals pre- and post-human hepatocytes transplantation. The FRG mice backcrossed onto the NOD background (FRG NOD) allowed full maturation of the *P. falciparum* liver stages up to the generation of infectious hepatic merozoites<sup>19</sup>. Here we have used TK-NOG mice that express the HSVtk transgene under the albumin promoter onto the NOD SCID IL2Rγ<sup>-/-</sup> background<sup>20</sup>. In this mouse strain, the loss of endogenous hepatocytes is inducible by a brief exposure to a non-toxic dose of gancyclovir, a method that is rapid and temporally restricted, and routinely leads to substantial hHEP repopulation (60–80%). These levels are comparable to those obtained in UpA-SCID and FRG mice<sup>13,14,19</sup>, and more importantly, they are maintained without the need for any additional treatment. Furthermore, similarly to FRG NOD mice, carriage of the SIRPα gene NOD allele prevents recognition of CD47 on the transplanted human cells, which highly facilitates engraftment with hRBC<sup>21</sup>.

The aim of our studies was to exploit the TK-NOG mice to obtain animals simultaneously engrafted with hHEP and hRBC, and to ascertain whether they could then sustain the full *P. falciparum* life cycle, from sporozoite inoculation to gametocyte production. During the course of the study, we also had the opportunity to infect the mice with *P. ovale* sporozoites and to follow-up the infection for a sufficiently long period to suggest the presence of hypnozoites.

## Results

***P. falciparum* hepatic development in TK-NOG mice.** Liver-humanized (LH) TK-NOG mice were inoculated with 1–3 million *P. falciparum* sporozoites, killed at different time points thereafter, and their livers were analysed for the presence of parasites by immunofluorescent staining of *Plasmodium* HSP70 (Fig. 1a). Human albumin (hAlb) plasma levels on the day of sporozoites inoculation varied between the mice (2–10 mg ml<sup>-1</sup>). In the mice where hAlb levels were approximately 5 mg ml<sup>-1</sup> (liver humanization ≥ 60%, *n* = 2) around 20 parasite forms could be observed in each 40–45 mm<sup>2</sup> liver section obtained on day 7 after inoculation with 3 million *P. falciparum* sporozoites (Supplementary Fig. 1a–b).

Hepatic schizonts were observed in liver sections made on day 5 and day 7 post-infection (Fig. 1a), with clearly individualized merozoites distinguishable in the mature day-7 schizonts. The diameter of the maturing liver forms ranged from 30.5 to 59.72 μm (*n* = 32, mean ± s.d. = 44.38 ± 8.09 μm) for the day 5 parasites, and from 60.2 to 105 μm (*n* = 27, mean ± s.d. = 80.73 ± 11.87 μm) for the day 7 parasites (Fig. 1b). These values are the double of those usually observed at equivalent time points in *in vitro*-cultured *P. falciparum*-infected primary human hepatocytes<sup>5,22</sup>. The parasites' mean area increased from 1203 ± 461 μm<sup>2</sup> on day 5 to 4165 ± 1370 μm<sup>2</sup> on day 7. We also confirmed that the parasites developed exclusively in the engrafted hHEP stained for hAlb (Supplementary Fig. 2). It was interesting to note that by contrast to *in vitro* observations of *P. falciparum* in primary human hepatocytes cultures<sup>23</sup>, uninucleate forms were not observed in the liver sections analysed.

To facilitate future investigations, we set up a medium throughput analysis using a fluorescent slide scanner (Nanozoomer) to screen liver sections. Identification, measurement and

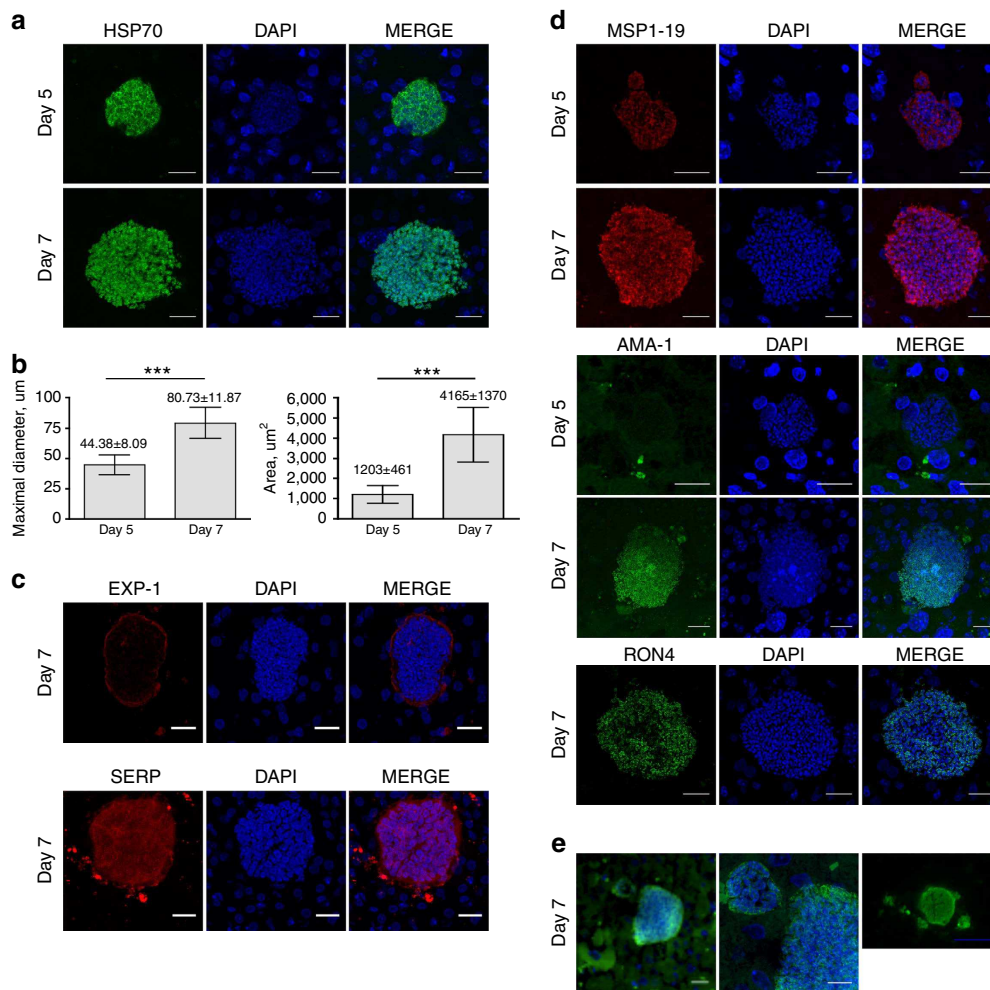


**Figure 1 | Hepatic development of *P. falciparum* in LH TK-NOG mice.** Representative pictures of *P. falciparum* schizonts at days 5 and 7 post-infection. Sixteen- $\mu\text{m}$  thick frozen and 5- $\mu\text{m}$  thick deparaffinized liver sections were stained by indirect immunofluorescence with antibodies specific to *P. falciparum* and DAPI to stain host cell and parasite nuclei. **(a)** Day-5 and day-7 schizonts stained for *Plasmodium* HSP70, scale bar, 20  $\mu\text{m}$ . **(b)** Maximal diameter and area of day-5 and day-7 schizonts;  $n = 32$  at day 5 and  $n = 27$  at day 7, both from 3 different lobes, mean  $\pm$  s.d. \*\*\* $P < 0.0001$ , Mann-Whitney *U*-test. **(c)** Day-7 schizonts stained for EXP-1 and SERP. **(d)** Schizonts were stained for MSP-1, AMA-1 and RON-4 at day 5 and day 7. Scale bar, 20  $\mu\text{m}$ . **(e)** Merosome-like structures stained for HSP70 and DAPI observed in day-7 schizonts, left picture, Scale bar, 20  $\mu\text{m}$ ; central picture, magnification of left picture showing merozoites nuclei in the merosome-like structure, Scale bar, 10  $\mu\text{m}$ ; right picture, Scale bar, 50  $\mu\text{m}$ .

quantification of day 7 *P. falciparum* schizonts were thereby rapid and accurate (Supplementary Fig. 1a,b).

Maturation of the liver forms was assessed by a panel of antibodies raised against different parasite proteins expressed at different stages of development. Day-7 schizonts in sections stained for *P. falciparum* Exported Protein-1 (*Pf*EXP-1, ref. 24), a mid to late liver stage antigen, showed circumferential staining consistent with its expected localization at the parasitophorous vacuole membrane (Fig. 1c, upper panel). We also noted that the serine-rich protein (SERP, ref. 25), a soluble protein secreted in the lumen of the parasitophorous vacuole in blood-stage parasites<sup>26</sup>, was also found in the parasitophorous vacuole of the day-7 hepatic parasites (Fig. 1c, lower panel). Day-5 hepatic parasites stained positively only for the Merozoite Surface Protein 1-p19 (MSP1<sub>19</sub>), whereas day-7 parasites additionally stained positively for the Apical Merozoite Antigen-1 (AMA-1, ref. 27) and the Rhoptry Neck Protein 4 (RON-4, ref. 28) (Fig. 1d). These results are consistent with a normal hepatic maturation in LH TK-NOG mice culminating in mature merozoites capable of invading RBC. This conclusion was further re-enforced by observation of merosome-like structures in the liver of day-6- and

day-7-infected LH TK-NOG mice (Fig. 1e). Merosomes, vesicles containing packets of merozoites, have been described for *Plasmodium* species that infect rodents as the means by which hepatic merozoites reach the blood stream *in vivo*<sup>29,30</sup>.

#### *P. falciparum* blood stages in sporozoite-infected TK-NOG mice.

Having established that TK-NOG mice sustain full maturation of the *P. falciparum* hepatic stages, we wished to establish whether the liver-to-blood transition could take place in these animals. It had been previously shown that NOG mice can be efficiently engrafted with hRBC and can sustain the multiplication of *P. falciparum* blood stages<sup>16,31</sup>. We first established that TK-NOG mice could also be humanized with hRBC through daily intraperitoneal (i.p.) injection of hRBC and without further immunosuppressive treatment, as described in NOD<sup>SCID</sup>/ $\beta 2m^{-/-}$  mice<sup>15</sup>. Thus, we obtained 50–60% hRBC chimerism within 6 days, and 80–99% by day 12. These levels remained at or above 80% thereafter in all the engrafted mice (Supplementary Fig. 3). We further obtained similar results in TK-NOG mice that had been previously engrafted with hHEP, and in these mice the high

levels of hRBC chimerism was maintained for up to 5 weeks (Supplementary Fig. 3).

Groups of TK-NOG mice were then first engrafted with hHEP and when plasma hAlb levels reached  $5.0\text{--}9.8\text{ mg ml}^{-1}$  (liver humanization  $\geq 60\%$ ), they were injected with hRBC daily for 6 days, before inoculation with  $1.75 \times 10^6$  to  $3.5 \times 10^6$  *P. falciparum* sporozoites. Daily injections of hRBC were continued until the end of the observations. In this manner, optimal levels of hRBC ( $\geq 80\%$ ) were present in the mice at the time (day 6) when the hepatic schizonts are expected to reach full maturity and release infective merozoites (Supplementary Table 1). At day-8 post-sporozoite inoculation a sample of 200  $\mu\text{l}$  of peripheral mouse blood was collected and used to initiate *in vitro* cultures that were then followed over the next 8 days to assess for the presence of *P. falciparum* blood stage parasites (Fig. 2a). In three independent experiments, cultured blood from all eight mice showed parasites within the first 4 days of *in vitro* culture (Fig. 2b). The robustness of the protocol is further underlined by the fact that three distinct batches of hHEP

and of sporozoites (though all from the same line, NF54) were used for these experiments.

Furthermore, the parasitaemia was monitored in thin and thick tail-blood smears collected daily in four of the mice above (from two independent experiments) starting from day-8 post-sporozoite inoculation. In all four mice, a patent parasitaemia was detected. In the first experiment, one mouse became positive from day 9 with the parasitaemia increasing to 1.52% by day 21 at which time the mouse was killed (Fig. 2c). In the second experiment, parasites were first detectable on day 8 post-sporozoite injection in all three mice but the parasitaemia remained low, never exceeding 0.016%, throughout the 4 weeks of follow-up (Fig. 2c). The reason for the difference in peak parasitaemia levels in the two experiments might be related to batch-to-batch variations in human primary hepatocyte receptivity or sporozoite infectivity (unpublished observations and ref. 4). Furthermore, two of the four mice above were monitored for gametocyte appearance and, in both mice, gametocytes were detected at day-26 post-sporozoite injection, with immature

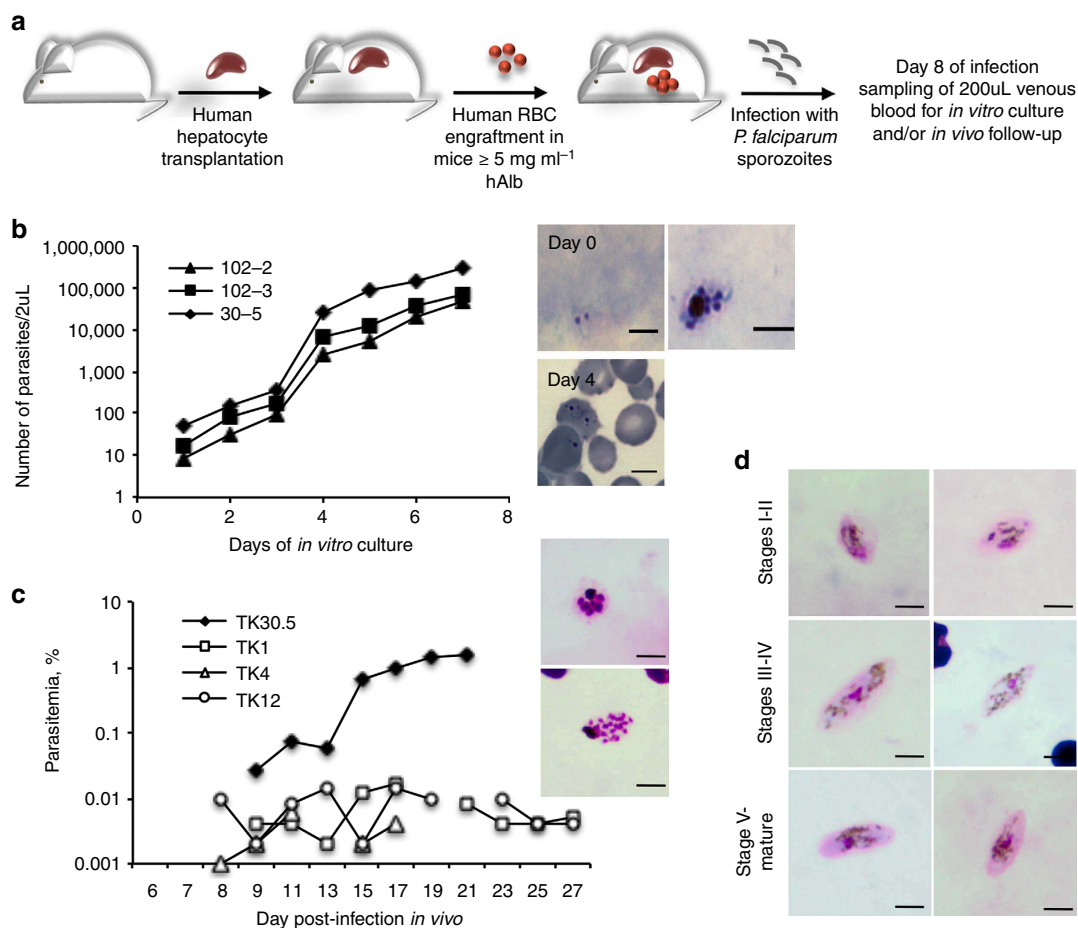


**Figure 2 | Asexual and sexual blood stages of *P. falciparum* in sporozoite-infected TK-NOG mice engrafted with human hepatocytes and RBC.**

(a). Experimental procedure for the double engraftment of TK-NOG mice with human hepatocytes and RBC before infection with *P. falciparum* sporozoites. (b). *In vitro* asexual blood stage culture: at day 8 of infection, 200  $\mu\text{l}$  of venous blood was put in culture to follow emergence of parasitaemia. Results of one experiment with three mice are expressed as the number of parasites within 2  $\mu\text{l}$  of blood for each mouse. Results are representative of three independent experiments performed with a total of eight mice. Representative pictures of a trophozoite and a schizont observed on Giemsa-stained thick blood smears at day 0 of *in vitro* culture (= day 8 of infection) and of trophozoites observed on Giemsa-stained thin blood smears at day 4 of culture. (c). *In vivo* asexual blood stage development: individual parasitaemias were determined using Giemsa-stained thin blood smears from a total of 4 mice from two independent experiments. Representative pictures of schizonts observed on Giemsa-stained thick blood smears during the course of infection, scale bar, 5  $\mu\text{m}$ . (d). *In vivo* sexual blood stage development: representative pictures of gametocytes at different stages of their development as observed in Giemsa-stained thick blood smears from two mice.

stages I–IV observed first and then with the progressive appearance of stage V mature gametocytes (Fig. 2d). Gametocytaemia was maintained thereafter, during the two additional weeks of follow-up, with the maximum proportion of total and mature gametocytes observed reaching 8.5% and 2.5% of the circulating parasites, respectively.

**LH-TK-NOG mice are suitable for investigations on a relapsing malaria parasite.** We had the opportunity to investigate the suitability of the TK-NOG mice for the study of *P. ovale*, a parasite prevalent in sub-tropical Africa, through the availability of two blood samples obtained from different patients with *P. ovale* infection. The sporozoites obtained from *Anopheles stephensi* mosquitoes that had fed on the *P. ovale*-infected blood samples, were used to inoculate LH TK-NOG mice.

Given that *P. ovale* liver stage maturation has been reported to take 9 days in humans<sup>32</sup>, we assessed the parasite's development in some of the TK-NOG mice on day 8 post-sporozoite inoculation, to search for mature schizonts and hypnozoites, and in other mice on day 21, with the aim to seek evidence for the presence of late-developing schizonts that would result from hypnozoite activation.

In a first experiment, 2 mice having 6.0 and 6.9 mg ml<sup>-1</sup> hAlb plasma levels were infected with 280,000 sporozoites. Large mature *P. ovale* schizonts were readily detectable in the engrafted hHEP at day-8 post-sporozoite inoculation (upper panel, Fig. 3a, Supplementary Fig. 4a). Their median  $\pm$  s.d. diameter was 52.63  $\pm$  13.01  $\mu$ m and areas 1664  $\pm$  671  $\mu$ m<sup>2</sup> ( $n = 35$ , Fig. 3c). In this experiment numerous developing schizonts were observed in liver sections (15–20 schizonts per 30–35 mm<sup>2</sup> liver section) and were easily identified using the fluorescent slide scanner (Supplementary Fig. 4b). We also observed small, round-shaped uninucleate parasites with a diameter of  $\sim$ 5  $\mu$ m (Fig. 3b, Supplementary Fig. 4b, lower panel) that could be hypnozoites, and that represented 15% of the total number of forms observed on day 8 (10 of the 65 forms detected in thick serial liver sections from two different lobes). Finally, we observed a single hepatic schizont, of 40- $\mu$ m diameter, among 123 sections from four pieces of different lobes analysed from a mouse sacrificed on day-21 post-sporozoite injection (Supplementary Fig. 4c), the only late parasite form that we could detect in this experiment. In a second infection with 200,000 sporozoites from another clinical isolate that were inoculated to two LH TK-NOG mice (1 and 1.7 mg ml<sup>-1</sup> plasma hAlb), fewer numbers of schizonts and uninucleate hypnozoite-like forms were observed on day 8, likely due to the low level of liver humanization of the mouse, but several schizonts were observed at day 21 (Fig. 3d). In neither experiment were any small forms observed on day 21. This suggests that all parasites had resumed their hepatic development or that the number of persisting quiescent parasites were too low to be detected. It should be noted that small forms were not observed in *P. falciparum*-infected mice sacrificed on day 5 or day-7 post-sporozoite inoculation, nor could any parasites forms be found in the liver of a *P. falciparum*-infected mouse sacrificed on day 21 post-infection.

## Discussion

We describe the successful double engraftment of TK-NOG mice with hHEP and hRBC, with efficiencies of 'humanization' reaching up to 90% for both cell types. In all the mice, the engrafted hHEP were receptive to infection by sporozoites from two of the species that infect humans, *P. falciparum* and *P. ovale*, and sustained maturation of the resulting hepatic stages.

Observations of the *P. ovale* hepatic stages are very few in number indeed. *In vivo* observations are restricted to a single

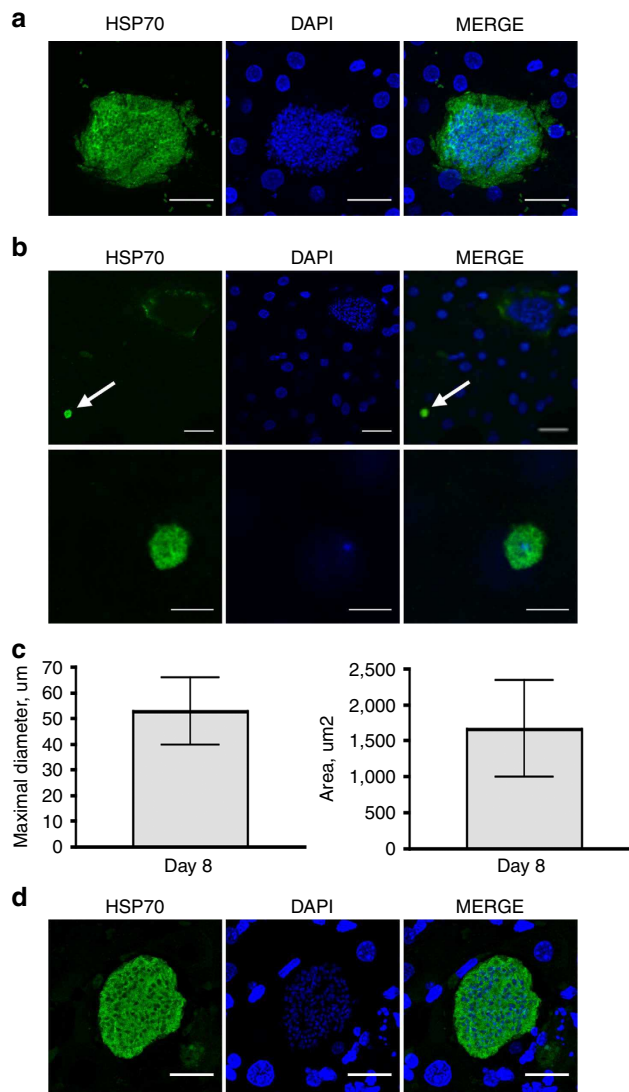


**Figure 3 | Hepatic development of *P. ovale* in LH-TK-NOG mice.**

Representative pictures of *P. ovale* schizonts and hypnozoites at days 8 and 21 post-infection. 50- $\mu$ m thick frozen (a,b) or 5- $\mu$ m thick deparaffinized liver sections (d) were stained by indirect immunofluorescence with immune serum specific to *Plasmodium* HSP70 and DAPI to stain host cell and parasite nuclei. (a). Day-8 schizonts, scale bar, 20  $\mu$ m. (b). Upper panel: day-8 schizont and—hypnozoite (white arrow), scale bar, 20  $\mu$ m. Lower panel: higher magnification of the hypnozoite showing the single nucleus within the 5  $\mu$ m round-shape parasite, scale bar, 5  $\mu$ m. (c) Maximal diameter and area of day-8 schizonts;  $n = 35$ , from three different lobes, mean  $\pm$  s.d. (d). Day-21 schizont, scale bar, 20  $\mu$ m.

occasion in humans<sup>32</sup>, and apart from one case where *Saimiri* monkeys were used<sup>33</sup>, the remainder were principally made on infected chimpanzees<sup>34,35</sup>. *In vitro* observations were also made only once using primary human hepatocytes<sup>36</sup> and once using primary *Saimiri* hepatocytes<sup>33</sup>. Experimental infections with *P. ovale* were last made in humans in the mid 1960s when five volunteers were inoculated with sporozoites<sup>37</sup>, and thereafter using chimpanzees. West African strains of the parasites were mainly used for these observations. The *P. ovale* sporozoites used in the current study were derived from two distinct *P. ovale* clinical isolates, collected 9 months apart from patients who acquired the infection in Africa. These sporozoites proved to be infectious to human primary hepatocytes engrafted in TK-NOG

mice, where they developed into mature hepatic schizonts of a size consistent with those observed in the human liver<sup>32</sup>. Despite the relatively low sporozoite inoculum (250,000 and 300,000), the resulting *P. ovale* hepatic forms were sufficiently numerous to allow easy detection in the liver sections screened 8 days following inoculation. Along these mature schizonts, we observed small round-shaped uninucleate parasite forms of ~5 µm in diameter. Furthermore, maturing schizonts were observed in liver sections taken on day-21 post-infection. The fact that the *P. ovale* hepatic stages normally complete their maturation in 9 days<sup>32</sup> and that early relapses can occur within the first month after the infective mosquito bite<sup>38</sup>, are consistent with a hypnozoite origin of the maturing forms observed on day 21. This is also supported by observations in TK-NOG mice inoculated with sporozoites of a non-relapsing species, *P. falciparum*, where neither small uninucleate forms could be observed on day 5 or 7 liver sections, nor any parasite forms could be found on those made on day 21. Nonetheless, conclusive proof of the occurrence of hypnozoites in TK-NOG mice awaits further observations.

For *P. falciparum*, we could demonstrate a successful transition from the hepatic to the erythrocytic stages of the infection, as all the mice inoculated with sporozoites developed a patent blood parasitaemia, which was maintained over 3–6 weeks of follow-up. It was further noted that *P. falciparum* gametocytogenesis culminating in the production of mature gametocytes was also observed, thus providing a laboratory mice model that recapitulates the complete life cycle of *P. falciparum*. Complete development of the *P. falciparum* hepatic stages had been previously obtained in immunocompromised mice. This was reported in Alb-UpA SCID mice by one group<sup>14</sup> but not by the other<sup>13</sup>, and more recently in FRG mice<sup>19</sup>. In these mice, treatment to maintain optimal conditions for engraftment had been administered, though this did not appear to have influenced parasite development. In these mice as well as the TK-NOG described here, the diameters of the hepatic schizonts on day-7 post-inoculation ranged from 50 to 100 µm. This is in accordance with observations of the hepatic stages of the same strain of *P. falciparum* (NF54) in chimpanzee livers (average diameter of 60 to 100 µm on day-6 post-inoculation)<sup>39</sup>. It is interesting to note that when different lines of *P. falciparum* were used, a Rumanian strain in humans<sup>40</sup> or a Liberian strain in chimpanzees<sup>41</sup>, the average sizes on days 6 were 60 and 35 µm, respectively. Given that these are the only *in vivo* observations made on the liver stages of *P. falciparum*, it is not possible to speculate on the nature of the size variations observed. On the other hand, it is clear that hepatic parasite maturation is slower in *in vitro*-cultured human primary hepatocytes than in hepatocytes engrafted in the immune-compromised mice<sup>5</sup>. Moreover, the uninucleate forms that are usually observed in *in vitro* culture of the *P. falciparum* hepatic stages<sup>23</sup>, presumably arrested forms, were not observed in any of the liver sections taken from the FRG<sup>19</sup> or the TK-NOG mice. Such arrested or retarded forms had not been reported from previous *in vivo* observations, which reinforces the quality and suitability of the hepatic environment for parasite development in the LH mice. The speed of maturation of the *P. ovale* hepatic parasites in the TK-NOG mice (average diameter of 65 µm on day 8) was also closer to that observed *in vivo*, where schizont sizes ranged from an average of 45 µm on day 5 to 75 µm on day 9 in humans<sup>32</sup>, and of 40 µm on day 8 in chimpanzee livers<sup>34</sup>. It is interesting to note that for this species, the speed of maturation *in vitro*<sup>36</sup> appears to mirror that observed, albeit on a limited number of occasions, in the human or chimpanzee hosts.

The detection of *P. falciparum* antigens expressed in the asexual blood stages (SERP) or in merozoites (MSP1<sub>19</sub>, AMA-1 and RON-4) strongly indicated that full maturation of the hepatic

schizonts to yield invasive merozoites was obtained in the TK-NOG mice. This was further supported by the observation of merozoite-like structures, merozoites being packets of merozoites that had been previously reported in the rodent malaria parasites as the means by which their hepatic merozoites reach the blood stream on hepatic schizont rupture<sup>29,30</sup>. Our observations of merozoite-like structures in the livers of *P. falciparum*-infected TK-NOG mice duplicate those made in FRG mice<sup>19</sup>, indicating that this strategy of parasite egress from the infected hepatocyte might be characteristic of all *Plasmodium* species. Incontrovertible proof that infectious *P. falciparum* merozoites were generated from the infected engrafted hHEP was obtained in double-engrafted TK-NOG mice (with hRBC). Thus, blood samples taken from all eight mice in three independent experiments (engrafted with distinct hHEP and infected with different *P. falciparum* sporozoite batches) were positive for blood stage parasites shortly after *in vitro* cultivation and, more importantly, four out of four mice from two of the experiments cited above developed a microscopically detectable blood parasitaemia from days 8 or 9 post-sporozoite inoculation, which was maintained over many weeks of follow-up. This transition was also reported in FRG mice<sup>19</sup>, although in that case, the blood stages could only be demonstrated through *in vitro* cultivation of total blood collected on day 7 post-inoculation in mice that had received injections of hRBC the previous day as well as 2 hours before killing.

To date, long-term maintenance of *P. falciparum* blood parasitaemias had been obtained in mice engrafted solely with hRBC that were: (a) inoculated with high numbers of infected RBC<sup>15</sup>; and/or (b) that were under additional immunosuppressive treatment (chlodronate-liposomes to eliminate macrophages, antibodies to deplete polymorphonuclear leukocytes)<sup>12,16,17,42</sup>; and/or (c) that were inoculated with a strain of *P. falciparum* that had been adapted to mice<sup>15,43</sup>. The presence of gametocytes was only reported in some of these previous studies<sup>12,16,17</sup>. The double-engrafted TK-NOG mice (with hHEP and hRBC) made it possible to overcome the limitations of previous models, such as the need to adapt the *P. falciparum* strain to the mice<sup>15,43</sup> or the necessity for continuous treatment with clodronate liposome to deplete macrophages<sup>16</sup>, and thus proved suitable to obtain all the stages of the *P. falciparum* life cycle. In particular, the TK-NOG mice offered an environment conducive to the production and maturation of the sexual blood stages. Indeed immature gametocytes were observed starting from day-26 post-sporozoite inoculation, with mature stage V forms gradually appearing throughout the follow-up period. The total gametocyte numbers could account for up to 8.5% of all the parasites forms observed, mature gametocytes reaching up to 2.5% of the circulating parasites. Similar to previous observations in other mouse strains<sup>12,16,17</sup>, gametocytes of all stages of maturity were observed in the mice's peripheral circulation, a situation that sharply contrasts with the situation in humans where maturation is completed in the bone marrow and the spleen before the release of the infective gametocytes to the periphery and eventual transmission to mosquitoes<sup>44</sup>. It would be of interest to elucidate the reasons for this difference. Recently, the full life cycle of *P. falciparum* was reported in humanized HLA-DR4.RagKO.IL2RγcKO.NOD (DRAG) mice<sup>45</sup> transplanted with CD34+ haematopoietic stem cells. Parasitaemia levels, where measured, did not exceed a few parasites per µl, and efficient transmission to mosquitoes required prior *in vitro* cultivation although direct transmission from one infected mouse was reported. Furthermore, the value of immunocompromised mice models for the study of relapsing parasites has been strongly enhanced by the recent successful demonstration of the

development of *P. vivax* hepatic stages, including hypnozoites, in FRG KO mice engrafted with human primary hepatocytes<sup>46</sup>.

The TK-NOG model used in our study has been recently shown to represent a suitable model for preclinical drug validations<sup>47,48</sup>. Here we show that this extends to investigations of the *Plasmodium* species that infect humans. The main advantages of the TK-NOG model are the freedom from additional treatment post-engraftment, the high levels and sustainability of the humanized compartments, and the potential for double engraftment that made it possible to obtain consistently all the stages of the *P. falciparum* life cycle within the same animal directly from a sporozoite inoculation. This makes it possible to envisage routine *in vivo* preclinical validation of compounds targeting *P. falciparum* liver stage, genetic crosses of *P. falciparum* strains that had become severely limited by the necessity to employ chimpanzees, and *in vivo* validation of *P. falciparum* attenuated live vaccines targeting the liver stages. In addition, obtaining mature *P. falciparum* gametocytes allows to envisage the use of this model for transmission to mosquitoes, and, if validated, for *in vivo* evaluation of transmission blocking interventions. Finally, the success in obtaining hHEP infected with sporozoites from two distinct *P. ovale* strains directly obtained from clinical isolates and observations of viable late-developing forms, probably activated hypnozoites, makes the TK-NOG model suitable for *in vivo* investigations of relapsing *Plasmodium* species hitherto restricted to primate models.

## Methods

**Ethics statement.** This study was carried out in strict accordance with the Guide for the Care and Use of Laboratory Animals from the Central Institute for Experimental Animals (CIEA) in Japan and with the French and European regulations (2010/63/EU). The experimental protocols were approved by the Animal Care Committee of the CIEA (Permit Number: 11029A) and by the Ministère de l'Éducation Nationale, de l'Enseignement Supérieur et de la Recherche (Authorization Number 01737.03). Human blood samples infected with *P. ovale* were obtained from adult after receiving written informed consent. The collection and use of this material was approved by the Institutional Review Board (Comité de Protection des Personnes) of the Centre Hospitalo-Universitaire Pitié-Salpêtrière, Assistance Publique-Hôpitaux de Paris, Paris, France.

**Liver- and RBC-humanization of TK-NOG mice.** TK-NOG mice were imported from Dr Hiroshi Suemizu's laboratory (CIEA, Japan) and bred at the Centre d'Expérimentation Fonctionnelle (CEF, La Pitié-Salpêtrière, Paris) under strict pathogen-free conditions. Given that transgenic males are hypofertile, non-transgenic males were bred with transgenic females, progeny was genotyped and transgenic males were engrafted with hHEP as described by Hasegawa *et al.*<sup>20</sup>. Only transgenic males were used for further hHEP engraftment because the higher expression of the HSVtk transgene in males as compared with that in females (Supplementary Fig. 5) allowed higher level of endogenous hepatocyte lysis and, subsequently, more efficient human hepatocyte engraftment. Briefly, 7–9 week-old transgenic males were injected with gancyclovir and lysis of endogenous hepatocytes was evaluated through alanine amino transferase (ALT) measurement on 32  $\mu$ l of heparinized plasma using a Reflovet chemistry analyzer (SciVet, France) at the CEF (La Pitié-Salpêtrière, Paris). When ALT level exceeded 100 IU l<sup>-1</sup>, mice were injected intrasplenically with 1 million thawed hHEP previously isolated and frozen in the lab from a 60-year-old male patient negative for HIV, HCV and HBV<sup>23</sup>. Efficiency of hHEP engraftment was then evaluated every month by quantifying human albumin within mouse plasma with the Human Albumin ELISA Quantitation Set (Bethyl laboratories) following manufacturer recommendations. Hasegawa *et al.*<sup>20</sup> previously showed that hAlb plasmatic level correlated with replacement index. Gancyclovir was not administered after transplantation.

Mice used for the present study were either bred and LH in the CEF as mentioned above, or imported already engrafted with commercial hHEP from H. Suemizu's laboratory (Supplementary Table S2), and had human albumin level ranging from 1 to 10 mg ml<sup>-1</sup>, corresponding to 15–90% of humanization<sup>20</sup>. For *P. falciparum* full life cycle experiments, LH TK-NOG mice showing hAlb levels  $\geq$  5 mg ml<sup>-1</sup> were selected for further engraftment with hRBC. hRBC group O were obtained from the Etablissement Français du Sang blood bank. Mice were injected daily through the i.p. route with 1 ml of hRBC, 50% haematocrit in RPMI medium, following a protocol adapted from Angulo-Barturen *et al.*<sup>15</sup>, starting 6 days before sporozoite injection. Volume 0.5  $\mu$ l of blood was taken at the tail vein to monitor hRBC engraftment by flow cytometry. Engraftment with hRBC was maintained up to 6 weeks post-sporozoite injection.

**Sporozoites and *in vivo* infection.** *P. falciparum* (NF54 strain) sporozoites were isolated by aseptic dissection of the salivary glands of infected *A. stephensi* obtained from the Department of Medical Microbiology, University Medical Centre, St Radboud, Nijmegen, The Netherlands. Anaesthetised mice were injected intravenously into the retro-orbital sinus vein with 1–3.5 million sporozoites. *P. ovale* sporozoites were obtained from infected *A. stephensi* salivary glands after a blood meal on *P. ovale*-infected blood. *P. ovale* species diagnosis was performed at the Service de Maladies Infectieuses, Centre National de Référence pour le Paludisme, Laveran Building, La Pitié-Salpêtrière, by microscopic examination of thick and thin blood smears by a highly experienced technician and was further confirmed by PCR<sup>49</sup>. Fresh heparinized blood from *P. ovale*-infected patients containing gametocytes was used to feed mosquitoes. Briefly, plasma and buffy coat were removed by centrifugation, pelleted RBC were then washed twice with RPMI and resuspended in human AB plasma at 50% haematocrit. All of this process was done at 37 °C to maintain gametocytes infectivity. Volume of 2.5 ml was used to fill a membrane-based feeder system and mosquitoes were fed for 1 h. Mosquitoes were then kept at 27 °C. Stomachs were analysed at day 8 post-infected blood meal to check for the presence of oocysts. Salivary glands were dissected on day 14 post-blood feeding for sporozoite isolation. Anaesthetised mice were injected intravenously into the retro-orbital sinus vein with sporozoites. Mice were inoculated with *Plasmodium* sporozoites at least 2 months after the gancyclovir treatment. Mice were killed at different days post-sporozoite injection. After removal of the gall bladder, the liver was cut into pieces and fixed in formalin for paraffin inclusion, or snap-frozen in liquid nitrogen before storage at –80 °C. Snap-frozen samples were further processed for immunohistology analysis on liver sections.

**Follow-up of *P. falciparum* blood stages *in vivo* and *in vitro*.** *P. falciparum* blood stage infection in liver- and RBC-humanized mice was monitored starting from day-8 post-sporozoite injection on thick and thin blood smears, done with, respectively, 2 and 4  $\mu$ l of fresh blood collected at the tail on EDTA. At day 8 post-sporozoite injection, 200  $\mu$ l of blood was taken at the retro-orbital sinus vein under anaesthesia for *in vitro* culture of blood stage parasites. Briefly, heparinized blood was washed twice with RPMI medium containing 0.5% albumax (Gibco), 20  $\mu$ g ml<sup>-1</sup> of gentamycin (Gibco), 0.23% of sodium bicarbonate (Gibco), and 0.1 mM Hypoxanthine (Sigma), and diluted half with fresh O hRBC for further culture in flask at 5% haematocrit, in a 5% CO<sub>2</sub> humid atmosphere. Medium was renewed every 48 h and 2- $\mu$ l thick or thin blood smears were made to monitor blood-stage parasite emergence and growth.

Fixed-permeabilized thick and thin blood smears were GIEMSA-stained before analysis for quantitation of asexual and sexual blood stages. Results were either expressed as the number of asexual/sexual forms per  $\mu$ l of blood after complete examination of thick blood smears, or percentage of parasitaemia estimated after analysis of at least 50 fields, magnification  $\times$  50, on thin blood smears (number of infected RBC  $\times$  100/total number of infected and uninfected RBC).

**Detection of hepatic parasites in liver sections.** Formalin-fixed liver samples were embedded in paraffin and processed at the Anatomic-Pathology Service of the Pitié-Salpêtrière Hospital, Paris. Briefly, automated paraffin inclusion was done in cassettes, 5- $\mu$ m thick serial sections were cut with a microtome, deparaffinized and either stained with Hematoxylin-Eosin-Safran at the Anatomic-Pathology Service, or processed for *Plasmodium* HSP70 staining at the laboratory. In this latter case, antigen retrieval was performed by incubating sections in a pH 8 - 1 mM EDTA buffer at 98 °C for 30 min, followed by 20 min at room temperature to allow samples temperature to cool down, and then washed twice in PBS before processing for HSP70 immunostaining as described below for frozen sections.

Sixteen- to fifty- $\mu$ m thick serial sections of frozen liver samples were made with a Cryostat HM500, air dried for 30 or 60 min before fixation in methanol for 5 min or 4% PFA for 20 min at room temperature. Sections were then washed twice in PBS before processing for HSP70 immunostaining. Briefly, 5- $\mu$ m thick deparaffinized sections and 16- $\mu$ m thick frozen sections were first incubated with normal goat serum diluted 1:500 for 1 h, washed twice in PBS, incubated with a mouse polyclonal anti-*Plasmodium* HSP70 serum diluted 1:1,000 (ref. 50) for 1 h, washed twice and finally incubated with a goat anti-mouse IgG coupled to Alexa-Fluor 488 or to Alexa-Fluor 594 diluted 1:500 (Life Technologies) and DAPI 1  $\mu$ g ml<sup>-1</sup> in the dark for 45 min. All incubations were done in PBS-1%BSA-0.2%Triton X-100 and at 37 °C. Staining with anti-Pf EXP-1 (1:200, ref. 24), SERP (1:400, ref. 25), AMA-1 (rat mAb 4G2, 1:100, ref. 27), MSP1<sub>19</sub> (1:50, ref. 51), RON-4 (mouse mAb 24C6 4F12, 1:100, ref. 28) and anti-human Aquaporin-9 (goat mAb C18, Santa Cruz Biotechnology, 1:40) were performed following the protocol described above, using either goat anti-mouse, goat anti-rabbit, goat anti-rat or donkey anti-goat IgG coupled to Alexa-Fluor 488 or Alexa-Fluor 594 diluted 1:500 (Life Technologies) as secondary antibodies. For parasite immunostaining in 50- $\mu$ m thick frozen sections, incubation with the anti-*Plasmodium* HSP70 immune serum was performed overnight at room temperature and all incubations were done in PBS-1%BSA-0.2%Triton X-100. All sections were washed twice in PBS before being mounted in anti-fading medium and stored at 4 °C before analysis. Immunostained sections were examined under a fluorescence microscope (Leica DMI 4000 B). Photomicrographs were obtained using a confocal microscope (Olympus FV-1000, Plateforme d'Imagerie Cellulaire PICPS, La Pitié-Salpêtrière,

Paris) and images were analysed using ImageJ software. Whole-slide imaging was done using a digital slide scanner Nanozoomer 2.0 HT equipped with the fluorescent unit option L11600-05 and a 3-CCD TDI camera using a x20 objective (Hamamatsu Photonics, Plateforme d'Imagerie, Institut de la Vision, Paris). Scanned images were analysed with the NDPView Nanozoomer associated software.

**In vivo hRBC monitoring by flow cytometry.** Volume of 0.5 µl of EDTA-blood were stained with anti-human-Glycophorin A mAb coupled to FITC (eBiosciences), washed in PBS, fixed in 0.2% PFA and analysed using a LSR Fortessa cytometer (Plateforme de cytométrie en flux CYPS, La Pitié-Salpêtrière, Paris). Analyses were performed using the FlowJo software 7.6.3.

**Statistical analyses.** The sizes and areas of *P. falciparum* schizonts at days 5 and 7 were compared using the Mann-Whitney *U*-test (GraphPad Prism software).

## References

1. W.H.O. World Malaria Report 2013 [http://www.who.int/malaria/publications/world\\_malaria\\_report\\_2013/en/](http://www.who.int/malaria/publications/world_malaria_report_2013/en/) (2013).
2. Galinski, M. R., Meyer, E. V. & Barnwell, J. W. *Plasmodium vivax*: modern strategies to study a persistent parasite's life cycle. *Adv. Parasitol.* **81**, 1–26 (2013).
3. Demebele, L. *et al.* Persistence and activation of malaria hypnozoites in long-term primary hepatocyte cultures. *Nat. Med.* **20**, 307–312 (2014).
4. March, S. *et al.* A microscale human liver platform that supports the hepatic stages of *Plasmodium falciparum* and *vivax*. *Cell. Host. Microbe.* **14**, 104–115 (2013).
5. Mazier, D. *et al.* Complete development of hepatic stages of *Plasmodium falciparum* *in vitro*. *Science* **227**, 440–442 (1985).
6. Sattabongkot, J. *et al.* Establishment of a human hepatocyte line that supports *in vitro* development of the exo-erythrocytic stages of the malaria parasites *Plasmodium falciparum* and *P. vivax*. *Am. J. Trop. Med. Hyg.* **74**, 708–715 (2006).
7. Zou, X., House, B. L., Zyzak, M. D., Richie, T. L. & Gerbasi, V. R. Towards an optimized inhibition of liver stage development assay (ILSDA) for *Plasmodium falciparum*. *Malar. J.* **12**, 394 (2013).
8. Hollingdale, M. R., Collins, W. E., Campbell, C. C. & Schwartz, A. L. *In vitro* culture of two populations (dividing and nondividing) of exoerythrocytic parasites of *Plasmodium vivax*. *Am. J. Trop. Med. Hyg.* **34**, 216–222 (1985).
9. Mazier, D. *et al.* Cultivation of the liver forms of *Plasmodium vivax* in human hepatocytes. *Nature* **307**, 367–369 (1984).
10. Mazier, D., Renia, L. & Snounou, G. A pre-emptive strike against malaria's stealthy hepatic forms. *Nat. Rev. Drug. Discov.* **8**, 854–864 (2009).
11. Legrand, N. *et al.* Humanized mice for modeling human infectious disease: challenges, progress, and outlook. *Cell Host Microbe.* **6**, 5–9 (2009).
12. Moore, J. M., Kumar, N., Shultz, L. D. & Rajan, T. V. Maintenance of the human malarial parasite, *Plasmodium falciparum*, in scid mice and transmission of gametocytes to mosquitoes. *J. Exp. Med.* **181**, 2265–2270 (1995).
13. Morosan, S. *et al.* Liver-stage development of *Plasmodium falciparum*, in a humanized mouse model. *J. Infect. Dis.* **193**, 996–1004 (2006).
14. Sacci, Jr. J. B. *et al.* *Plasmodium falciparum* infection and exoerythrocytic development in mice with chimeric human livers. *Int. J. Parasitol.* **36**, 353–360 (2006).
15. Angulo-Barturen, I. *et al.* A murine model of *falciparum*-malaria by *in vivo* selection of competent strains in non-myelodepleted mice engrafted with human erythrocytes. *PLoS ONE* **3**, e2252 (2008).
16. Arnold, L. *et al.* Further improvements of the *P. falciparum* humanized mouse model. *PLoS ONE* **6**, e18045 (2011).
17. Moreno, A. *et al.* The course of infections and pathology in immunomodulated NOD/LtSz-SCID mice inoculated with *Plasmodium falciparum* laboratory lines and clinical isolates. *Int. J. Parasitol.* **36**, 361–369 (2006).
18. Azuma, H. *et al.* Robust expansion of human hepatocytes in *Fah<sup>-/-</sup>/Rag2<sup>-/-</sup>/Il2rg<sup>-/-</sup>* mice. *Nat. Biotechnol.* **25**, 903–910 (2007).
19. Vaughan, A. M. *et al.* Complete *Plasmodium falciparum* liver-stage development in liver-chimeric mice. *J. Clin. Invest.* **122**, 3618–3628 (2012).
20. Hasegawa, M. *et al.* The reconstituted 'humanized liver' in TK-NOG mice is mature and functional. *Biochem. Biophys. Res. Commun.* **405**, 405–410 (2011).
21. Hu, Z., Van Rooijen, N. & Yang, Y. G. Macrophages prevent human red blood cell reconstitution in immunodeficient mice. *Blood* **118**, 5938–5946 (2011).
22. Jeffery, G. M., Wolcott, G. B., Young, M. D. & Williams, Jr. D. Exo-erythrocytic stages of *Plasmodium falciparum*. *Am. J. Trop. Med. Hyg.* **1**, 917–925 (1952).
23. Demebele, L. *et al.* Towards an *in vitro* model of *Plasmodium* hypnozoites suitable for drug discovery. *PLoS ONE* **6**, e18162 (2011).
24. Gunther, K. *et al.* An exported protein of *Plasmodium falciparum* is synthesized as an integral membrane protein. *Mol. Biochem. Parasitol.* **46**, 149–157 (1991).
25. Ragge, K. *et al.* *In vitro* biosynthesis and membrane translocation of the serine rich protein of *Plasmodium falciparum*. *Mol. Biochem. Parasitol.* **42**, 93–100 (1990).
26. Delplace, P., Dubremetz, J. F., Fortier, B. & Vernes, A. A 50 kilodalton exoantigen specific to the merozoite release-reinvasion stage of *Plasmodium falciparum*. *Mol. Biochem. Parasitol.* **17**, 239–251 (1985).
27. Kocken, C. H. *et al.* Precise timing of expression of a *Plasmodium falciparum*-derived transgene in *Plasmodium berghei* is a critical determinant of subsequent subcellular localization. *J. Biol. Chem.* **273**, 15119–15124 (1998).
28. Roger, N. *et al.* Characterization of a 225 kilodalton rhoptry protein of *Plasmodium falciparum*. *Mol. Biochem. Parasitol.* **27**, 135–141 (1988).
29. Baer, K., Klotz, C., Kappe, S. H., Schnieder, T. & Frevert, U. Release of hepatic *Plasmodium yoelii* merozoites into the pulmonary microvasculature. *PLoS Pathog.* **3**, e171 (2007).
30. Sturm, A. *et al.* Manipulation of host hepatocytes by the malaria parasite for delivery into liver sinusoids. *Science* **313**, 1287–1290 (2006).
31. Dreyer, A. M. *et al.* Passive immunoprotection of *Plasmodium falciparum*-infected mice designates the CyRPA as candidate malaria vaccine antigen. *J. Immunol.* **188**, 6225–6237 (2012).
32. Garnham, P. C. *et al.* The pre-erythrocytic stage of *Plasmodium ovale*. *Trans. R. Soc. Trop. Med. Hyg.* **49**, 158–167 (1955).
33. Millet, P. *et al.* *Plasmodium ovale*: observations on the parasite development in Saimiri monkey hepatocytes *in vivo* and *in vitro* in contrast with its inability to induce parasitemia. *Exp. Parasitol.* **78**, 394–399 (1994).
34. Bray, R. S. & Gunders, A. E. Studies on malaria in chimpanzees. XI. The early forms of the pre-erythrocytic phase of *Laverania falcipara*. *Am. J. Trop. Med. Hyg.* **12**, 13–18 (1963).
35. Collins, W. E. *et al.* Infection of chimpanzees with Nigerian I/CDC strain of *Plasmodium ovale*. *Am. J. Trop. Med. Hyg.* **37**, 455–459 (1987).
36. Mazier, D. *et al.* *Plasmodium ovale*: *in vitro* development of hepatic stages. *Exp. Parasitol.* **64**, 393–400 (1987).
37. Chin, W., Contacos, P. G. & Buxbaum, J. N. The transmission of a West African strain of *Plasmodium ovale* by *Anopheles freeborni* and *Anopheles maculatus*. *Am. J. Trop. Med. Hyg.* **15**, 690–693 (1966).
38. Chin, W. & Coatney, G. R. Relapse activity in sporozoite-induced infections with a West African strain of *Plasmodium ovale*. *Am. J. Trop. Med. Hyg.* **20**, 825–827 (1971).
39. Meis, J. F. *et al.* *Plasmodium falciparum*: studies on mature exoerythrocytic forms in the liver of the chimpanzee, *Pan troglodytes*. *Exp. Parasitol.* **70**, 1–11 (1990).
40. Shortt, H. E., Fairley, N. H., Covell, G., Shute, P. G. & Garnham, P. C. The pre-erythrocytic stage of *Plasmodium falciparum*. *Trans. R. Soc. Trop. Med. Hyg.* **44**, 405–419 (1951).
41. Bray, R. S. & Gunders, A. E. Studies on malaria in chimpanzees. IX. The distribution of the pre-erythrocytic forms of *Laverania falcipara*. *Am. J. Trop. Med. Hyg.* **11**, 437–439 (1962).
42. Badell, E. *et al.* Human malaria in immunocompromised mice: an *in vivo* model to study defense mechanisms against *Plasmodium falciparum*. *J. Exp. Med.* **192**, 1653–1660 (2000).
43. Jimenez-Diaz, M. B. *et al.* Improved murine model of malaria using *Plasmodium falciparum* competent strains and non-myelodepleted NOD-*scid* IL2Rγ<sup>null</sup> mice engrafted with human erythrocytes. *Antimicrob. Agents Chemother.* **53**, 4533–4536 (2009).
44. Talman, A. M., Domarle, O., McKenzie, F. E., Ariey, F. & Robert, V. Gametocytogenesis: the puberty of *Plasmodium falciparum*. *Malar. J.* **3**, 24 (2004).
45. Wijayalath, W. *et al.* Humanized HLA-DR4.RagKO.IL2Rγ<sup>macKO</sup>.NOD (DRAG) mice sustain the complex vertebrate life cycle of *Plasmodium falciparum* malaria. *Malar. J.* **13**, 386 (2014).
46. Mikolajczak, S. A. *et al.* *Plasmodium vivax* liver stage development and hypnozoite persistence in human liver-chimeric mice. *Cell Host Microbe.* **17**, 526–535 (2015).
47. Xu, D. *et al.* Fialuridine induces acute liver failure in chimeric TK-NOG mice: a model for detecting hepatic drug toxicity prior to human testing. *PLoS Med.* **11**, e1001628 (2014).
48. Hu, Y., Wu, M., Nishimura, T., Zheng, M. & Peltz, G. Human pharmacogenetic analysis in chimeric mice with 'humanized livers'. *Pharmacogenet. Genomics* **23**, 78–83 (2013).
49. Rougemont, M. *et al.* Detection of four *Plasmodium* species in blood from humans by 18S rRNA gene subunit-based and species-specific real-time PCR assays. *J. Clin. Microbiol.* **42**, 5636–5643 (2004).
50. Renia, L. *et al.* A malaria heat-shock-like determinant expressed on the infected hepatocyte surface is the target of antibody-dependent cell-mediated cytotoxic mechanisms by nonparenchymal liver cells. *Eur. J. Immunol.* **20**, 1445–1449 (1990).
51. Faber, B. W. *et al.* Diversity covering AMA1-MSP119 fusion proteins as malaria vaccines. *Infect. Immun.* **81**, 1479–1490 (2013).

## Acknowledgements

We are grateful to Prof. K. Lingelbach (FB Biology, Philipps-University, Marburg, Germany) for his gift of the antibodies to Pf-SERP and Pf-EXPI, to Dr Ed Remarque (Biomedical Primate Research Center, Rijswijk, The Netherlands) for the antibodies to Pf-MSP1<sub>19</sub>, to Dr Dubremetz (UMR5235, CNRS, Université de Montpellier 2, Montpellier, France) for the antibodies to Pf-RON4, to C. Enond (Centre d'Expérimentation Fonctionnelle, UMS28, La Pitié-Salpêtrière, Paris) for her help with TK-NOG housing and breeding, to Pr. R. Sauerwein and G.J. Van Gemert (Department of Medical Microbiology, Radboud University Nijmegen Medical Centre, Nijmegen, The Netherlands) for the provision of *P. falciparum*-infected mosquitoes, to Pr. C. Hennequin (Service de Parasitologie-Myologie, Hôpital Saint-Antoine, CIMI-Paris, UPMC, Paris, France) for his help with the recruitment of one of the *P. ovale*-infected patient, to Pr. L. Hannoun (Service de Chirurgie Digestive, Hépatobilio-Pancréatique et Transplantation Hépatique, AP-HP, Centre Hospitalo-Universitaire Pitié-Salpêtrière, Paris, France) for providing us with hepatic resections, to A. Lesot (Service d'Anatomie et Cytologie Pathologiques, AP-HP, Groupe Hospitalier Pitié-Salpêtrière, Paris) for her precious help with the processing of paraffin-embedded liver samples, to T. Houpert, V. Ok, E. Tepaz and Y. Terres for their help with mosquito breeding, infection and processing of liver sections, to L. Ciceron and N. Chartrel for their invaluable help with *Plasmodium* species diagnosis, to M. Bauzou and G. Pieumi for their support with quantification of *P. falciparum* blood stage parasites, to A. Dauphin and C. Lovo for their help with confocal microscopy (Plateforme d'Imagerie Cellulaire de la Pitié-Salpêtrière PICPS, Paris, France), to C. Blanc and B. Hoareau-Coudert for their help with flow cytometry analyses (Cytometry Platform of the Pitié-Salpêtrière CYPS, Paris, France), to S. Fouquet and D. Godefroy for their help with the digital scanning of liver sections (Imaging Platform, Institut de la Vision, Paris, France). This work was supported by the MaTuRe Project funded by the French National Agency for research (ANR), the Fondation pour la Recherche Médicale (grant DPM20121125558), the MultiMalVax project (Grant Agreement number: 305282) and the PathCo project (Grant Agreement n°HEALTH-F3-2012-305578) both funded by the European Community's Seventh Framework Programme [FP7-2007-2013], the PARAFRAP LabEx of the French Parasitology Alliance For Health Care, and a DIM Malinf grant from the Ile-de-France

region. V.S. was a recipient of a postdoctoral fellowship from the MaTuRe and the MultiMalVax projects; C.R. was a recipient from a DIM Malinf postdoctoral fellowship from the Ile-de-France region.

## Author contributions

V.S., H.B.V., A.L., J.F.F., G.S., A.M.S. and D.M. conceived, planned and designed experiments. V.S., H.B.V., A.L., C.R., J.F.F., G.Z., M.B., M.T., M.T., S.M., H.S. and A.M.S. conducted experiments. V.S., H.B.V., A.L., C.R., J.F.F., G.Z., M.B., M.T., M.T., G.L.N., F.C., H.S., G.S., A.M.S. and D.M. analysed the data. V.S., H.S., G.S., A.M.S. and D.M. wrote the manuscript. All authors reviewed the manuscript.

## Additional information

**Supplementary Information** accompanies this paper at <http://www.nature.com/naturecommunications>

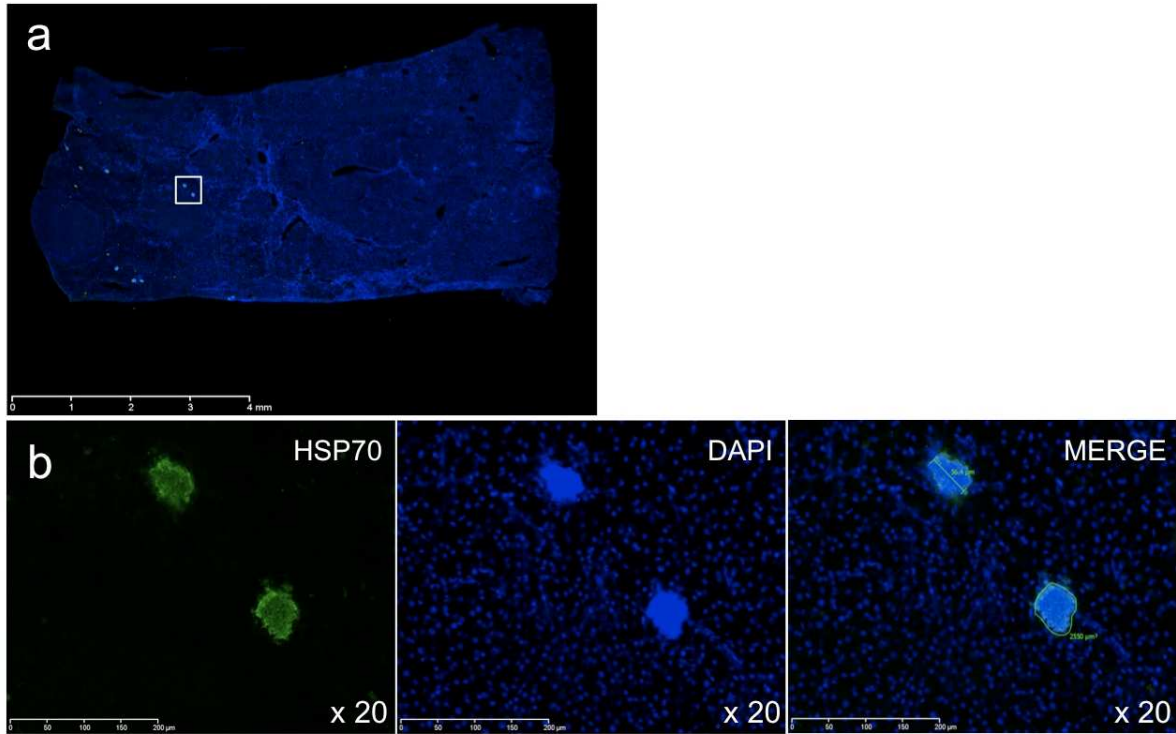
**Competing financial interests:** The authors declare no competing financial interests.

**Reprints and permission** information is available online at <http://npg.nature.com/reprintsandpermissions/>

**How to cite this article:** Soulard, V. *et al.* *Plasmodium falciparum* full life cycle and *Plasmodium ovale* liver stages in humanized mice. *Nat. Commun.* 6:7690 doi: 10.1038/ncomms8690 (2015).

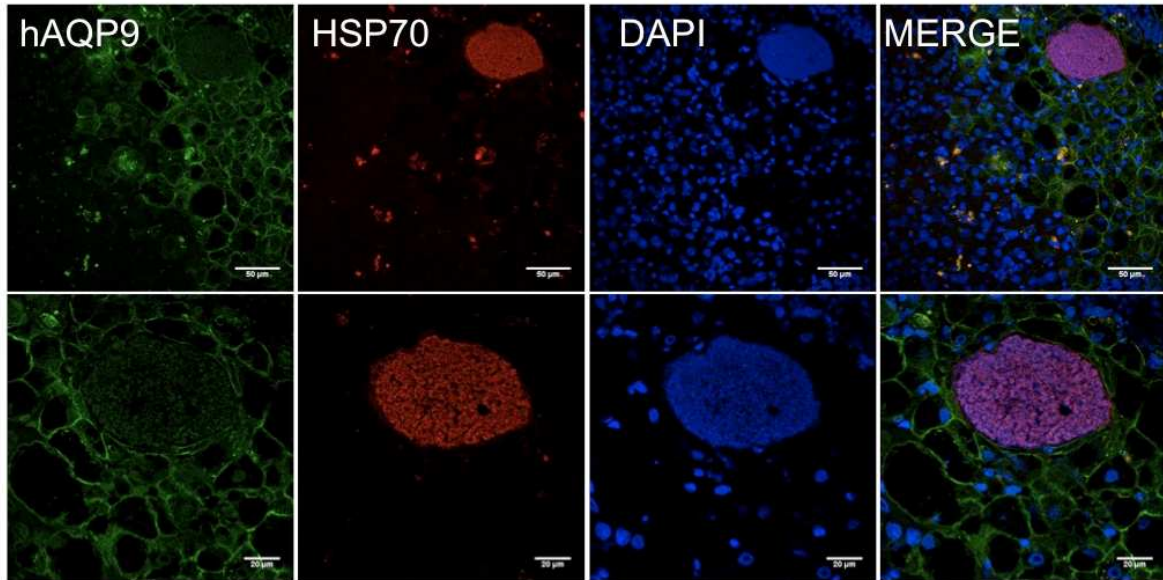


This work is licensed under a Creative Commons Attribution 4.0 International License. The images or other third party material in this article are included in the article's Creative Commons license, unless indicated otherwise in the credit line; if the material is not included under the Creative Commons license, users will need to obtain permission from the license holder to reproduce the material. To view a copy of this license, visit <http://creativecommons.org/licenses/by/4.0/>



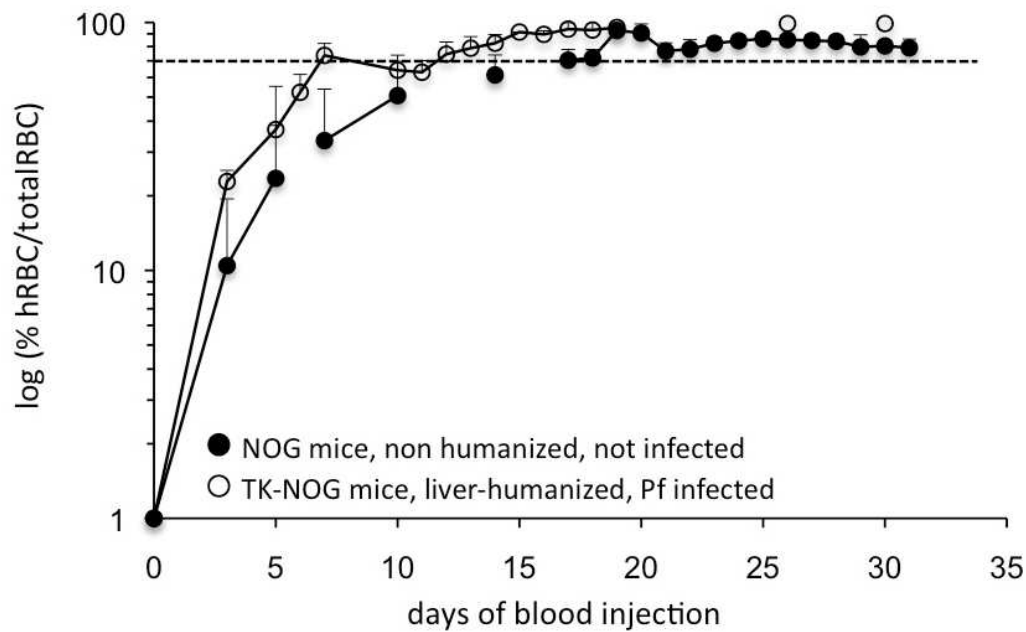
**Supplementary figure 1: Medium throughput analysis of *P. falciparum* hepatic development through the use of a fluorescence slide scanner.**

50 μm-thick liver sections were stained for *Plasmodium* HSP70 and DAPI and analyzed with a fluorescence slide scanner. **A.** Picture of a whole liver section stained for HSP70 and DAPI showing numerous day 7-schizonts. **B.** Magnification x20 of two mature schizonts.



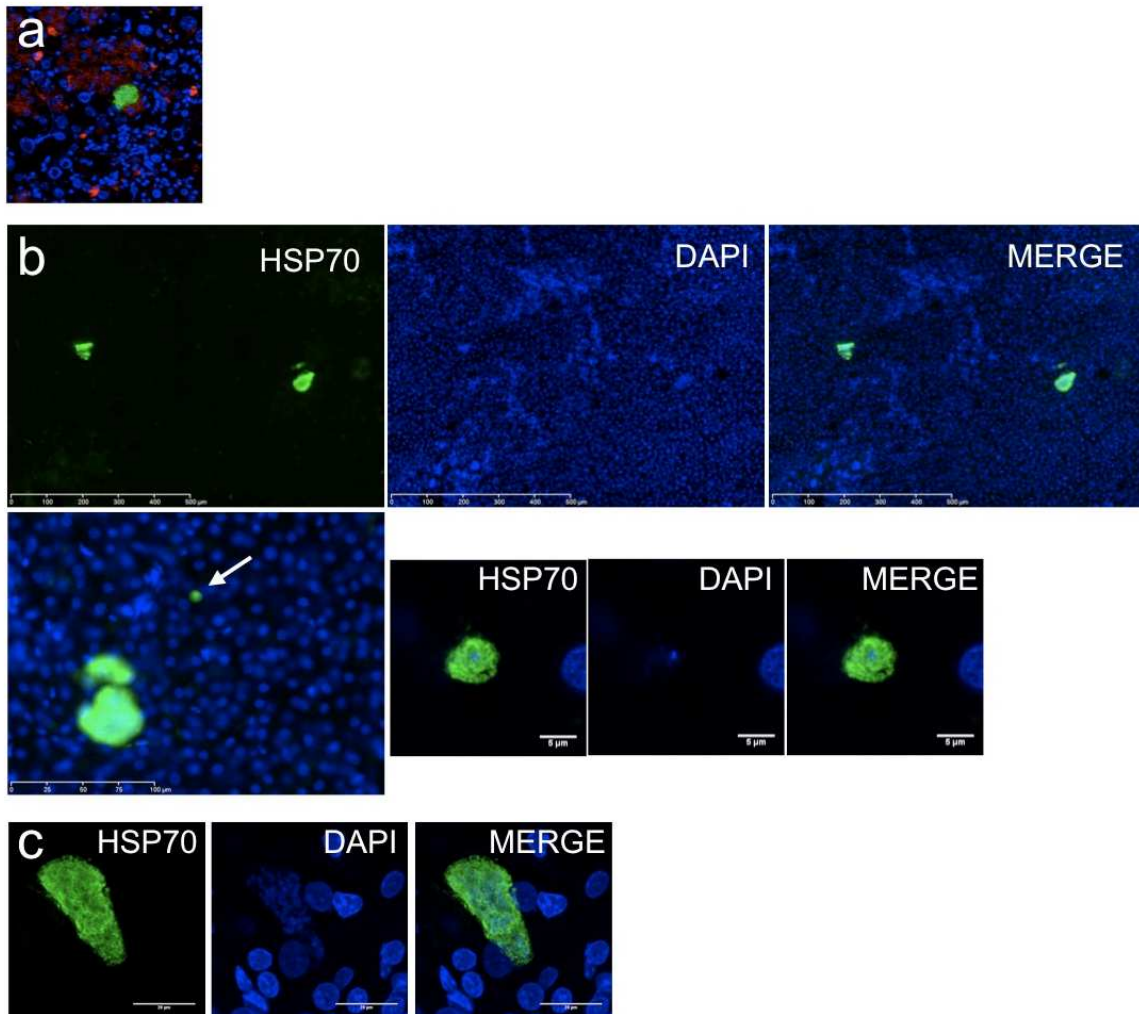
**Supplementary figure 2: *P. falciparum* develops within engrafted hHEP in LH TK-NOG mice.**

Triple staining for human membrane AQP9 protein (green), *Plasmodium* HSP70 (red) and DAPI (blue) showing parasite growth within human engrafted hepatocyte. Upper panel, bar = 50 μm. The lower panel is a higher magnification of the schizont showed above, bar = 20 μm.



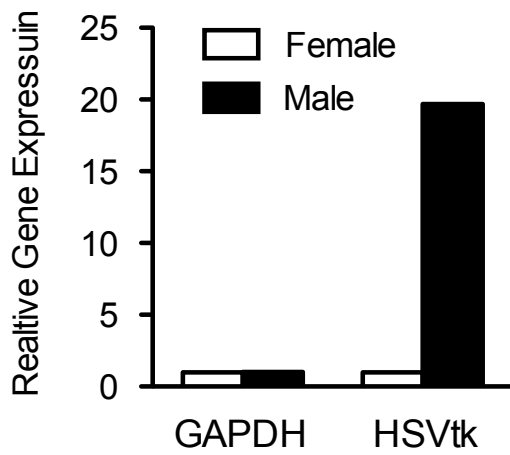
**Supplementary figure 3 : hRBC engraftment in TK-NOG mice.**

TK-NOG non transgenic mice (NOG mice), non humanized and not infected (n = 4 mice), and LH-TK NOG mice, infected with *P. falciparum* sporozoites at day 6 of hRBC injection (n = 8, 3 independent experiments), were daily injected with hRBC and the percentage of hRBC in the peripheral blood was monitored by flow cytometry. Results are expressed as the percentage of hRBC among total RBC (mean  $\pm$  SD). The dashed line shows 70% of humanization.



**Supplementary figure 4 : *P. ovale* hepatic development in LH-TK NOG mice.**

Representative pictures of *P. ovale* schizonts and hypnozoites at days 8 and 21 of infection stained by indirect immunofluorescence on 16- and 50  $\mu\text{m}$ -thick frozen liver sections. **A.** Triple staining for *Plasmodium* HSP70 (green), human albumine (red) and DAPI (blue) showing parasite growth within human engrafted hepatocyte; bar = 20  $\mu\text{m}$ . **B.** Fluorescent slide scanner pictures showing two *P. ovale* mature schizonts (upper panel), and a schizont close to a hypnozoite (white arrow, left picture of lower panel). Lower panel, right pictures: higher magnification of the hypnozoite showing the unique nucleus of the round shaped 5  $\mu\text{m}$  diameter parasite; bar = 5  $\mu\text{m}$ . **C.** Picture of the day 21-schizont found in the first *P. ovale* infection; bar = 20  $\mu\text{m}$ .



**Supplementary Figure 5: Gender difference in transgene expression.**

Comparison of HSVtk transgene expression between female and male TK-NOG mice of same age (8 weeks old) by RT-qPCR. The expression of HSVtk transgene was normalized to the expression of glyceraldehyde 3-phosphate dehydrogenase (GAPDH).

	Mouse #	hAlb (mg/mL) <sup>a</sup>	%hRBC <sup>b</sup>
<b>Exp #1</b>	1 <sup>†</sup>	5.2	84.6
	2	5.1	77.8
<b>Exp #2</b>	3 <sup>†</sup>	5.7	82.7
	4 <sup>†</sup>	7.4	97.9
	5 <sup>†</sup>	9.8	98.1
<b>Exp #3</b>	6	9.3	83.7
	7	5.5	93.4
	9	7.2	98.2

**Supplementary Table 1: Levels of liver- and RBC-humanization in doubly engrafted TK-NOG mice.**

<sup>a</sup>Level of human albumin within two weeks before starting engraftment of hRBC, one week before inoculation of sporozoites.

<sup>b</sup>Percentage of hRBC measured between day 6 and 8 post-sporozoite inoculation.

All three experiments were performed with distinct batches of human hepatocytes, human RBC and *P. falciparum* sporozoites.

<sup>†</sup>Mice #1, 3, 4 and 5 were monitored for parasitemia *in vivo*.

	<b>Batch</b>	<b>Gender</b>	<b>Age</b>
<b>Lonza CC-2591S<sup>a</sup></b>	7F3063	F	4 Y
<b>BPI HEP187<sup>a</sup></b>	HEP187266-TA05	M	5 Y

**Supplementary Table 2: Human hepatocytes used for engraftment of TK-NOG mice in CIEA. <sup>a</sup>Negative for HIV, HBV, HCV**



## ARTICLE 2

### ***Plasmodium falciparum* PfSET7: enzymatic characterization and cellular localization of a novel protein methyltransferase in sporozoite, liver and erythrocytic stage parasites**

Chen, Ding, Zanghi et al, *Scientific Reports*, 2016

Histone post-translational modifications (PTMs) have been linked to several key biological processes in the blood stage development of *P. falciparum*. Amongst the well-characterized PTMs, the methylation of lysine 4 and 9 of Histone H3 (H3K4me or H3K9me) play a central role in the regulation of the clonally variant gene families responsible for *P. falciparum* virulence. However, to date, the enzymes that are responsible for generating these marks, the histone methyltransferases, HKMTs, have been poorly characterized. The *P. falciparum* genome encodes 10 HKMTs containing the catalytic SET domain. In this paper, we characterize PfSET7, a putative HKMT of unknown specificity. For the first time, we produced recombinant *P. falciparum* PKMT and demonstrated that it possesses high methyltransferase activity towards H3K9 and H3K4. To our surprise, PfSET7 preferentially methylated these residues in the context of pre-existing H3K14Ac. By using anti-PfSET7 antibodies, immunofluorescence assays localized the protein to different foci near the nucleus of erythrocytic and liver stage *P. falciparum* parasites, but in sporozoites the protein was more spread out in the cytoplasm. The production of the first active PfSET protein will allow for the screening of different small molecule inhibitors of methyltransferase activity that can be subsequently be used to investigate the biological role of HKMTs in the *Plasmodium* life cycle, and eventually lead to the development of new antimalarial drugs.

**In this study, my contribution was to investigate PfSET7 localization in pre-erythrocytic stages of *P. falciparum*. I characterized this using anti-PfSET7 antibodies and performing immunofluorescence assays in sporozoites and fully mature liver schizonts obtained from the infection of TK-NOG humanized mice described in the previous chapter.**



# SCIENTIFIC REPORTS



OPEN

## *Plasmodium falciparum* PfSET7: enzymatic characterization and cellular localization of a novel protein methyltransferase in sporozoite, liver and erythrocytic stage parasites

Received: 09 December 2015

Accepted: 01 February 2016

Published: 23 February 2016

Patty B. Chen<sup>1,2,3,\*</sup>, Shuai Ding<sup>1,2,3,\*</sup>, Gigliola Zanghi<sup>4</sup>, Valérie Soulard<sup>4</sup>, Peter A. DiMaggio<sup>6</sup>, Matthew J. Fuchter<sup>7</sup>, Salah Mecheri<sup>1,2,3</sup>, Dominique Mazier<sup>4,5</sup>, Artur Scherf<sup>1,2,3</sup> & Nicholas A. Malmquist<sup>1,2,3</sup>

Epigenetic control via reversible histone methylation regulates transcriptional activation throughout the malaria parasite genome, controls the repression of multi-copy virulence gene families and determines sexual stage commitment. *Plasmodium falciparum* encodes ten predicted SET domain-containing protein methyltransferases, six of which have been shown to be refractory to knock-out in blood stage parasites. We have expressed and purified the first recombinant malaria methyltransferase in sufficient quantities to perform a full enzymatic characterization and reveal the ill-defined PfSET7 is an AdoMet-dependent histone H3 lysine methyltransferase with highest activity towards lysines 4 and 9. Steady-state kinetics of the PfSET7 enzyme are similar to previously characterized histone methyltransferase enzymes from other organisms, however, PfSET7 displays specific protein substrate preference towards nucleosomes with pre-existing histone H3 lysine 14 acetylation. Interestingly, PfSET7 localizes to distinct cytoplasmic foci adjacent to the nucleus in erythrocytic and liver stage parasites, and throughout the cytoplasm in salivary gland sporozoites. Characterized recombinant PfSET7 now allows for target based inhibitor discovery. Specific PfSET7 inhibitors can aid in further investigating the biological role of this specific methyltransferase in transmission, hepatic and blood stage parasites, and may ultimately lead to the development of suitable antimalarial drug candidates against this novel class of essential parasite enzymes.

While global mortality due to malaria has decreased since the beginning of this century, this parasitic disease continues to claim approximately 0.6 million lives per year, particularly in the vulnerable populations of children under five years of age and pregnant women<sup>1</sup>. Malaria eradication efforts have been hindered by the incredible ability of the parasite to develop resistance to existing antimalarials, prompting the search for novel essential factors to serve as potential drug targets. The complex life cycle of human malaria parasites involves an insect vector phase, a liver stage at the onset of infection, an asexual blood stage responsible for disease pathogenesis

<sup>1</sup>Unité Biologie des Interactions Hôte-Parasite, Département de Parasites et Insectes Vecteurs, Institut Pasteur, Paris 75015, France. <sup>2</sup>CNRS, ERL 9195, Paris 75015, France. <sup>3</sup>INSERM, UMR 1201, Paris 75015, France. <sup>4</sup>Sorbonne Universités, UPMC Univ Paris 06, INSERM U1135, CNRS ERL 8255, Centre d'Immunologie et des Maladies Infectieuses (CIMI-Paris), 91 Bd de l'hôpital, 75013, Paris, France. <sup>5</sup>AP HP, Centre Hospitalo-Universitaire Pitié-Salpêtrière, 75013 Paris, France. <sup>6</sup>Department of Chemical Engineering, Imperial College London, South Kensington Campus, London SW7 2AZ, United Kingdom. <sup>7</sup>Department of Chemistry, Imperial College London, South Kensington Campus, London SW7 2AZ, United Kingdom. \*These authors contributed equally to this work. Correspondence and requests for materials should be addressed to N.A.M. (email: nicholas.malmquist@pasteur.fr)

and a sexual stage permitting disease transmission. Transition through the various stages of the complex parasite life cycle is a highly controlled process regulated at the level of transcriptional gene activation. Indeed, in the experimentally tractable asexual blood stage, a clear stage-specific transcriptional cascade as been observed<sup>2</sup>. Aside from the recent discovery of a plant-derived family of transcription factors<sup>3</sup>, no canonical gene regulatory elements have been identified in *P. falciparum*. However, a variety of distinct epigenetic mechanisms have been discovered which contribute to the transcriptional control of single copy genes as well as the orchestration of clonally variant virulence gene families<sup>4–8</sup>.

Histone post-translational modifications (PTMs) play a particularly important role in the developmental progression of blood stage malaria parasites. The role of histone PTMs was first demonstrated in the monoallelic expression of a virulence gene family known as the *var* genes, which are involved in antigenic variation and pathogenesis<sup>4</sup>. Subsequent studies have shown that transcriptional activation and silencing of virtually all genes is associated with histone methylation or acetylation<sup>5,6</sup>. The tri-methylation of histone H3 lysine 4 (H3K4me3) and acetylation of histone H3 lysine 9 (H3K9ac), associated with transcriptional activation in the conserved histone code, is indeed associated with actively transcribed genes, including the single expressed *var* gene, in *P. falciparum*<sup>5,6</sup>. Tri-methylation of histone H3 lysine 9 (H3K9me3), a repressive mark in the conserved histone code, stands out in malaria parasites for its association with the variegated gene expression of clonally variant gene families and genes encoding a parasite-induced erythrocyte permeation pathway and with regulating the commitment to transmission stage parasites<sup>5,6,9,10</sup>. Importantly, H3K9me3 is not associated with general transcriptional repression across the genome<sup>5,6</sup>. Tri-methylation of histone H3 lysine 36 (H3K36), an activation mark in the conserved histone code, plays a dual function in *P. falciparum*, as H3K36me3 is associated with transcriptionally active genes throughout the genome but also is associated with silenced members of *var* genes and other clonally variant gene families<sup>11</sup>. Additional methylation PTMs exist on *P. falciparum* histones, some of which are conserved throughout eukaryotes while others are unique to *Plasmodium*<sup>12</sup>. These methylation marks exist in combination with other PTMs such as acetylation and phosphorylation<sup>13</sup>, but their functions, either singly or in combination, remain to be elucidated.

Protein methyltransferase enzymes (PMTs) catalyze the mono-, di- or tri-methylation of lysine residues (PKMTs) or the mono- or di-methylation of arginine residues (PRMTs). PKMTs and PRMTs were initially thought to be specific for the methylation of a single protein substrate, and while some members of this class of enzyme do exhibit a high degree of protein substrate specificity, it is widely recognized that certain individual PMTs are able to methylate multiple protein substrates, including both histones in the nucleus and non-histone proteins in the cytosol<sup>14</sup>. Since both PKMTs and PRMTs have been associated with a variety of diseases including cancer, neurodegenerative and inflammatory diseases, PMT enzymes have emerged as a target class for drug discovery against human disease<sup>15</sup>.

Recently, we have expanded our fundamental research on the role of histone PTMs in malaria parasite gene regulation to include translational research into discovering PKMT inhibitors for both the further study of parasite biology using a chemical biology approach and for the potential development of novel classes of future antimalarials. In the absence of recombinant target parasite enzymes we initiated an approach based on targeting malaria parasite histone methylation using a known inhibitor of a human PKMT, BIX-01294<sup>16–18</sup>. These studies established histone methylation to be a viable target for antimalarial drug discovery, as BIX-01294 and its derivatives cause rapid and specific parasite death with the concomitant reduction in parasite histone methylation levels<sup>16</sup>. These inhibitor-based results have motivated increased efforts into recombinant PfPKMT enzyme production to both fully characterize these enzymes and to enable a target-based approach to discovering specific malaria parasite enzyme inhibitors.

Computational analysis predicts ten PKMTs and three PRMTs in the *P. falciparum* genome. All ten identified PfPKMT genes contain a catalytic methyltransferase SET domain, named after the *Drosophila* chromatin-modifying enzymes *Su(var)3–9*, *Enhancer of zeste*, and *Trithorax*<sup>19</sup>. SET domain containing proteins were initially studied in the context of specifically methylating lysine residues of histones, but subsequent work has revealed numerous non-histone protein substrates for SET domain proteins<sup>20</sup>. Knock-out studies have indicated a subset of PfPKMTs are essential in blood stage parasites<sup>11</sup>. Despite significant efforts, the molecular characterization of PfPKMT enzyme activity has been constrained by the inability to produce sufficient quantities of recombinant proteins. Cui *et al.* were able to express four PfPKMTs (PfSET1, PfSET2, PfSET3, PfSET8) using a wheat germ expression system, but only assign histone H4 lysine 20 (H4K20) methyltransferase activity to PfSET8 and histone H3 methyltransferase activity to PfSET2 through Western blots analysis and autoradiography of enzyme reactions containing nucleosomes as protein substrates<sup>21</sup>. PfSET2, since re-named PfSETvs, was confirmed to have H3K36 methyltransferase activity through the observed reduction of this mark along *var* genes in PfSETvs knock-out parasites<sup>11</sup>. Volz, *et al.* were able to detect low-level H3K4 methyltransferase activity for an affinity-tagged version of endogenous PfSET10 immunoprecipitated from transgenic parasites<sup>22</sup>. To date, no isolated PfPKMT enzymes have undergone biochemical characterization to determine substrate specificity and enzyme kinetic parameters.

In this report we describe the first large-scale production and enzymatic characterization of a recombinant *P. falciparum* PKMT, the poorly understood PfSET7, purified from a baculovirus expression system. Recombinant PfSET7 displays comparable kinetics to other characterized PKMTs from human and mouse with regards to enzyme turnover and AdoMet methyl-donor utilization. Nucleosome labeling experiments reveal that PfSET7 extensively methylates H3K4 and H3K9, but modifies the latter particularly in the presence of pre-existing acetylated histone H3 lysine 14 (H3K14ac). Immunofluorescence imaging of blood stage parasites, however, reveals PfSET7 to localize to distinct foci outside of the parasite nucleus. PfSET7 was also identified by immunofluorescence to be present in motile salivary gland sporozoite stage parasites and in liver stage parasite forms. Since PfSET7 was refractory to genetic knock-out in blood-stage parasites<sup>11</sup>, this enzyme is presumed to be essential in at least that stage, and therefore represents a promising antimalarial drug target candidate. With a

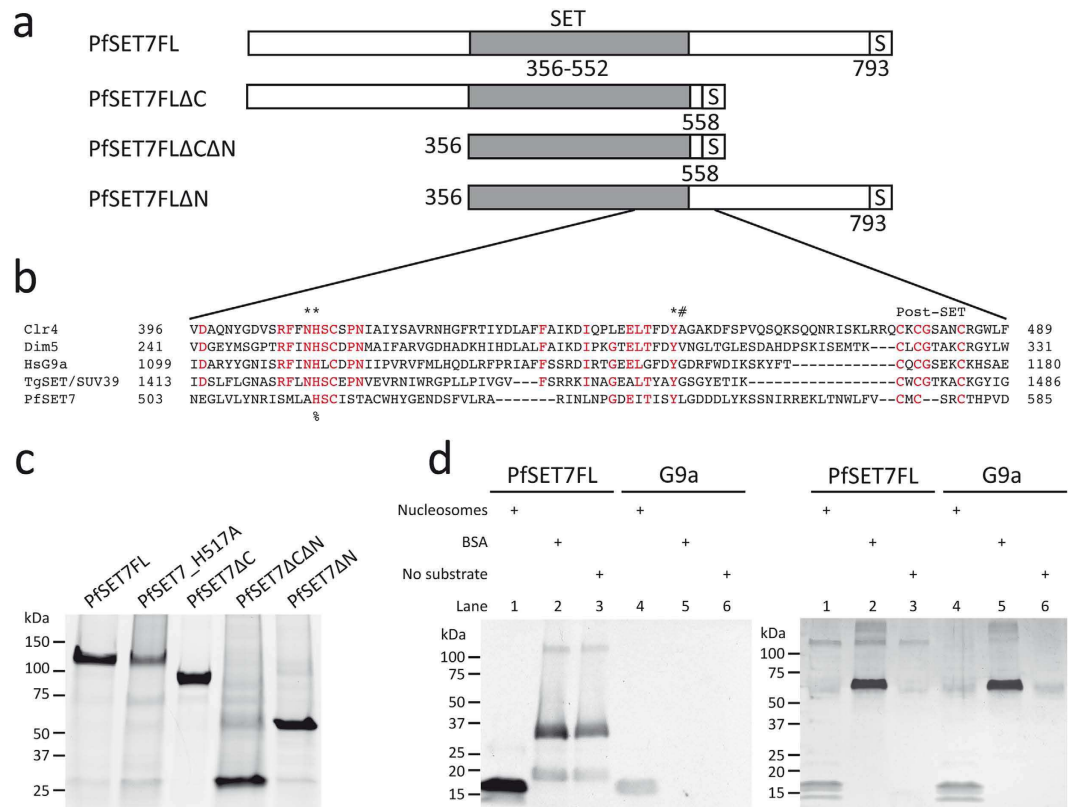


**Figure 1. Protein production and purification.** (a) Schematic of the PfSET7 full-length protein and truncated proteins, all expressed as recombinant affinity-tagged proteins. SET, SET domain; S, 2 × strep-tag. (b) Alignment of the C-terminal part of the SET domain and post-SET domains of H3K9 methyltransferases from *Schizosaccharomyces pombe* Clr4 (O60016), *Neurospora crassa* Dim5 (Q8X225), *Homo sapiens* HsG9a (Q96KQ7), *Toxoplasma gondii* SET/SUV39 (TGME49\_255970), *Plasmodium falciparum* PfSET7 (PF3D7\_1115200). Conserved residues are highlighted in red. (\*) Residues involved in catalysis. (#) Final amino acid of the SET domain. (%) Indicates residue mutated in the catalytic mutant PfSET7\_H517A. Post-SET, post-SET domain. (c) SDS-PAGE of recombinant PfSET7FL, the catalytic mutant PfSET7\_H517A, PfSET7ΔC, PfSET7ΔCΔN and PfSET7ΔN. (d) Autoradiograph (left panel) of enzyme reactions with PfSET7FL (lanes 1, 2 and 3) and MmG9a (lanes 4, 5 and 6) with nucleosomes, BSA and enzyme alone. Film was exposed 72h. Duplicate reactions were resolved by SDS-PAGE and silver stained (right panel).

biochemically characterized enzyme amenable to large-scale expression and purification, target based inhibitor discovery can proceed. Specific PfSET7 inhibitors will be useful tools to further explore the biological function of PfSET7 and have potential to be developed into a novel class of future antimalarials.

## Results

**Expression and purification of recombinant wild-type and mutant PfSET7.** The 793 amino acid PfSET7 protein contains a central catalytic SET domain followed by a short post-SET domain, which is flanked by a 355 amino acid N-terminal arm and 240 amino acid C-terminal arm (Fig. 1a). The SET domain is identifiable due to its homology with PKMTs from other species<sup>21</sup>. The C-terminal region of the PfSET7 SET domain (Fig. 1b), which contains the catalytic residues, shows higher homology to other organisms compared to the N-terminal region<sup>21</sup>. As with most of the *Plasmodium* genome, the PfSET7 gene contains a high percentage (72%) of AT nucleotides. To reduce the high AT content for heterologous recombinant protein expression we obtained a codon optimized version of wild-type full-length PfSET7 (PfSET7FL). In anticipation of potential recombinant protein production in secretory systems, two potential N-glycosylation sites were mutated. Recombinant protein expression attempts in mammalian cells and wheat germ were unsuccessful. Ultimately, an active recombinant PfSET7 enzyme fused to a C-terminal 2x-strep tag was successfully produced in a baculovirus-based Sf9 insect cell expression system.

To study the impact of the N- and C-termini on methyltransferase activity, truncated mutants of PfSET7 (Fig. 1a) were made by removing the N-terminus or the C-terminus or both termini, leaving only the SET domain. Finally, to confirm that our purified methyltransferase activity is specific to PfSET7, a catalytically inactive mutant, PfSET7\_H517A, was produced by the mutation of a single conserved catalytic residue.

Purified PfSET7FL and PfSET7\_H517A are expected to migrate at 98 kDa, though a single protein band is consistently observed at approximately 120 kDa (Fig. 1c). PfSET7ΔC is expected at 70 kDa but migrates at

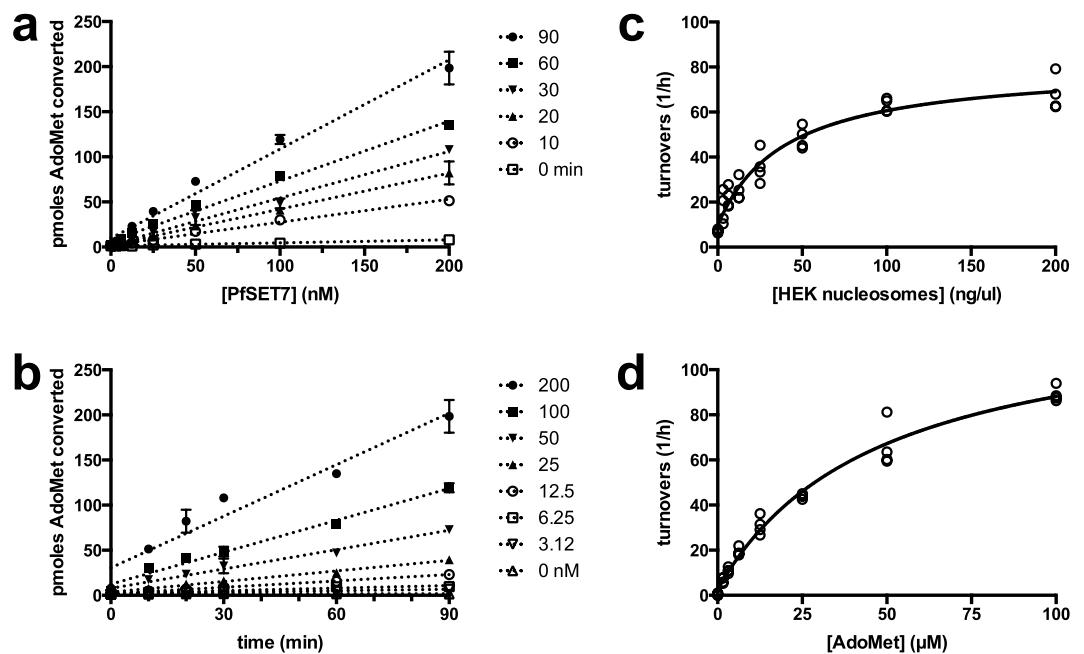


**Figure 2. Steady state enzyme kinetics of PfSET7FL.** (a) Enzyme concentration and (b) time dependent enzyme activity. (c) Saturation kinetics for HEK nucleosomes yield a  $K_m$  value of  $40 \pm 9$  ng/ul. (d) Saturation kinetics for methyl-donor AdoMet yield a  $K_m$  value of  $48 \pm 7$   $\mu$ M. Data in (a,b) are mean  $\pm$  SD of one representative experiment. Data in (c,d) are replicate values from duplicate experiments and were fitted to the Michaelis-Menton equation using GraphPad Prism software.

85 kDa. PfSET7 $\Delta$ C $\Delta$ N and PfSET7 $\Delta$ N are both expressed at an expected size of 27 and 55 kDa, respectively. Recombinant PfSET7 proteins nonetheless were purified to homogeneity.

**Steady state enzyme kinetics.** To investigate the methyltransferase activity of PfSET7FL, the purified enzyme was tested in a PKMT assay using methyl- $^3$ H-AdoMet as the methyl donor. Mouse G9a, a known histone H3K9 PKMT was used as a positive control. Both enzymes were tested for methyltransferase activity in the presence of nucleosomes as a protein substrate, with BSA as a general protein substrate, or without a protein substrate. Enzyme reaction contents were migrated on SDS-PAGE and exposed to film (Fig. 1d left panel). A second gel loaded with identical reactions using unlabelled AdoMet was silver stained to show total protein content (Fig. 1d right panel). Methyltransferase activity of PfSET7FL was confirmed by the presence of bands on the autoradiograph. In reactions with PfSET7FL and G9a with nucleosomes (Lanes 1 & 4), a band at 17 kDa corresponding to histone H3 is apparent. PfSET7FL produces a second band below H3, corresponding to histone H4. There was no methyl transfer to BSA by either enzyme (lanes 2 & 5). However, in the absence of nucleosomes or in the presence of BSA, PfSET7FL transfers methyl groups to proteins that migrate at 19 kDa, 32 kDa and 125 kDa (Lanes 2 & 3). The band at 125 kDa co-migrates with PfSET7FL and could represent automethylation of the enzyme occurring in the absence of nucleosomes, as these bands are absent when nucleosomes are present<sup>23</sup>. The two lower bands could be methylation of degradation fragments of the full-length enzyme, as there are no other common proteins added to these reactions. These results suggest PfSET7FL is primarily a histone H3 methyltransferase, with possible additional activity toward histone H4.

To characterize the enzymatic properties of PfSET7FL, time and enzyme concentration dependent activity of PfSET7FL was examined using radiometric assays (Fig. 2a,b). Enzyme activity was linear from 12.5–200 nM for up to 90 minutes of reaction time. Subsequent experiments therefore used 25 nM enzyme in 60 minutes reactions to remain in this linear range. Nucleosome-dependent activity was tested at nucleosome concentrations of 0–200 ng/ul, revealing a  $K_m$   $40 \pm 9$  ng/ul (Fig. 2c). AdoMet-dependent activity was examined at AdoMet concentrations of 0–100  $\mu$ M, yielding a  $K_m$  for AdoMet of  $48 \pm 7$   $\mu$ M (Fig. 2d). Subsequent experiments used nucleosome and AdoMet at saturating concentrations of 200 ng/ul and 100  $\mu$ M, respectively. PfSET7FL revealed a turnover of between 80 to 150  $h^{-1}$ , which is comparable to other characterized PKMTs such as mouse G9a at 88  $h^{-1}$ <sup>24</sup> and Dim5 at 180  $h^{-1}$ <sup>25</sup>.

Experiments to test pH dependence showed PfSET7FL to display peak activity near pH 8.8 (Fig. 3a), with activity decreasing above and below this pH value. Performing enzyme reactions at three different temperatures of 4  $^{\circ}$ C, 25  $^{\circ}$ C and 37  $^{\circ}$ C showed the highest activity at 25  $^{\circ}$ C (Fig. 3b). The presence of monovalent salts has been reported to be detrimental to PKMT activity for certain recombinant enzymes. However, up to 250 mM NaCl or 200 mM KCl (Fig. 3c) does not appear to affect PfSET7FL enzyme activity. Various PKMT characterization buffers reported in the literature contain divalent magnesium cations. To investigate any role for magnesium on PfSET7FL,  $MgCl_2$  was added at 100  $\mu$ M but did not appear to alter PfSET7FL enzyme activity. SET domain

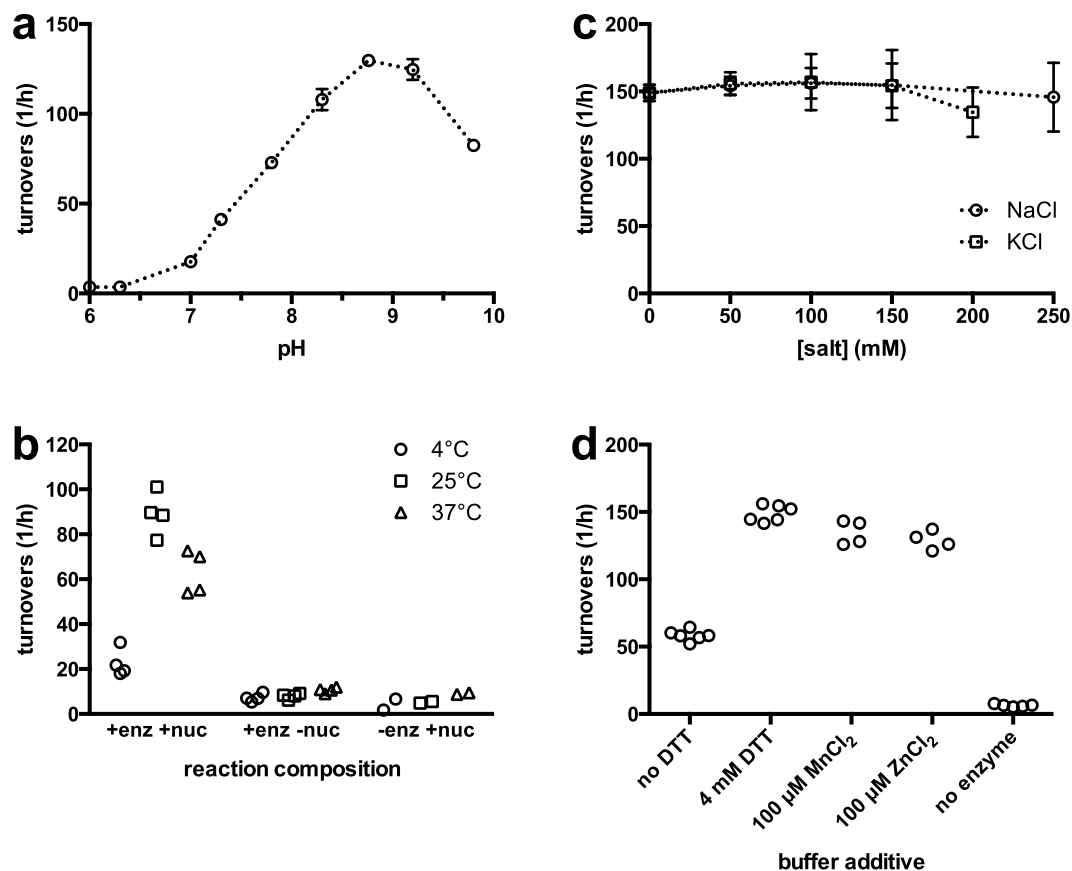


**Figure 3. Characterization of PfSET7FL enzyme reaction conditions.** (a) PKMT reactions were performed to determine pH dependent enzyme activity on a pH range of 6–10. (b) Temperature dependent enzyme activity where reactions were carried out at 4°C (circles), 25°C (squares), or 37°C (triangles). Control reactions without nucleosomes or without enzyme were performed in parallel. (c) The effect of two common salts NaCl (circles) and KCl (squares) were tested up to 250 mM or 200 mM, respectively. (d) The effect of removing DTT or adding divalent metal ions on enzyme activity. All reactions, except where noted, contain 4 mM DTT. Reactions contained 100 μM MnCl<sub>2</sub> or ZnCl<sub>2</sub> where noted. Data from at least two independent experiments are represented in (a,c) as mean ± SD. Individual data from two independent experiments are presented in (b,d).

proteins are known to contain zinc binding sites<sup>26</sup>, thus the effect of zinc ions on PfSET7FL enzyme activity was tested. The data show supplementing reactions with 100 μM zinc has little effect on apparent enzyme activity. Finally, the presence of the reducing agent dithiothreitol (DTT) was tested, and the data reveal 4 mM DTT results in increased apparent PfSET7 enzyme catalysis relative to no reducing agent present (Fig. 3d). These data define the optimal assay conditions for PfSET7FL for the present analyses for any future *in vitro* PfSET7FL studies, including further enzyme characterization or subsequent inhibitor discovery.

**PfSET7 mutational analysis.** To identify functionally important regions of PfSET7, truncation mutants were examined for catalytic activity (Fig. 4). PfSET7ΔN demonstrated PKMT activity similar to that of the full-length enzyme, indicating that the N-terminus of PfSET7 is not essential for enzyme activity.

While some PKMT enzymes contain only a catalytic SET domain<sup>27</sup>, others also possess a cysteine rich post-SET domain that is implicated in protein folding and formation of the active site<sup>28</sup>. In proteins containing a post-SET domain, this domain has been shown to be necessary for enzyme activity<sup>29</sup>. PfSET7 contains a cysteine rich putative post-SET domain similar to post-SET domains from other PKMTs, though the canonical CxCxxxxC motif as seen in Dim5 and G9a is a CxCxxC motif in PfSET7 (Fig. 1b). To test if the putative post-SET domain of PfSET7 is essential for enzyme activity, two mutants lacking the post-SET domain, PfSET7ΔC and PfSET7ΔCΔN, were produced. These mutants display no enzyme activity, indicating that the putative post-SET domain of PfSET7 may indeed be necessary for catalysis as seen in other PKMT enzymes containing post-SET domains.

Wild-type PfSET7 has two conserved catalytic residues in the SET domain (Fig. 1b), H517 and Y551<sup>21</sup>. A third catalytic residue, N516, is present in PKMTs such as Clr4, Dim5 and HsG9a, but absent in PfSET7, which contains an arginine at this location. Mutation of the conserved H517 has been shown to abolish PKMT activity<sup>30,31</sup>. Accordingly, the catalytic mutant PfSET7\_H517A shows no HKMT activity compared to PfSET7FL (Fig. 4). This confirms that the methyltransferase activity we observe is specific to PfSET7 and that mutation of a single conserved residue is sufficient to abolish the activity of this purified recombinant enzyme.

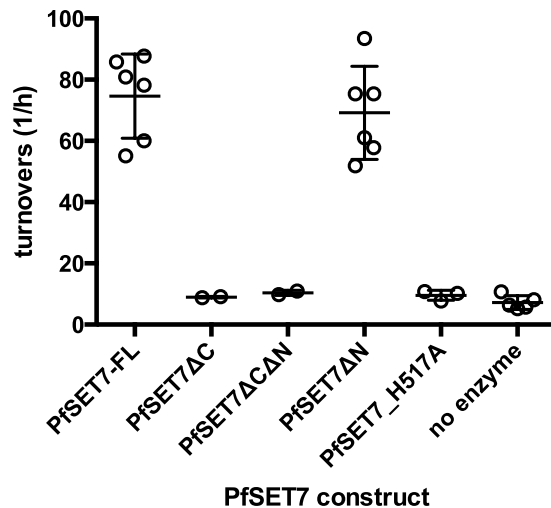


**Figure 4. PfSET7 mutational analysis.** Enzyme activity of full-length, truncated and catalytic dead versions of PfSET7. Data from two independent experiments are represented as mean  $\pm$  SD.

**Mass spectrometry identification of PfSET7 histone lysine methylation targets.** To identify the target amino acid specificity of PfSET7, we employed deuterium-labeled AdoMet (CD3-AdoMet) and isolated human nucleosomes in a mass spectrometry based enzyme assay. These experiments have the advantage of providing a protein substrate containing a range of pre-existing histone PTMs and can identify an enzyme preference for specific target residues and any influence of modifications to neighboring residues. Recombinant PfSET7 enzyme (1  $\mu$ M) was incubated with human nucleosomes (0.1 mg/mL, isolated from HEK293 nuclei) and CD3-AdoMet (1 mM) for 3 hours. Histones were prepared for mass spectrometry analysis (as described in the Methods section) to identify the lysine targets that were methylated by PfSET7, which are distinguishable from existing methylations by a CD3 mass shift (+3 Daltons) in the  $m/z$  of the modified peptide. A mass shift of 3 Daltons is necessary to sufficiently distinguish new methyl groups added by the recombinant HKMT from previously existing histone methylation, as naturally occurring isotopes (e.g.  $^{13}\text{C}$ ,  $^{15}\text{N}$ , etc) and their combinations result in abundant isotopic peaks that are +1 and +2 Daltons after the monoisotopic peak (i.e. the mass based on the most abundant isotopes:  $^{12}\text{C}$ ,  $^{14}\text{N}$ ,  $^{16}\text{O}$ , etc). The same *in vitro* labeling experiment was performed using recombinant mouse G9a as a reference control as it is known to methylate H3K9. For instance, the right panels of Figures S1 and S2 reveal significant levels of mouse G9a methylation for H3K9me3K14ac and H3K9me2K14un, respectively, where the isotopic peak cluster for every methylation event has been colour-coded based on the total number of CD3 methyl groups (blue, green and red isotopic peaks represent the signal for 1, 2 and 3 CD3 methyl groups, respectively).

Extensive labeling of H3K4 di- and tri-methylation (H3K4me2, H3K4me3) was observed for PfSET7 (left panel of Fig. 5 for H3K4me3; H3K4me2 in Fig. S1 and corresponding tandem mass spectra in Figures S3–S7), but not for mouse G9a. Interestingly, PfSET7 appears to modify H3K4 to its highest methyl occupancy, as observed by the peak intensities in the mass spectrum (in the left panel of Fig. 5, the highest intensity peak corresponds to H3K4me3 with three new CD3 methyl groups; similar trend observed in Fig. S1 for H3K4me2). PfSET7 was also observed to methylate H3K9 in the presence of existing K14 acetylation on nucleosome substrates (right panel of Fig. 5 for H3K9me3K14ac; corresponding tandem mass spectra in Figures S8–S13) to the same extent as mouse G9a (compare Figs. 5 to S1). However, whereas mouse G9a exhibited a similar degree of H3K9 methylation activity for unmodified H3K14 substrates (right panels of Figs S1 and S2), the extent of PfSET7-mediated K9 methylation was orders of magnitude lower in the absence of H3K14 acetylation, as shown in Fig. S2 for H3K9me2K14un (see also tandem MS in Figures S14–S17). This implies PfSET7 preferentially recognizes nucleosome substrates containing acetylation on H3K14.

To a lesser extent PfSET7 was also observed to methylate H3K36, particularly when H3K27 is unmodified (see Figures S18 and S19 for H3K36me1 and H3K36me3, respectively). A tandem mass spectrum was identified to support evidence of PfSET7 methylation of H3K27me2 substrates to H3K27me3 (Fig. S20). However, it should be noted that methylation activity for H3K27me2/me3 is also observed for mouse G9a, which can occur under *in vitro* conditions since the amino acid sequences around H3K9 and H3K27 are homologous (ARKST and ARKSA, respectively). Methylation of other common lysine targets (i.e. H3K18, H3K23, H3K79 and H4K20) was not observed for PfSET7.

**Cellular localization of PfSET7 in blood stage parasites.** To identify the cellular location of PfSET7 in parasites, a Pf3D7-SET7-HA-glmS integrant transfected line was generated through markerless insertion at the PfSET7 genomic locus of a  $3 \times$  HA affinity tag and the glmS ribozyme using the CRISPR/Cas9 genome editing tool. Correct genomic integration of this transgenic parasite line was confirmed by PCR and endogenous tagged protein expression was confirmed by Western Blot (Fig. S21). This glmS construct was designed to produce an inducible knock-down parasite line, but was found to be inefficient at PfSET7 mRNA and protein reduction in the presence of glucosamine inducer, and induced parasites displayed no obvious growth phenotype (Fig. S22).

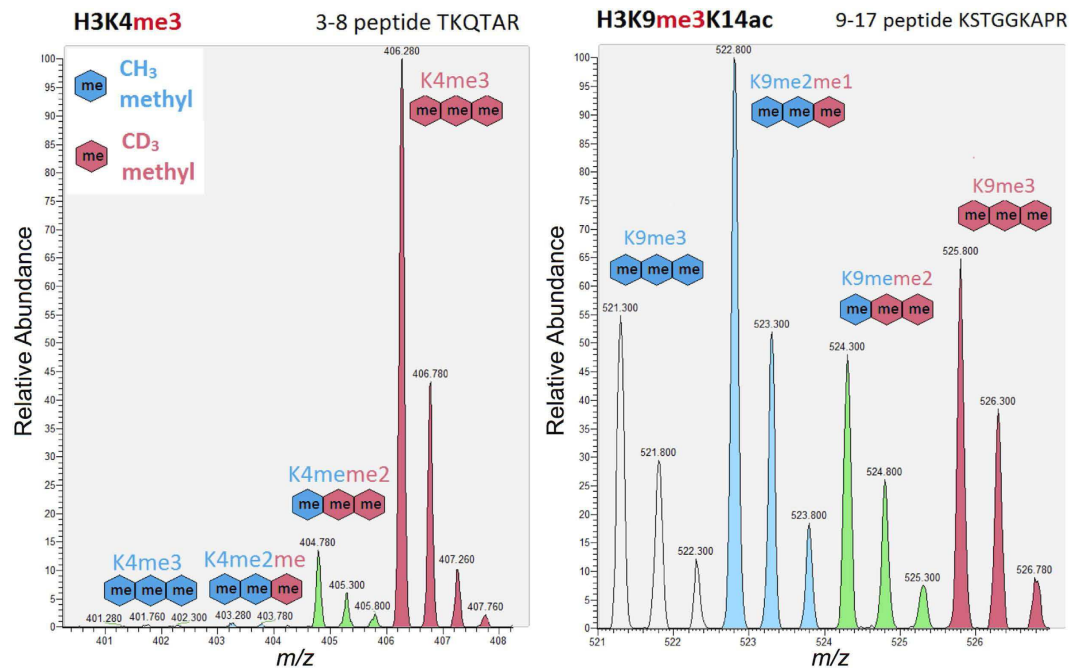


**Figure 5. PfSET7 extensively methylates H3K4 and H3K9 in the presence of H3K14ac.** Recombinant PfSET7 enzyme was incubated with human nucleosomes and CD3-labeled S-adenosyl-methionine to identify the histone lysine targets of PfSET7, which are distinguishable from existing methylations (blue colored ‘me’ symbols) by a CD3 mass shift (+3 Daltons; red colored ‘me’ symbols) in the  $m/z$  of the modified peptide. Significant labeling of H3K4me2 and H3K4me3 by PfSET7 was observed (shown for H3K4me3 in the left panel), where the major product is the fully methylated H3K4 substrate. Extensive labeling of H3K9me2 and H3K9me3 by PfSET7 was also observed, but particularly in the presence of existing H3K14 acetylation on nucleosome substrates (shown for H3K9me3K14ac in the right panel), implying this methyltransferase exhibits some degree of nucleosome specificity (compare extent of labeling of H3K9me2K14un substrate by PfSET7 and mG9a in Supplementary Fig. S2). Annotated tandem mass spectra for all observed labeled histone peptides are provided in the Supplementary Figures.

To determine the subcellular distribution of PfSET7, whole cell extracts of the integrant Pf3D7-SET7-HA-glmS line were biochemically separated into nuclear and cytoplasmic fractions, which were examined by Western Blot for PfSET7-HA via the HA-tag and for aldolase or histone H3 for cytoplasmic or nuclear protein controls, respectively. The results show PfSET7 is present in the cytoplasmic fraction but not visible in the nuclear fraction (Fig. 6). These results suggest PfSET7 may have a role outside of the nucleus, which is unexpected for an apparent histone methyltransferase.

**PfSET7 localizes to a distinct cytoplasmic compartment in blood stages.** To assess the intracellular localization of PfSET7, *P. falciparum* parasites were analyzed by immunofluorescence microscopy (IF) using monoclonal anti-HA or polyclonal anti-PfSET7 antibodies in PfSET7-HA-glmS or wild-type parasites, respectively. Staining patterns using either antibody are virtually identical, suggesting both antibodies are equivalent in detecting PfSET7, and that affinity tagging the endogenous protein does not lead to aberrant expression or localization. (Fig. S23). Through the three major asexual blood stages, PfSET7 signal exhibited a punctate pattern adjacent to the nucleus, with a concomitant increase in staining during progression through mature trophozoites and schizonts (Fig. S24). To determine whether PfSET7 is localized at the nuclear periphery or outside of the nucleus, PfSET7 staining was compared to that of PfHP1, which localizes to discrete foci within the nucleus but at the nuclear periphery<sup>32</sup>. Consistent with the biochemical fractionation experiments, PfSET7 staining is distinct from the nuclear periphery marker PfHP1 (Fig. 7a), further supporting PfSET7 cytoplasmic localization. The punctate fluorescent signal suggests PfSET7 could be localized to a cytoplasmic organelle rather than evenly distributed throughout the cytoplasm.

The discrete IF staining of PfSET7 led us to explore whether the protein localizes to other DNA-containing organelles in malaria parasites, namely the single parasite mitochondrion or the apicoplast, an organelle specific to the phylum apicomplexa. A previous study reported PfSET5 localizes to the mitochondria, but did not examine PfSET7<sup>33</sup>. To determine if PfSET7 is in the parasite mitochondrion, we combined IF staining for PfSET7 and MitoTracker Deep Red FM staining for the mitochondrion. The data show PfSET7 does not co-localize with mitochondrial staining and is therefore not located within this organelle (Fig. 7a). To determine if PfSET7 is in the apicoplast we used a parasite line expressing HA-tagged triosephosphate transporter (PfoTPT-HA), a polytopic membrane protein of the apicoplast<sup>34</sup>. The IF images show no signal overlap between PfSET7 and PfoTPT, indicating PfSET7 is not located in the parasite apicoplast (Fig. 7a). Other markers for organelles whose ontogeny begins in early stage were used to evaluate their proximity to PfSET7, including anti-Bip for the endoplasmic

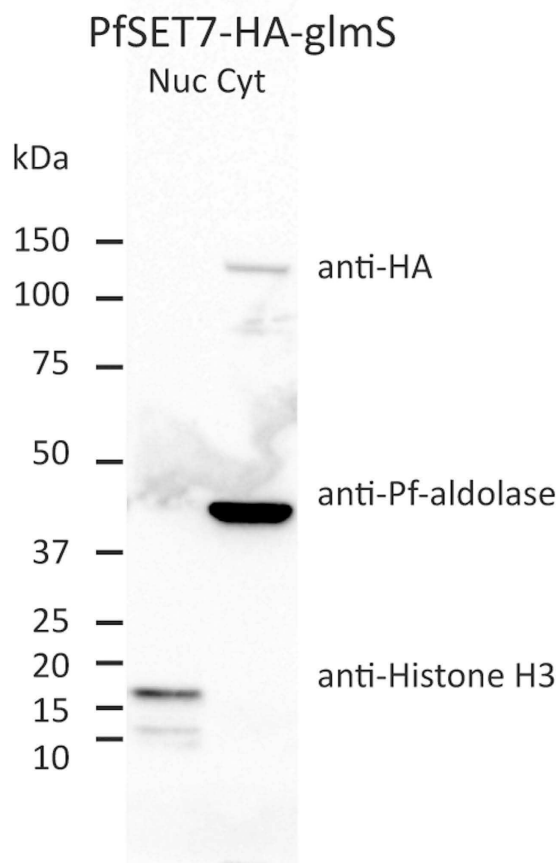


**Figure 6. PfSET7 expression and cytoplasmic localization.** Western blot of nuclear and cytoplasmic fractions of asynchronous parasites using anti-HA antibodies against PfSET7-HA-glmS. The two fractions were monitored for purity using control antibodies anti-Pf-aldolase (predicted MW: 29 kDa) for the cytoplasm and anti-histone H3 (predicted MW: 15 kDa) for the nucleus. Anti-HA recognized the PfSET7-HA band of >100 kDa (predicted MW: 98 kDa) in the cytoplasm.

reticulum and anti-EDR2 for the cis-golgi apparatus (Fig. 7a). Results from IF studies utilizing markers for these two organelles reveal that PfSET7 does not co-localize with either the endoplasmic reticulum or the cis-golgi. These combined IF results suggest PfSET7 is localized to a distinct compartment in the cytoplasm.

**PfSET7 expression in *P. falciparum* sporozoites and in liver stage schizonts.** To characterize PfSET7 expression in pre-erythrocytic parasite stages, immunofluorescence imaging was performed on *P. falciparum* mosquito salivary gland stage sporozoites and on hepatic forms. As motile sporozoites productively invade hepatocytes, these forms undergo a radical morphological remodeling, a process first discernible by a bulbous expansion that progressively enlarges to become the early spherical hepatic stage<sup>35</sup>. PfSET7 staining of freshly isolated sporozoites shows an uneven and clustered localization in the cytoplasm (Fig. 7b). Upon sporozoite transformation into early hepatic forms under axenic conditions, a similar cytoplasmic staining is observed with a more intense focal signal at the growing bulb (Fig. 7b). Nearly fully mature hepatic schizonts (just prior to merozoite egress) were imaged in liver sections from humanized mice seven days post-sporozoite inoculation (Fig. 7c). PfSET7 is found in these hepatic schizonts in a punctate pattern as distinct dots observed near the nucleus of each forming merozoite. This cytoplasmic and nucleus-associated fluorescence pattern is similar to that observed in asexual blood stage parasites.

## Discussion

Epigenetic gene regulation plays a critical role in malaria parasites in the control of general transcriptional regulation, monoallelic expression of virulence genes and in the commitment to transmission stage development. A major mechanism of epigenetic regulation in *P. falciparum* is mediated by histone post-translational modifications, which have been linked to transcriptional activation throughout the *Plasmodium* genome and to transcriptional repression of *P. falciparum* multi-copy gene families<sup>36</sup>. Building upon our fundamental research into parasite gene regulation, we have taken a chemical biology approach to target malaria methyltransferase enzymes in an effort to identify the biological role of individual PfPKMTs, ideally through the development of specific enzyme inhibitors. We have recently reported the identification and development of one PKMT inhibitor series entirely through phenotypic readouts<sup>16–18</sup>, but the inability to produce functional recombinant PfPKMTs has

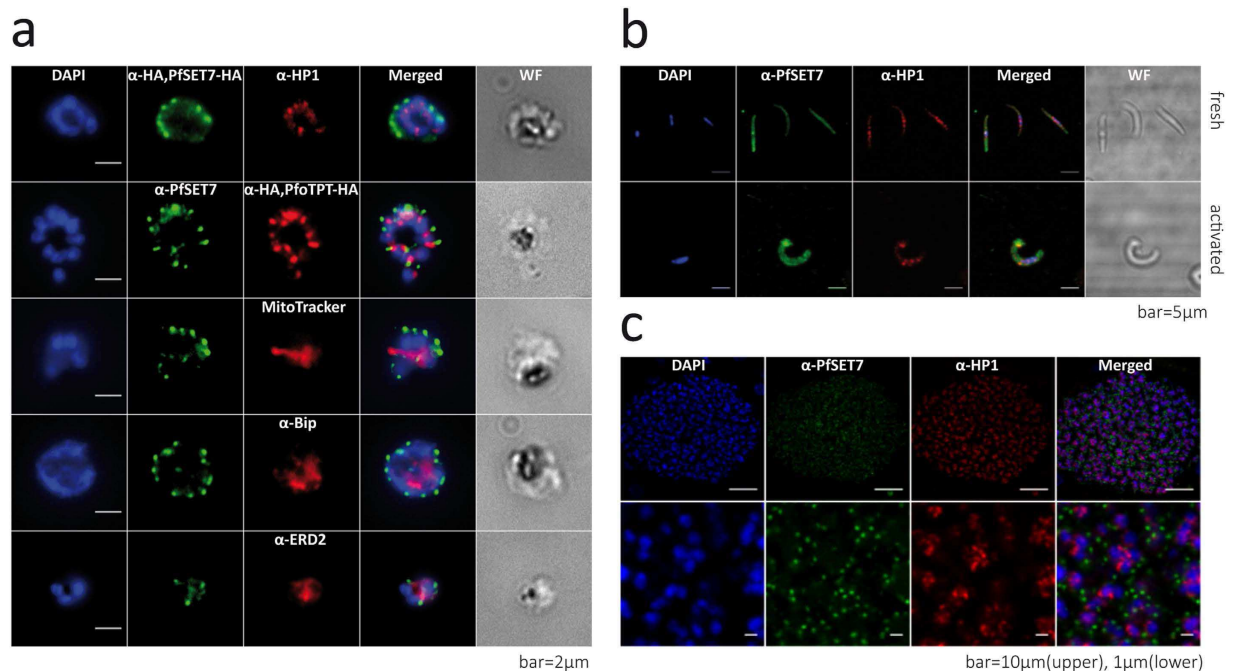


**Figure 7. Immunofluorescence localization of PfSET7 at different stages of the *Plasmodium falciparum* life cycle.** (a) Asexual blood stage parasites. Markers used were: DAPI as a DNA marker, anti-HA in PfSET7-HA parasites, anti-PfSET7 in wild-type parasites, anti-HP1 as a nuclear periphery marker, anti-HA in PfoTPT-HA parasites as an apicoplast marker, MitoTracker Deep Red FM staining for the mitochondrion, anti-Bip as an ER marker and anti-ERD2 as a cis-golgi marker. The scale bars correspond to 2  $\mu$ m. (b) Mosquito salivary gland stage sporozoites. The PfSET7 is expressed in fresh (upper panel) and activated sporozoites (lower panel) characterized by the transformation bulb. Sporozoites are visualized by DAPI staining, anti-PfSET7 and anti-HP1 immunostaining. The scale bars correspond to 5  $\mu$ m. (c) Liver stage parasites. Upper panel: liver stage schizonts from TK-NOG humanized mice were immunostained with anti-PfSET7 and anti-HP1 at day 7 post-infection. The scale bar corresponds to 10  $\mu$ m. Lower panel: higher magnification of the image above. The scale bar corresponds to 1  $\mu$ m.

greatly limited our ability to take a target-based approach to PfPKMT inhibitor discovery. Indeed, the difficulty with producing recombinant PfPKMT enzymes by us and other researchers has greatly limited the functional understanding of this entire class of parasite enzymes. Notably, we tested numerous bacterial, eukaryotic and *in vitro* protein expression systems before successfully producing sufficient quantities of active PfSET7 enzyme using a baculovirus-based insect cell expression system.

Here we report the first large-scale production of an active full-length recombinant PfPKMT, allowing a detailed *in vitro* enzyme kinetics investigation of this important enzyme class in malaria parasites. PfSET7 exhibits kinetic characteristics similar to other PKMTs from other organisms in terms of steady-state AdoMet cofactor utilization, peak activity at pH ~9 and a dependence upon a catalytic histidine residue<sup>24,27,37</sup>. Mutational analysis of truncated PfSET7 enzymes revealed at least the post-SET domain of the C-terminal protein beyond the SET domain is required for PKMT activity, as truncated enzymes lacking this segment of the protein were inactive. PfSET7 does not exhibit decreased activity at increased salt concentrations, as has been reported for some PKMT enzymes when using peptide substrates but not nucleosome protein substrates, a result that has previously been suggested to support the interpretation that nucleosomes are the physiological substrate of a given PKMT<sup>38</sup>. Methyl transfer to isolated nucleosome protein substrates is saturable, further suggesting histones are a legitimate protein substrate for PfSET7. As additional support that PfSET7 is a histone methyltransferase, nucleosome labeling studies using heavy-labeled AdoMet reveals that PfSET7 extensively methylates H3K4 and H3K9, the latter target particularly in the presence of a pre-existing H3K14ac mark. Despite the specific methylation of histones, which are overwhelmingly present in the parasite nucleus, Western blot analysis and immunofluorescence localization reveal PfSET7 is detected primarily in the cytosol in blood stage parasites. Additional immunofluorescence localization in salivary gland sporozoites and liver stage parasites reveals PfSET7 to be localized throughout the cell in sporozoites and, in liver stage parasites, located at distinct foci in the cytosol adjacent to parasite nuclei similar to blood stage parasites. The specific role of PKMT enzymes in sporozoites has not been studied. PKMT enzymes in liver stage hypnozoite forms of *P. cynomolgi* malaria parasites have been linked to the maintenance of quiescence<sup>39</sup>, though no specific PfPKMT has been implicated in this process.

The functional significance of H3K4, H3K9 and to a lesser extent H3K36 methylation by PfSET7 is not presently understood. The methylation of H3K9 in the presence of existing H3K14 acetylation has been reported previously in mass spectrometry-based analyses of *P. falciparum* histones<sup>12</sup>, indicating this is indeed a bona fide histone PTM combination present in malaria parasites. By ChIP analysis, the H3K9me3 mark in *P. falciparum*

has been closely linked to the monoallelic expression of genes encoding variant surface antigens<sup>5,6</sup>. Importantly, these ChIP studies used commercially available antibodies specific for the single H3K9me3 histone modification, which would presumably not discriminate between the presence or absence of H3K14ac with regards to H3K9me3. Further investigation could therefore determine whether the H3K9me3K14ac mark is responsible for regulating a subset of the genes associated with H3K9me3, and thus implicate PfSET7 in an even finer level of epigenetic control over multi-copy gene families. This finding also highlights the strengths of using mass spectrometry to detect heavy methyl labeling of modified nucleosome substrates, as assays employing unmodified histone substrates (peptides, histone proteins or nucleosomes) would fail to detect such activity. While methylation of H3K4 and H3K9 (in the presence of K14ac) methylation by PfSET7 were observed to be most abundant, further studies will be required to elucidate the significance of the H3K27 and H3K36 methylations observed in lower abundance (Figs S18–S20). Notably, the control experiment using mouse G9a enzyme reveals similar methylation of H3K27me3, perhaps resulting from the sequence homology between H3K9 and H3K27, and thus could represent a consequence of the *in vitro* assay conditions. However, the PfSET7 mediated methylation of H3K36 in the context of unmethylated H3K27 substrates is not observed in the mouse G9a enzyme control, and thus may represent an additional interesting target to investigate further.

The primarily cytosolic localization of PfSET7 in asexual blood stage parasites was unanticipated for a putative histone methyltransferase. However, PKMT enzymes which are localized in both the nucleus and the cytosol have been reported, including the human histone H3K9 specific PKMT SetDB1<sup>40</sup>. As well, newly synthesized histones have been reported in other organisms to be methylated at H3K9 and acetylated at H3K14 within histone-chaperone protein complexes in the cytoplasm<sup>41,42</sup>. This opens the possibility that PfSET7 is a cytosolic histone methyltransferase acting on newly synthesized histones in a PfSET7-defined subcellular cytosolic compartment. Future pull-down studies could confirm whether similar histone-chaperone protein complexes exist in *Plasmodium*. Alternatively, PfSET7 may methylate recycled, pre-modified histones. Very little is known about the order of addition of histone PTMs or histone recycling in *Plasmodium*, and additional investigation of PfSET7 through genetic or chemical attenuation may be able to address the cytosolic role of PfSET7 on the methylation of newly synthesized or recycled histones. Alternatively, many PKMT enzymes which were originally reported to be histone methyltransferases were subsequently found to possess one or more additional non-histone protein substrates<sup>15</sup>. As such, it is entirely possible that PfSET7 has additional non-histone protein substrates in the parasite cytosol, though further studies would be required to address this hypothesis.

Altogether, the production and enzymatic characterization of recombinant PfSET7 enzyme now allows for small molecule inhibitor discovery against this histone methyltransferase previously reported to be essential in blood stage parasites<sup>11</sup>. Inhibitors identified through target-based discovery can be used as tools to dissect the biological role of PfSET7 with regards to histone and potential non-histone protein methylation, and the role of the H3K9me3K14ac histone PTM combination for which PfSET7 appears to be specific. Chemical biology experiments using PfSET7 specific inhibitors can be corroborated using, for example, inducible knock-down of PfSET7 in blood stage parasites, the stage in which various genetic techniques have been established and continue to be developed. However, chemical genetics investigations using specific PfSET7 inhibitors may prove much more powerful in determining the biological role of PfSET7 in sporozoite and liver stage parasites, which are much less amenable to genetic manipulation, but present fascinating biology as the obligate initial stage of malaria infection and are responsible for malaria relapses in *P. vivax* and *P. ovale* infections. Ultimately, successfully developed small molecule inhibitors of PfSET7 may enter the antimalarial drug discovery pipeline as a much needed new chemical entity against this novel target class.

## Methods

**Protein expression constructs.** Codon optimized full-length PfSET7 (PfSET7FL) gene (PlasmoDB Gene ID PF3D7\_1115200) was synthesized (Genscript), fused to a C-terminal double Strep-tag and ligated into the transfer vector pVL1393. Two potential glycosylation sites in PfSET7FL, S122A and T784A, were mutated to allow expression in secretory systems. The SET domain of PfSET7 was identified using Prosite (prosite.expasy.org). Truncated constructs of PfSET7 were generated by PCR (Pfu Ultra II, Agilent Technologies) using specific primers (Table S1). PfSET7 $\Delta$ C (residues 1–558), PfSET7 $\Delta$ C $\Delta$ N (residues 356–558), PfSET7 $\Delta$ N (residues 356–793) and the double strep-tag, were amplified and inserted into pVL1393 via Gibson assembly (NEB). The PfSET7\_H517A catalytic mutant was generated by site directed mutagenesis using PfSET7FL as template (primers in Table S1). Clones were verified to be error free and in frame by sequencing (GATC).

**Protein expression and purification.** Recombinant proteins were expressed using a baculoviral expression system following manufacturer's instructions. Briefly, 5  $\mu$ g of plasmid, 500 ng linearised baculovirus DNA (BestBac 2.0, Expression Systems) was transfected with Cellfectin (Life Technologies) into Sf9 insect cells grown in media (Insect Xpress, Lonza) supplemented with 5% fetal bovine serum and 50  $\mu$ g/ml gentamycin. Positive baculoviral clones were selected and viral stocks for protein production were made by several cycles of viral amplification. Recombinant proteins were purified using StrepTrap HP columns (GE Healthcare). Briefly, pellets from infected Sf9 insect cells were resuspended in lysis buffer (10 mM TRIS, pH 7.5, 300 mM NaCl, 1% Triton X-100, 10% Glycerol and protease inhibitors), lysed by sonication using 6 bursts of 15 seconds (Vibra-Cell, Sonics and Materials) with a 1 minute pause on ice between bursts. The lysate was clarified by centrifugation (20 000  $\times$  g, Beckman Coulter) for 1h at 4  $^{\circ}$ C. The cleared lysate was filtered through 0.45  $\mu$ m filters (Durapore, Millipore), loaded onto the column, washed with wash buffer (10 mM TRIS, pH 8, 150 mM NaCl, 1 mM EDTA with protease inhibitors), then eluted (10 mM TRIS, pH 8, 150 mM NaCl, 1 mM EDTA and 2.5 mM desthiobiotin). Protein concentration was determined by Bradford Assay (Bio-Rad Protein Assay, Bio-Rad). Purified recombinant proteins were aliquoted, flash frozen in liquid nitrogen and stored at  $-80^{\circ}$ C until use. All proteins were judged to be >90% pure by SDS-PAGE.

**Nucleosome extraction.** To isolate nuclei, HEK cell pellets were resuspended in lysis buffer (20 mM HEPES, pH 7.5, 250 mM sucrose, 4 mM MgCl<sub>2</sub>, 0.5% NP-40, 0.4 mM PMSF and 5 mM TCEP), homogenized with a dounce (Wheaton), then centrifuged at 2000 × *g* for 15 minutes at 4 °C. The nuclear pellet was suspended in wash buffer (20 mM HEPES, pH 7.5, 250 mM sucrose, 4 mM MgCl<sub>2</sub>, 0.4 mM PMSF and 5 mM TCEP), centrifuged and nuclei were resuspended in wash buffer. To 0.5 ml of suspended nuclei, 20 ml of 0.65 M NaCl-sodium phosphate buffer (0.65 M NaCl, 50 mM phosphate, pH 6.8, 0.4 mM PMSF and 5 mM TCEP) was added dropwise with constant stirring, then vortexed for 1 hour at 4 °C. The nuclear lysate was passed through a column loaded with pre-wet Hydroxylapatite Fast Flow (Calbiochem) then washed with 0.65 M NaCl-sodium phosphate buffer. Nucleosomes were isolated with elution buffer (2.5 M NaCl, 50 mM phosphate, pH 6.8, 0.4 mM PMSF and 5 mM TCEP). Fractions containing nucleosomes were pooled and buffer-exchanged (HiPrep Desalting, GE Healthcare) into 50 mM sodium phosphate, pH 6.8. Pooled fractions were concentrated to 1 mg/ml by centrifugation (Amicon Ultra, Millipore) and stored at −20 °C.

***In vitro* methyltransferase assay.** Standard reactions were performed in a total volume of 25 μl in KMT buffer (50 mM TRIS, pH 8.8, 5 mM MgCl<sub>2</sub>, 4 mM dithiothreitol), with HEK nucleosomes (0.2 mg/ml final) as substrate, unless otherwise stated. For autoradiography, 2.5 μl of S-[<sup>3</sup>H-methyl]-adenosyl-L-methionine (<sup>3</sup>H-AdoMet) was added (3.7 μM final, 15 Ci/mmol, Perkin-Elmer). For kinetic characterization, <sup>3</sup>H-AdoMet was diluted with unlabeled AdoMet (Sigma) to give a final concentration of 100 μM at 0.025 Ci/mmol. PfSET7 enzyme was used at 25 nM and reactions were incubated at room temperature for 1 hour unless otherwise stated. HKMT reactions at various pH values were performed using citrate-HEPES-CHES buffer (50 mM Tri-Sodium Citrate, 50 mM HEPES, 50 mM CHES, 5 mM MgCl<sub>2</sub> and 4 mM DTT)<sup>43</sup>. 10 μl of each reaction was spotted in duplicate onto P81 Filters (Unifilter 96 well plate, Whatman), washed with 200 mM ammonium bicarbonate, dried, overlaid with scintillation fluid (Betaplate Scint, Perkin-Elmer) and read in a scintillation counter (MicroBeta2, Perkin-Elmer) and counts were converted to enzyme turnover. Analysis by fluorography was performed by resolving 20 μl of standard HKMT reactions (25 nM of PfSET7FL or G9a, 20 μg/ml of either BSA or nucleosomes, 2.5 μl of <sup>3</sup>H-AdoMet at 15 Ci/mmol, in a total volume of 25 μl in KMT buffer) on 4–15% SDS-PAGE, the gel was rinsed in EN<sup>3</sup>HANCE (Perkin-Elmer) according to manufacturer's instructions, dried and exposed to film (BioMax MR Film, Carestream). Duplicate reactions were performed with unlabeled AdoMet, resolved on 4–15% SDS-PAGE and silver stained (Dodeca, Silver Stain Kit, Bio-Rad). Mutational analysis experiments tested enzymes at 25 nM and 100 nM.

**Histone extraction and LC-MS/MS.** Deuterium labeled S-[<sup>2</sup>H<sub>3</sub>-methyl]-adenosyl-L-methionine (CD3-AdoMet) was synthesized using iodomethane-d<sub>3</sub>, AgOTf and HCOOH, according to the method of Stecher<sup>44</sup>. Nano-liquid chromatography tandem mass spectrometry (nanoLC-MS/MS) was utilized to identify sites of PfSET7 methylation on histone variants H3 and H4 based on the observation of mass shifts resulting from the incorporation of CD3 from CD3-AdoMet. Histones were acid extracted from the *in vitro* reaction buffer and processed for nanoLC-MS/MS analysis as previously described<sup>45</sup>. Briefly, the histone proteins were propionylated to label unmodified and monomethylated lysines with a propionyl group (+56 Da), which will result in a trypsin digest cleaving only at arginine residues. This produces the same histone peptide sequences regardless of any post-translational modifications present on lysine residues, and thus enables relative quantitation between different modifications on the same peptide based on signal intensity in the mass spectrometer. Subsequent propionylation of the N-termini of the corresponding histone peptides results in enhanced chromatographic resolution of isobaric (i.e. same mass) peptides (e.g. trimethylation [42.0469 Da] and acetylation [42.0106 Da] of lysine) based on their degree of hydrophobicity, thereby eliminating issues relating to signal interference and increasing confidence in PTM identification<sup>46</sup>. Approximately 1 μg of histone peptides were chromatographically resolved using an Ultimate 3000 RS-LC-nano System (Dionex), with an Acclaim PepMap100, C18 stationary phase, 2 μm particle size, 100 Å pore size, 75 μm internal diameter × 15 cm length column (Thermo Fisher). The nanoLC gradient started at 1% B (5% H<sub>2</sub>O, 95% MeCN, and 0.1% formic acid) and 99% A (0.1% formic acid and 100% H<sub>2</sub>O) and increased to 30% B over 35 min followed by an increase to 95% B over 30 mins. Real-time tandem mass spectra were acquired on an LTQ Velos Pro linear ion trap (Thermo Scientific) with a 110 min acquisition time. Targeted zoom scans were performed for *m/z* values corresponding to the modified histone peptides to mitigate dynamic range issues and tandem mass spectra corresponding to methylated histone peptides were acquired using a priority queue.

**Transgenic parasite plasmid constructs.** The CRISPR/Cas9 genome editing approach was employed to generate HA-tagged PfSET7 transgenic parasite line as described previously<sup>47</sup>. We used Protospacer Workbench to identify sgRNA sequences for PfSET7 and computationally predict off-target sites<sup>48</sup>. A 20-nt gRNA target sequence (5'-CACTGATGCTCCTCAAATTG-3') directing Cas9 cleavage near the C-terminal end of PfSET7 was cloned into the sgRNA-expression cassette in the pL6 plasmid. Two homology regions were inserted in separate cloning steps using Gibson assembly to generate the pL6-Pfset7 plasmid. The primers used are listed in Table S1. A second plasmid, pUF1-Cas9, containing an engineered *S. pyogenes* endonuclease Cas9 cassette and regulatory elements of *Pfalciparum* U6 snRNA was reported previously<sup>47</sup>.

**Parasite culture and transfections.** Asexual blood-stage parasites were cultivated using standard methods, and synchronous cultures were obtained by sorbitol treatment and plasmion enrichment. Parasites were transfected using the pre-loaded red blood cells method<sup>49</sup>. Positive selection using 2.66 nM WR99210 and 1.5 μM DSM1 and negative selection using 40 μM 5-fluorocytosine were applied sequentially in culture until the integrant transfected line was established. Genomic integration was verified by PCR.

**PfSET7 antibody production.** C57BL/6 and BALB/C mice were immunized 4 times at 14-day intervals with 20 µg doses of purified recombinant PfSET7-FL in Freund's Complete Adjuvant for the initial injection and Freund's Incomplete Adjuvant for booster injections to generate a polyclonal anti-PfSET7 antibody. Specificity of immune sera was determined by Western blot (Fig. S25).

**Subcellular fractionation and western blotting.** Subcellular extract preparations were prepared as described previously<sup>50</sup>. Equal amounts of protein were loaded and separated on 4–12% SDS-PAGE gel (Invitrogen), and analyzed by western blot using antibodies anti-PfSET7 (mouse), anti-HA (mouse, Roche 12CA5 or rat, Roche 3F10), anti-Pf-aldolase (Abcam ab38905) or anti-Histone H3 (mouse, Abcam ab1791), all at 1:2000 dilution. Secondary antibodies were anti-rabbit IgG-HRP (GE NA934V, Lot 9568295) and anti-mouse IgG-HRP (GE NA931V, Lot 9648752), both at 1:4000. Blots were developed using ECL (Thermo Scientific).

**Immunofluorescence microscopy.** Immunofluorescence microscopy on extracellular and intracellular parasites was performed as described previously<sup>51</sup>. Antibody dilutions are as follows: anti-PfHP1 (rabbit, Genscript) 1:4000, anti-PfSET7 (mouse) 1:2000, anti-HA (mouse or rat, Roche) 1:2000, anti-Bip (rabbit, MR4) 1:1000, anti-ERD2 (rat, MR4) 1:1000, and secondary goat anti-rat/rabbit/mouse Alexa-Fluor 488 or 568 conjugates (Invitrogen), all at 1:2500. Mitochondria were stained with 100 nM MitoTracker-DeepRedFM for 20 minutes at 37 °C in the dark before fixation and permeabilization. Images were captured using a Nikon Eclipse 80i microscope with a CoolSnapHQ2 camera (Photometrics). NIS Elements version 3.0 software was used for image acquisition, and Fiji software was used for analysis.

*P. falciparum* (NF54) sporozoites were isolated by aseptic dissection of the salivary glands of infected *Anopheles stephensi* obtained from the Department of Medical Microbiology, University Medical Centre, St Radboud, Nijmegen, the Netherlands.  $5 \times 10^4$  sporozoites placed on poly-L-lysine coated coverslips were either fixed or activated for 1 h at 37 °C and then fixed in 4% PFA for 10 min at room temperature. Samples were blocked in normal goat serum diluted 1:500 for 2 h at 37 °C, washed twice in PBS and incubated with anti-PfSET7 antibody at 1:1000 and anti-PfHP1 at 1:2000 for 1 h, washed twice in PBS, then incubated with secondary goat anti-mouse IgG coupled to Alexa-Fluor 488 or 594 diluted 1:500 with DAPI 1 µg/ml in the dark for 1 h.

Fifty micron thick serial sections of frozen liver from humanized TK-NOG mice infected with *P. falciparum* were prepared as previously described<sup>52</sup>. Sections were incubated overnight with anti-PfSET7 antibody diluted 1:1000 and anti-PfHP1 antibody diluted 1:2000, washed twice in PBS, then incubated with secondary antibodies and DAPI as above, at 37 °C. All antibodies were diluted in PBS containing 1% BSA and 0.2% Triton X-100. All sections were washed twice in PBS before being mounted in anti-fading medium and stored at 4 °C before analysis. Immunostained sporozoites and liver sections were examined under a confocal microscope (Olympus FV-1000, Plateforme d'Imagerie Cellulaire PICPS, La Pitié-Salpêtrière, Paris) and images were analysed using ImageJ software.

**Ethics Statement.** All animal care and experiments involving mice were conducted at the Institut Pasteur, approved by the 'Direction Départementale des Services Vétérinaires' de Paris, France (Permit Number N° 75-066 issued on September 14, 2009) and performed in compliance with institutional guidelines and European regulations ([http://ec.europa.eu/environment/chemical?s/lab\\_animals/home\\_en.htm](http://ec.europa.eu/environment/chemical?s/lab_animals/home_en.htm)). A statement of compliance with the French Government's ethical and animal experiment regulations was issued by the Ministère de l'Enseignement Supérieur et de la Recherche under the number 00218.01.

## References

- World Health Organization. *World Malaria Report 2014*. WHO (2014). at <[http://www.who.int/malaria/publications/world\\_malaria\\_report\\_2014/report/en/](http://www.who.int/malaria/publications/world_malaria_report_2014/report/en/)> Date of access: 15/01/2016.
- Bozdech, Z. *et al.* The transcriptome of the intraerythrocytic developmental cycle of *Plasmodium falciparum*. *PLoS Biol.* **1**, E5 (2003).
- De Silva, E. K. *et al.* Specific DNA-binding by apicomplexan AP2 transcription factors. *Proc. Natl. Acad. Sci. USA* **105**, 8393–8 (2008).
- Freitas-Junior, L. H. *et al.* Telomeric heterochromatin propagation and histone acetylation control mutually exclusive expression of antigenic variation genes in malaria parasites. *Cell* **121**, 25–36 (2005).
- Lopez-Rubio, J. J., Mancio-Silva, L. & Scherf, A. Genome-wide Analysis of Heterochromatin Associates Clonally Variant Gene Regulation with Perinuclear Repressive Centers in Malaria Parasites. *Cell Host Microbe* **5**, 179–190 (2009).
- Salcedo-Amaya, A. M. *et al.* Dynamic histone H3 epigenome marking during the intraerythrocytic cycle of *Plasmodium falciparum*. *Proc. Natl. Acad. Sci. USA* **106**, 9655–60 (2009).
- Shock, J. L., Fischer, K. F. & DeRisi, J. L. Whole-genome analysis of mRNA decay in *Plasmodium falciparum* reveals a global lengthening of mRNA half-life during the intra-erythrocytic development cycle. *Genome Biol.* **8**, R134 (2007).
- Gunasekera, A. M. *et al.* Widespread distribution of antisense transcripts in the *Plasmodium falciparum* genome. *Mol. Biochem. Parasitol.* **136**, 35–42 (2004).
- Cortés, A. *et al.* Epigenetic silencing of *Plasmodium falciparum* genes linked to erythrocyte invasion. *PLoS Pathog.* **3**, e107 (2007).
- Kafsack, B. F. C. *et al.* A transcriptional switch underlies commitment to sexual development in malaria parasites. *Nature* **507**, 248–52 (2014).
- Jiang, L. *et al.* PfSETvs methylation of histone H3K36 represses virulence genes in *Plasmodium falciparum*. *Nature* **499**, 223–7 (2013).
- Trelle, M. B., Salcedo-Amaya, A. M., Cohen, A. M., Stunnenberg, H. G. & Jensen, O. N. Global histone analysis by mass spectrometry reveals a high content of acetylated lysine residues in the malaria parasite *Plasmodium falciparum*. *J. Proteome Res.* **8**, 3439–50 (2009).
- Dastidar, E. G. *et al.* Comprehensive Histone Phosphorylation Analysis and Identification of Pf14-3-3 Protein as a Histone H3 Phosphorylation Reader in Malaria Parasites. *PLoS One* **8**, e53179 (2013).
- Hamamoto, R., Saloura, V. & Nakamura, Y. Critical roles of non-histone protein lysine methylation in human tumorigenesis. *Nat. Rev. Cancer* **15**, 110–24 (2015).
- Copeland, R. A., Solomon, M. E. & Richon, V. M. Protein methyltransferases as a target class for drug discovery. *Nat. Rev. Drug Discov.* **8**, 724–732 (2009).

16. Malmquist, N. A., Moss, T. A., Mecheri, S., Scherf, A. & Fuchter, M. J. Small-molecule histone methyltransferase inhibitors display rapid antimalarial activity against all blood stage forms in *Plasmodium falciparum*. *Proc. Natl. Acad. Sci.* **109**, 16708–16713 (2012).
17. Sundriyal, S. *et al.* Development of Diaminoquinazoline Histone Lysine Methyltransferase Inhibitors as Potent Blood-Stage Antimalarial Compounds. *Chem. Med. Chem.* **9**, 2360–2373 (2014).
18. Malmquist, N. A. *et al.* Histone Methyltransferase Inhibitors Are Orally Bioavailable, Fast-Acting Molecules with Activity against Different Species Causing Malaria in Humans. *Antimicrob. Agents Chemother.* **59**, 950–959 (2015).
19. Jenuwein, T., Laible, G., Dorn, R. & Reuter, G. SET domain proteins modulate chromatin domains in eu- and heterochromatin. *Cell. Mol. Life Sci.* **54**, 80–93 (1998).
20. Biggar, K. K. & Li, S. S.-C. Non-histone protein methylation as a regulator of cellular signalling and function. *Nat. Rev. Mol. Cell Biol.* **16**, 5–17 (2015).
21. Cui, L. L., Fan, Q., Cui, L. L. & Miao, J. Histone lysine methyltransferases and demethylases in *Plasmodium falciparum*. *Int. J. Parasitol.* **38**, 1083–1097 (2008).
22. Volz, J. C. *et al.* PfSET10, a *Plasmodium falciparum* Methyltransferase, Maintains the Active var Gene in a Poised State during Parasite Division. *Cell Host Microbe* **11**, 7–18 (2012).
23. Chin, H. G. *et al.* Automethylation of G9a and its implication in wider substrate specificity and HP1 binding. *Nucleic Acids Res.* **35**, 7313–7323 (2007).
24. Patnaik, D. *et al.* Substrate specificity and kinetic mechanism of mammalian G9a histone H3 methyltransferase. *J. Biol. Chem.* **279**, 53248–58 (2004).
25. Rathert, P., Cheng, X. & Jeltsch, A. Continuous enzymatic assay for histone lysine methyltransferases. *Biotechniques* **43**, 602–608 (2007).
26. Xiao, B., Wilson, J. R. & Gamblin, S. J. SET domains and histone methylation. *Curr. Opin. Struct. Biol.* **13**, 699–705 (2003).
27. Fang, J. *et al.* Purification and functional characterization of SET8, a nucleosomal histone H4-lysine 20-specific methyltransferase. *Curr. Biol.* **12**, 1086–1099 (2002).
28. Min, J., Zhang, X., Cheng, X., Grewal, S. I. S. S. & Xu, R.-M. Structure of the SET domain histone lysine methyltransferase Clr4. *Nat. Struct. Biol.* **9**, 828–832 (2002).
29. Rea, S. *et al.* Regulation of chromatin structure by site-specific histone H3 methyltransferases. *Nature* **406**, 593–599 (2000).
30. Lachner, M., O'Carroll, D., Rea, S., Mechtler, K. & Jenuwein, T. Methylation of histone H3 lysine 9 creates a binding site for HP1 proteins. *Nature* **410**, 116–120 (2001).
31. Gerace, E. L., Halic, M. & Moazed, D. The methyltransferase activity of Clr4Suv39h triggers RNAi independently of histone H3K9 methylation. *Mol. Cell* **39**, 360–72 (2010).
32. Flueck, C. *et al.* *Plasmodium falciparum* heterochromatin protein 1 marks genomic loci linked to phenotypic variation of exported virulence factors. *PLoS Pathog.* **5**, e1000569 (2009).
33. Volz, J. *et al.* Potential epigenetic regulatory proteins localise to distinct nuclear sub-compartments in *Plasmodium falciparum*. *Int. J. Parasitol.* **40**, 109–21 (2010).
34. Botté, C. Y. *et al.* Atypical lipid composition in the purified relict plastid (apicoplast) of malaria parasites. *Proc. Natl. Acad. Sci. USA* **110**, 7506–11 (2013).
35. Kaiser, K., Camargo, N. & Kappe, S. H. I. Transformation of sporozoites into early exoerythrocytic malaria parasites does not require host cells. *J. Exp. Med.* **197**, 1045–50 (2003).
36. Doerig, C., Rayner, J. C., Scherf, A. & Tobin, A. B. Post-translational protein modifications in malaria parasites. *Nat. Rev. Microbiol.* **13**, 160–172 (2015).
37. Trievel, R. C., Beach, B. M., Dirk, L. M. a., Houtz, R. L. & Hurley, J. H. Structure and catalytic mechanism of a SET domain protein methyltransferase. *Cell* **111**, 91–103 (2002).
38. Xiao, B. *et al.* Specificity and mechanism of the histone methyltransferase Pr-Set7. *Genes Dev.* **19**, 1444–54 (2005).
39. Dembélé, L. *et al.* Persistence and activation of malaria hypnozoites in long-term primary hepatocyte cultures. *Nat. Med.* **20**, 307–312 (2014).
40. Loyola, A. *et al.* The HP1alpha-CAF1-SetDB1-containing complex provides H3K9me1 for Suv39-mediated K9me3 in pericentric heterochromatin. *EMBO Rep.* **10**, 769–775 (2009).
41. Alvarez, F. *et al.* Sequential establishment of marks on soluble histones H3 and H4. *J. Biol. Chem.* **286**, 17714–17721 (2011).
42. Loyola, A., Bonaldi, T., Roche, D., Imhof, A. & Almouzni, G. PTMs on H3 Variants before Chromatin Assembly Potentiate Their Final Epigenetic State. *Mol. Cell* **24**, 309–316 (2006).
43. Newman, J. Novel buffer systems for macromolecular crystallization. *Acta Crystallogr. D. Biol. Crystallogr.* **60**, 610–2 (2004).
44. Stecher, H. *et al.* Biocatalytic Friedel-Crafts Alkylation Using Non-natural Cofactors. *Angew. Chemie Int. Ed.* **48**, 9546–9548 (2009).
45. Leroy, G. *et al.* A quantitative atlas of histone modification signatures from human cancer cells. *Epigenetics Chromatin* **6**, 20 (2013).
46. Bartke, T., Borgel, J. & DiMaggio, P. a. Proteomics in epigenetics: new perspectives for cancer research. *Brief. Funct. Genomics* **12**, 205–18 (2013).
47. Ghorbal, M., Gorman, M., Macpherson, C. R., Martins, R. M. & Scherf, A. Genome editing in the human malaria parasite *Plasmodium falciparum* using the CRISPR-Cas9 system. *Nat. Biotechnol.* **2**, (2014).
48. MacPherson, C. R. & Scherf, A. Flexible guide-RNA design for CRISPR applications using Protospacer Workbench. *Nat. Biotechnol.* **33**, 805–6 (2015).
49. Deitsch, K. W. Transformation of malaria parasites by the spontaneous uptake and expression of DNA from human erythrocytes. *Nucleic Acids Res.* **29**, 850–853 (2001).
50. Lanzer, M., de Bruin, D. & Ravetch, J. V. A sequence element associated with the *Plasmodium falciparum* KAHRP gene is the site of developmentally regulated protein-DNA interactions. *Nucleic Acids Res.* **20**, 3051–6 (1992).
51. Guizetti, J., Martins, R. M., Guadagnini, S., Claes, A. & Scherf, A. Nuclear pores and perinuclear expression sites of var and ribosomal DNA genes correspond to physically distinct regions in *Plasmodium falciparum*. *Eukaryot. Cell* **12**, 697–702 (2013).
52. Soulard, V. *et al.* *Plasmodium falciparum* full life cycle and *Plasmodium ovale* liver stages in humanized mice. *Nat. Commun.* **6**, 7690 (2015).

## Acknowledgements

We thank Stéphane Petres and the Recombinant Proteins in Eukaryotes platform, Institut Pasteur, Paris, for providing us with the pVL1393 plasmid, for making the PfSET7FL enzyme and for valuable advice. We thank Cyrille Y. Botté and Geoff McFadden for providing us with the parasite line expressing PfoTPT-HA. We gratefully acknowledge Katie Addison and Nicole Trainor for contributing to the synthesis of heavy-labeled AdoMet. The expression plasmid for mouse G9a enzyme was kindly provided by Thomas Jenuwein, Max Planck Institute, Freiburg. This work was funded by European Research Council Advanced Grants (PlasmoEscape 250320 and PlasmoSilencing 670301), the French Parasitology Consortium ParaFrap (ANR-11-LABX0024) and the Agence Nationale de Recherche (HypEpiC ANR-14 CE 160013 02).

### Author Contributions

P.B.C. expressed and purified enzymes and performed enzyme characterization and kinetics experiments. S.D. performed cellular localization experiments in blood stage parasites. G.Z. performed cellular localization experiments in sporozoite and liver stage parasites. V.S. provided frozen mouse liver sections infected with *P. falciparum*. P.A.D. designed, performed, analyzed and interpreted mass spectrometry experiments. P.A.D. and M.J.F. supervised synthesis of heavy-labeled AdoMet. S.M. supervised anti-PfSET7 antibody production. D.M. and A.S. supervised the project and interpreted the results. N.A.M. designed, performed, analyzed and interpreted enzyme kinetics experiments, designed and performed nucleosome labeling experiments, interpreted and synthesized all results and wrote the manuscript with input from all authors. All authors contributed to the writing of and reviewed the manuscript.

### Additional Information

**Supplementary information** accompanies this paper at <http://www.nature.com/srep>

**Competing financial interests:** The authors declare no competing financial interests.

**How to cite this article:** Chen, P. B. *et al.* *Plasmodium falciparum* PfSET7: enzymatic characterization and cellular localization of a novel protein methyltransferase in sporozoite, liver and erythrocytic stage parasites. *Sci. Rep.* **6**, 21802; doi: 10.1038/srep21802 (2016).



This work is licensed under a Creative Commons Attribution 4.0 International License. The images or other third party material in this article are included in the article's Creative Commons license, unless indicated otherwise in the credit line; if the material is not included under the Creative Commons license, users will need to obtain permission from the license holder to reproduce the material. To view a copy of this license, visit <http://creativecommons.org/licenses/by/4.0/>

## Title

*Plasmodium falciparum* PfSET7: enzymatic characterization and cellular localization of a novel protein methyltransferase in sporozoite, liver and erythrocytic stage parasites

## Authors

Patty B. Chen<sup>1,2,3,§</sup>, Shuai Ding<sup>1,2,3,§</sup>, Gigliola Zanghi<sup>4</sup>, Valérie Soulard<sup>4</sup>, Peter A. DiMaggio Jr<sup>6</sup>, Matthew J. Fuchter<sup>7</sup>, Salah Mecheri<sup>1,2,3</sup>, Dominique Mazier<sup>4,5</sup>, Artur Scherf<sup>1,2,3</sup>, Nicholas A. Malmquist<sup>1,2,3,\*</sup>

<sup>1</sup> Unité Biologie des Interactions Hôte-Parasite, Département de Parasites et Insectes Vecteurs, Institut Pasteur, Paris 75015, France. <sup>2</sup> CNRS, ERL 9195, Paris 75015, France. <sup>3</sup> INSERM, UMR 1201, Paris 75015, France. <sup>4</sup> Sorbonne Universités, UPMC Univ Paris 06, INSERM U1135, CNRS ERL 8255, Centre d'Immunologie et des Maladies Infectieuses (CIMI-Paris), 91 Bd de l'hôpital, 75013, Paris, France. <sup>5</sup> AP HP, Centre Hospitalo-Universitaire Pitié-Salpêtrière, 75013 Paris, France. <sup>6</sup> Department of Chemical Engineering, Imperial College London, South Kensington Campus, London SW7 2AZ, United Kingdom. <sup>7</sup> Department of Chemistry, Imperial College London, South Kensington Campus, London SW7 2AZ, United Kingdom.

\*Correspondence and requests for materials should be addressed to N.A.M (e-mail: [nicholas.malmquist@pasteur.fr](mailto:nicholas.malmquist@pasteur.fr))

§These authors contributed equally to this work.

## Supplementary Data

Product	Primer	Sequence
PfSET7ΔC	Primer 1F Primer 3R	5'-CATCGGGCGCGGATCCATGGAACTATTTTTAGGAACTC-3' 5'-ATAGAGGTCATCGTCGCCAGGTA-3'
PfSET7ΔCΔN	Primer 2F Primer 3R	5'-CATCGGGCGCGGATCCATGAACGACGTGGAAATCTTCAATGTCA-3' 5'-ATAGAGGTCATCGTCGCCAGGTA-3'
PfSET7ΔN	Primer 2F Primer 5R	5'-CATCGGGCGCGGATCCATGAACGACGTGGAAATCTTCAATGTCA-3' 5'-AGATCTGCAGCGGCCGGATCAGCGGGTTTAACTCACTTCTC-3'
Strep-Tag	Primer 4F Primer 5R	5'-GACGATGACCTCTATGACGATGACGATAAGGCCGGTTG-3' 5'-AGATCTGCAGCGGCCGGATCAGCGGGTTTAACTCACTTCTC-3'
PfSET7_H517A	Primer 6F Primer 7R	5'-CGCATCTCTATGCTGGCAGCCTCATGCATTAGTACAGCCTG-3' 5'-CAGGCTGTACTAATGCATGAGGCTGCCAGCATAGAGATGCG-3'
pL6-Pfset7 plasmid Homology Region 1	Primer 8F Primer 9R	5'-TTCCGCGGGGAGGACTAGTCCAATTATTTCCAAGTGAATGT-3' 5'-TATCCACCGCCTGGCGGCCCTCTTCGATCTGAGGAGCAT-3'
pL6-Pfset7 plasmid Homology Region 2	Primer 10F Primer 11R	5'-TGTAGGAGGGGACGGCGCCATATATTTAGCAATAACTTC-3' 5'-AATTTTTTTTACAAAATGCTTAAGTACCTTAGAACAAATAGG-3'
Integration confirmation	Primer 12F Primer 13R Primer 14F Primer 15R	5'-GTATGTATGTGTAGTAGGTGACTCATCC-3' 5'-GCATAGTCTGGTACGTCATAGGGATACG-3' 5'-CATGGGGACAACAATGGGGAGAAAGAGG-3' 5'-GCTTAGTTGACGAGGATGGAGGTTATCG-3'
PfSET7 qPCR	Primer qF Primer qR	5'-GATTTGTCTGATGCCTTAGC-3' 5'-TTTCCCATTGAGATGTATCC-3'

Table S1 | Primers for generating PfSET7 mutants, pL6-Pfset7 constructs and quantitative PCR.







x2

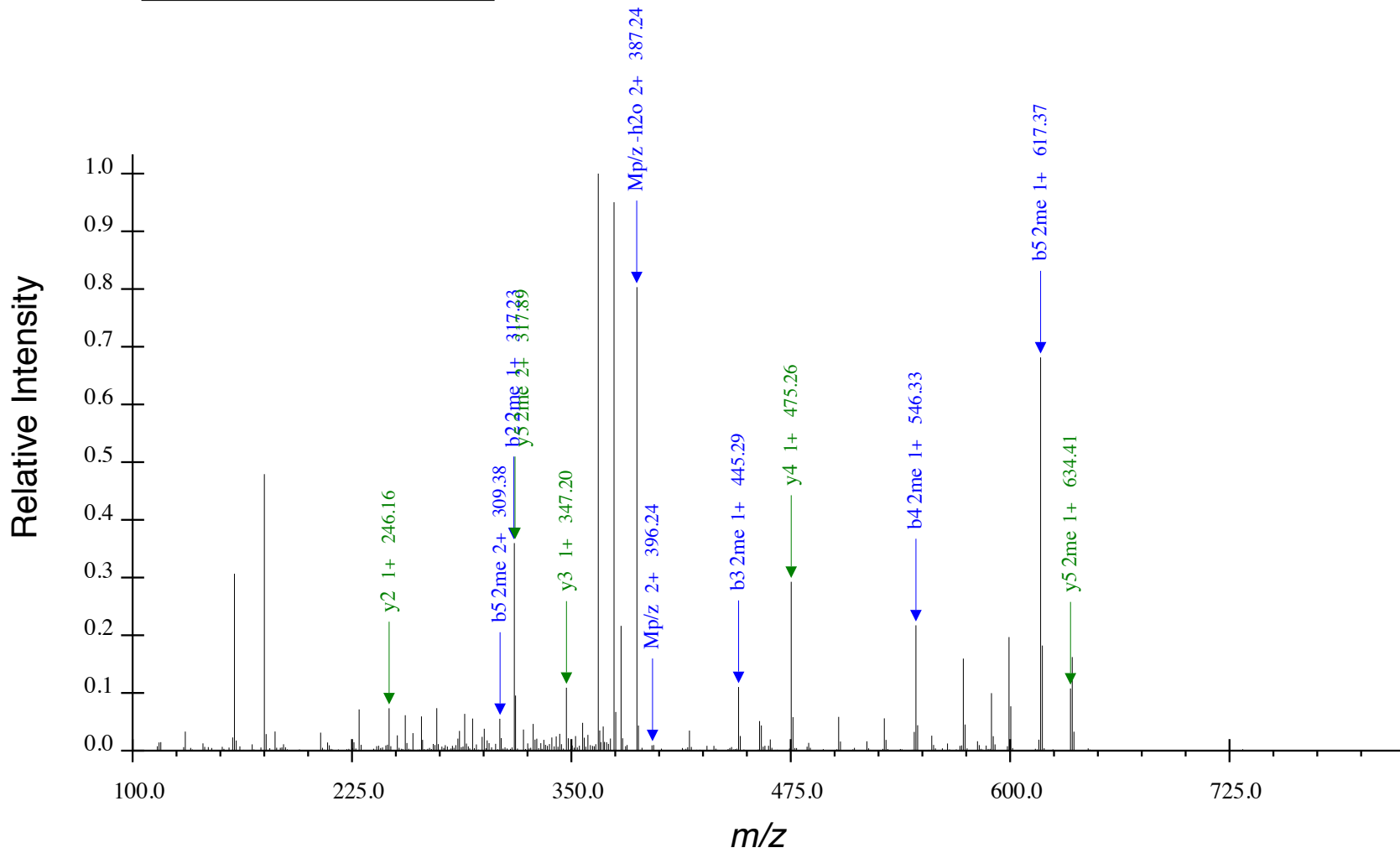


**Figure S3** | Annotated CID tandem mass spectrum for H3K4me2(CH<sub>3</sub>, CD<sub>3</sub>),  $z = 2$ ,  $Mp/z = 396.24$ . N-terminus has been propionylated (+56.0627 Da).

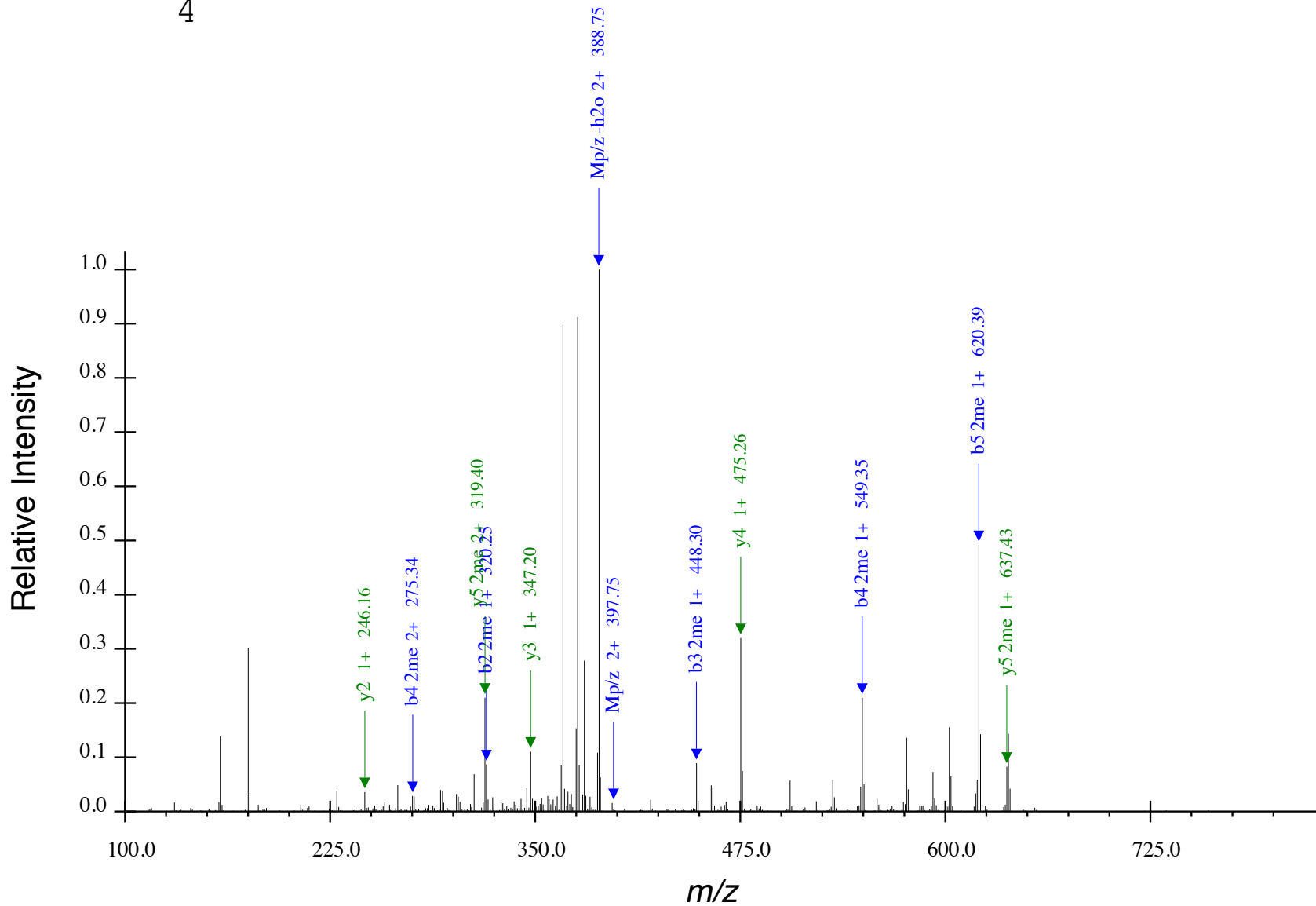


**Figure S4** | Annotated CID tandem mass spectrum for H3K4me2(2CD<sub>3</sub>), z = 2, Mp/z = 397.75. N-terminus has been propionylated (+56.0627 Da).

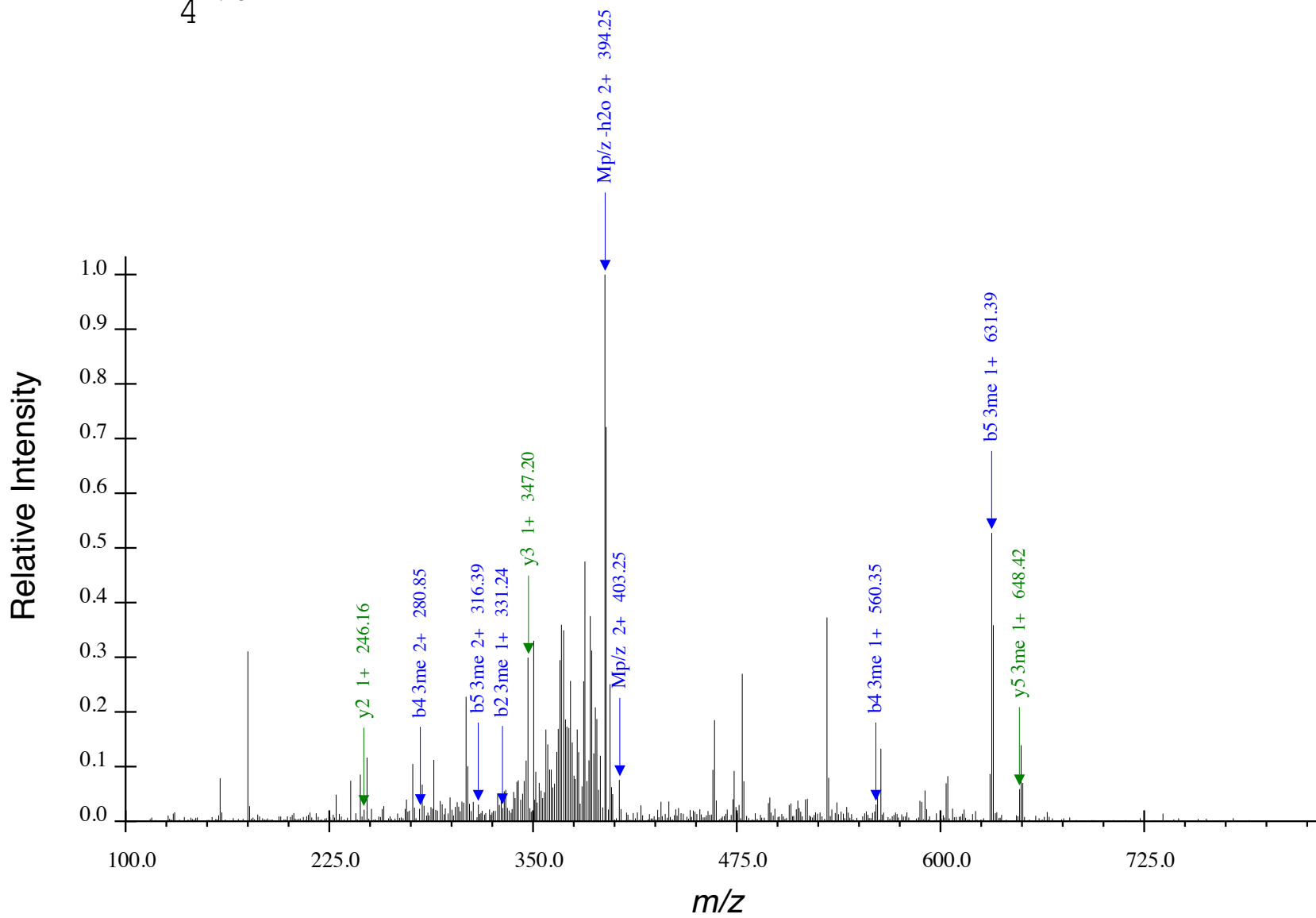


**Figure S5** | Annotated CID tandem mass spectrum for H3K4me3(2CH<sub>3</sub>, CD<sub>3</sub>), z = 2, Mp/z = 403.25. N-terminus has been propionylated (+56.0627 Da).

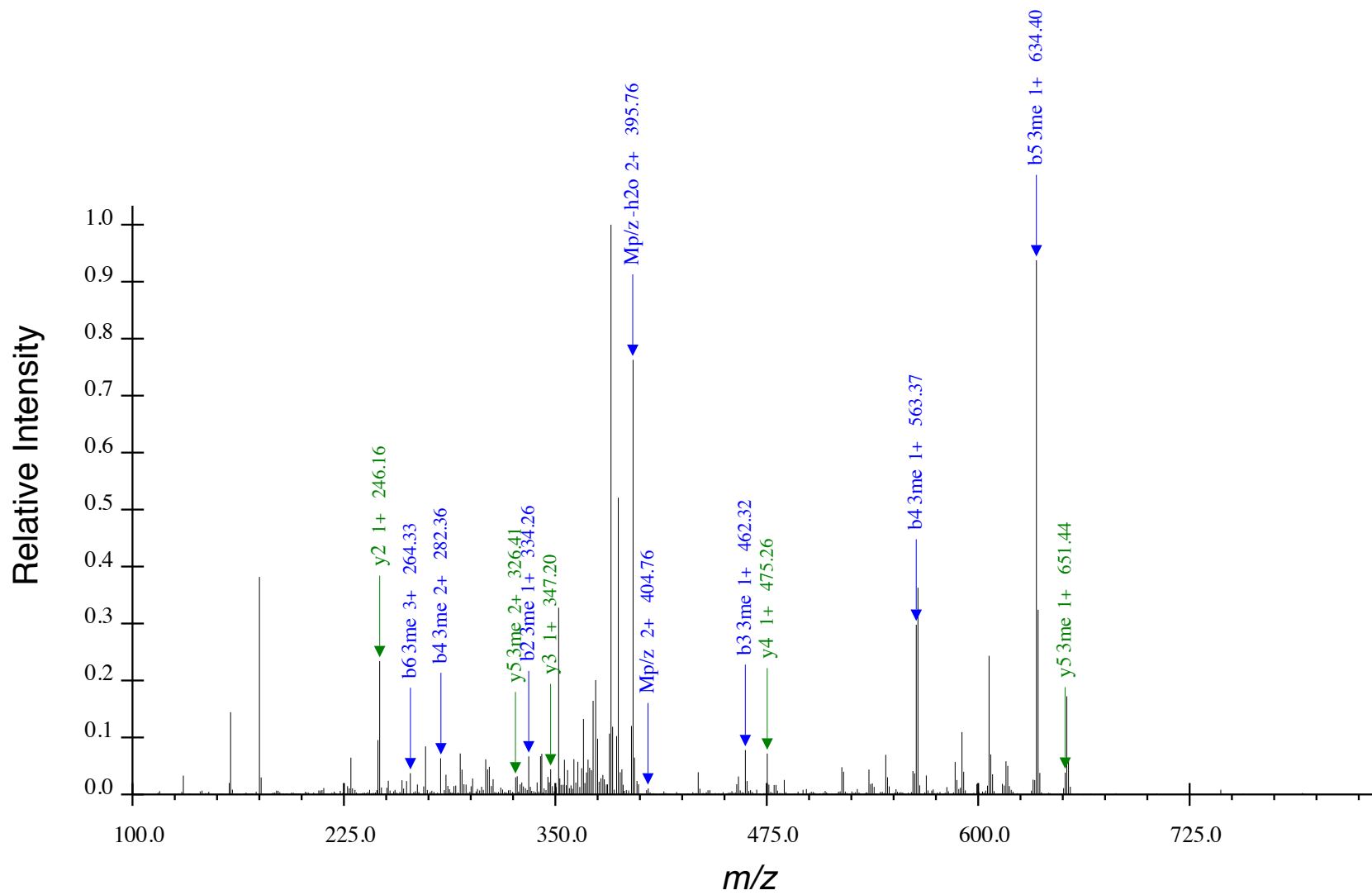


**Figure S6** | Annotated CID tandem mass spectrum for H3K4me3(CH<sub>3</sub>,2CD<sub>3</sub>),  $z = 2$ ,  $Mp/z = 404.76$ . N-terminus has been propionylated (+56.0627 Da).

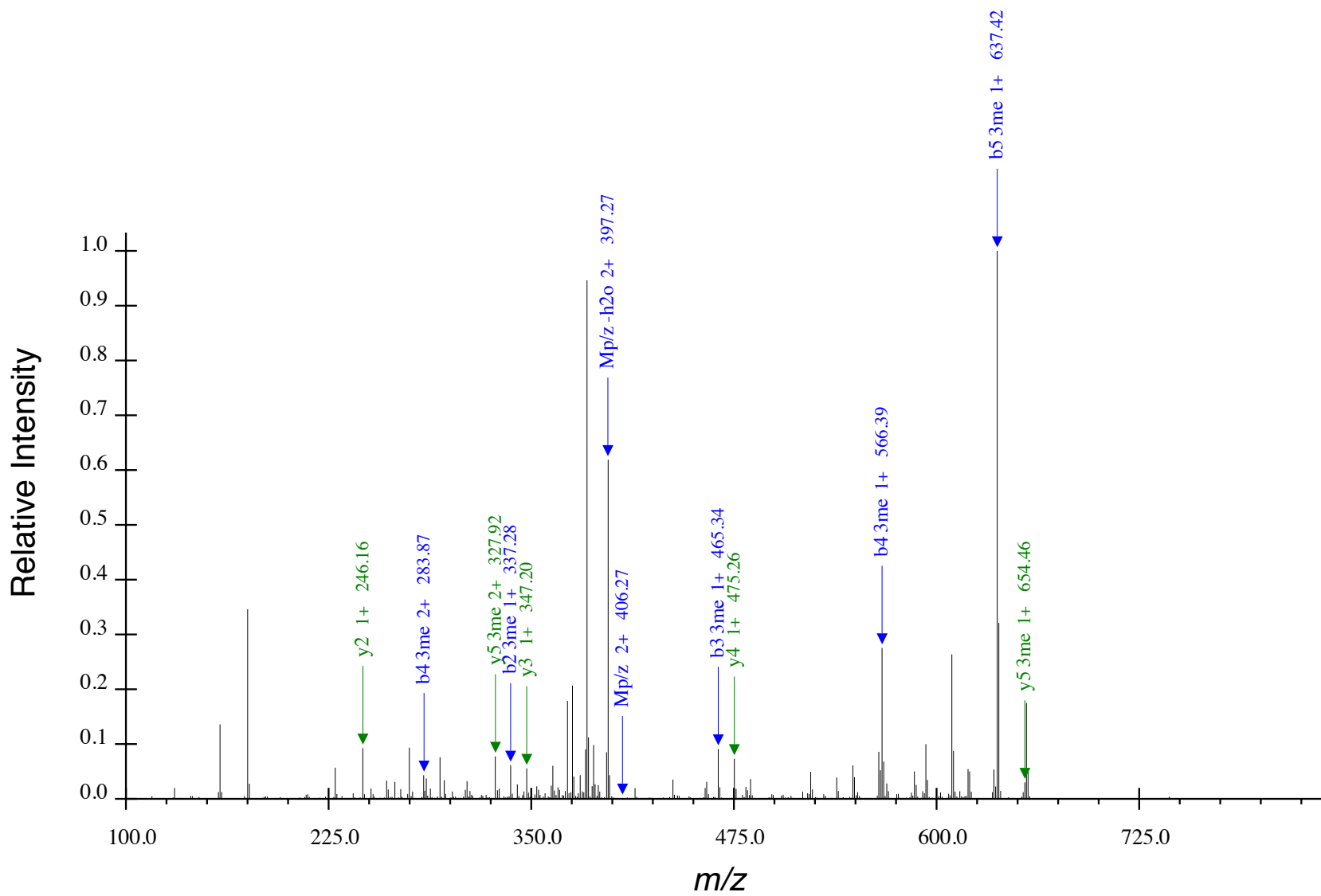


**Figure S7** | Annotated CID tandem mass spectrum for H3K4me3(3CD<sub>3</sub>),  $z = 2$ ,  $Mp/z = 406.27$ .  
N-terminus has been propionylated (+56.0627 Da).

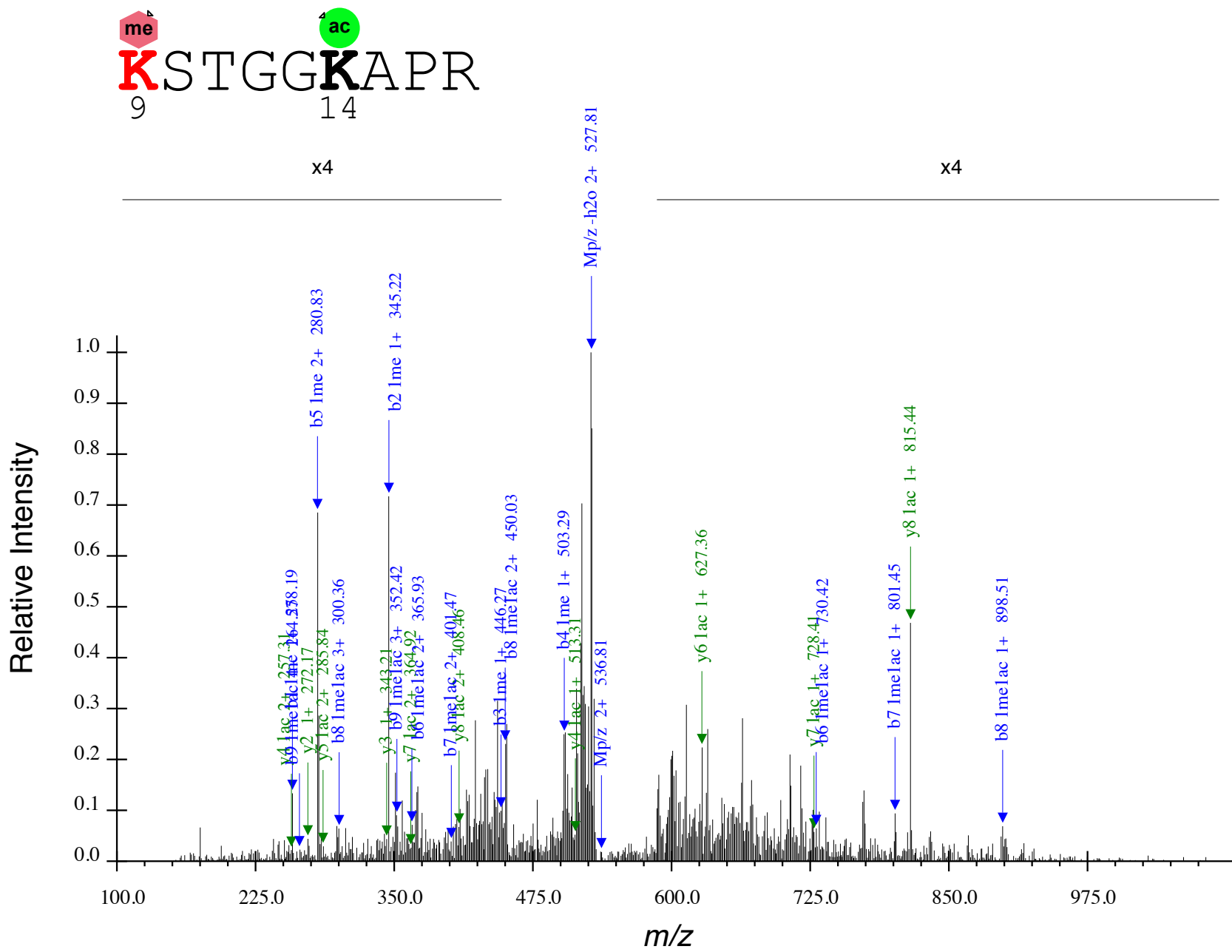


**Figure S8** | Annotated CID tandem mass spectrum for H3K9me1(CD<sub>3</sub>)K14ac, z = 2, Mp/z = 536.81. N-terminus and K9 have been propionylated (+56.0627 Da).



x4

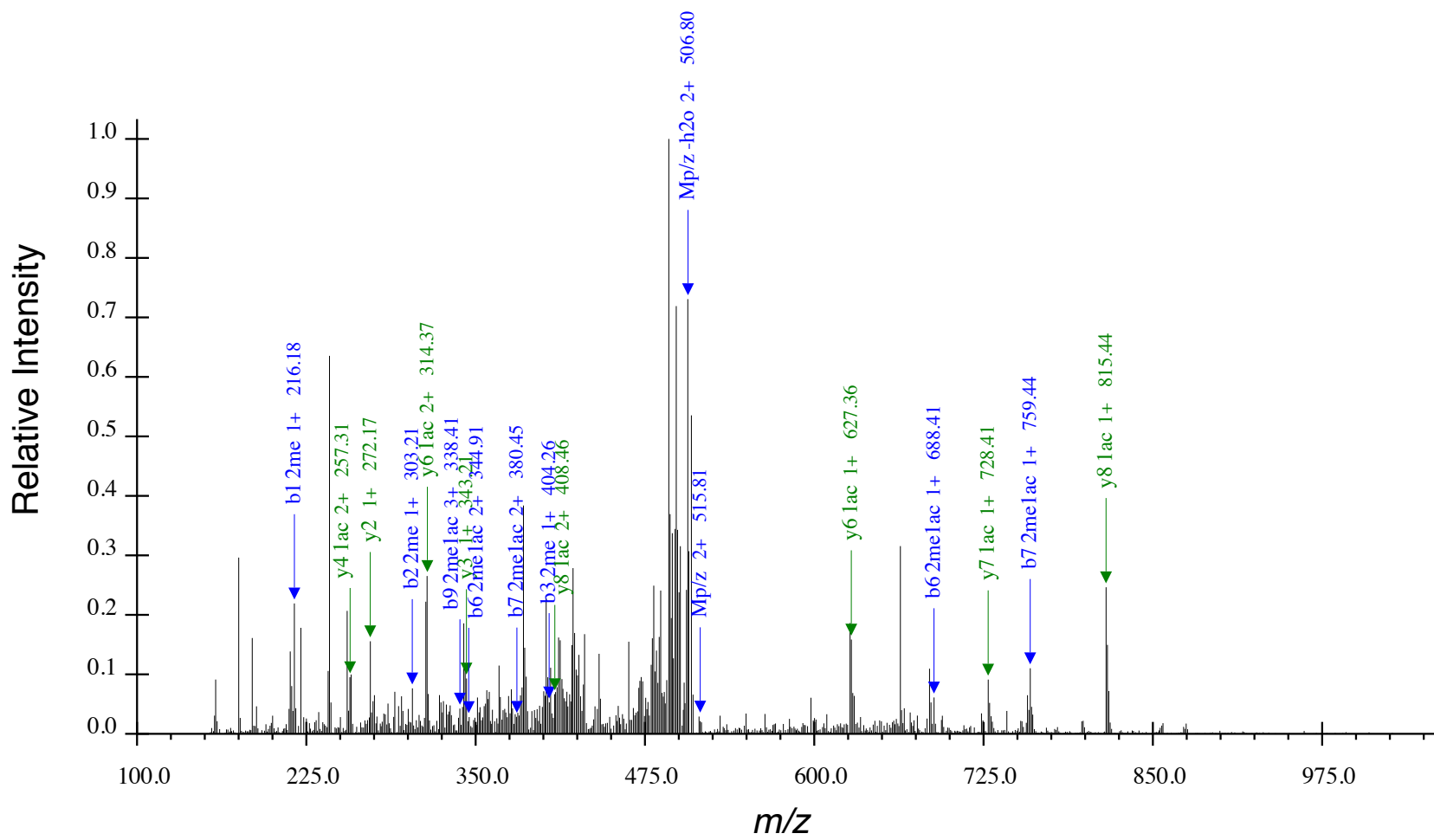


**Figure S9** | Annotated CID tandem mass spectrum for H3K9me2(CH<sub>3</sub>,CD<sub>3</sub>)K14ac, z = 2, Mp/z = 515.81. N-terminus has been propionylated (+56.0627 Da).

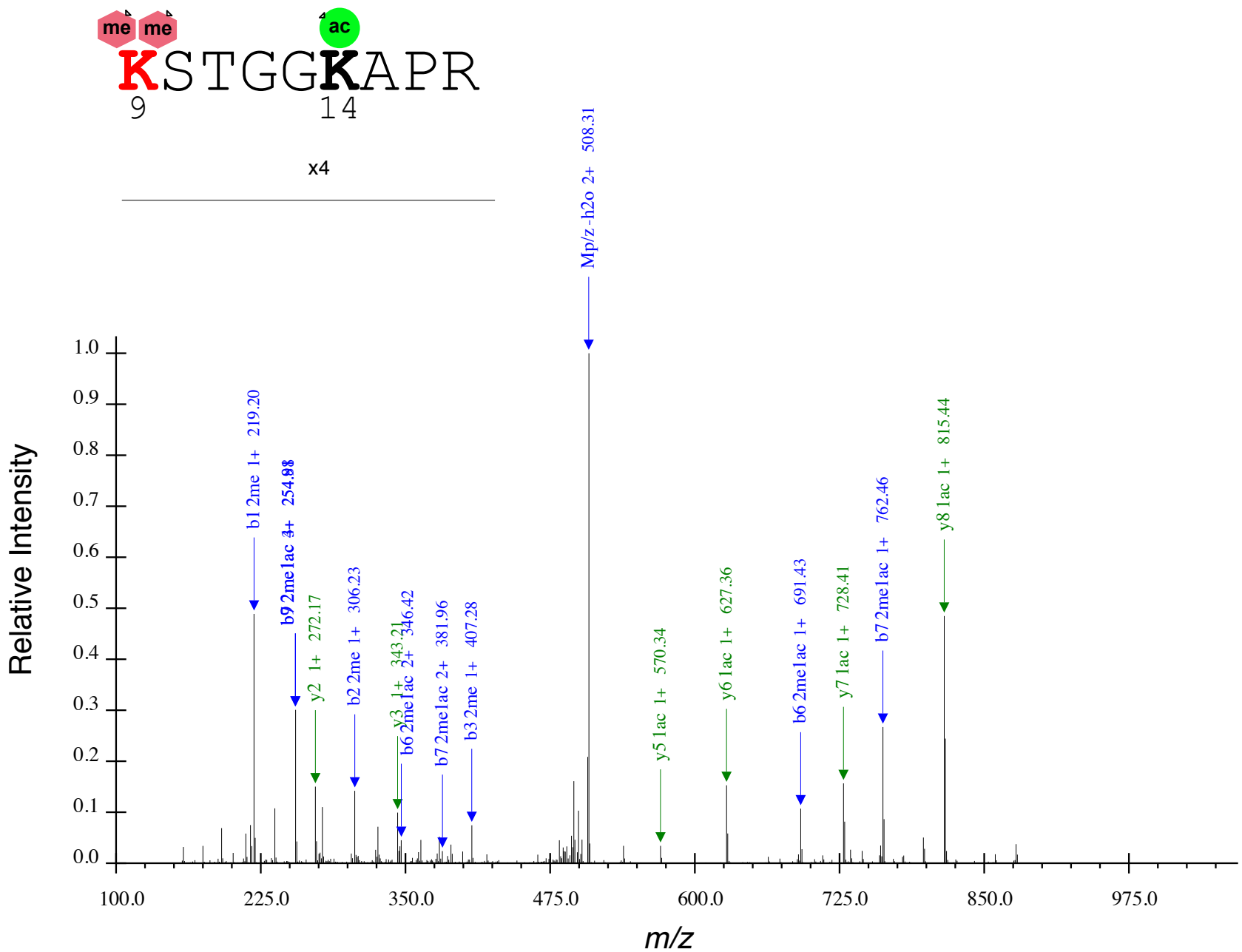


**Figure S10** | Annotated CID tandem mass spectrum for H3K9me2(2CD<sub>3</sub>)K14ac, z = 2, Mp/z = 517.31. N-terminus has been propionylated (+56.0627 Da).

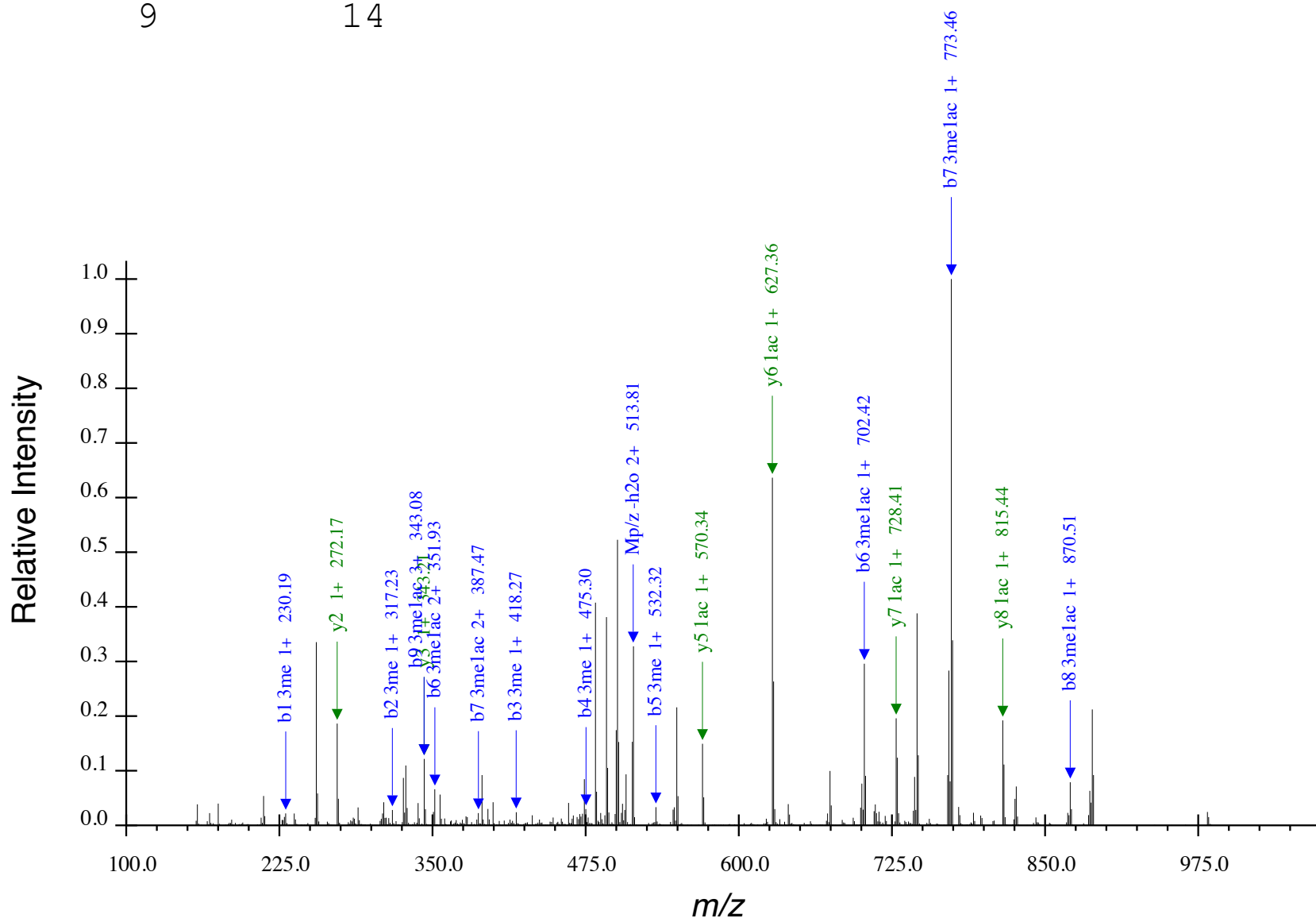


**Figure S11** | Annotated CID tandem mass spectrum for H3K9me3(2CH<sub>3</sub>,CD<sub>3</sub>)K14ac, z = 2, Mp/z = 522.82. N-terminus has been propionylated (+56.0627 Da).

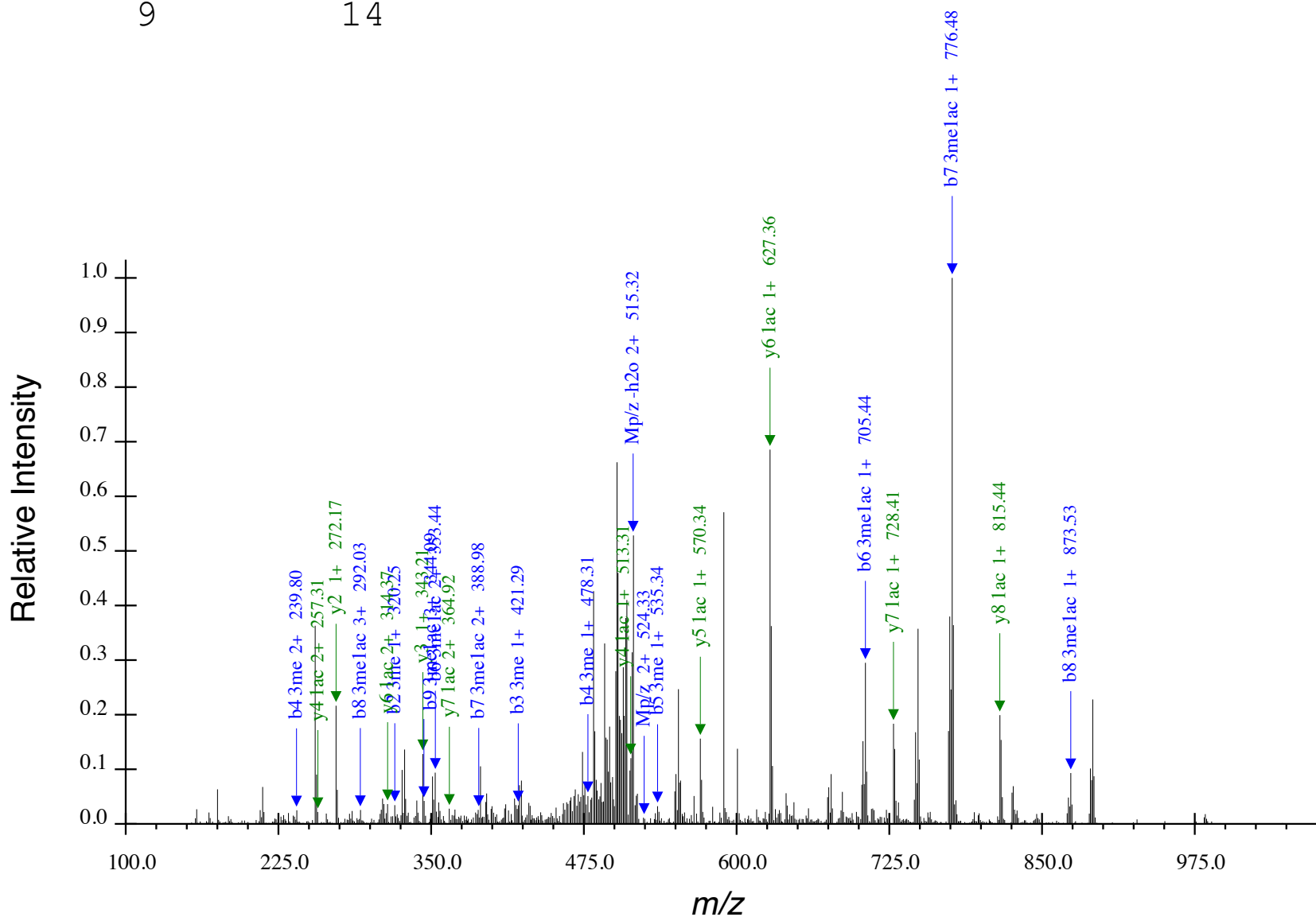
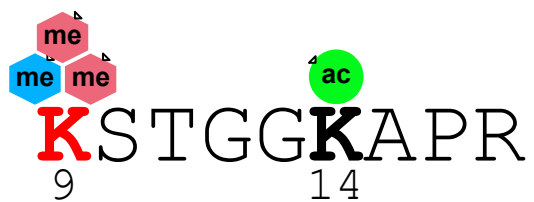


**Figure S12** | Annotated CID tandem mass spectrum for H3K9me3(CH<sub>3</sub>,2CD<sub>3</sub>)K14ac, z = 2, Mp/z = 524.33. N-terminus has been propionylated (+56.0627 Da).

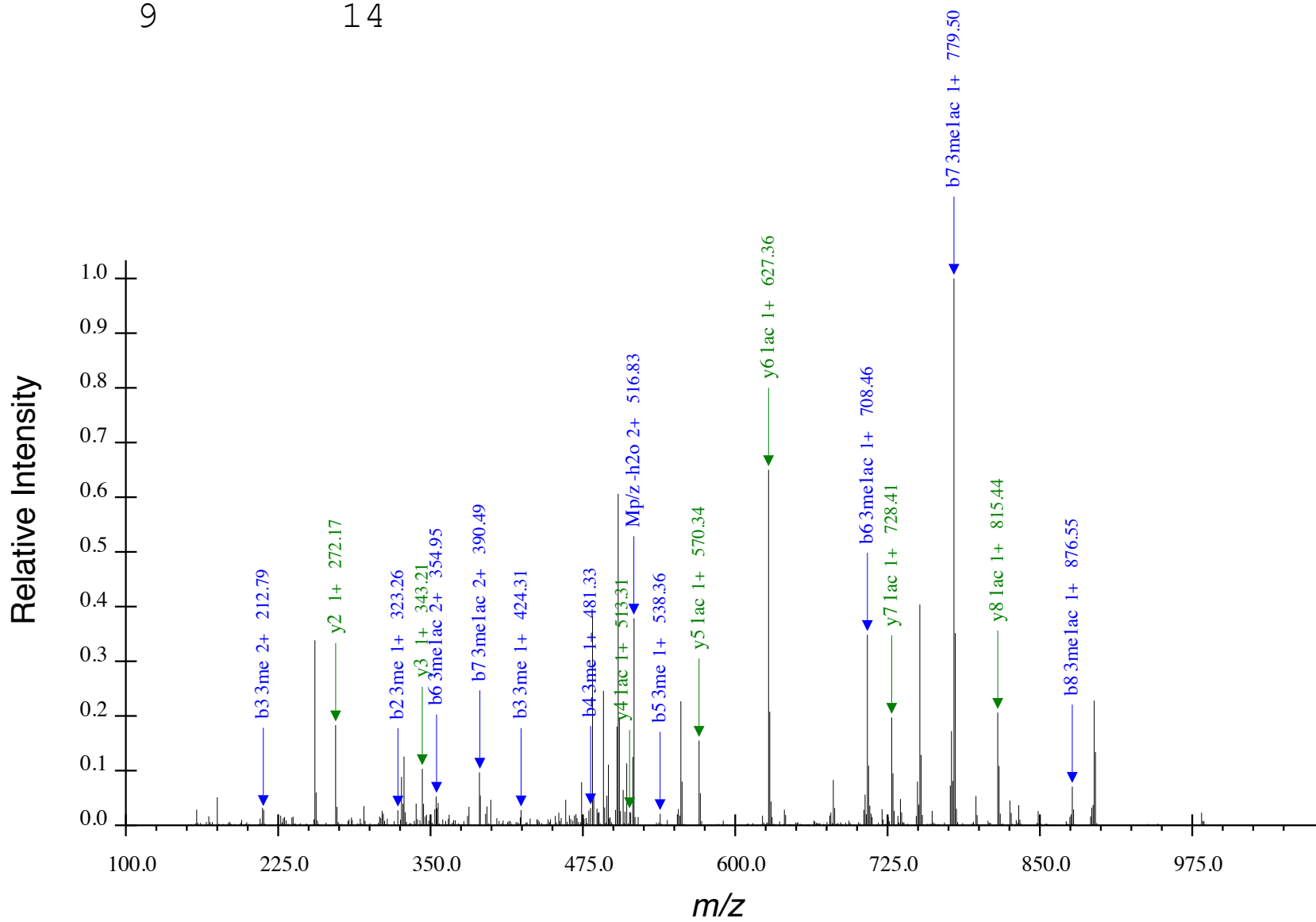
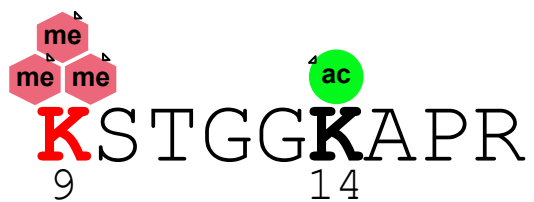


**Figure S13** | Annotated CID tandem mass spectrum for H3K9me3(3CD<sub>3</sub>)K14ac, z = 2, Mp/z = 525.84. N-terminus has been propionylated (+56.0627 Da).

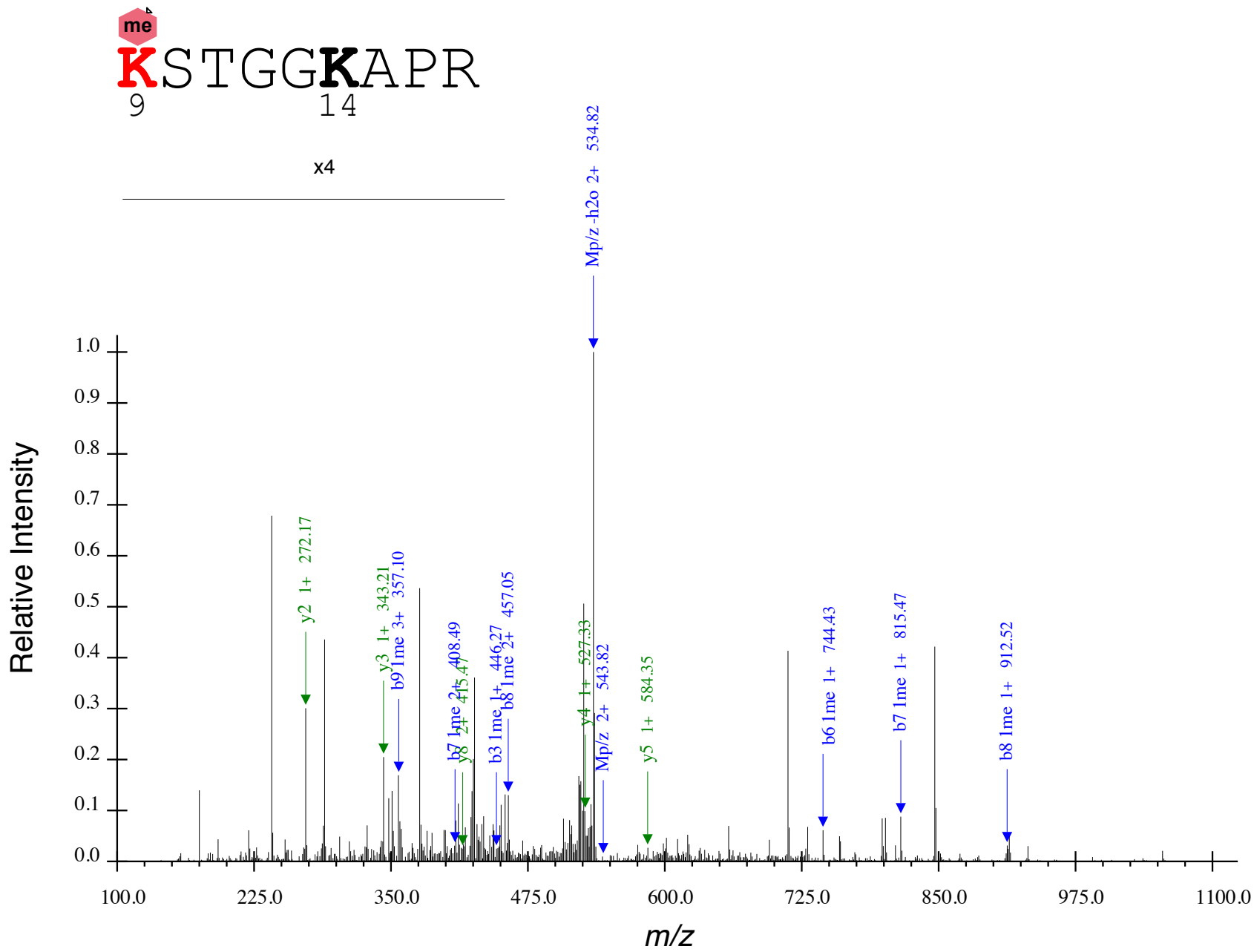


**Figure S14** | Annotated CID tandem mass spectrum for H3K9me1(CD<sub>3</sub>)K14un, z = 2, Mp/z = 543.82. N-terminus, K9 and K14 have been propionylated (+56.0627 Da).

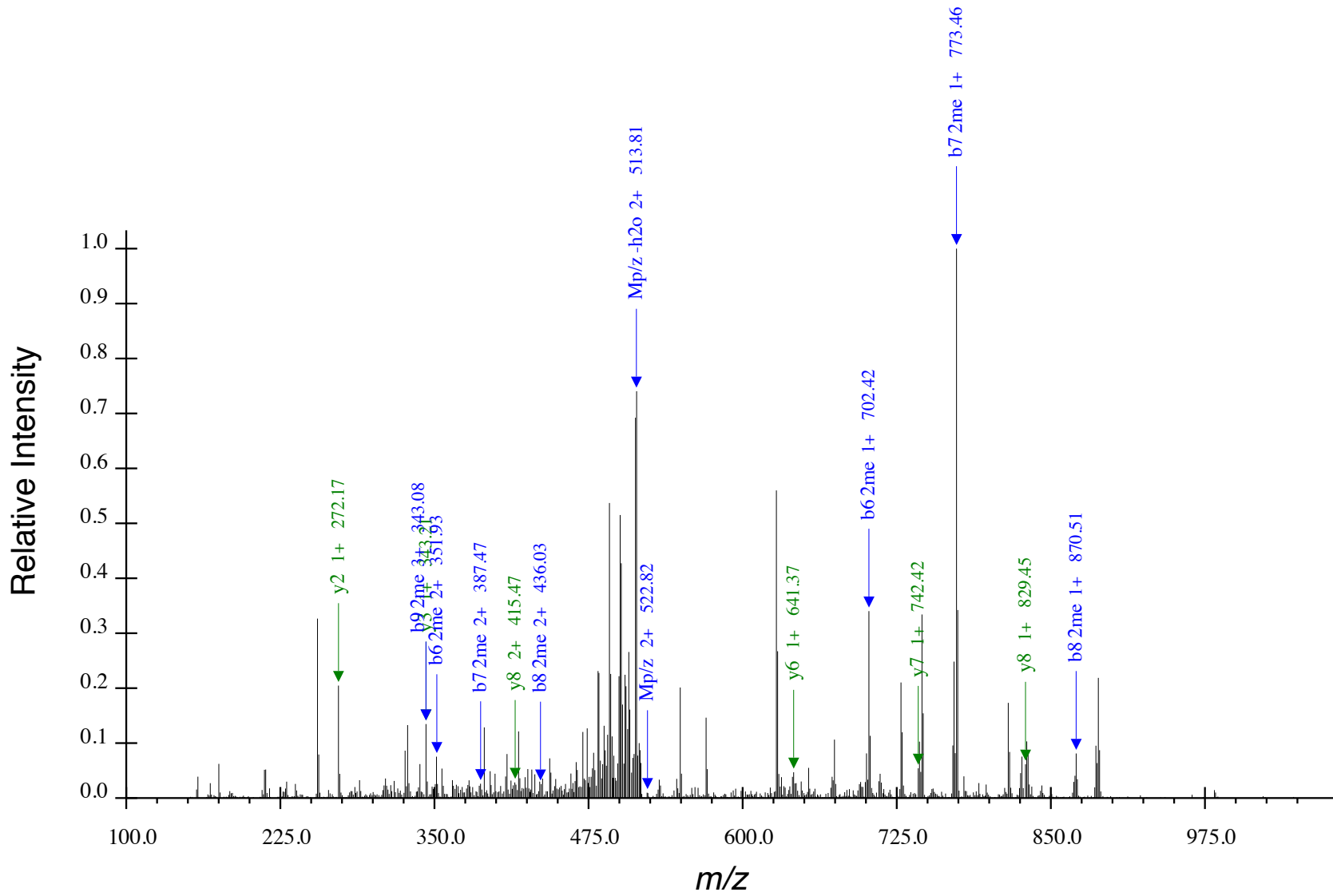


**Figure S15** | Annotated CID tandem mass spectrum for H3K9me2(CH<sub>3</sub>,CD<sub>3</sub>)K14un, z = 2, Mp/z = 522.82. N-terminus and K14 have been propionylated (+56.0627 Da).

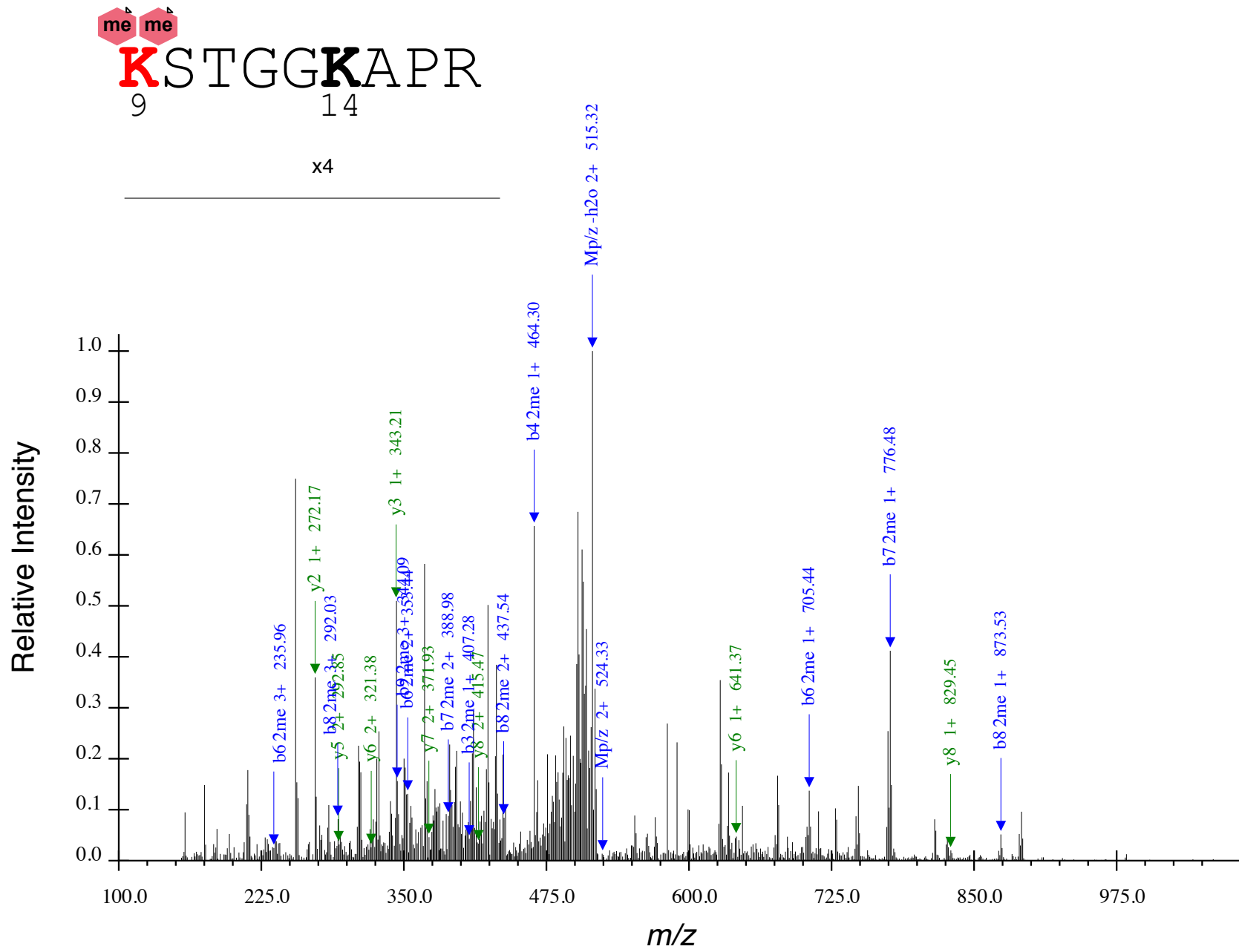


**Figure S16** | Annotated CID tandem mass spectrum for H3K9me2(2CD<sub>3</sub>)K14un, z = 2, Mp/z = 524.33. N-terminus and K14 have been propionylated (+56.0627 Da).



x4

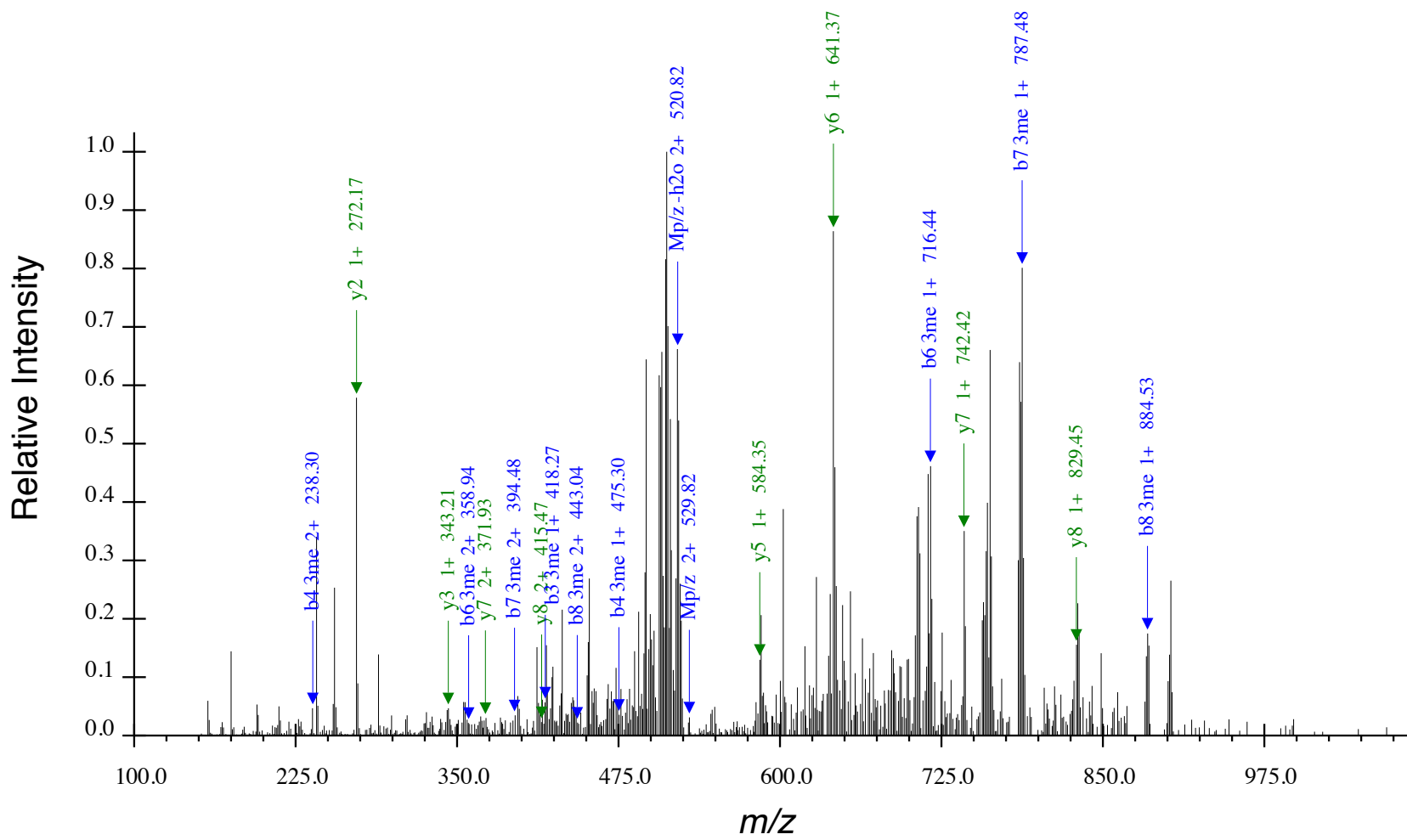


**Figure S17** | Annotated CID tandem mass spectrum for H3K9me3(2CH<sub>3</sub>,CD<sub>3</sub>)K14un, z = 2, Mp/z = 529.82. N-terminus and K14 have been propionylated (+56.0627 Da).

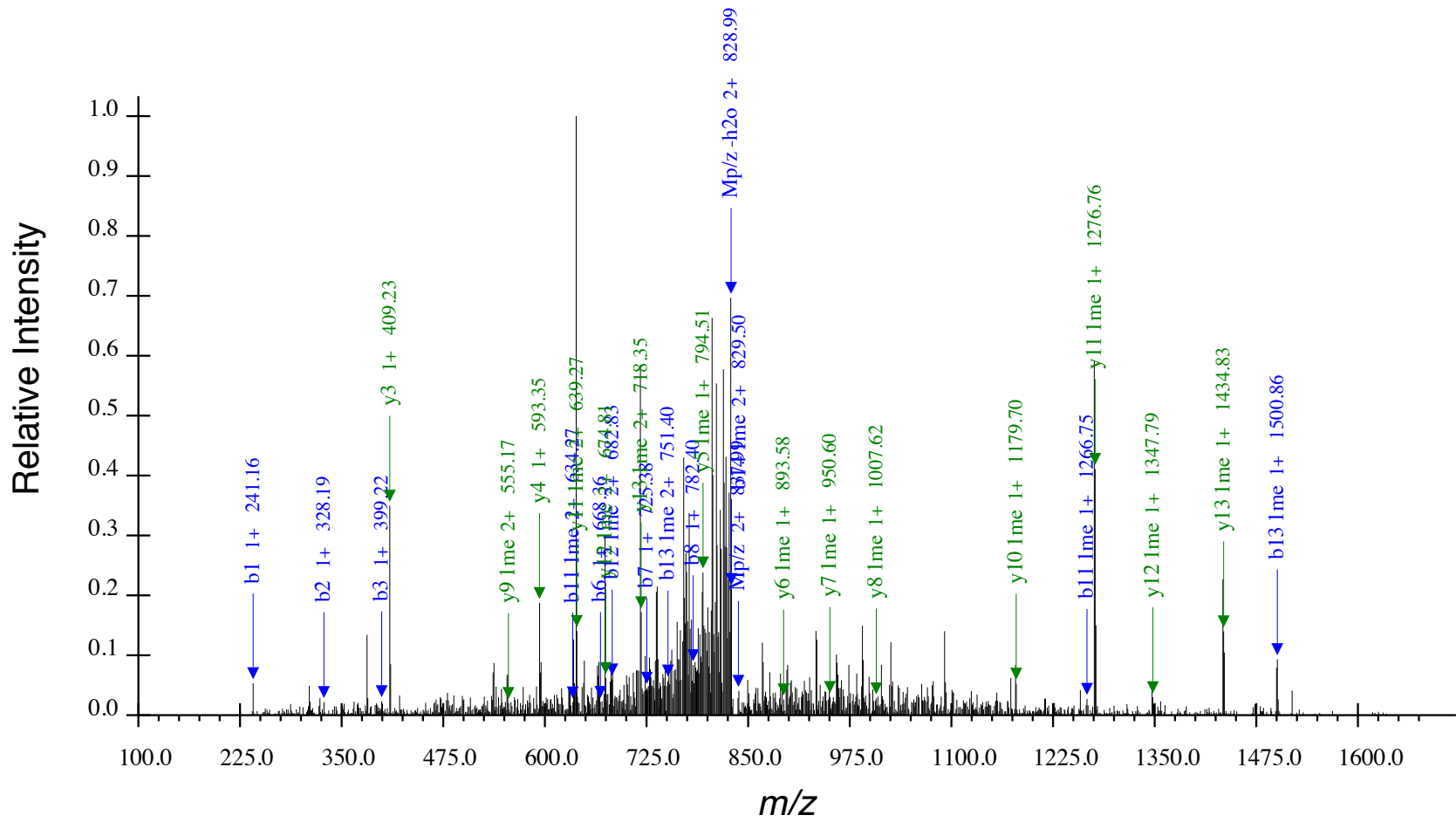


**Figure S18** | Annotated CID tandem mass spectrum for H3K27unK36me1(CD<sub>3</sub>), z = 2, Mp/z = 837.99. N-terminus, K27, K36 and K37 have been propionylated (+56.0627 Da).

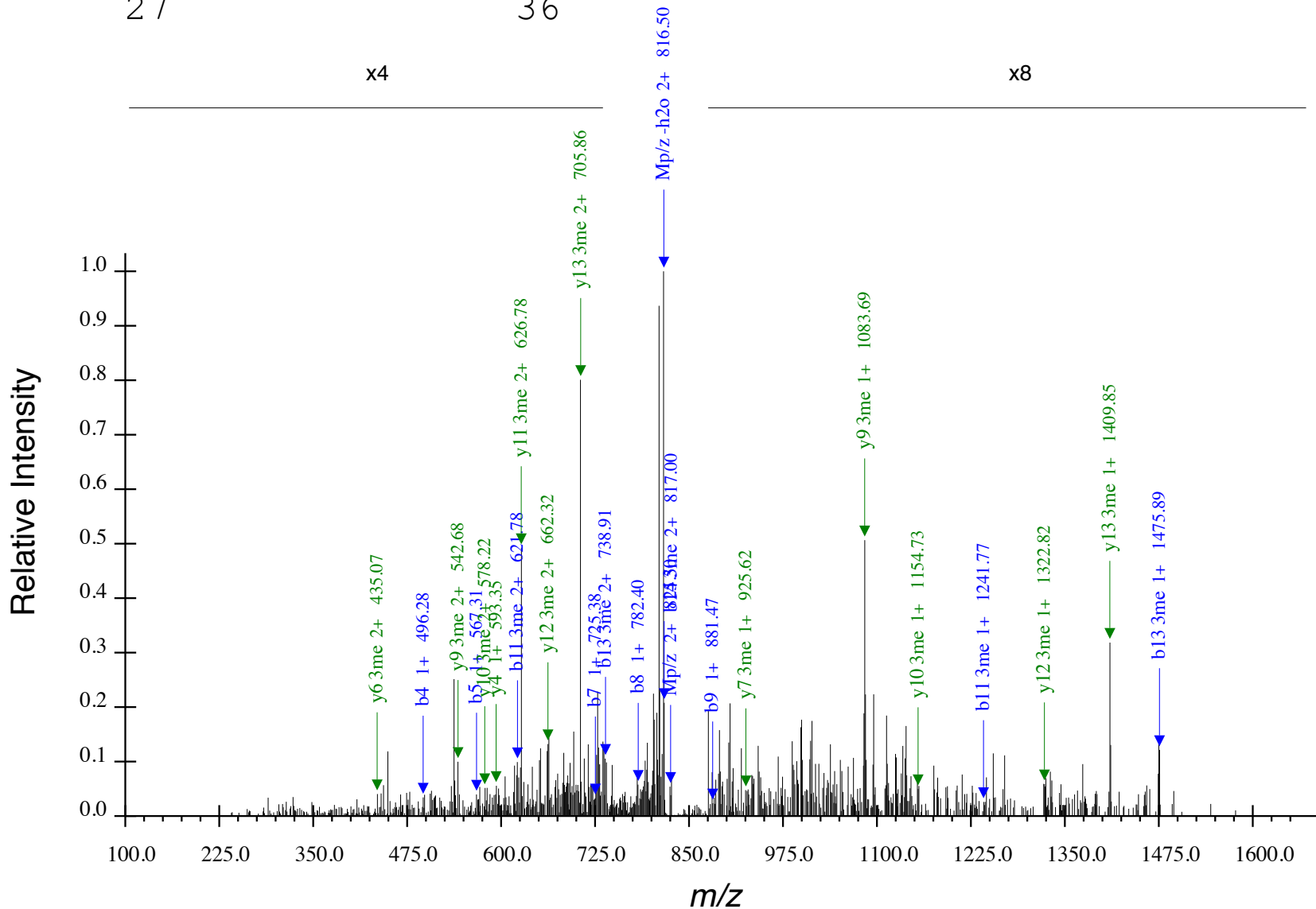


**Figure S19** | Annotated CID tandem mass spectrum for H3K27unK36me3(CH<sub>3</sub>,2CD<sub>3</sub>),  $z = 2$ ,  $Mp/z = 825.50$ . N-terminus, K27 and K37 have been propionylated (+56.0627 Da).

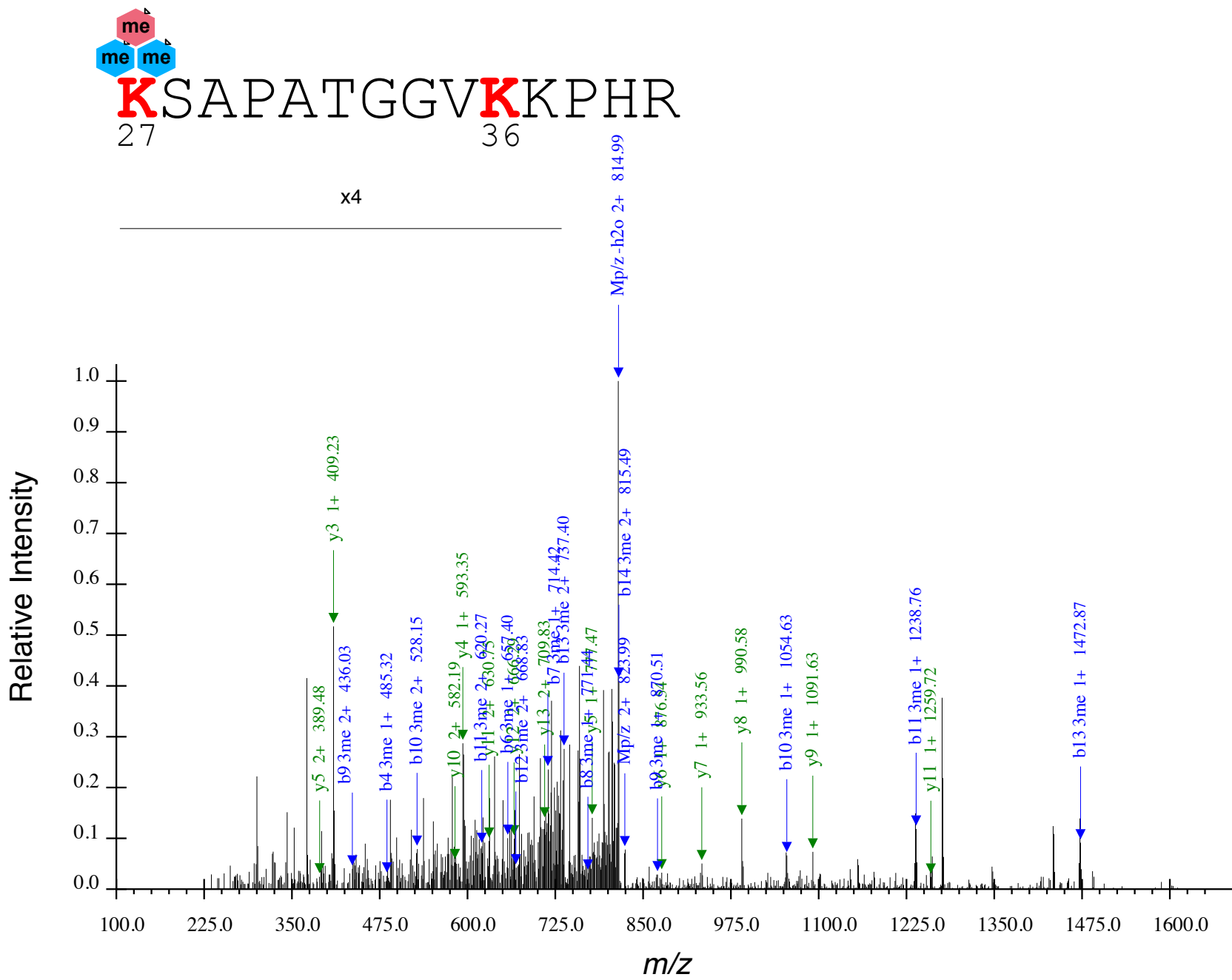
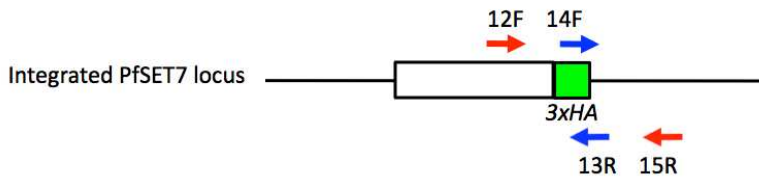
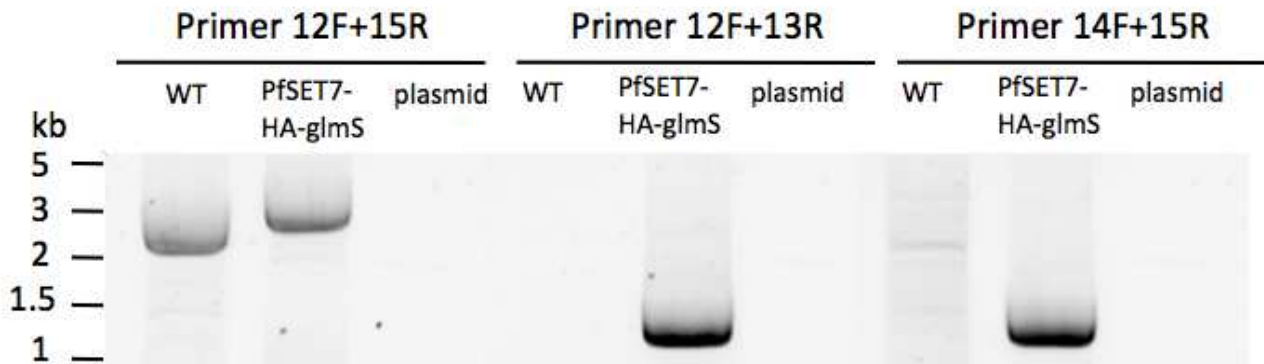


**Figure S20** | Annotated CID tandem mass spectrum for H3K27me3(2CH<sub>3</sub>, CD<sub>3</sub>)K36un, z = 2, Mp/z = 823.99. N-terminus, K36 and K37 have been propionylated (+56.0627 Da).

a



b



c

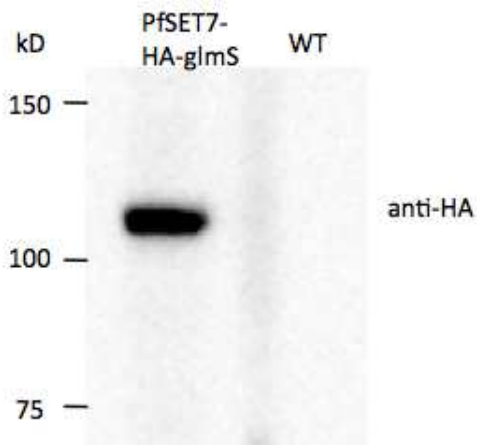
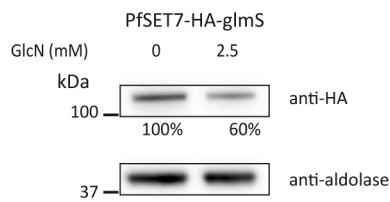
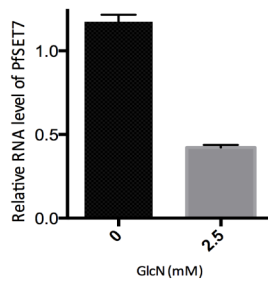
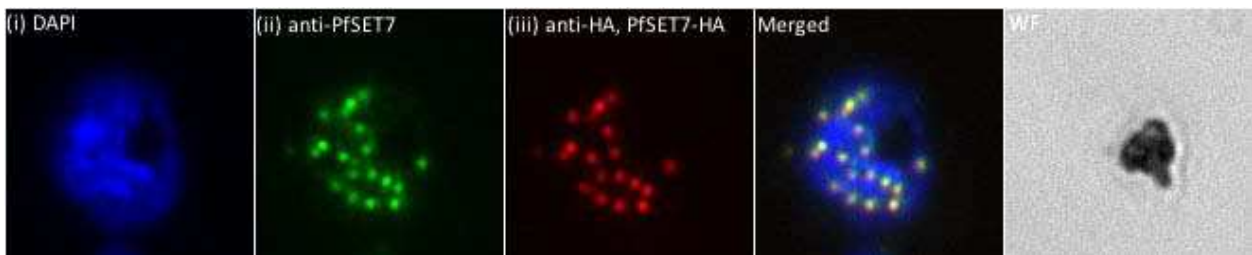


Figure S21 | **Confirmation of PfSET7-HA-glmS integration.** (a) Schematic of the PCR verification of PfSET7-HA-glmS integration. White rectangles represent the wild PfSET7 locus and green box indicate the 3xHA tag. Red arrows represent the primers used to identify the upstream and downstream of homologous region. Blue arrows represent the primers located in HA tag sequence. (b) Agarose gel electrophoresis of the upstream, downstream and insertion confirmation PCRs. Left panel: Either wild-type (2248 bp) or the integrated allele (2615 bp) are visualized after amplification with 12F+15R. Middle and right panel: note the presence of integration after amplification with 12F+13R (1230 bp) and 14F+15R (1247 bp). (c) Western blot of PfSET7 in transgenic PfSET7-HA-glmS line and wild-type parasite lines. The anti-HA antibody recognizes a band of >100 kDa (PfSET7-HA predicted MW: 98 kDa).

**a****b**

**Figure S22 | Generation of a PfSET7 knock-down line after 2 generations of glucosamine treatment.** (a) Western blot analysis of treated PfSET7-HA-glmS parasites shows 40% decrease in protein levels compared to the control. The PfSET7 expression was normalized to the protein aldolase. The blot image presented has been cropped to the area used for densitometry. (b) Quantitative PCR analysis showing 60% reduction of PfSET7 mRNA levels in treated parasites. Seryl-tRNA synthetase (PF07\_0073) was used as an endogenous control. The  $\Delta\text{CT}$  for the PfSET7 gene was determined by subtracting the PfSET7 gene CT value from the seryl-tRNA synthetase gene CT value. Copy number was then converted using the formula (copy number =  $2^{-\Delta\text{Ct}}$ ). Data are presented as mean  $\pm$  SD of two independent experiments.



**Figure S23 | Comparison of anti-PfSET7 and anti-HA antibodies in the PfSET7-HA-glmS parasite line.** Both anti-PfSET7 and anti-HA produced a strong punctate staining dots that are consistent with each other. They are equivalent in detecting PfSET7.

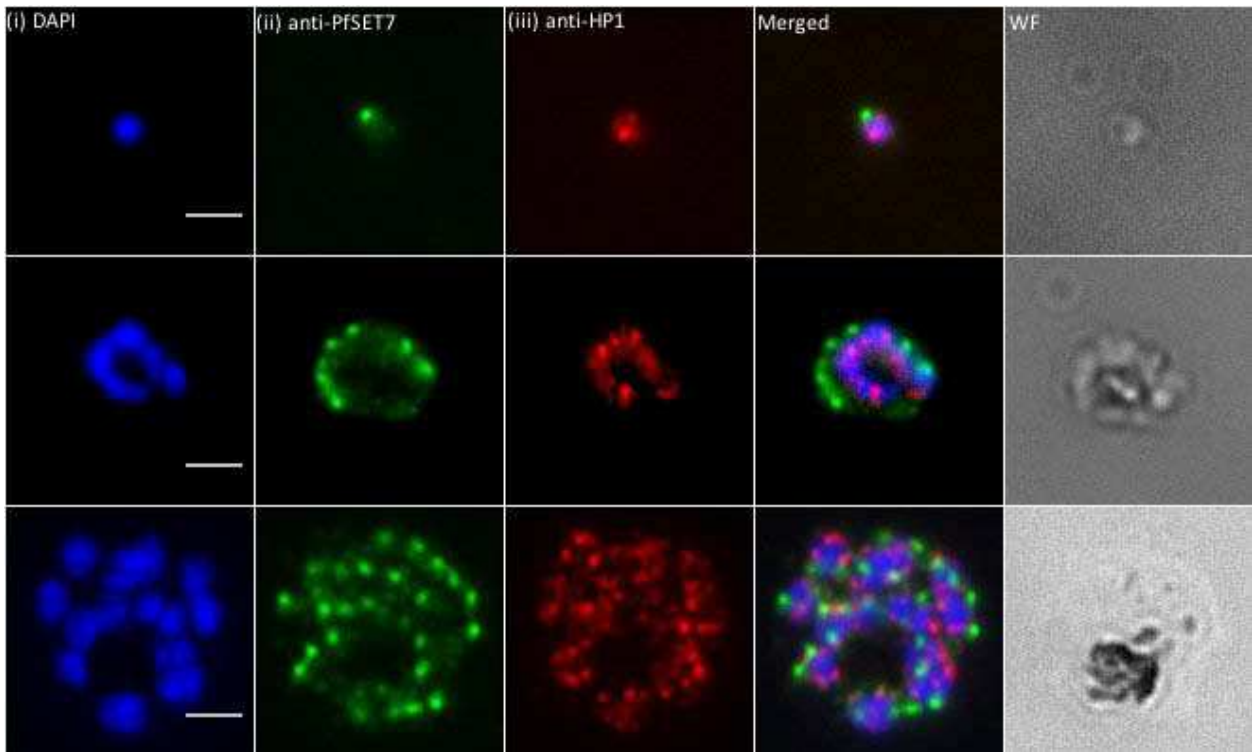


Figure S24 | **Cellular localization of PfSET7 at different blood cell stages.** IF of *P. falciparum* erythrocytic stage rings, trophozoites and schizonts using anti-PfSET7 combined with the nuclear periphery marker PfHP1. Throughout the three asexual blood stages, PfSET7 shows a punctate pattern adjacent to nucleus and distant from nuclear periphery. Scale bar is 2  $\mu$ m.

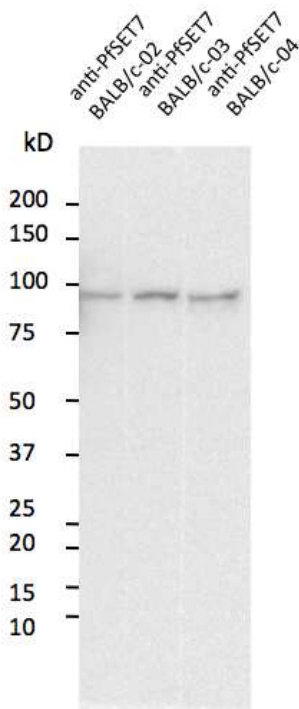


Figure S25 | **Western blot of parasite lysates using the native PfSET7 antibody.**

The anti-PfSET7 antibody from three separate animals all recognize a single band representing the 94 kDa native PfSET7 protein. Identical lanes from a single membrane were cut, probed with the three antibodies individually and then imaged together as oriented on the original membrane.



## ARTICLE 3

### **A SMYD-type methyltransferase PfSET6 associates with a subset of gene loci of *Plasmodium falciparum* and forms multiple cytoplasmic foci during asexual, sexual blood stage and sporozoite stage**

Ding, Chen, Baumgarten, Vembar, **Zanghì et al, in preparation**

Having characterized PfSET7 in the previous chapter (Articl 2), in this work we focused on PfSET6, a SMYD-type methyltransferase that is essential for *P. falciparum* blood stage development. Recombinant PfSET6 showed histone methyltransferase activity *in vitro*, but to a much lower level than PfSET7, indicating that it either functions in the presence of activating co-factors or on different non-histone substrates. Using anti-PfSET6 antibodies in immunofluorescence assays, we found that PfSET6 localization is dynamic during blood stage development, with a partial overlap with the repression centers of *var* genes, as analyzed by PfHP1 co-staining. Moreover, chromatin immunoprecipitation and next generation sequencing analysis revealed that PfSET6 may play a role in transcriptional repression in ring stages, and may regulate genes that are associated with H3K9me3 and PfHP1.

**In this work, I determined PfSET6 distribution in sporozoites using indirect immunofluorescence microscopy with anti-PfSET6 antibodies.**



**A SMYD-type methyltransferase PfSET6 associates with a subset of gene loci of *Plasmodium falciparum* and forms multiple cytoplasmic foci during asexual, sexual blood stage and sporozoite stage**

Ding Shuai<sup>1,2,3</sup> Chen Patty B. <sup>1,2,3</sup>, Baumgarten Sebastian<sup>1,2,3</sup>, Vembar Shruthi<sup>1,2,3</sup>, Zanghì Gigliola<sup>4,5,6</sup>, Mecheri Salah<sup>1,2,3</sup>, Mazier Dominique<sup>4,5,6</sup> and Scherf Artur<sup>1,2,3</sup> \*

<sup>1</sup>*Unité Biologie des Interactions Hôte-Parasite, Département de Parasites et Insectes Vecteurs, Institut Pasteur, Paris 75015, France;*

<sup>2</sup>*CNRS, ERL 9195, Paris 75015, France;*

<sup>3</sup>*INSERM, Unit U1201, Paris 75015, France;*

<sup>4</sup>*Sorbonne Universités, Université Pierre et Marie Curie-Paris 6, UMR S945 Paris, F-75013 France*

<sup>5</sup>*Institut National de la Santé et de la Recherche Médicale U945, F-75013 Paris, France*

<sup>6</sup>*AP-HP, Groupe Hospitalier Pitié-Salpêtrière, Service Parasitologie-Mycologie, Paris, F-75013, France*

- *Corresponding author: Scherf Artur email: artur.scherf@pasteur.fr*

## Abstract

Epigenetic control via reversible histone methylation regulates transcriptional activation of *Plasmodium falciparum* blood stage development activation including sexual stage commitment and default silencing of clonally variant virulence gene families. *P. falciparum* encodes ten predicted histone lysine methyltransferases (HKMTs) with a predicted catalytic SET (Su(var)3-9 and 'Enhancer of zeste') protein domain. HKMTs represent attractive drug targets but only PfSET2, PfSET7 and PfSET10 have been characterized to a limited extent in malaria parasites. PfSET6 was shown refractory to genetic disruption in blood stages, indicating an essential role in parasite development. Here we have expressed the recombinant full length PfSET6 in insect cells. Purified PfSET6 showed methyltransferase activity to histone H3. Immunofluorescence (IF) assays using antibodies raised against recombinant PfSET6 revealed a nuclear localization pattern in ring stage and a punctuated pattern in the cytoplasm of mature stage parasites. This cellular distribution is supported by cellular fractionation and western blot analysis, which showed that anti-PfSET6 detect a band of the expected size (60 kDa) in nuclear and cytoplasmic fractions of parasite cell lysates. In addition, PfSET6 is enriched within foci-like structures in the cytoplasm of sexual stage gametocytes and forms discrete foci in the cytoplasm and nucleus of salivary gland sporozoites. Genome-wide chromatin immunoprecipitation assays of ring stage parasites, when PfSET6 is nuclear, showed an enrichment of PfSET6 within the promoter and gene body of a subset of genes including select clonally variant *var* genes in subtelomeric and chromosome-internal regions. In summary, our work suggests that PfSET6 may have a cytoplasmic role in addition to the predicted nuclear function during the life cycle. Given that PfSET6 apparently targets multiple substrates during the parasite life cycle, this could explain its essentiality during blood stage growth.

## INTRODUCTION

Despite major efforts, malaria remains the most significant human parasitic disease of humans and claims approximately 0.6 million lives per year (WHO, 2015). Global efforts to control malaria have been hampered by the development of drug resistance in parasites and insecticide resistance in mosquitoes, and the lack of an effective vaccine. The human malaria parasites, such as *Plasmodium falciparum* and *P. vivax*, undergo a complex life cycle within the mosquito vector and the human host. Development within the human host involves a pre-erythrocytic liver stage, asexual intra-erythrocytic stages responsible for all disease pathology, and sexual stages permitting disease transmission. Stage transitions in the multistage life cycle are highly regulated and orchestrated by distinct programs of gene activation. Of the transcriptional waves in *P. falciparum*, the intra-erythrocytic developmental cycle (IDC) is the best studied. It revealed that the ring, trophozoite and schizont stages of the IDC have distinct transcriptomic profiles resulting in a cascade of gene expression, with every mRNA reaching peak levels at only one timepoint of this 48 hour cycle (Bozdech et al., 2003; Foth et al., 2011).

A variety of epigenetic and post-transcriptional mechanisms have been found to contribute to orchestrate gene activation or repression in *P. falciparum* (Doerig et al., 2015b; Guizetti and Scherf, 2013; Scherf et al., 2008a). Genome-wide analysis of histone post-translational modifications (PTMs) provide the evidence linking histone methylation and acetylation to a gene's transcriptional status (Salcedo-Amaya et al., 2009), particularly for the well-known clonally variant gene family *var*, which is responsible for antigenic variation in *P. falciparum* blood stage pathogenesis. Acetylation and methylation of N-terminal histone lysines are the two most common PTMs with distinct distributions along both euchromatin and heterochromatin in *P. falciparum* (Saraf et al., 2016b; Trelle et al., 2009). The overarching observation is that the euchromatic marks H3K9ac (acetylation of histone H3 lysine 9) and H3K4me3 (tri-methylation of histone H3 lysine 4) are widely distributed across the genome, including in intergenic regions, and are enriched at promoters of actively transcribed genes (Salcedo-Amaya et al., 2009) (Lopez-Rubio et al., 2007; J. J. Lopez-Rubio et al., 2009). In contrast, the heterochromatin marker H3K9me3 (tri-methylation of histone H3 lysine 9) is distributed in broad domains over silenced regions (Chookajorn et al., 2007; Lopez-Rubio et

al., 2007; J. J. Lopez-Rubio et al., 2009). Specifically, H3K9me3 is associated with multigene families such as *var*, *rifin* and *stevor*, and genes encoding a parasite-induced erythrocyte permeation pathway and with regulating the commitment to sexual differentiation (J. J. Lopez-Rubio et al., 2009). The therapeutic implication from the above mentioned findings is that the rational drug design against histone modification machineries could potentially interfere with all life cycle stage. Preliminary studies indicated that a known anti-cancer drug BIX-01294, which is a diaminoquinazoline that targets the human SET domain protein G9a, and one of its analogues TM2-115 caused rapid and specific parasite death with a concomitant reduction in parasite histone methylation levels (Malmquist et al., 2012, 2015; Sundriyal et al., 2014). Of interest, the same drugs also affected the quiescent state of *Plasmodium* hypnozoites by waking them thus allowing their develop into mature dividing forms (Demb et al., 2014). These studies established histone methylation can be an attractive direction in antimalarial drug discovery. Moreover, given that particular histone methylation states are linked to important biological processes of *P. falciparum*, specific inhibitors could be potentially used to explore the fascinating biology of this parasite.

As the most essential components of histone methylation mark writers, protein methyltransferase (PKMTs) catalyze the mono-, di- or tri-methylation of lysine residues or the mono- or di-methylation of arginine residues (PRMTs). The Su(var)3-9–Enhancer of zeste–Trithorax (SET) domain was demonstrated to be the catalytic domain for lysine methylation, consisting of binding sites for histone substrate and methyl donor molecule S-(5'-Adenosyl)-L-methionine (SAM). In *P. falciparum*, ten SET domain-containing HKMTs have been bioinformatically predicted (Cui et al., 2008). Six of the ten PfSET genes were refractory to knock-out attempts via double crossover homologous recombination, suggesting that these genes play a role in development of asexual blood stage parasites (Jiang et al., 2013). Until now, three PfSET proteins have been characterized in *P. falciparum* to a certain limit. PfSET10, a putative H3K4 methyltransferase implicated in clonally variant gene expression, localizes to a single spot within the nuclear periphery of all asexual blood stages, coinciding with the perinuclear poised *var* expression site (Volz et al., 2010; Jennifer C. Volz et al., 2012). PfSET2, also called PfSETvs, is predicted to mediate H3K36-specific methylation. Disruption of PfSETvs causes loss of H3K36me3 at the transcription start site of all silent *var* genes and leads to their de-repression, indicating it plays a pivotal role in broadly silencing *var* genes (Jiang et al., 2013). PfSET7, the only *P. falciparum* SET-domain protein that has been purified and enzymatically characterized, shows robust methyltransferase activity *in*

*in vitro* and localizes to apical organelles in schizont stages of the IDC (Chen et al., 2016). Moreover, PfSET7 methylates histone H3K4 and H3K9 in the presence of pre-existing acetylated histone H3 lysine 14 (H3K14ac). However, because gene knockout and mRNA knockdown of PfSET7 was not achieved, its *in vivo* function remains unknown.

In this report we produced recombinant full length PfSET6 and investigated the biological function of PfSET6 in different life cycle stages. We showed that the cellular localization of PfSET6 changes during the IDC and partially overlaps with *var* repression centres, putative mRNA-containing granules and apical organelles. This points to non-histone PfSET6 targets outside the nucleus. Moreover, genome-wide occupancy analyses indicated that PfSET6 associates with particular genome regions in a manner that correlates with transcriptional repression.

## RESULTS

### Recombinant PfSET6 possesses histone methyltransferase activity

The PfSET6 open reading frame of 1,530 nucleotides (PF3D7\_1355300) encodes a 509 amino acid protein containing a SET domain (codons 1-250) and Myeloid-Nervy-DEAF1 (MYND) domain (codons 62-100) at the amino terminus (Figure 1a), suggesting that PfSET6 belongs to the SMYD3 family of methyltransferases. Notably, the conserved SET domain is split into two parts by the MYND domain (Figure 1a). Phylogenetic analysis of PfSET6 orthologues in Apicomplexans using EggNOG indicated that while *Plasmodium* SET6 proteins are well conserved with 85.7% identity, they are genetically divergent from *Toxoplasma* and *Cryptosporidium* SET proteins (Supplementary Figure 1).

Next, to determine whether PfSET6 possesses methyltransferase activity *in vitro*, we expressed recombinant full-length PfSET6 fused to a C-terminal 2x-Streptavidin tag using a baculovirus-based Sf9 insect cell expression system (Figure 1a). Due to the high AT-content of the *set6* gene (76.1%), for heterologous protein expression, we utilized a codon-optimized version of *set6*. The resulting protein was purified using StrepTrap HP columns and resolved using denaturing gel electrophoresis. When visualized by Bio-Rad Stain-Free detection, the gel revealed two migrating bands, one of approximately 60kDa, and the other band which was consistently observed at 50kDa and has been validated as a recombinant PfSET6 by western blotting using anti-Streptavidin antibodies (Figure 1b).

Biochemical characterization of methyltransferase activity of recombinant PfSET6 was performed using a radioactive assay described earlier (Chen et al., 2016). We used purified histones to measure the incorporation of radiolabeled methyl groups from a S-adenosyl methionine (SAM) donor over time. We observed that recombinant PfSET6 exhibited histone methyltransferase activity that was 3-fold higher than the control (Figure 1c). However, this was significantly lower than PfSET7 or human G9a methyltransferase activity (Chen et al., 2016). It has previously been shown that SMYD3 proteins optimally function in the presence of co-factors such as chaperone hsp90. Therefore, we repeated the methyltransferase assay in the presence of total parasite lysates. However, we did not observe an increase in PfSET6 activity over time indicating that such interaction probably has less reciprocal effect on methyltransferase activity and nuclear chaperone activity compared with *in vivo* (data not shown).

To explore the enzyme specificity, we performed a second independent analysis of PfSET6 activity. The methyltransferase reaction was resolved by denaturing gel electrophoresis and radiolabeled proteins detected using autoradiography. As shown in Figure 1d, a single methylated band at 17kDa corresponding to histone H3 was apparent in reactions containing both PfSET6 and nucleosomes (lane 1). In the absence of nucleosomes or in the presence of an unrelated substrate BSA, there was no methyl transfer, suggesting that PfSET6 is indeed a histone H3 methyltransferase.

### **PfSET6 localizes to the nucleus and cytoplasm of asexual blood stage parasites in a dynamic and punctate pattern**

Anti-PfSET6 antibodies generated in mice against recombinant full-length of PfSET6 were used to determine cellular localization of PfSET6 during blood stage growth. First, the specificity of the anti-PfSET6 antibodies was assessed using western blotting of either parasite lysates (Supplementary Figure 2, left lane) or purified PfSET6 (right lane). These results showed that the anti-PfSET6 antibodies recognize a single band representing the 60kDa native PfSET6 protein in parasite lysates.

Second, to determine the sub-cellular distribution of PfSET6, whole parasites extracts were biochemically separated into nuclear and cytoplasmic fractions, and examined by western blotting with anti-PfSET6 antibodies. Antibodies against PfAldolase or histone H3 were used as controls for cytoplasmic and nuclear fraction, respectively. Figure 2a shows that PfSET6 is

present in both cytoplasmic and nuclear fractions of extracts prepared from an asynchronous parasite culture, suggesting that PfSET6 may methylates non-histone substrates in the cytoplasm and have unique roles outside of the nucleus.

To assess the intracellular localization of PfSET6, *P. falciparum* asexual erythrocytic stage parasites were analyzed by immunofluorescence microscopy (IF). As shown in Figure 2b, PfSET6 exhibits a predominantly perinuclear distribution in ring stages, with this pattern changing in trophozoites and schizonts, where the PfSET6 signal is more diffuse throughout the parasite cytoplasm, albeit with distinct foci of enrichment. Notably, nuclear PfSET6 staining is maintained in trophozoites and schizonts. Taken together, these results suggested that PfSET6 cellular localization is dynamic during the IDC.

To determine whether the punctate pattern of PfSET6 in ring stages coincided with the well-characterized epigenetic regulator and marker of facultative heterochromatin, PfHP1, co-IF assays were performed with anti-PfSET6 and anti-PfHP1 antibodies. In rings and schizonts, PfSET6 staining partially overlapped with PfHP1 foci at the nuclear periphery (Figure 3a), implying a role for PfSET6 in gene regulation. PfSET6 staining in schizonts was also compared to other known markers of cytoplasmic organelles: BiP for the endoplasmic reticulum, ERD2 for the *cis*-golgi, CLAG3.2 for rhoptries and EBA175 for micronemes. As shown in Figure 3b, PfSET6 staining partially overlapped with BiP and EBA175, but not the other marker analyzed. This indicated that PfSET6 involved in some critical cellular processes, such as protein synthesis, and some important biological process like invasion. Finally, because the punctate cytoplasmic pattern of PfSET6 was reminiscent of mRNA-containing ribonucleoprotein (mRNA) granules, we combined PfSET6 staining with mRNP markers such as members of the DNA/RNA-binding PfAlba family. As shown in Figure 3c, PfSET6 signals partially overlapped with PfAlba1, 2 or 4 staining, suggesting the role of protein methyltransferases in post-transcriptional gene regulation or mRNA regulation or translational repression has been described previously (Dastidar et al., 2012; Vembar et al., 2015).

### **PfSET6 localizes to distinct foci in different sub-compartments of *P. falciparum* transmission stages**

To determine if PfSET6 continues to be expressed after the parasite differentiates into sexual erythrocytic stages, we performed co-IF assays with anti-Pfg377 antibodies. The reference

marker Pfg377 is a gametocyte antigen associated with osmiophilic bodies, membrane-bound vesicles that are found in female gametocytes and become progressively more abundant as gametocyte reaches full maturity; that are believed to be involved in gamete egress from the host cell (Sannella et al., 2012). Figure 4a shows that in stage IV and V gametocytes, PfSET6 predominantly localized at the parasite membrane, with a low dispersed signal in the cytoplasm, which partially overlapped with Pfg377. Additionally, we observed that PfSET6 localizes in discrete cytoplasmic foci and co-localizes with the nucleus of salivary gland sporozoites (Figure 4b). These combined IF suggest that PfSET6 localizes to different cellular sub-compartments during parasite development in a dynamic manner, indicating that it may methylate both histone and non-histone substrates to achieve its biological function.

### **Identification of PfSET6 genome-wide occupancy**

Given that PfSET6 is predicted to be a HKMT and that it shows a nuclear localization pattern that partially coincides with an epigenetic regulator, we next asked whether PfSET6 could play a role in transcriptional regulation. We analyzed the genome-wide distribution of PfSET6 in ring stages by performing chromatin-immunoprecipitation with anti-PfSET6 antibodies (Supplementary Figure S3) and next generation sequencing (ChIP-seq). As shown in the circular genome-wide map of Figure 5a, we observed that PfSET6 localized to all chromosomes, with no apparent enrichment at chromosomal ends. Moreover, when we performed peak enrichment analysis using MACS2, we found that PfSET6 occupied hundreds genomic positions, near promoters, within gene bodies and within intergenic regions. These corresponded to a total of 94 genes, reflecting less than 2% of the parasite's coding genome (supplementary Table 1).

Specifically, PfSET6 bound to select subtelomeric *var* genes on chromosome 1, 2, 3, 5, 6, 7, 9 and 13, as well as chromosome-central *var* gene clusters in chromosome 4. Notably, PfSET6 occupancy was not restricted to *var* loci, but also included other clonally variant gene families such as *rifin* and *stevor*. Other PfSET6-bound genes encode exported proteins (of the *epf1*, *epf3*, *epf4* families), liver stage antigen (*lsa1*), the gametocyte-specific protein (*Pf11-1*), histone phosphosite binding protein (14-3-3I), heterochromatin protein (*hp1*), DNA/RNA-binding protein (*alba2*), ribosomal RNA loci and hypothetical conserved proteins.

Next, we asked whether PfSET6 chromosomal occupancy coincided with known epigenetic regulators (i.e., PfHP1) and histone post-translational modifications (i.e., H3K9me3, a

repressive mark, and H3K4me3, the predicted modification of PfSET6). On the gross genomic level, we did not observe a significant overlap between PfSET6 distribution and the distribution of any of these marks, as shown in Figure 6a. However, in select cases, PfSET6 occupancy coincided with the repressive chromatin markers PfHP1 and H3K9me3 (Figure 6b), validating the IF observations of Figure 3a. Notably, there was no correlation between PfSET6 and H3K4me3 distribution indicating that they are functionally unrelated.

## DISCUSSION

Histone methylation has been shown to play an important role in the control of general transcriptional regulation, monoallelic expression of virulence genes, and in the commitment to transmission stage development in *P. falciparum* (Scherf et al., 2008a). These important biological processes are still ill-defined. SET domain proteins have been associated to histone methyltransferase activity in malaria parasites, however the biological role of most *plasmodial* SET domain encoding genes remains unknown. Here we report the expression, purification and biological characterization of PfSET6, a protein lysine methyltransferase which was refractory to classical genetic disruption in asexual blood stages. PfSET6 has an unusual domain structure belonging to the SET and MYND domain-containing proteins (SMYD), that are a special class of protein lysine methyltransferases involved in methylation of histones and non-histone targets in other eukaryotes. It has been linked to cardiomyocyte differentiation and cardiac morphogenesis and proliferation of cancer cells (Gottlieb et al., 2002; Hamamoto et al., 2004).

PfSET6 enzymatic activity showed specific histone H3 methylation using radiolabeled SAM as a methyl donor and histones as substrate. Many efforts have been made to produce an KMT active PfSET proteins, and the only example of a recombinant enzyme that shows a very high KMT activity on histones was reported recently for PfSET7 (Chen et al., 2016). Although we used the same expression and purification protocol, the full length PfSET6 showed weak activity when compared to PfSET7. One explanation for this maybe that the assay conditions used in this study such as PH, temperature, substrate and enzyme concentration are not optimal for PfSET6 function. Changing these conditions could improve the rate of PfSET6 catalysis *in vitro*. Alternatively, in human cancer research, it was shown that SMYD3-mediated di- and tri-methylation of histone H3K4 was enhanced by interaction with heat shock protein 90 $\alpha$  (HSP90 $\alpha$ ) (Silva et al., 2008). This suggests that plasmodial SET6 may require interacting partners such as chaperon for full activity. Pull-down experiments using anti-PfSET6 antibodies may reveal such partners and help to improve its KMT activity, a feature needed to high-throughput small inhibitor screening assay development.

We observed the changes in the localization of PfSET6 during asexual blood stage development: from nuclear in rings to cytoplasmic in trophozoites and schizonts (Figure 2);

this is consistent with the dual nuclear and cytoplasmic localization pattern of SMYD3 (Mazur et al., 2016). In the nucleus, PfSET6 staining partially co-localized with the heterochromatin marker PfHP1 (Figure 3a), suggesting a potential role in transcriptional repression. In the cytoplasm, PfSET6 distribution was not restricted to any specific sub-cellular compartment but was weakly diffused with partial enrichment in the ER, microneme and mRNA granules (Figure 3b, c). This points to a possible role in targeting RNA complexes, that have been shown to be involved in translational delay and repression of invasion genes (Dastidar et al., 2012; Vembar et al., 2015). The IFA staining show that most substrates of PfSET6 reside in the cytoplasm, suggesting that PfSET6 catalytic efficiency may be orders of magnitude higher on non-histone targets as compared to histones. In *P. falciparum*, although considerable research has been devoted to explore the role of histone PTMs, very little is known about more general protein PTMs and how they are regulated. Further pull down studies could reveal PfSET6 interacting partners and shed light on substrates that are methylated.

The PfSET6 ChIP-Seq data in ring stage parasites was unanticipated for a putative H3K4 methyltransferases, but there was no correlation between PfSET6 and H3K4me3 distribution. By contrast, some genes associated with PfSET6 were also enriched in the transcriptional repressor HP1, together with H3K9me3. Notably, the majority of rest PfSET6-demarcated gene code for proteins which are exported into the host erythrocyte or assisted the exportation process and closely related to the pathogenesis. Moreover, the association of PfSET6 with liver stage antigen *I*sa1 and gametocyte-specific protein Pf11-1 provide information about its potential involvement in parasites developmental decision-making. It is noteworthy that 14-3-3i coding for the histone phosphor-site binding protein was also shown in the list of gene set enrichment. In malaria parasites how the hierarchy of multiple modifications is regulated and how distinct combinatorial modification patterns are established or maintained remains to be explored. One possible explanation for the silencing-associated occupancies of PfSET6 could be the various mechanisms of SMYD3 mediated. SMYD3 contains a conserved MYND-type domain, which contains a zinc finger motif that facilitating protein-protein interaction, and other DNA-binding consensus motifs. Due to its localization within the catalytic SET domain, the DNA-interaction mediated by MYND could prevent the methyltransferase enzyme catalyzing modifications to histone lysine residue properly (Mazur et al., 2016).

Altogether, the production of full length recombinant PfSET6 in insect cells demonstrated histone methyltransferase activity. Although several attempts to generate a knock-down

transgenic line failed, the rapid and inducible knock-down of PfSET6 are still hoping to be established in the near future, providing answers to questions regarding to its essentiality for parasite survival, impact on genome-wide transcriptome and proteome-wide methylation, and even the mechanisms of action for PfSET6 in parasite development. Given that PfSET6 is expressed in all life cycle stages so far analyzed and may target distinct biology pathways, this makes this protein a very good novel target for drug development against multiple parasite stages.

## REFERENCE

- Almelli, T., Ndam, N.T., Ezimegnon, S., Alao, M.J., Ahouansou, C., Sagbo, G., Amoussou, A., Deloron, P., Tahar, R., 2014. Cytoadherence phenotype of Plasmodium falciparum-infected erythrocytes is associated with specific pfemp-1 expression in parasites from children with cerebral malaria. *Malar. J.* 13. doi:10.1186/1475-2875-13-333
- Amino, R., Thiberge, S., Martin, B., Celli, S., Shorte, S., Frischknecht, F., Ménard, R., 2006. Quantitative imaging of Plasmodium transmission from mosquito to mammal. *Nat. Med.* 12, 220–224. doi:10.1038/nm1350
- Amit-Avraham, I., Pozner, G., Eshar, S., Fastman, Y., Kolevzon, N., Yavin, E., Dzikowski, R., 2015. Antisense long noncoding RNAs regulate var gene activation in the malaria parasite Plasmodium falciparum. *Proc. Natl. Acad. Sci. U. S. A.* 112, E982-991. doi:10.1073/pnas.1420855112
- Andrews, K.T., Tran, T.N., Fairlie, D.P., 2012. Towards histone deacetylase inhibitors as new antimalarial drugs. *Curr. Pharm. Des.* 18, 3467–3479.
- Andrews, K.T., Tran, T.N., Lucke, A.J., Kahnberg, P., Le, G.T., Boyle, G.M., Gardiner, D.L., Skinner-Adams, T.S., Fairlie, D.P., 2008. Potent Antimalarial Activity of Histone Deacetylase Inhibitor Analogues. *Antimicrob. Agents Chemother.* 52, 1454–1461. doi:10.1128/AAC.00757-07
- Annoura, T., Ploemen, I.H.J., van Schaijk, B.C.L., Sajid, M., Vos, M.W., van Gemert, G.-J., Chevalley-Maurel, S., Franke-Fayard, B.M.D., Hermsen, C.C., Gego, A., Franetich, J.-F., Mazier, D., Hoffman, S.L., Janse, C.J., Sauerwein, R.W., Khan, S.M., 2012. Assessing the adequacy of attenuation of genetically modified malaria parasite vaccine candidates. *Vaccine* 30, 2662–2670. doi:10.1016/j.vaccine.2012.02.010
- Ashley, E.A., Dhorda, M., Fairhurst, R.M., Amaratunga, C., Lim, P., Suon, S., Sreng, S., Anderson, J.M., Mao, S., Sam, B., Sopha, C., Chuor, C.M., Nguon, C., Sovannaroth, S., Pukrittayakamee, S., Jittamala, P., Chotivanich, K., Chutasmit, K., Suchatsoonthorn, C., Runcharoen, R., Hien, T.T., Thuy-Nhien, N.T., Thanh, N.V., Phu, N.H., Htut, Y., Han, K.-T., Aye, K.H., Mokuolu, O.A., Olaosebikan, R.R., Folaranmi, O.O., Mayxay, M., Khanthavong, M., Hongvanthong, B., Newton, P.N., Onyamboko, M.A., Fanello, C.I., Tshefu, A.K., Mishra, N., Valecha, N., Phyto, A.P., Nosten, F., Yi, P., Tripura, R., Borrmann, S., Bashraheil, M., Peshu, J., Faiz, M.A., Ghose, A., Hossain, M.A., Samad, R., Rahman, M.R., Hasan, M.M., Islam, A., Miotto, O., Amato, R., MacInnis, B., Stalker, J., Kwiatkowski, D.P., Bozdech, Z., Jeeyapant, A., Cheah, P.Y., Sakulthaew, T., Chalk, J., Intharabut, B., Silamut, K., Lee, S.J., Vihokhern, B., Kunasol, C., Imwong, M., Tarning, J., Taylor, W.J., Yeung, S., Woodrow, C.J., Flegg, J.A., Das, D., Smith, J., Venkatesan, M., Plowe, C.V.,

- Stepniewska, K., Guerin, P.J., Dondorp, A.M., Day, N.P., White, N.J., 2014. Spread of Artemisinin Resistance in *Plasmodium falciparum* Malaria. *N. Engl. J. Med.* 371, 411–423. doi:10.1056/NEJMoa1314981
- Bachmann, A., Petter, M., Krumkamp, R., Esen, M., Held, J., Scholz, J.A.M., Li, T., Sim, B.K.L., Hoffman, S.L., Kremsner, P.G., Mordmüller, B., Duffy, M.F., Tannich, E., 2016. Mosquito Passage Dramatically Changes var Gene Expression in Controlled Human *Plasmodium falciparum* Infections. *PLoS Pathog.* 12. doi:10.1371/journal.ppat.1005538
- Baer, K., Klotz, C., Kappe, S.H.I., Schnieder, T., Frevort, U., 2007. Release of Hepatic *Plasmodium yoelii* Merozoites into the Pulmonary Microvasculature. *PLoS Pathog.* 3. doi:10.1371/journal.ppat.0030171
- Balaji, S., Babu, M.M., Iyer, L.M., Aravind, L., 2005. Discovery of the principal specific transcription factors of Apicomplexa and their implication for the evolution of the AP2-integrase DNA binding domains. *Nucleic Acids Res.* 33, 3994–4006. doi:10.1093/nar/gki709
- Baldacci, P., Ménard, R., 2004. The elusive malaria sporozoite in the mammalian host. *Mol. Microbiol.* 54, 298–306. doi:10.1111/j.1365-2958.2004.04275.x
- Balu, B., Maher, S.P., Pance, A., Chauhan, C., Naumov, A.V., Andrews, R.M., Ellis, P.D., Khan, S.M., Lin, J.-W., Janse, C.J., Rayner, J.C., Adams, J.H., 2011. CCR4-associated factor 1 coordinates the expression of *Plasmodium falciparum* egress and invasion proteins. *Eukaryot. Cell* 10, 1257–1263. doi:10.1128/EC.05099-11
- Bannister, A.J., Kouzarides, T., 2011. Regulation of chromatin by histone modifications. *Cell Res.* 21, 381–395. doi:10.1038/cr.2011.22
- Barragan, A., Brossier, F., Sibley, L.D., 2005. Transepithelial migration of *Toxoplasma gondii* involves an interaction of intercellular adhesion molecule 1 (ICAM-1) with the parasite adhesin MIC2. *Cell. Microbiol.* 7, 561–568. doi:10.1111/j.1462-5822.2005.00486.x
- Barry, A.E., Arnott, A., 2014. Strategies for designing and monitoring malaria vaccines targeting diverse antigens. *Microb. Immunol.* 5, 359. doi:10.3389/fimmu.2014.00359
- Baruch, D.I., Gormely, J.A., Ma, C., Howard, R.J., Pasloske, B.L., 1996. *Plasmodium falciparum* erythrocyte membrane protein 1 is a parasitized erythrocyte receptor for adherence to CD36, thrombospondin, and intercellular adhesion molecule 1. *Proc. Natl. Acad. Sci. U. S. A.* 93, 3497–3502.
- Baruch, D.I., Ma, X.C., Singh, H.B., Bi, X., Pasloske, B.L., Howard, R.J., 1997. Identification of a region of PfEMP1 that mediates adherence of *Plasmodium falciparum* infected erythrocytes to CD36: conserved function with variant sequence. *Blood* 90, 3766–3775.
- Baruch, D.I., Pasloske, B.L., Singh, H.B., Bi, X., Ma, X.C., Feldman, M., Taraschi, T.F., Howard, R.J., 1995. Cloning the *P. falciparum* gene encoding PfEMP1, a malarial variant antigen and adherence receptor on the surface of parasitized human erythrocytes. *Cell* 82, 77–87. doi:10.1016/0092-8674(95)90054-3
- Baum, J., Papenfuss, A.T., Mair, G.R., Janse, C.J., Vlachou, D., Waters, A.P., Cowman, A.F., Crabb, B.S., de Koning-Ward, T.F., 2009. Molecular genetics and comparative genomics reveal RNAi is not functional in malaria parasites. *Nucleic Acids Res.* 37, 3788–3798. doi:10.1093/nar/gkp239
- Baum, J., Richard, D., Healer, J., Rug, M., Krnajski, Z., Gilberger, T.-W., Green, J.L., Holder, A.A., Cowman, A.F., 2006. A conserved molecular motor drives cell invasion and gliding motility across malaria life cycle stages and other apicomplexan parasites. *J. Biol. Chem.* 281, 5197–5208. doi:10.1074/jbc.M509807200

- Bengtsson, A., Joergensen, L., Rask, T.S., Olsen, R.W., Andersen, M.A., Turner, L., Theander, T.G., Hviid, L., Higgins, M.K., Craig, A., Brown, A., Jensen, A.T.R., 2013. A novel domain cassette identifies Plasmodium falciparum PfEMP1 proteins binding ICAM-1 and is a target of cross-reactive, adhesion-inhibitory antibodies. *J. Immunol. Baltim. Md 1950* 190, 240–249. doi:10.4049/jimmunol.1202578
- Besteiro, S., Dubremetz, J.-F., Lebrun, M., 2011. The moving junction of apicomplexan parasites: a key structure for invasion. *Cell. Microbiol.* 13, 797–805. doi:10.1111/j.1462-5822.2011.01597.x
- Billker, O., Lindo, V., Panico, M., Etienne, A.E., Paxton, T., Dell, A., Rogers, M., Sinden, R.E., Morris, H.R., 1998. Identification of xanthurenic acid as the putative inducer of malaria development in the mosquito. *Nature* 392, 289–292. doi:10.1038/32667
- Bougdour, A., Maubon, D., Baldacci, P., Ortet, P., Bastien, O., Bouillon, A., Barale, J.-C., Pelloux, H., Ménard, R., Hakimi, M.-A., 2009. Drug inhibition of HDAC3 and epigenetic control of differentiation in Apicomplexa parasites. *J. Exp. Med.* 206, 953–966. doi:10.1084/jem.20082826
- Bozdech, Z., Llin??s, M., Pulliam, B.L., Wong, E.D., Zhu, J., DeRisi, J.L., 2003. The transcriptome of the intraerythrocytic developmental cycle of Plasmodium falciparum. *PLoS Biol.* 1, 85–100. doi:10.1371/journal.pbio.0000005
- Brancucci, N.M.B., Bertschi, N.L., Zhu, L., Niederwieser, I., Chin, W.H., Wampfler, R., Freymond, C., Rottmann, M., Felger, I., Bozdech, Z., Voss, T.S., 2014. Heterochromatin Protein 1 Secures Survival and Transmission of Malaria Parasites. *Cell Host Microbe* 16, 165–176. doi:10.1016/j.chom.2014.07.004
- Bull, P.C., Abdi, A.I., 2016. The role of PfEMP1 as targets of naturally acquired immunity to childhood malaria: prospects for a vaccine. *Parasitology* 143, 171–186. doi:10.1017/S0031182015001274
- Bunnik, E.M., Le Roch, K.G., 2015. PfAlba1: master regulator of translation in the malaria parasite. *Genome Biol.* 16, 221. doi:10.1186/s13059-015-0795-x
- Carlson, J., Helmsby, H., Hill, A.V., Brewster, D., Greenwood, B.M., Wahlgren, M., 1990. Human cerebral malaria: association with erythrocyte rosetting and lack of anti-rosetting antibodies. *Lancet Lond. Engl.* 336, 1457–1460.
- Carman, C.V., Springer, T.A., 2004. A transmigratory cup in leukocyte diapedesis both through individual vascular endothelial cells and between them. *J. Cell Biol.* 167, 377–388. doi:10.1083/jcb.200404129
- Carruthers, V.B., Sibley, L.D., 1997. Sequential protein secretion from three distinct organelles of Toxoplasma gondii accompanies invasion of human fibroblasts. *Eur. J. Cell Biol.* 73, 114–123.
- Cary, C., Lamont, D., Dalton, J.P., Doerig, C., 1994. Plasmodium falciparum chromatin: nucleosomal organisation and histone-like proteins. *Parasitol. Res.* 80, 255–258.
- Chaal, B.K., Gupta, A.P., Wastuwidyaningtyas, B.D., Luah, Y.-H., Bozdech, Z., 2010. Histone Deacetylases Play a Major Role in the Transcriptional Regulation of the Plasmodium falciparum Life Cycle. *PLOS Pathog* 6, e1000737. doi:10.1371/journal.ppat.1000737
- Chen, P.B., Ding, S., Zanghì, G., Soulard, V., DiMaggio, P.A., Fuchter, M.J., Mecheri, S., Mazier, D., Scherf, A., Malmquist, N.A., 2016. Plasmodium falciparum PfSET7: enzymatic characterization and cellular localization of a novel protein methyltransferase in sporozoite, liver and erythrocytic stage parasites. *Sci. Rep.* 6, 21802. doi:10.1038/srep21802
- Chen, Q., Barragan, A., Fernandez, V., Sundström, A., Schlichtherle, M., Sahlén, A., Carlson, J., Datta, S., Wahlgren, M., 1998. Identification of Plasmodium falciparum

- erythrocyte membrane protein 1 (PfEMP1) as the rosetting ligand of the malaria parasite *P. falciparum*. *J. Exp. Med.* 187, 15–23.
- Chen, Q., Heddini, A., Barragan, A., Fernandez, V., Pearce, S.F., Wahlgren, M., 2000. The semiconserved head structure of *Plasmodium falciparum* erythrocyte membrane protein 1 mediates binding to multiple independent host receptors. *J. Exp. Med.* 192, 1–10.
- Chêne, A., Vembar, S.S., Rivière, L., Lopez-Rubio, J.J., Claes, A., Siegel, T.N., Sakamoto, H., Scheidig-Benatar, C., Hernandez-Rivas, R., Scherf, A., 2012. PfAlbas constitute a new eukaryotic DNA/RNA-binding protein family in malaria parasites. *Nucleic Acids Res.* 40, 3066–3077. doi:10.1093/nar/gkr1215
- Chitnis, C.E., Sharma, A., 2008. Targeting the *Plasmodium vivax* Duffy-binding protein. *Trends Parasitol.* 24, 29–34. doi:10.1016/j.pt.2007.10.004
- Chookajorn, T., Dzikowski, R., Frank, M., Li, F., Jiwani, A.Z., Hartl, D.L., Deitsch, K.W., 2007. Epigenetic memory at malaria virulence genes. *Proc. Natl. Acad. Sci. U. S. A.* 104, 899–902. doi:10.1073/pnas.0609084103
- Clyde, D.F., 1990. Immunity to *falciparum* and *vivax* malaria induced by irradiated sporozoites: a review of the University of Maryland studies, 1971-75. *Bull. World Health Organ.* 68 Suppl, 9–12.
- Cogswell, F.B., 1992. The hypnozoite and relapse in primate malaria. *Clin. Microbiol. Rev.* 5, 26–35.
- Contreras, C.E., Santiago, J.I., Jensen, J.B., Udeinya, I.J., Bayoumi, R., Kennedy, D.D., Druilhe, P., 1988. RESA-IFA assay in *Plasmodium falciparum* malaria, observations on relationship between serum antibody titers, immunity, and antigenic diversity. *J. Parasitol.* 74, 129–134.
- Cottrell, G., Musset, L., Hubert, V., Le Bras, J., Clain, J., 2014. Emergence of Resistance to Atovaquone-Proguanil in Malaria Parasites: Insights from Computational Modeling and Clinical Case Reports. *Antimicrob. Agents Chemother.* 58, 4504–4514. doi:10.1128/AAC.02550-13
- Counihan, N.A., Kalanon, M., Coppel, R.L., de Koning-Ward, T.F., 2013. *Plasmodium* rhoptry proteins: why order is important. *Trends Parasitol.* 29, 228–236. doi:10.1016/j.pt.2013.03.003
- Cowman, A.F., Crabb, B.S., 2006. Invasion of red blood cells by malaria parasites. *Cell* 124, 755–766. doi:10.1016/j.cell.2006.02.006
- Cui, L., Miao, J., 2010. Chromatin-Mediated Epigenetic Regulation in the Malaria Parasite *Plasmodium falciparum*. *Eukaryot. Cell* 9, 1138–1149. doi:10.1128/EC.00036-10
- Cui, L., Miao, J., Furuya, T., Li, X., Su, X., Cui, L., 2007. PfGCN5-Mediated Histone H3 Acetylation Plays a Key Role in Gene Expression in *Plasmodium falciparum*. *Eukaryot. Cell* 6, 1219–1227. doi:10.1128/EC.00062-07
- Cui, L.L., Fan, Q., Cui, L.L., Miao, J., 2008. Histone lysine methyltransferases and demethylases in *Plasmodium falciparum*. *Int. J. Parasitol.* 38, 1083–1097. doi:10.1016/j.ijpara.2008.01.002
- da Silva, H.B., Caetano, S.S., Monteiro, I., Gómez-Conde, I., Hanson, K., Penha-Gonçalves, C., Olivieri, D.N., Mota, M.M., Marinho, C.R., D’Imperio Lima, M.R., Tadokoro, C.E., 2012. Early skin immunological disturbance after *Plasmodium*-infected mosquito bites. *Cell. Immunol.* 277, 22–32. doi:10.1016/j.cellimm.2012.06.003
- Darkin-Rattray, S.J., Gurnett, A.M., Myers, R.W., Dulski, P.M., Crumley, T.M., Allocco, J.J., Cannova, C., Meinke, P.T., Colletti, S.L., Bednarek, M.A., Singh, S.B., Goetz, M.A., Dombrowski, A.W., Polishook, J.D., Schmatz, D.M., 1996. Apicidin: A novel antiprotozoal agent that inhibits parasite histone deacetylase. *Proc. Natl. Acad. Sci. U. S. A.* 93, 13143–13147.

- Dastidar, E.G., Dayer, G., Holland, Z.M., Dorin-Semblat, D., Claes, A., Chene, A., Sharma, A., Hamelin, R., Moniatte, M., Lopez-Rubio, J.-J., Scherf, A., Doerig, C., 2012. Involvement of Plasmodium falciparum protein kinase CK2 in the chromatin assembly pathway. *BMC Biol.* 10, 5. doi:10.1186/1741-7007-10-5
- Demb, L., Franetich, L., Lorthiois, A., Gego, A., Zeeman, A.-M., M Kocken, C.H., Le Grand, R., Dereuddre-Bosquet, N., van Gemert, G.-J., Sauerwein, R., Vaillant, J.-C., Hannoun, L., Fuchter, M.J., Diagana, T.T., Malmquist, N.A., Scherf, A., Snounou, G., Mazier, D., 2014. Persistence and activation of malaria hypnozoites in long-term primary hepatocyte cultures. doi:10.1038/nm.3461
- Dembélé, L., Franetich, J.-F., Lorthiois, A., Gego, A., Zeeman, A.-M., Kocken, C.H.M., Le Grand, R., Dereuddre-Bosquet, N., van Gemert, G.-J., Sauerwein, R., Vaillant, J.-C., Hannoun, L., Fuchter, M.J., Diagana, T.T., Malmquist, N.A., Scherf, A., Snounou, G., Mazier, D., 2014. Persistence and activation of malaria hypnozoites in long-term primary hepatocyte cultures. *Nat. Med.* 20, 307–312. doi:10.1038/nm.3461
- Doerig, C., Rayner, J.C., Scherf, A., Tobin, A.B., 2015a. Post-translational protein modifications in malaria parasites. *Nat. Rev. Microbiol.* 13, 160–172. doi:10.1038/nrmicro3402
- Doerig, C., Rayner, J.C., Scherf, A., Tobin, A.B., 2015b. Post-translational protein modifications in malaria parasites. *Nat. Rev. Microbiol.* 13, 160–172. doi:10.1038/nrmicro3402
- Douglas, A.D., Williams, A.R., Illingworth, J.J., Kamuyu, G., Biswas, S., Goodman, A.L., Wyllie, D.H., Crosnier, C., Miura, K., Wright, G.J., Long, C.A., Osier, F.H., Marsh, K., Turner, A.V., Hill, A.V.S., Draper, S.J., 2011. The Blood-Stage Malaria Antigen PfRH5 is Susceptible to Vaccine-Inducible Cross-Strain Neutralizing Antibody. *Nat. Commun.* 2, 601. doi:10.1038/ncomms1615
- Douglas, R.G., Amino, R., Sinnis, P., Frischknecht, F., 2015. Active migration and passive transport of malaria parasites. *Trends Parasitol.* 31, 357–362. doi:10.1016/j.pt.2015.04.010
- Dowse, T., Soldati, D., 2004. Host cell invasion by the apicomplexans: the significance of microneme protein proteolysis. *Curr. Opin. Microbiol.* 7, 388–396. doi:10.1016/j.mib.2004.06.013
- Drew, D.R., Beeson, J.G., 2015. PfRH5 as a candidate vaccine for Plasmodium falciparum malaria. *Trends Parasitol.* 31, 87–88. doi:10.1016/j.pt.2015.02.001
- Dudareva, M., Andrews, L., Gilbert, S.C., Bejon, P., Marsh, K., Mwacharo, J., Kai, O., Nicosia, A., Hill, A.V.S., 2009. Prevalence of serum neutralizing antibodies against chimpanzee adenovirus 63 and human adenovirus 5 in Kenyan Children, in the context of vaccine vector efficacy. *Vaccine* 27, 3501–3504. doi:10.1016/j.vaccine.2009.03.080
- Ewer, K.J., O’Hara, G.A., Duncan, C.J.A., Collins, K.A., Sheehy, S.H., Reyes-Sandoval, A., Goodman, A.L., Edwards, N.J., Elias, S.C., Halstead, F.D., Longley, R.J., Rowland, R., Poulton, I.D., Draper, S.J., Blagborough, A.M., Berrie, E., Moyle, S., Williams, N., Siani, L., Folgari, A., Colloca, S., Sinden, R.E., Lawrie, A.M., Cortese, R., Gilbert, S.C., Nicosia, A., Hill, A.V.S., 2013. Protective CD8+ T-cell immunity to human malaria induced by chimpanzee adenovirus-MVA immunisation. *Nat. Commun.* 4. doi:10.1038/ncomms3836
- Fairhurst, R.M., 2015. Understanding artemisinin-resistant malaria: what a difference a year makes. *Curr. Opin. Infect. Dis.* 28, 417–425. doi:10.1097/QCO.000000000000199
- Fan, Q., Miao, J., Cui, L., Cui, L., 2009. Characterization of PRMT1 from Plasmodium falciparum. *Biochem. J.* 421, 107–118. doi:10.1042/BJ20090185

- Figueiredo, L.M., Pirrit, L.A., Scherf, A., Pirritt, L.A., 2000. Genomic organisation and chromatin structure of *Plasmodium falciparum* chromosome ends. *Mol. Biochem. Parasitol.* 106, 169–174.
- Florens, L., Washburn, M.P., Raine, J.D., Anthony, R.M., Grainger, M., Haynes, J.D., Moch, J.K., Muster, N., Sacci, J.B., Tabb, D.L., Witney, A.A., Wolters, D., Wu, Y., Gardner, M.J., Holder, A.A., Sinden, R.E., Yates, J.R., Carucci, D.J., 2002. A proteomic view of the *Plasmodium falciparum* life cycle. *Nature* 419, 520–526.  
doi:10.1038/nature01107
- Flueck, C., Bartfai, R., Volz, J., Niederwieser, I., Salcedo-Amaya, A.M., Alako, B.T.F., Ehlgén, F., Ralph, S.A., Cowman, A.F., Bozdech, Z., Stunnenberg, H.G., Voss, T.S., 2009a. *Plasmodium falciparum* Heterochromatin Protein 1 Marks Genomic Loci Linked to Phenotypic Variation of Exported Virulence Factors. *PLoS Pathog.* 5.  
doi:10.1371/journal.ppat.1000569
- Flueck, C., Bartfai, R., Volz, J., Niederwieser, I., Salcedo-Amaya, A.M., Alako, B.T.F., Ehlgén, F., Ralph, S.A., Cowman, A.F., Bozdech, Z., Stunnenberg, H.G., Voss, T.S., 2009b. *Plasmodium falciparum* heterochromatin protein 1 marks genomic loci linked to phenotypic variation of exported virulence factors. *PLoS Pathog.* 5, e1000569.  
doi:10.1371/journal.ppat.1000569
- Foth, B.J., Zhang, N., Chaal, B.K., Sze, S.K., Preiser, P.R., Bozdech, Z., 2011. Quantitative time-course profiling of parasite and host cell proteins in the human malaria parasite *Plasmodium falciparum*. *Mol. Cell. Proteomics MCP* 10, M110.006411.  
doi:10.1074/mcp.M110.006411
- Freitas-Junior, L.H., Hernandez-Rivas, R., Ralph, S.A., Montiel-Condado, D., Ruvalcaba-Salazar, O.K., Rojas-Meza, A.P., Mâncio-Silva, L., Leal-Silvestre, R.J., Gontijo, A.M., Shorte, S., Scherf, A., 2005. Telomeric Heterochromatin Propagation and Histone Acetylation Control Mutually Exclusive Expression of Antigenic Variation Genes in Malaria Parasites. *Cell* 121, 25–36. doi:10.1016/j.cell.2005.01.037
- Frevert, U., 2004. Sneaking in through the back entrance: the biology of malaria liver stages. *Trends Parasitol.* 20, 417–424. doi:10.1016/j.pt.2004.07.007
- Frevert, U., Engelmann, S., Zougbedé, S., Stange, J., Ng, B., Matuschewski, K., Liebes, L., Yee, H., 2005. Intravital Observation of *Plasmodium berghei* Sporozoite Infection of the Liver. *PLoS Biol.* 3. doi:10.1371/journal.pbio.0030192
- Frevert, U., Nacer, A., Cabrera, M., Movila, A., Leberl, M., 2014. Imaging *Plasmodium* Immunobiology in Liver, Brain, and Lung. *Parasitol. Int.* 63.  
doi:10.1016/j.parint.2013.09.013
- Frevert, U., Sinnis, P., Cerami, C., Shreffler, W., Takacs, B., Nussenzweig, V., 1993. Malaria circumsporozoite protein binds to heparan sulfate proteoglycans associated with the surface membrane of hepatocytes. *J. Exp. Med.* 177, 1287–1298.
- Fried, M., Duffy, P.E., 1996. Adherence of *Plasmodium falciparum* to chondroitin sulfate A in the human placenta. *Science* 272, 1502–1504.
- Frischknecht, F., Baldacci, P., Martin, B., Zimmer, C., Thiberge, S., Olivo-Marin, J.-C., Shorte, S.L., Ménard, R., 2004. Imaging movement of malaria parasites during transmission by *Anopheles* mosquitoes. *Cell. Microbiol.* 6, 687–694.  
doi:10.1111/j.1462-5822.2004.00395.x
- García-Martínez, J., Aranda, A., Pérez-Ortín, J.E., 2004. Genomic run-on evaluates transcription rates for all yeast genes and identifies gene regulatory mechanisms. *Mol. Cell* 15, 303–313. doi:10.1016/j.molcel.2004.06.004
- Gardner, M.J., Hall, N., Fung, E., White, O., Berriman, M., Hyman, R.W., Carlton, J.M., Pain, A., Nelson, K.E., Bowman, S., Paulsen, I.T., James, K., Eisen, J.A., Rutherford, K., Salzberg, S.L., Craig, A., Kyes, S., Chan, M.-S., Nene, V., Shallom, S.J., Suh, B.,

- Peterson, J., Angiuoli, S., Pertea, M., Allen, J., Selengut, J., Haft, D., Mather, M.W., Vaidya, A.B., Martin, D.M.A., Fairlamb, A.H., Fraunholz, M.J., Roos, D.S., Ralph, S.A., McFadden, G.I., Cummings, L.M., Subramanian, G.M., Mungall, C., Venter, J.C., Carucci, D.J., Hoffman, S.L., Newbold, C., Davis, R.W., Fraser, C.M., Barrell, B., 2002a. Genome sequence of the human malaria parasite *Plasmodium falciparum*. *Nature* 419. doi:10.1038/nature01097
- Gardner, M.J., Hall, N., Fung, E., White, O., Berriman, M., Hyman, R.W., Carlton, J.M., Pain, A., Nelson, K.E., Bowman, S., Paulsen, I.T., James, K., Eisen, J.A., Rutherford, K., Salzberg, S.L., Craig, A., Kyes, S., Chan, M.-S., Nene, V., Shallom, S.J., Suh, B., Peterson, J., Angiuoli, S., Pertea, M., Allen, J., Selengut, J., Haft, D., Mather, M.W., Vaidya, A.B., Martin, D.M.A., Fairlamb, A.H., Fraunholz, M.J., Roos, D.S., Ralph, S.A., McFadden, G.I., Cummings, L.M., Subramanian, G.M., Mungall, C., Venter, J.C., Carucci, D.J., Hoffman, S.L., Newbold, C., Davis, R.W., Fraser, C.M., Barrell, B., 2002b. Genome sequence of the human malaria parasite *Plasmodium falciparum*. *Nature* 419. doi:10.1038/nature01097
- Garnham, P.C., Bird, R.G., Baker, J.R., 1963. Electron microscope studies of motile stages of malaria parasites. IV. The fine structure of the sporozoites of four species of *Plasmodium*. *Trans. R. Soc. Trop. Med. Hyg.* 57, 27–31.
- Garver, L.S., Dong, Y., Dimopoulos, G., 2009. Caspar Controls Resistance to *Plasmodium falciparum* in Diverse Anopheline Species. *PLoS Pathog.* 5. doi:10.1371/journal.ppat.1000335
- Goel, S., Palmkvist, M., Moll, K., Joannin, N., Lara, P., Akhouri, R.R., Moradi, N., Öjemalm, K., Westman, M., Angeletti, D., Kjellin, H., Lehtiö, J., Blixt, O., Idestrom, L., Gahmberg, C.G., Storry, J.R., Hult, A.K., Olsson, M.L., von Heijne, G., Nilsson, I., Wahlgren, M., 2015. RIFINs are adhesins implicated in severe *Plasmodium falciparum* malaria. *Nat. Med.* 21, 314–317. doi:10.1038/nm.3812
- Gottlieb, P.D., Pierce, S. a, Sims, R.J., Yamagishi, H., Weihe, E.K., Harriss, J. V, Maika, S.D., Kuziel, W. a, King, H.L., Olson, E.N., Nakagawa, O., Srivastava, D., 2002. Bop encodes a muscle-restricted protein containing MYND and SET domains and is essential for cardiac differentiation and morphogenesis. *Nat. Genet.* 31, 25–32. doi:10.1038/ng866
- Graewe, S., Stanway, R.R., Rennenberg, A., Heussler, V.T., 2012. Chronicle of a death foretold: *Plasmodium* liver stage parasites decide on the fate of the host cell. *FEMS Microbiol. Rev.* 36, 111–130. doi:10.1111/j.1574-6976.2011.00297.x
- Greenwalt, D.E., Lipsky, R.H., Ockenhouse, C.F., Ikeda, H., Tandon, N.N., Jamieson, G.A., 1992. Membrane glycoprotein CD36: a review of its roles in adherence, signal transduction, and transfusion medicine. *Blood* 80, 1105–1115.
- Gueirard, P., Tavares, J., Thiberge, S., Bernex, F., Ishino, T., Milon, G., Franke-Fayard, B., Janse, C.J., Ménard, R., Amino, R., 2010. Development of the malaria parasite in the skin of the mammalian host. *Proc. Natl. Acad. Sci. U. S. A.* 107, 18640–18645. doi:10.1073/pnas.1009346107
- Guizetti, J., Barcons-Simon, A., Scherf, A., 2016. Trans-acting GC-rich non-coding RNA at var expression site modulates gene counting in malaria parasite. *Nucleic Acids Res.* gkw664. doi:10.1093/nar/gkw664
- Guizetti, J., Scherf, A., 2013. Silence, activate, poise and switch! Mechanisms of antigenic variation in *Plasmodium falciparum*. *Cell. Microbiol.* doi:10.1111/cmi.12115
- Hafalla, J.C.R., Cockburn, I.A., Zavala, F., 2006. Protective and pathogenic roles of CD8+ T cells during malaria infection. *Parasite Immunol.* 28, 15–24. doi:10.1111/j.1365-3024.2006.00777.x

- Hamamoto, R., Furukawa, Y., Morita, M., Iimura, Y., Silva, F.P., Li, M., Yagyu, R., Nakamura, Y., 2004. SMYD3 encodes a histone methyltransferase involved in the proliferation of cancer cells. *Nat. Cell Biol.* 6, 731–740. doi:10.1038/ncb1151
- Hawkins, R.D., Hon, G.C., Lee, L.K., Ngo, Q., Lister, R., Pelizzola, M., Edsall, L.E., Kuan, S., Luu, Y., Klugman, S., Antosiewicz-Bourget, J., Ye, Z., Espinoza, C., Agarwahl, S., Shen, L., Ruotti, V., Wang, W., Stewart, R., Thomson, J.A., Ecker, J.R., Ren, B., 2010. Distinct Epigenomic Landscapes of Pluripotent and Lineage-Committed Human Cells. *Cell Stem Cell* 6, 479–491. doi:10.1016/j.stem.2010.03.018
- Hemmer, C.J., Holst, F.G.E., Kern, P., Chiwakata, C.B., Dietrich, M., Reisinger, E.C., 2006. Stronger host response per parasitized erythrocyte in *Plasmodium vivax* or *ovale* than in *Plasmodium falciparum* malaria. *Trop. Med. Int. Health* 11, 817–823. doi:10.1111/j.1365-3156.2006.01635.x
- Hernandez-Rivas, R., Pérez-Toledo, K., Herrera Solorio, A.-M., Delgadillo, D.M., Vargas, M., 2010. Telomeric Heterochromatin in *Plasmodium falciparum*. *J. Biomed. Biotechnol.* 2010. doi:10.1155/2010/290501
- Hoffman, S.L., Subramanian, G.M., Collins, F.H., Venter, J.C., 2002. *Plasmodium*, human and *Anopheles* genomics and malaria. *Nature* 415, 702–709. doi:10.1038/415702a
- Holder, A.A., 2009. The carboxy-terminus of merozoite surface protein 1: structure, specific antibodies and immunity to malaria. *Parasitology* 136, 1445–1456. doi:10.1017/S0031182009990515
- Howard, R.J., Barnwell, J.W., Rock, E.P., Neequaye, J., Ofori-Adjei, D., Maloy, W.L., Lyon, J.A., Saul, A., 1988. Two approximately 300 kilodalton *Plasmodium falciparum* proteins at the surface membrane of infected erythrocytes. *Mol. Biochem. Parasitol.* 27, 207–223.
- Huang, B., Deng, C., Yang, T., Xue, L., Wang, Q., Huang, S., Su, X., Liu, Y., Zheng, S., Guan, Y., Xu, Q., Zhou, J., Yuan, J., Bacar, A., Abdallah, K.S., Attoumane, R., Mliva, A.M.S.A., Zhong, Y., Lu, F., Song, J., 2015. Polymorphisms of the artemisinin resistant marker (K13) in *Plasmodium falciparum* parasite populations of Grande Comore Island 10 years after artemisinin combination therapy. *Parasit. Vectors* 8. doi:10.1186/s13071-015-1253-z
- Hviid, L., Jensen, A.T.R., 2015. Chapter Two - PfEMP1 – A Parasite Protein Family of Key Importance in *Plasmodium falciparum* Malaria Immunity and Pathogenesis, in: Stothard, D.R. and J.R. (Ed.), *Advances in Parasitology*. Academic Press, pp. 51–84.
- Ishino, T., Chinzei, Y., Yuda, M., 2005. A *Plasmodium* sporozoite protein with a membrane attack complex domain is required for breaching the liver sinusoidal cell layer prior to hepatocyte infection. *Cell. Microbiol.* 7, 199–208. doi:10.1111/j.1462-5822.2004.00447.x
- Iwanaga, S., Kaneko, I., Kato, T., Yuda, M., 2012. Identification of an AP2-family Protein That Is Critical for Malaria Liver Stage Development. *PLOS ONE* 7, e47557. doi:10.1371/journal.pone.0047557
- Jiang, L., Mu, J., Zhang, Q., Ni, T., Srinivasan, P., Rayavara, K., Yang, W., Turner, L., Lavstsen, T., Theander, T.G., Peng, W., Wei, G., Jing, Q., Wakabayashi, Y., Bansal, A., Luo, Y., Ribeiro, J.M.C., Scherf, A., Aravind, L., Zhu, J., Zhao, K., Miller, L.H., 2013. PfSETvs methylation of histone H3K36 represses virulence genes in *Plasmodium falciparum*. *Nature* 499. doi:10.1038/nature12361
- Jones, D.O., Mattei, M.G., Horsley, D., Cowell, I.G., Singh, P.B., 2001. The gene and pseudogenes of Cbx3/mHP1 gamma. *DNA Seq. J. DNA Seq. Mapp.* 12, 147–160.
- Josling, G.A., Petter, M., Oehring, S.C., Gupta, A.P., Dietz, O., Wilson, D.W., Schubert, T., Längst, G., Gilson, P.R., Crabb, B.S., Moes, S., Jenoe, P., Lim, S.W., Brown, G.V., Bozdech, Z., Voss, T.S., Duffy, M.F., 2015. A *Plasmodium Falciparum* Bromodomain

- Protein Regulates Invasion Gene Expression. *Cell Host Microbe* 17, 741–751.  
doi:10.1016/j.chom.2015.05.009
- Josling, G.A., Selvarajah, S.A., Petter, M., Duffy, M.F., 2012. The Role of Bromodomain Proteins in Regulating Gene Expression. *Genes* 3, 320–343.  
doi:10.3390/genes3020320
- Kafsack, B.F.C., Rovira-Graells, N., Clark, T.G., Bancells, C., Crowley, V.M., Campino, S.G., Williams, A.E., Drought, L.G., Kwiatkowski, D.P., Baker, D.A., Cortés, A., Llinás, M., 2014. A transcriptional switch underlies commitment to sexual development in human malaria parasites. *Nature* 507, 248–252.  
doi:10.1038/nature12920
- Kaiser, K., Camargo, N., Kappe, S.H.I., 2003. Transformation of Sporozoites into Early Exoerythrocytic Malaria Parasites Does Not Require Host Cells. *J. Exp. Med.* 197, 1045–1050. doi:10.1084/jem.20022100
- Kanoh, J., Sadaie, M., Urano, T., Ishikawa, F., 2005. Telomere Binding Protein Taz1 Establishes Swi6 Heterochromatin Independently of RNAi at Telomeres. *Curr. Biol.* 15, 1808–1819. doi:10.1016/j.cub.2005.09.041
- Kappe, S.H.I., Buscaglia, C.A., Nussenzweig, V., 2004. Plasmodium Sporozoite Molecular Cell Biology. *Annu. Rev. Cell Dev. Biol.* 20, 29–59.  
doi:10.1146/annurev.cellbio.20.011603.150935
- Kariu, T., Ishino, T., Yano, K., Chinzei, Y., Yuda, M., 2006. CelTOS, a novel malarial protein that mediates transmission to mosquito and vertebrate hosts. *Mol. Microbiol.* 59, 1369–1379. doi:10.1111/j.1365-2958.2005.05024.x
- Keeley, A., Soldati, D., 2004. The glideosome: a molecular machine powering motility and host-cell invasion by Apicomplexa. *Trends Cell Biol.* 14, 528–532.  
doi:10.1016/j.tcb.2004.08.002
- Kimani, D., Jagne, Y.J., Cox, M., Kimani, E., Bliss, C.M., Gitau, E., Ogwang, C., Afolabi, M.O., Bowyer, G., Collins, K.A., Edwards, N., Hodgson, S.H., Duncan, C.J.A., Spencer, A.J., Knight, M.G., Drammeh, A., Anagnostou, N.A., Berrie, E., Moyle, S., Gilbert, S.C., Soipei, P., Okebe, J., Colloca, S., Cortese, R., Viebig, N.K., Roberts, R., Lawrie, A.M., Nicosia, A., Imoukhuede, E.B., Bejon, P., Chilengi, R., Bojang, K., Flanagan, K.L., Hill, A.V.S., Urban, B.C., Ewer, K.J., 2014. Translating the Immunogenicity of Prime-boost Immunization With ChAd63 and MVA ME-TRAP From Malaria Naive to Malaria-endemic Populations. *Mol. Ther.* 22, 1992–2003.  
doi:10.1038/mt.2014.109
- Kirchner, S., Power, B.J., Waters, A.P., 2016a. Recent advances in malaria genomics and epigenomics. *Genome Med.* 8. doi:10.1186/s13073-016-0343-7
- Kirchner, S., Power, B.J., Waters, A.P., 2016b. Recent advances in malaria genomics and epigenomics. *Genome Med.* 8. doi:10.1186/s13073-016-0343-7
- Kouzarides, T., 2007. SnapShot: Histone-modifying enzymes. *Cell* 131, 822.  
doi:10.1016/j.cell.2007.11.005
- Kun, J.F., Schmidt-Ott, R.J., Lehman, L.G., Lell, B., Luckner, D., Greve, B., Matousek, P., Kremsner, P.G., 1998. Merozoite surface antigen 1 and 2 genotypes and rosetting of Plasmodium falciparum in severe and mild malaria in Lambaréné, Gabon. *Trans. R. Soc. Trop. Med. Hyg.* 92, 110–114.
- Langreth, S.G., Reese, R.T., Motyl, M.R., Trager, W., 1979. Plasmodium falciparum: loss of knobs on the infected erythrocyte surface after long-term cultivation. *Exp. Parasitol.* 48, 213–219.
- Lasonder, E., Janse, C.J., van Gemert, G.-J., Mair, G.R., Vermunt, A.M.W., Douradinha, B.G., van Noort, V., Huynen, M.A., Luty, A.J.F., Kroeze, H., Khan, S.M., Sauerwein, R.W., Waters, A.P., Mann, M., Stunnenberg, H.G., 2008. Proteomic profiling of

- Plasmodium sporozoite maturation identifies new proteins essential for parasite development and infectivity. *PLoS Pathog.* 4, e1000195.  
doi:10.1371/journal.ppat.1000195
- Lavstsen, T., Salanti, A., Jensen, A.T., Arnot, D.E., Theander, T.G., 2003. Sub-grouping of *Plasmodium falciparum* 3D7 var genes based on sequence analysis of coding and non-coding regions. *Malar. J.* 2, 27. doi:10.1186/1475-2875-2-27
- Lavstsen, T., Turner, L., Saguti, F., Magistrado, P., Rask, T.S., Jespersen, J.S., Wang, C.W., Berger, S.S., Baraka, V., Marquard, A.M., Seguin-Orlando, A., Willerslev, E., Gilbert, M.T.P., Lusingu, J., Theander, T.G., 2012. *Plasmodium falciparum* erythrocyte membrane protein 1 domain cassettes 8 and 13 are associated with severe malaria in children. *Proc. Natl. Acad. Sci. U. S. A.* 109, E1791-1800.  
doi:10.1073/pnas.1120455109
- Le Roch, K.G., Zhou, Y., Blair, P.L., Grainger, M., Moch, J.K., Haynes, J.D., De La Vega, P., Holder, A.A., Batalov, S., Carucci, D.J., Winzeler, E.A., 2003. Discovery of gene function by expression profiling of the malaria parasite life cycle. *Science* 301, 1503–1508. doi:10.1126/science.1087025
- Leech, J.H., Barnwell, J.W., Miller, L.H., Howard, R.J., 1984. Identification of a strain-specific malarial antigen exposed on the surface of *Plasmodium falciparum*-infected erythrocytes. *J. Exp. Med.* 159, 1567–1575.
- Lopez-Rubio, J.J., Gontijo, A.M., Nunes, M.C., Issar, N., Hernandez Rivas, R., Scherf, A., 2007. 5' Flanking Region of Var Genes Nucleate Histone Modification Patterns Linked To Phenotypic Inheritance of Virulence Traits in Malaria Parasites. *Mol. Microbiol.* 66, 1296–1305. doi:10.1111/j.1365-2958.2007.06009.x
- Lopez-Rubio, J.J., Mancio-Silva, L., Scherf, A., 2009. Genome-wide Analysis of Heterochromatin Associates Clonally Variant Gene Regulation with Perinuclear Repressive Centers in Malaria Parasites. *Cell Host Microbe* 5, 179–190.  
doi:10.1016/j.chom.2008.12.012
- Lopez-Rubio, J.-J., Mancio-Silva, L., Scherf, A., 2009. Genome-wide Analysis of Heterochromatin Associates Clonally Variant Gene Regulation with Perinuclear Repressive Centers in Malaria Parasites. *Cell Host Microbe* 5, 179–190.  
doi:10.1016/j.chom.2008.12.012
- Lopez-Rubio, J.-J., Siegel, T.N., Scherf, A., 2013. Genome-wide chromatin immunoprecipitation-sequencing in *Plasmodium*. *Methods Mol. Biol. Clifton NJ* 923, 321–333. doi:10.1007/978-1-62703-026-7\_23
- Maier, A.G., Cooke, B.M., Cowman, A.F., Tilley, L., 2009. Malaria parasite proteins that remodel the host erythrocyte. *Nat. Rev. Microbiol.* 7, 341–354.  
doi:10.1038/nrmicro2110
- Malmquist, N.A., Moss, T.A., Mecheri, S., Scherf, A., Fuchter, M.J., 2012. Small-molecule histone methyltransferase inhibitors display rapid antimalarial activity against all blood stage forms in *Plasmodium falciparum*. *Proc. Natl. Acad. Sci.* 109, 16708–16713. doi:10.1073/pnas.1205414109
- Malmquist, N.A., Sundriyal, S., Caron, J., Chen, P., Witkowski, B., Menard, D., Suwanarusk, R., Renia, L., Nosten, F., Jimenez-Diaz, M.B., Angulo-Barturen, I., Martinez, M.S., Ferrer, S., Sanz, L.M., Gamo, F.J., Wittlin, S., Duffy, S., Avery, V.M., Ruecker, A., Delves, M.J., Sinden, R.E., Fuchter, M.J., Scherf, A., 2015. Histone methyltransferase inhibitors are orally bioavailable, fast-acting molecules with activity against different species causing malaria in humans. *Antimicrob. Agents Chemother.* doi:10.1128/AAC.04419-14

- Matuschewski, K., Nunes, A.C., Nussenzweig, V., Ménard, R., 2002a. Plasmodium sporozoite invasion into insect and mammalian cells is directed by the same dual binding system. *EMBO J.* 21, 1597–1606. doi:10.1093/emboj/21.7.1597
- Matuschewski, K., Ross, J., Brown, S.M., Kaiser, K., Nussenzweig, V., Kappe, S.H.I., 2002b. Infectivity-associated changes in the transcriptional repertoire of the malaria parasite sporozoite stage. *J. Biol. Chem.* 277, 41948–41953. doi:10.1074/jbc.M207315200
- Mazur, P.K., Gozani, O., Sage, J., Reynoird, N., 2016. Novel insights into the oncogenic function of the SMYD3 lysine methyltransferase. *Transl. Cancer Res.* 5, 330–333. doi:10.21037/tcr.2016.06.26
- McRobert, L., Preiser, P., Sharp, S., Jarra, W., Kaviratne, M., Taylor, M.C., Renia, L., Sutherland, C.J., 2004. Distinct Trafficking and Localization of STEVOR Proteins in Three Stages of the Plasmodium falciparum Life Cycle. *Infect. Immun.* 72, 6597–6602. doi:10.1128/IAI.72.11.6597-6602.2004
- Medana, I.M., Turner, G.D.H., 2006. Human cerebral malaria and the blood–brain barrier. *Int. J. Parasitol., Blood-brain Barrier in Parasitic Disease* 36, 555–568. doi:10.1016/j.ijpara.2006.02.004
- Ménard, R., Tavares, J., Cockburn, I., Markus, M., Zavala, F., Amino, R., 2013. Looking under the skin: the first steps in malarial infection and immunity. *Nat. Rev. Microbiol.* 11, 701–712. doi:10.1038/nrmicro3111
- Merrick, C.J., Duraisingh, M.T., 2007. Plasmodium falciparum Sir2: an Unusual Sirtuin with Dual Histone Deacetylase and ADP-Ribosyltransferase Activity. *Eukaryot. Cell* 6, 2081–2091. doi:10.1128/EC.00114-07
- Miao, J., Fan, Q., Cui, L., Li, J., Li, J., Cui, L., 2006. The malaria parasite Plasmodium falciparum histones: organization, expression, and acetylation. *Gene* 369, 53–65. doi:10.1016/j.gene.2005.10.022
- Miao, J., Fan, Q., Parker, D., Li, X., Li, J., Cui, L., 2013. Puf mediates translation repression of transmission-blocking vaccine candidates in malaria parasites. *PLoS Pathog.* 9, e1003268. doi:10.1371/journal.ppat.1003268
- Miao, J., Li, J., Fan, Q., Li, X., Li, X., Cui, L., 2010. The Puf-family RNA-binding protein PfPuf2 regulates sexual development and sex differentiation in the malaria parasite Plasmodium falciparum. *J. Cell Sci.* 123, 1039–1049. doi:10.1242/jcs.059824
- Miller, L.H., 1969. Distribution of mature trophozoites and schizonts of Plasmodium falciparum in the organs of Aotus trivirgatus, the night monkey. *Am. J. Trop. Med. Hyg.* 18, 860–865.
- Mishra, S., Nussenzweig, R.S., Nussenzweig, V., 2012. Antibodies to Plasmodium circumsporozoite protein (CSP) inhibit sporozoite's cell traversal activity. *J. Immunol. Methods* 377, 47. doi:10.1016/j.jim.2012.01.009
- Morrisette, N.S., Sibley, L.D., 2002. Cytoskeleton of apicomplexan parasites. *Microbiol. Mol. Biol. Rev. MMBR* 66, 21–38; table of contents.
- Mota, M.M., Rodriguez, A., 2004. Migration through host cells: the first steps of Plasmodium sporozoites in the mammalian host. *Cell. Microbiol.* 6, 1113–1118. doi:10.1111/j.1462-5822.2004.00460.x
- Mota, M.M., Rodriguez, A., 2001. Migration through host cells by apicomplexan parasites. *Microbes Infect.* 3, 1123–1128.
- Mueller, A.-K., Camargo, N., Kaiser, K., Andorfer, C., Frevert, U., Matuschewski, K., Kappe, S.H.I., 2005a. Plasmodium liver stage developmental arrest by depletion of a protein at the parasite–host interface. *Proc. Natl. Acad. Sci. U. S. A.* 102, 3022–3027. doi:10.1073/pnas.0408442102

- Mueller, A.-K., Labaied, M., Kappe, S.H.I., Matuschewski, K., 2005b. Genetically modified Plasmodium parasites as a protective experimental malaria vaccine. *Nature* 433, 164–167. doi:10.1038/nature03188
- Niang, M., Bei, A.K., Madhani, K.G., Pelly, S., Dankwa, S., Kanjee, U., Gunalan, K., Amaladoss, A., Yeo, K.P., Bob, N.S., Malleret, B., Duraisingh, M.T., Preiser, P.R., 2014. STEVOR is a Plasmodium falciparum erythrocyte binding protein that mediates merozoite invasion and rosetting. *Cell Host Microbe* 16, 81–93. doi:10.1016/j.chom.2014.06.004
- Nussenzweig, R.S., Vanderberg, J., Most, H., Orton, C., 1967. Protective immunity produced by the injection of x-irradiated sporozoites of plasmodium berghei. *Nature* 216, 160–162.
- Offeddu, V., Thathy, V., Marsh, K., Matuschewski, K., 2012. Naturally acquired immune responses against Plasmodium falciparum sporozoites and liver infection. *Int. J. Parasitol., Molecular Approaches to Malaria 2012 (MAM 2012)* 42, 535–548. doi:10.1016/j.ijpara.2012.03.011
- Ogwang, C., Afolabi, M., Kimani, D., Jagne, Y.J., Sheehy, S.H., Bliss, C.M., Duncan, C.J.A., Collins, K.A., Garcia Knight, M.A., Kimani, E., Anagnostou, N.A., Berrie, E., Moyle, S., Gilbert, S.C., Spencer, A.J., Soipei, P., Mueller, J., Okebe, J., Colloca, S., Cortese, R., Viebig, N.K., Roberts, R., Gantlett, K., Lawrie, A.M., Nicosia, A., Imoukhuede, E.B., Bejon, P., Urban, B.C., Flanagan, K.L., Ewer, K.J., Chilengi, R., Hill, A.V.S., Bojang, K., 2013. Safety and Immunogenicity of Heterologous Prime-Boost Immunisation with Plasmodium falciparum Malaria Candidate Vaccines, ChAd63 ME-TRAP and MVA ME-TRAP, in Healthy Gambian and Kenyan Adults. *PLoS ONE* 8. doi:10.1371/journal.pone.0057726
- Painter, H.J., Campbell, T.L., Llinás, M., 2011. The Apicomplexan AP2 family: Integral factors regulating Plasmodium development. *Mol. Biochem. Parasitol.* 176, 1–7. doi:10.1016/j.molbiopara.2010.11.014
- Patel, V., Mazitschek, R., Coleman, B., Nguyen, C., Urgaonkar, S., Cortese, J., Barker, R.H., Greenberg, E., Tang, W., Bradner, J.E., Schreiber, S.L., Duraisingh, M.T., Wirth, D.F., Clardy, J., 2009. Identification and Characterization of Small Molecule Inhibitors of a Class I Histone Deacetylase from Plasmodium falciparum. *J. Med. Chem.* 52, 2185–2187. doi:10.1021/jm801654y
- Peccarelli, M., Kebaara, B.W., 2014. Regulation of natural mRNAs by the nonsense-mediated mRNA decay pathway. *Eukaryot. Cell* 13, 1126–1135. doi:10.1128/EC.00090-14
- Peeters, E., Driessen, R.P.C., Werner, F., Dame, R.T., 2015. The interplay between nucleoid organization and transcription in archaeal genomes. *Nat. Rev. Microbiol.* 13, 333–341. doi:10.1038/nrmicro3467
- Pérez-Toledo, K., Rojas-Meza, A.P., Mancio-Silva, L., Hernández-Cuevas, N.A., Delgadillo, D.M., Vargas, M., Martínez-Calvillo, S., Scherf, A., Hernandez-Rivas, R., 2009. Plasmodium falciparum heterochromatin protein 1 binds to tri-methylated histone 3 lysine 9 and is linked to mutually exclusive expression of var genes. *Nucleic Acids Res.* 37, 2596–2606. doi:10.1093/nar/gkp115
- Pimenta, P.F., Touray, M., Miller, L., 1994. The Journey of Malaria Sporozoites in the Mosquito Salivary Gland. *J. Eukaryot. Microbiol.* 41, 608–624. doi:10.1111/j.1550-7408.1994.tb01523.x
- Ponnudurai, T., Lensen, A.H., van Gemert, G.J., Bolmer, M.G., Meuwissen, J.H., 1991. Feeding behaviour and sporozoite ejection by infected Anopheles stephensi. *Trans. R. Soc. Trop. Med. Hyg.* 85, 175–180.

- Portugal, S., Pierce, S.K., Crompton, P.D., 2013. Young Lives Lost as B Cells Falter: What We Are Learning About Antibody Responses in Malaria. *J. Immunol.* 190, 3039–3046. doi:10.4049/jimmunol.1203067
- Pradel, G., Garapaty, S., Frevet, U., 2002. Proteoglycans mediate malaria sporozoite targeting to the liver. *Mol. Microbiol.* 45, 637–651.
- Prudêncio, M., Mota, M.M., 2007. To Migrate or to Invade: Those Are the Options. *Cell Host Microbe* 2, 286–288. doi:10.1016/j.chom.2007.10.008
- Prusty, D., Mehra, P., Srivastava, S., Shivange, A.V., Gupta, A., Roy, N., Dhar, S.K., 2008. Nicotinamide inhibits *Plasmodium falciparum* Sir2 activity in vitro and parasite growth. *FEMS Microbiol. Lett.* 282, 266–272. doi:10.1111/j.1574-6968.2008.01135.x
- Quakyi, I.A., Carter, R., Rener, J., Kumar, N., Good, M.F., Miller, L.H., 1987. The 230-kDa gamete surface protein of *Plasmodium falciparum* is also a target for transmission-blocking antibodies. *J. Immunol.* 139, 4213–4217.
- Ralph, S.A., Scherf, A., 2005. The epigenetic control of antigenic variation in *Plasmodium falciparum*. *Curr. Opin. Microbiol.* 8, 434–440. doi:10.1016/j.mib.2005.06.007
- Rask, T.S., Hansen, D.A., Theander, T.G., Gorm Pedersen, A., Lavstsen, T., 2010. *Plasmodium falciparum* erythrocyte membrane protein 1 diversity in seven genomes--divide and conquer. *PLoS Comput. Biol.* 6. doi:10.1371/journal.pcbi.1000933
- Remarque, E.J., Faber, B.W., Kocken, C.H.M., Thomas, A.W., 2008. Apical membrane antigen 1: a malaria vaccine candidate in review. *Trends Parasitol.* 24, 74–84. doi:10.1016/j.pt.2007.12.002
- Rener, J., Graves, P.M., Carter, R., Williams, J.L., Burkot, T.R., 1983. Target antigens of transmission-blocking immunity on gametes of *plasmodium falciparum*. *J. Exp. Med.* 158, 976–981. doi:10.1084/jem.158.3.976
- Rieger, H., Yoshikawa, H.Y., Quadt, K., Nielsen, M.A., Sanchez, C.P., Salanti, A., Tanaka, M., Lanzer, M., 2015. Cytoadhesion of *Plasmodium falciparum*-infected erythrocytes to chondroitin-4-sulfate is cooperative and shear enhanced. *Blood* 125, 383–391. doi:10.1182/blood-2014-03-561019
- Roch, K.G.L., Johnson, J.R., Florens, L., Zhou, Y., Santosyan, A., Grainger, M., Yan, S.F., Williamson, K.C., Holder, A.A., Carucci, D.J., Yates, J.R., Winzeler, E.A., 2004. Global analysis of transcript and protein levels across the *Plasmodium falciparum* life cycle. *Genome Res.* 14, 2308–2318. doi:10.1101/gr.2523904
- Rodriguez, M.H., Hernández-Hernández, F. de la C., 2004. Insect–malaria parasites interactions: the salivary gland. *Insect Biochem. Mol. Biol., Molecular and population biology of mosquitoes* 34, 615–624. doi:10.1016/j.ibmb.2004.03.014
- Roestenberg, M., McCall, M., Hopman, J., Wiersma, J., Luty, A.J.F., van Gemert, G.J., van de Vegte-Bolmer, M., van Schaijk, B., Teelen, K., Arens, T., Spaarman, L., de Mast, Q., Roeffen, W., Snounou, G., Rénia, L., van der Ven, A., Hermsen, C.C., Sauerwein, R., 2009. Protection against a malaria challenge by sporozoite inoculation. *N. Engl. J. Med.* 361, 468–477. doi:10.1056/NEJMoa0805832
- Rosenberg, R., Wirtz, R.A., Schneider, I., Burge, R., 1990. An estimation of the number of malaria sporozoites ejected by a feeding mosquito. *Trans. R. Soc. Trop. Med. Hyg.* 84, 209–212.
- Rowe, A., Obeiro, J., Newbold, C.I., Marsh, K., 1995. *Plasmodium falciparum* rosetting is associated with malaria severity in Kenya. *Infect. Immun.* 63, 2323–2326.
- Rowe, J.A., Moulds, J.M., Newbold, C.I., Miller, L.H., 1997. *P. falciparum* rosetting mediated by a parasite-variant erythrocyte membrane protein and complement-receptor 1. *Nature* 388, 292–295. doi:10.1038/40888
- Salanti, A., Dahlbäck, M., Turner, L., Nielsen, M.A., Barfod, L., Magistrado, P., Jensen, A.T.R., Lavstsen, T., Ofori, M.F., Marsh, K., Hviid, L., Theander, T.G., 2004.

- Evidence for the involvement of VAR2CSA in pregnancy-associated malaria. *J. Exp. Med.* 200, 1197–1203. doi:10.1084/jem.20041579
- Salanti, A., Staalsoe, T., Lavstsen, T., Jensen, A.T.R., Sowa, M.P.K., Arnot, D.E., Hviid, L., Theander, T.G., 2003. Selective upregulation of a single distinctly structured var gene in chondroitin sulphate A-adhering *Plasmodium falciparum* involved in pregnancy-associated malaria. *Mol. Microbiol.* 49, 179–191.
- Salcedo-Amaya, A.M., van Driel, M.A., Alako, B.T., Trelle, M.B., van den Elzen, A.M.G., Cohen, A.M., Janssen-Megens, E.M., van de Vegte-Bolmer, M., Selzer, R.R., Iniguez, A.L., Green, R.D., Sauerwein, R.W., Jensen, O.N., Stunnenberg, H.G., 2009. Dynamic histone H3 epigenome marking during the intraerythrocytic cycle of *Plasmodium falciparum*. *Proc. Natl. Acad. Sci. U. S. A.* 106, 9655–60. doi:10.1073/pnas.0902515106
- Sannella, A.R., Olivieri, A., Bertuccini, L., Ferrè, F., Severini, C., Pace, T., Alano, P., 2012. Specific tagging of the egress-related osmiophilic bodies in the gametocytes of *Plasmodium falciparum*. *Malar. J.* 11, 88. doi:10.1186/1475-2875-11-88
- Santos, J.M., Lebrun, M., Daher, W., Soldati, D., Dubremetz, J.-F., 2009. Apicomplexan cytoskeleton and motors: key regulators in morphogenesis, cell division, transport and motility. *Int. J. Parasitol.* 39, 153–162. doi:10.1016/j.ijpara.2008.10.007
- Saraf, A., Cervantes, S., Bunnik, E.M., Ponts, N., Sardu, M.E., Chung, D.-W.D., Prudhomme, J., Varberg, J.M., Wen, Z., Washburn, M.P., Florens, L., Le Roch, K.G., 2016a. Dynamic and Combinatorial Landscape of Histone Modifications during the Intraerythrocytic Developmental Cycle of the Malaria Parasite. *J. Proteome Res.* 15, 2787–2801. doi:10.1021/acs.jproteome.6b00366
- Saraf, A., Cervantes, S., Bunnik, E.M., Ponts, N.P., Sardu, M.E., Chung, D.-W.D., Prudhomme, J., Varberg, J., Wen, Z., Washburn, M.P., Florens, L.A., Le Roch, K.G., 2016b. Dynamic and combinatorial landscape of histone modifications during the intra-erythrocytic developmental cycle of the malaria parasite. *J. Proteome Res.* acs.jproteome.6b00366. doi:10.1021/acs.jproteome.6b00366
- Sauerwein, R.W., Bousema, T., 2015. Transmission blocking malaria vaccines: Assays and candidates in clinical development. *Vaccine, Malaria Vaccines 2015* 33, 7476–7482. doi:10.1016/j.vaccine.2015.08.073
- Scherf, A., Figueiredo, L.M., Freitas-Junior, L.H., 2001. *Plasmodium* telomeres: a pathogen's perspective. *Curr. Opin. Microbiol.* 4, 409–414. doi:10.1016/S1369-5274(00)00227-7
- Scherf, A., Lopez-Rubio, J.J., Riviere, L., 2008a. Antigenic variation in *Plasmodium falciparum*. *Annu. Rev. Microbiol.* 62, 445–470. doi:10.1146/annurev.micro.61.080706.093134
- Scherf, A., Rivière, L., Lopez-Rubio, J.J., 2008b. SnapShot: var Gene Expression in the Malaria Parasite. *Cell* 134, 190–190.e1. doi:10.1016/j.cell.2008.06.042
- Seder, R.A., Chang, L.-J., Enama, M.E., Zephir, K.L., Sarwar, U.N., Gordon, I.J., Holman, L.A., James, E.R., Billingsley, P.F., Gunasekera, A., Richman, A., Chakravarty, S., Manoj, A., Velmurugan, S., Li, M., Ruben, A.J., Li, T., Eappen, A.G., Stafford, R.E., Plummer, S.H., Hendel, C.S., Novik, L., Costner, P.J.M., Mendoza, F.H., Saunders, J.G., Nason, M.C., Richardson, J.H., Murphy, J., Davidson, S.A., Richie, T.L., Sedegah, M., Sutamihardja, A., Fahle, G.A., Lyke, K.E., Laurens, M.B., Roederer, M., Tewari, K., Epstein, J.E., Sim, B.K.L., Ledgerwood, J.E., Graham, B.S., Hoffman, S.L., VRC 312 Study Team, 2013. Protection against malaria by intravenous immunization with a nonreplicating sporozoite vaccine. *Science* 341, 1359–1365. doi:10.1126/science.1241800
- Shimp, R.L., Rowe, C., Reiter, K., Chen, B., Nguyen, V., Aebig, J., Rausch, K.M., Kumar, K., Wu, Y., Jin, A.J., Jones, D.S., Narum, D.L., 2013. Development of a Pfs25-EPA

- malaria transmission blocking vaccine as a chemically conjugated nanoparticle. *Vaccine* 31, 2954–2962. doi:10.1016/j.vaccine.2013.04.034
- Sidjanski, S., Vanderberg, J.P., 1997. Delayed migration of Plasmodium sporozoites from the mosquito bite site to the blood. *Am. J. Trop. Med. Hyg.* 57, 426–429.
- Silva, F.P., Hamamoto, R., Kunizaki, M., Tsuge, M., Nakamura, Y., Furukawa, Y., 2008. Enhanced methyltransferase activity of SMYD3 by the cleavage of its N-terminal region in human cancer cells. *Oncogene* 27, 2686–92. doi:10.1038/sj.onc.1210929
- Silvie, O., Semblat, J.P., Franetich, J.F., Hannoun, L., Eling, W., Mazier, D., 2002. Effects of irradiation on Plasmodium falciparum sporozoite hepatic development: implications for the design of pre-erythrocytic malaria vaccines. *Parasite Immunol.* 24, 221–223.
- Sinha, A., Hughes, K.R., Modrzynska, K.K., Otto, T.D., Pfander, C., Dickens, N.J., Religa, A.A., Bushell, E., Graham, A.L., Cameron, R., Kafsack, B.F.C., Williams, A.E., Llinás, M., Berriman, M., Billker, O., Waters, A.P., 2014. A cascade of DNA-binding proteins for sexual commitment and development in Plasmodium. *Nature* 507, 253–257. doi:10.1038/nature12970
- Smith, J.D., Chitnis, C.E., Craig, A.G., Roberts, D.J., Hudson-Taylor, D.E., Peterson, D.S., Pinches, R., Newbold, C.I., Miller, L.H., 1995. Switches in expression of plasmodium falciparum var genes correlate with changes in antigenic and cytoadherent phenotypes of infected erythrocytes. *Cell* 82, 101–110. doi:10.1016/0092-8674(95)90056-X
- Spring, M., Murphy, J., Nielsen, R., Dowler, M., Bennett, J.W., Zarlino, S., Williams, J., de la Vega, P., Ware, L., Komisar, J., Polhemus, M., Richie, T.L., Epstein, J., Tamminga, C., Chuang, I., Richie, N., O’Neil, M., Heppner, D.G., Healer, J., O’Neill, M., Smithers, H., Finney, O.C., Mikolajczak, S.A., Wang, R., Cowman, A., Ockenhouse, C., Krzych, U., Kappe, S.H.I., 2013. First-in-human evaluation of genetically attenuated Plasmodium falciparum sporozoites administered by bite of Anopheles mosquitoes to adult volunteers. *Vaccine* 31, 4975–4983. doi:10.1016/j.vaccine.2013.08.007
- Strahl, B.D., Allis, C.D., 2000. The language of covalent histone modifications. *Nature* 403, 41–45. doi:10.1038/47412
- Su, X., Heatwole, V.M., Wertheimer, S.P., Guinet, F., Herrfeldt, J.A., Peterson, D.S., Ravetch, J.A., Wellems, T.E., 1995. The large diverse gene family var encodes proteins involved in cytoadherence and antigenic variation of plasmodium falciparum-infected erythrocytes. *Cell* 82, 89–100. doi:10.1016/0092-8674(95)90055-1
- Sultan, A.A., Thathy, V., Frevert, U., Robson, K.J.H., Crisanti, A., Nussenzweig, V., Nussenzweig, R.S., Ménard, R., 1997. TRAP Is Necessary for Gliding Motility and Infectivity of Plasmodium Sporozoites. *Cell* 90, 511–522. doi:10.1016/S0092-8674(00)80511-5
- Sundriyal, S., Malmquist, N. a, Caron, J., Blundell, S., Liu, F., Chen, X., Srimongkolpithak, N., Jin, J., Charman, S. a, Scherf, A., Fuchter, M.J., 2014. Development of Diaminoquinazoline Histone Lysine Methyltransferase Inhibitors as Potent Blood-Stage Antimalarial Compounds. *ChemMedChem* 9, 2360–2373. doi:10.1002/cmde.201402098
- Swerlick, R.A., Lee, K.H., Wick, T.M., Lawley, T.J., 1992. Human dermal microvascular endothelial but not human umbilical vein endothelial cells express CD36 in vivo and in vitro. *J. Immunol.* 148, 78–83.
- Takala, S.L., Plowe, C.V., 2009. Genetic diversity and malaria vaccine design, testing, and efficacy: Preventing and overcoming “vaccine resistant malaria.” *Parasite Immunol.* 31, 560–573. doi:10.1111/j.1365-3024.2009.01138.x
- Tamminga, C., Sedegah, M., Maiolatesi, S., Fedders, C., Reyes, S., Reyes, A., Vasquez, C., Alcorta, Y., Chuang, I., Spring, M., Kavanaugh, M., Ganeshan, H., Huang, J.,

- Belmonte, M., Abot, E., Belmonte, A., Banania, J., Farooq, F., Murphy, J., Komisar, J., Richie, N.O., Bennett, J., Limbach, K., Patterson, N.B., Bruder, J.T., Shi, M., Miller, E., Dutta, S., Diggs, C., Soisson, L.A., Hollingdale, M.R., Epstein, J.E., Richie, T.L., 2013. Human adenovirus 5-vectored *Plasmodium falciparum* NMRC-M3V-Ad-PfCA vaccine encoding CSP and AMA1 is safe, well-tolerated and immunogenic but does not protect against controlled human malaria infection. *Hum. Vaccines Immunother.* 9, 2165–2177. doi:10.4161/hv.24941
- Tavares, J., Formaglio, P., Thiberge, S., Mordelet, E., Van Rooijen, N., Medvinsky, A., Ménard, R., Amino, R., 2013. Role of host cell traversal by the malaria sporozoite during liver infection. *J. Exp. Med.* 210, 905–915. doi:10.1084/jem.20121130
- Taylor, H.M., Kyes, S.A., Newbold, C.I., 2000. Var gene diversity in *Plasmodium falciparum* is generated by frequent recombination events. *Mol. Biochem. Parasitol.* 110, 391–397. doi:10.1016/S0166-6851(00)00286-3
- Tonkin, C.J., Carret, C.K., Duraisingh, M.T., Voss, T.S., Ralph, S.A., Hommel, M., Duffy, M.F., Silva, L.M. da, Scherf, A., Ivens, A., Speed, T.P., Beeson, J.G., Cowman, A.F., 2009. Sir2 paralogues cooperate to regulate virulence genes and antigenic variation in *Plasmodium falciparum*. *PLoS Biol.* 7, e84. doi:10.1371/journal.pbio.1000084
- Trelle, M.B., Salcedo-Amaya, A.M., Cohen, A.M., Stunnenberg, H.G., Jensen, O.N., 2009. Global histone analysis by mass spectrometry reveals a high content of acetylated lysine residues in the malaria parasite *Plasmodium falciparum*. *J. Proteome Res.* 8, 3439–50. doi:10.1021/pr9000898
- Treutiger, C.J., Hedlund, I., Helmbj, H., Carlson, J., Jepson, A., Twumasi, P., Kwiatkowski, D., Greenwood, B.M., Wahlgren, M., 1992. Rosette formation in *Plasmodium falciparum* isolates and anti-rosette activity of sera from Gambians with cerebral or uncomplicated malaria. *Am. J. Trop. Med. Hyg.* 46, 503–510.
- Turner, L., Lavstsen, T., Berger, S.S., Wang, C.W., Petersen, J.E.V., Avril, M., Brazier, A.J., Freeth, J., Jespersen, J.S., Nielsen, M.A., Magistrado, P., Lusingu, J., Smith, J.D., Higgins, M.K., Theander, T.G., 2013. Severe malaria is associated with parasite binding to endothelial protein C receptor. *Nature* 498, 502–505. doi:10.1038/nature12216
- van Dijk, M.R., Douradinha, B., Franke-Fayard, B., Heussler, V., van Dooren, M.W., van Schaijk, B., van Gemert, G.-J., Sauerwein, R.W., Mota, M.M., Waters, A.P., Janse, C.J., 2005. Genetically attenuated, P36p-deficient malarial sporozoites induce protective immunity and apoptosis of infected liver cells. *Proc. Natl. Acad. Sci. U. S. A.* 102, 12194–12199. doi:10.1073/pnas.0500925102
- Vanderberg, J., Nussenzweig, R., Most, H., 1969. Protective immunity produced by the injection of x-irradiated sporozoites of *Plasmodium berghei*. V. In vitro effects of immune serum on sporozoites. *Mil. Med.* 134, 1183–1190.
- Vembar, S.S., Droll, D., Scherf, A., 2016. Translational regulation in blood stages of the malaria parasite *Plasmodium* spp.: systems-wide studies pave the way. *Wiley Interdiscip. Rev. RNA* 7, 772–792. doi:10.1002/wrna.1365
- Vembar, S.S., Macpherson, C.R., Sismeiro, O., Coppée, J.-Y., Scherf, A., 2015. The PfAlba1 RNA-binding protein is an important regulator of translational timing in *Plasmodium falciparum* blood stages. *Genome Biol.* 16, 212. doi:10.1186/s13059-015-0771-5
- Vembar, S.S., Scherf, A., Siegel, T.N., 2014. Noncoding RNAs as emerging regulators of *Plasmodium falciparum* virulence gene expression. *Curr. Opin. Microbiol.* 20, 153–161. doi:10.1016/j.mib.2014.06.013
- Vermeulen, A.N., Ponnudurai, T., Beckers, P.J., Verhave, J.P., Smits, M.A., Meuwissen, J.H., 1985. Sequential expression of antigens on sexual stages of *Plasmodium falciparum*

- accessible to transmission-blocking antibodies in the mosquito. *J. Exp. Med.* 162, 1460–1476.
- Vlachou, D., Schlegelmilch, T., Runn, E., Mendes, A., Kafatos, F.C., 2006. The developmental migration of *Plasmodium* in mosquitoes. *Curr. Opin. Genet. Dev.*, Pattern formation and developmental mechanisms 16, 384–391. doi:10.1016/j.gde.2006.06.012
- Volz, J., Carvalho, T.G., Ralph, S.A., Gilson, P., Thompson, J., Tonkin, C.J., Langer, C., Crabb, B.S., Cowman, A.F., 2010. Potential epigenetic regulatory proteins localise to distinct nuclear sub-compartments in *Plasmodium falciparum*. *Int. J. Parasitol.* doi:10.1016/j.ijpara.2009.09.002
- Volz, J.C., Bártfai, R., Petter, M., Langer, C., Josling, G.A., Tsuboi, T., Schwach, F., Baum, J., Rayner, J.C., Stunnenberg, H.G., Duffy, M.F., Cowman, A.F., 2012. PfSET10, a *Plasmodium falciparum* Methyltransferase, Maintains the Active var Gene in a Poised State during Parasite Division. *Cell Host Microbe* 11, 7–18. doi:10.1016/j.chom.2011.11.011
- Volz, J.C., Bártfai, R., Petter, M., Langer, C., Josling, G.A., Tsuboi, T., Schwach, F., Baum, J., Rayner, J.C., Stunnenberg, H.G., Duffy, M.F., Cowman, A.F., 2012. PfSET10, a *Plasmodium falciparum* Methyltransferase, Maintains the Active var Gene in a Poised State during Parasite Division. *Cell Host Microbe.* doi:10.1016/j.chom.2011.11.011
- Wang, Q., Fujioka, H., Nussenzweig, V., 2005. Exit of *Plasmodium* sporozoites from oocysts is an active process that involves the circumsporozoite protein. *PLoS Pathog.* 1, e9. doi:10.1371/journal.ppat.0010009
- Warren, A., Bertolino, P., Benseler, V., Fraser, R., McCaughan, G.W., Le Couteur, D.G., 2007. Marked changes of the hepatic sinusoid in a transgenic mouse model of acute immune-mediated hepatitis. *J. Hepatol.* 46, 239–246. doi:10.1016/j.jhep.2006.08.022
- Wassmer, S.C., Combes, V., Candal, F.J., Juhan-Vague, I., Grau, G.E., 2006. Platelets Potentiate Brain Endothelial Alterations Induced by *Plasmodium falciparum*. *Infect. Immun.* 74, 645–653. doi:10.1128/IAI.74.1.645-653.2006
- Wertheimer, S.P., Barnwell, J.W., 1989. *Plasmodium vivax* interaction with the human Duffy blood group glycoprotein: identification of a parasite receptor-like protein. *Exp. Parasitol.* 69, 340–350.
- WHO, 2015. World Malaria Report 2015. Who.
- Wisse, E., De Zanger, R.B., Charels, K., Van Der Smissen, P., McCuskey, R.S., 1985. The liver sieve: considerations concerning the structure and function of endothelial fenestrae, the sinusoidal wall and the space of Disse. *Hepatology* 5, 683–692.
- Yadava, A., Hall, C.E., Sullivan, J.S., Nace, D., Williams, T., Collins, W.E., Ockenhouse, C.F., Barnwell, J.W., 2014. Protective Efficacy of a *Plasmodium vivax* Circumsporozoite Protein-Based Vaccine in *Aotus nancymae* Is Associated with Antibodies to the Repeat Region. *PLoS Negl. Trop. Dis.* 8. doi:10.1371/journal.pntd.0003268
- Yamauchi, L.M., Coppi, A., Snounou, G., Sinnis, P., 2007. *Plasmodium* sporozoites trickle out of the injection site. *Cell. Microbiol.* 9, 1215–1222. doi:10.1111/j.1462-5822.2006.00861.x
- Yayon, A., Vande Waa, J.A., Yayon, M., Geary, T.G., Jensen, J.B., 1983. Stage-dependent effects of chloroquine on *Plasmodium falciparum* in vitro. *J. Protozool.* 30, 642–647.
- Yuda, M., Iwanaga, S., Shigenobu, S., Kato, T., Kaneko, I., 2010. Transcription factor AP2-Sp and its target genes in malarial sporozoites. *Mol. Microbiol.* 75, 854–863. doi:10.1111/j.1365-2958.2009.07005.x
- Yuda, M., Iwanaga, S., Shigenobu, S., Mair, G.R., Janse, C.J., Waters, A.P., Kato, T., Kaneko, I., 2009. Identification of a transcription factor in the mosquito-invasive stage

- of malaria parasites. *Mol. Microbiol.* 71, 1402–1414. doi:10.1111/j.1365-2958.2009.06609.x
- Zhang, M., Fennell, C., Ranford-Cartwright, L., Sakthivel, R., Gueirard, P., Meister, S., Caspi, A., Doerig, C., Nussenzweig, R.S., Tuteja, R., Sullivan, W.J., Roos, D.S., Fontoura, B.M.A., Ménard, R., Winzeler, E.A., Nussenzweig, V., 2010. The Plasmodium eukaryotic initiation factor-2 $\alpha$  kinase IK2 controls the latency of sporozoites in the mosquito salivary glands. *J. Exp. Med.* 207, 1465–1474. doi:10.1084/jem.20091975
- Zhang, Q., Huang, Y., Zhang, Y., Fang, X., Claes, A., Duchateau, M., Namane, A., Lopez-Rubio, J.-J., Pan, W., Scherf, A., 2011. A critical role of perinuclear filamentous actin in spatial repositioning and mutually exclusive expression of virulence genes in malaria parasites. *Cell Host Microbe* 10, 451–463. doi:10.1016/j.chom.2011.09.013
- Zhang, Q., Siegel, T.N., Martins, R.M., Wang, F., Cao, J., Gao, Q., Cheng, X., Jiang, L., Hon, C.-C., Scheidig-Benatar, C., Sakamoto, H., Turner, L., Jensen, A.T.R., Claes, A., Guizetti, J., Malmquist, N.A., Scherf, A., 2014. Exonuclease-mediated degradation of nascent RNA silences genes linked to severe malaria. *Nature* 513, 431–435. doi:10.1038/nature13468

## MATERIALS AND METHODS

**Protein expression construct.** Codon optimized full length PfSET6 (PlasmoDB Gene ID PF3D7\_1355300) was synthesized (Genscript), fused to a C-terminal double Strep-tag and ligated into the transfer vector pVL1393. A single potential glycosylation site S325A was removed for possible expression in secretory systems. The SET and SMYD domains of PfSET6 were identified using Prosite (prosite.expasy.org). Clones were verified to be error free and in frame by sequencing (GATC).

**Protein expression and purification.** To identify construct that provided sufficient amounts of Strep-tagged proteins, small-scale expression and purification was performed as described previously<sup>21</sup>. Briefly, recombinant PfSET6 was expressed using a baculoviral expression system following manufacturer's instructions. Proteins were then purified using StrepTrap HP columns (GE Healthcare). Final protein concentration was determined by Bradford Assay (Bio-Rad Protein Assay, Bio-Rad), and samples were aliquoted, flash frozen in liquid nitrogen and stored at -80°C until use.

**In vitro methytransferase assay.** Standard reactions were performed in a total volume of 25  $\mu$ l in KMT buffer (50 mM TRIS, pH 8.8, 5 mM MgCl<sub>2</sub>, 4 mM dithiothreitol), with HEK nucleosomes (0.2 mg/ml final) as substrate and 2.5  $\mu$ l of S-[3H-methyl]-adenosyl-L-methionine (3H-AdoMet) was added (3.7  $\mu$ M final, 15 Ci/mmol, Perkin-Elmer). PfSET6 enzyme was used at 1  $\mu$ M and reactions were incubated at room temperature for 1 hour.

Analysis by fluorography was performed by resolving 20 µl of standard HKMT reactions (2 µM of PfSET6, 20 µg/ml of either BSA or nucleosomes, 2.5 µl of methyl<sup>3</sup>H-AdoMet at 15Ci/mmol, in a total volume of 25 µl in KMT buffer) and incubated at room temperature for 2 hours. Reactions were separated on 4-15% SDS-PAGE gel, after migration the gel was rinsed in EN3HANCE (Perkin-Elmer) according to manufacturer's instructions, dried and exposed to film (BioMax MR Film, Carestream). 20 µl of each reaction was spotted in duplicate onto P81 Filters (Unifilter 96 well plate, Whatman), washed with 200 mM ammonium bicarbonate, dried, overlaid with scintillation fluid (Betaplate Scint, Perkin-Elmer) and read in a scintillation counter (MicroBeta2, Perkin-Elmer).

**Transgenic parasite plasmid constructs.** The CRISPR/Cas9 genome editing approach was employed to generate different PfSET6 transgenic parasite line as described previously. A 20-nt gRNA target sequence directing Cas9 cleavage near the C-terminal end and in the SET domain were cloned into the sgRNA-expression cassette in the pL6 plasmid, respectively. For each constructs, two homology regions of approximately 300-400bp were inserted in separate cloning steps using Gibson assembly. We generated a series of plasmid to knockdown PfSET6 that include: pL6-SET6-HA-glms, pL6-SET6-glms, pL6-SET6-HA-glms-hsp86, pL6-SET6-DiCre. A second plasmid, pUF1-Cas9, contained an engineered *S. pyogenes* endonuclease Cas9 cassette and regulatory elements of *P. falciparum* U6 snRNA.

**Parasite culture and transfections.** Asexual blood-stage parasites were cultivated using standard methods, and synchronous cultures were obtained by sorbitol treatment and plasmion enrichment. Parasites were transfected using the pre-loaded red blood cells method. Positive selection using 2.66 nM WR99210 and 1.5 µM DSM1 and negative selection using 40 µM 5-fluorocytosine were applied sequentially in culture until the integrant transfected line was established. To verify the integration and integration breakpoints, PCR was performed on genomic DNA from transgenic line or wild type strain.

**PfSET6 antibody production.** C57BL/6 and BALB/C mice were immunized 4 times every 14 days with 20ug doses of purified recombinant PfSET6 in Freund's Complete Adjuvant for the initial injection and Freund's Incomplete Adjuvant for booster injections to generate a polyclonal anti-PfSET6 antibody. Specificity of immune sera was determined by western blot.

**Subcellular fractionation and western blotting.** Subcellular extracts preparation was prepared as described previously. Equal amounts of protein were loaded and separated on 4-

12% SDS-PAGE gel (Invitrogen), and analyzed by western blot using antibodies anti-PfSET6 (mouse) at 1:500 dilutions, anti-Pf-Aldolase (Abcam ab38905) or anti-Histone H3 (mouse, Abcam ab1791) at 1:2000 dilution. Secondary antibodies were anti-rabbit IgG-HRP (GE NA934V, Lot 9568295) and anti-mouse IgG-HRP (GE NA931V, Lot 9648752), both at 1:4000. Blots were developed using ECL (Thermo Scientific).

**Immunofluorescence microscopy.** Immunofluorescence microscopy were performed as described previously. Antibody dilutions are as follows: anti-PfSET6 (mouse) 1:1000, anti-PfHP1 (rabbit, Genscript) 1:4000, anti-BiP (rabbit, MR4) 1:1000, anti-ERD2 (rat, MR4) 1:1000, anti-PfEBA175 (rabbit, MR4) 1:1000, anti-PfCLAG3.2 (rabbit, MR4) 1:1000, anti-PfAlba1 (rabbit, peptide antibody) 1:200, anti-PfAlba2 (rabbit, peptide antibody) 1:200, anti-PfAlba4 (rabbit, peptide antibody) 1:200, anti-Pfg377 (rabbit, MR4) 1:1000, and secondary goat anti-rat/rabbit/mouse Alexa-Fluor 488 or 568 conjugates (Invitrogen), all at 1:2500. Images were captured using a Nikon Eclipse 80i microscope with a CoolSnapHQ2 camera (Photometrics). NIS Elements version 3.0 software was used for image acquisition, and Fiji software was used for analysis.

**ChIP-Seq and data analysis.** Synchronous cultures of ring stage wild-type 3D7 parasites clone G10 were used. Cross-linked chromatin was prepared by adding formaldehyde to the culture followed by addition of glycine. Nuclei were isolated by homogenization suspended in SDS buffer. Chromatin was sheared by sonication in a Bioruptor® Pico to a size of 300bp. The commercially available antibodies to H3K9me3, H3K4me3, monoclonal anti-HP1, homemade polyclonal anti-PfSET6 were added and incubated at 4°C overnight. The antibody-protein-DNA complex is affinity purified using Magna ChIP™ ProteinG Magnetic Beads (Millipore, 16-662). As controls, DNA corresponding to the ChIP input or DNA immunoprecipitated using rabbit IgG were processed. Reverse cross-linking was followed by RNase treatment and Proteinase K digestion, DNA purification using the DNA Clean column. The MicroPlex Library Preparation kit (Diagenode, c05010012) is used for preparing libraries for sequencing. Pooled, multiplexed libraries were sequenced on an Illumina NextSeq® 500/550 system as a 150 nucleotide single-end run.

The resulting data were demultiplexed using bcl2fastq2 (Illumina) to obtain fastq files for downstream analysis. A minimum of two biological replicates was analyzed for each antibody and each parasite stage. Quality control of fastq files was performed using the FastQC software. Sequencing reads were mapped to the *P. falciparum* genome (v.3, GeneDB) with the Burrows-Wheeler Alignment tool (BWA MEM) using default parameters. After unique

read mapping and deduplication, the aligned reads were considered for peak-calling analysis with the MACS2 software 5 after controlling for a false discovery rate of 5% (default setting of MACS2) using Benjamini and Hochberg's correction method. For the genome-wide representation of PfSET6 from ring stage parasites, the coverages were calculated as average RPKM (reads per kilobase of genome sequence per one million mapped reads) over bins of 1000bp width using bamCoverage from the package deepTools2 (v2.2.4, PMID: 27079975). Coverage differences between the PfSET6 ChIP experiment, Mouse IgG mock and the input control (Fig. X) were calculated using bamCompare from the same package. Circular and linear coverage plots were generated using circos (v0.69, PMID: 19541911) and the Integrated Genomics Viewer (v2.3.72, PMID: 22517427).

## FIGURE LEGENDS

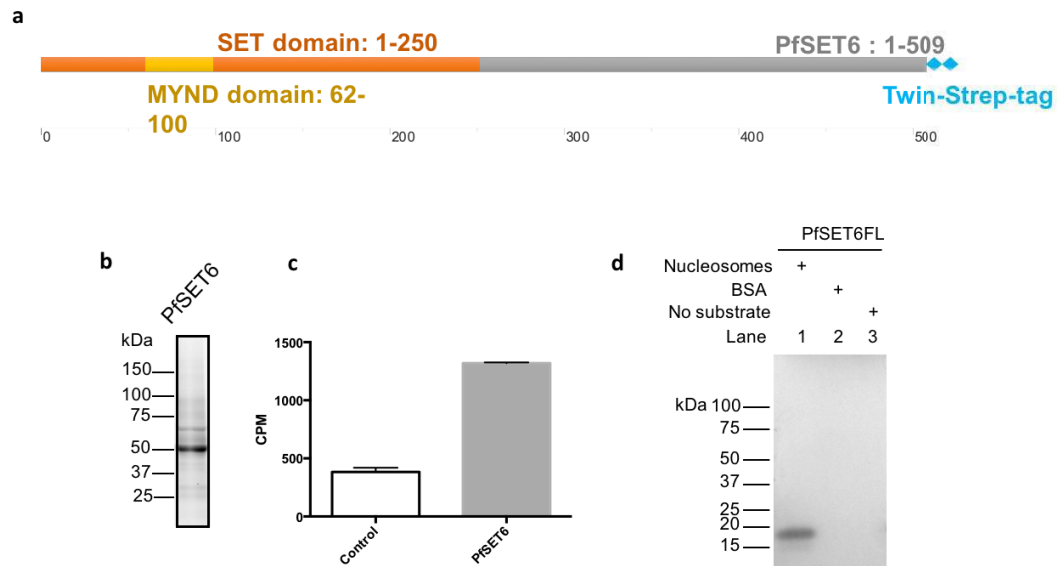
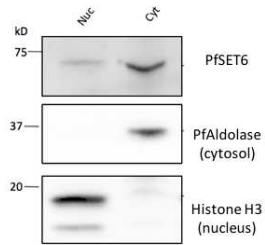


**Figure 1 PfSET6 is a *bona fide* histone methyltransferase.** a. Schematic representation of the domain organization of PfSET6 protein. The location of the 2x-Streptavidin tag for recombinant protein expression is indicated. b. Purified full-length recombinant PfSET6 was visualized by Bio-Rad Stain-Free detection (left) and was validated by western blotting using anti-Strep (right). c. Enzymatic assays with with radiolabeled S-adenosylmethionine as a methyl donor and histones as substrate and quantified as counts per minute (cpm). d. Autoradiograph of enzyme reactions with PfSET6 with nucleosomes, BSA and enzyme alone (lanes 1,2 and 3). Film was exposed 72h.

**a.**



**b.**

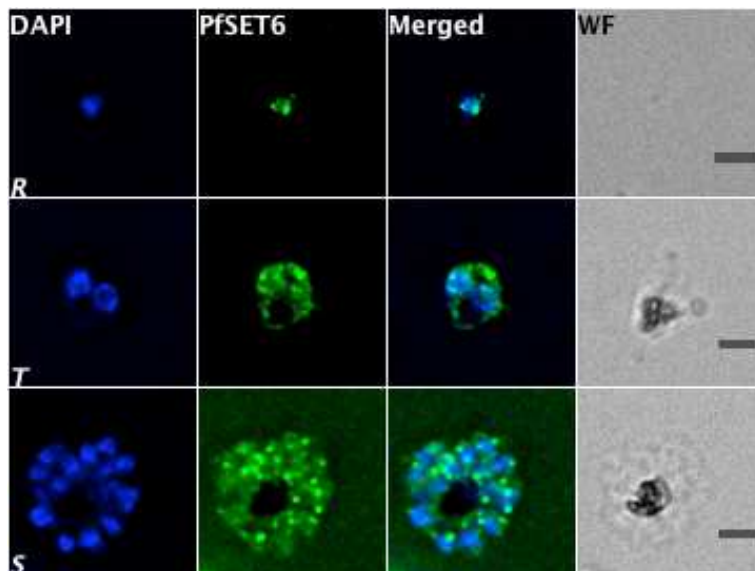


**Figure 2 PfSET6 localizes to the nucleus and cytoplasm of asexual blood stage parasites.** a. Western blotting of parasite nuclear and cytoplasmic fractions of asynchronized parasites using anti-PfSET6 antibodies. b. IF localization of PfSET6 in rings, trophozoites and schizonts. The scale bars correspond to 2 μm.

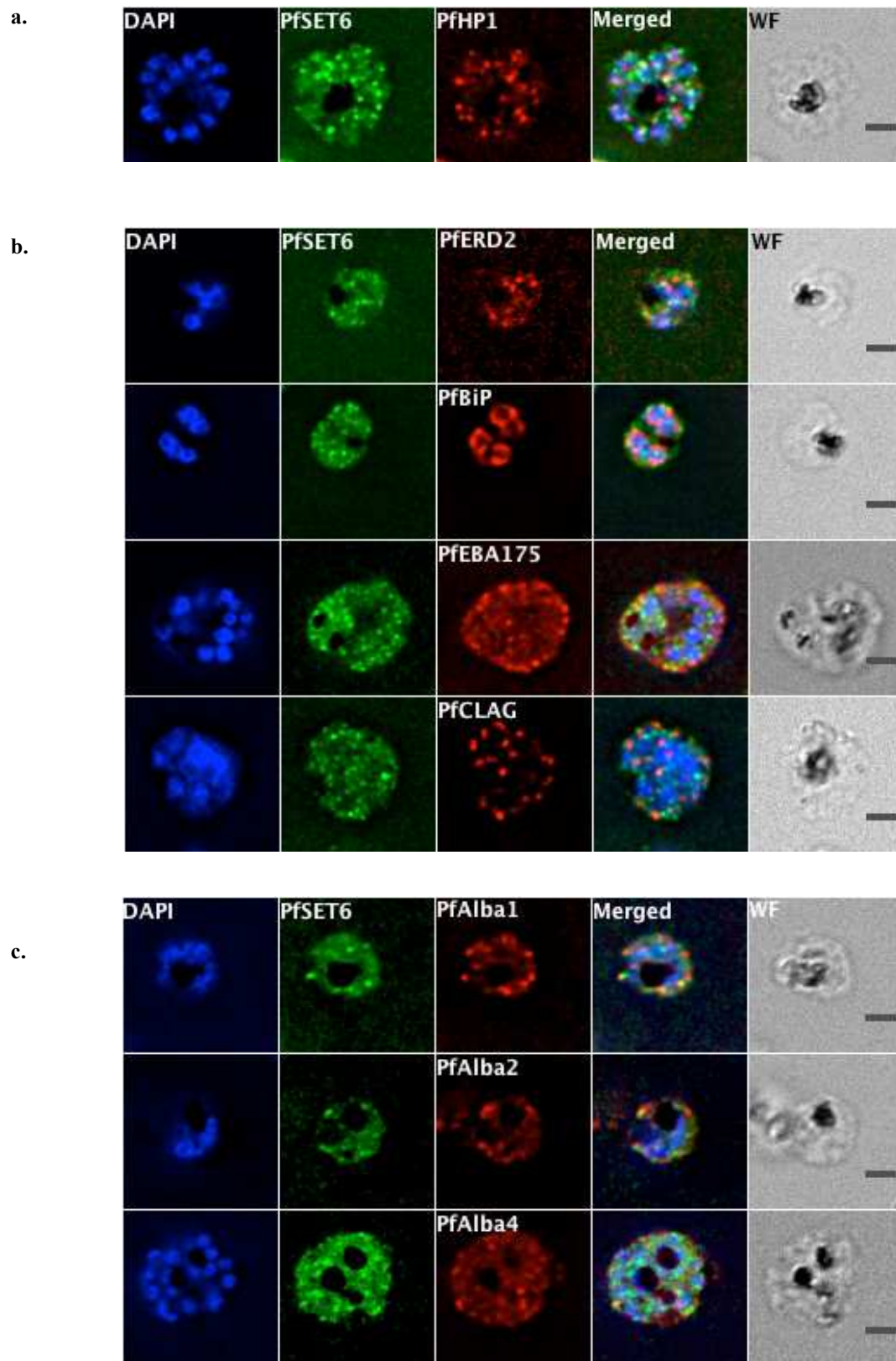
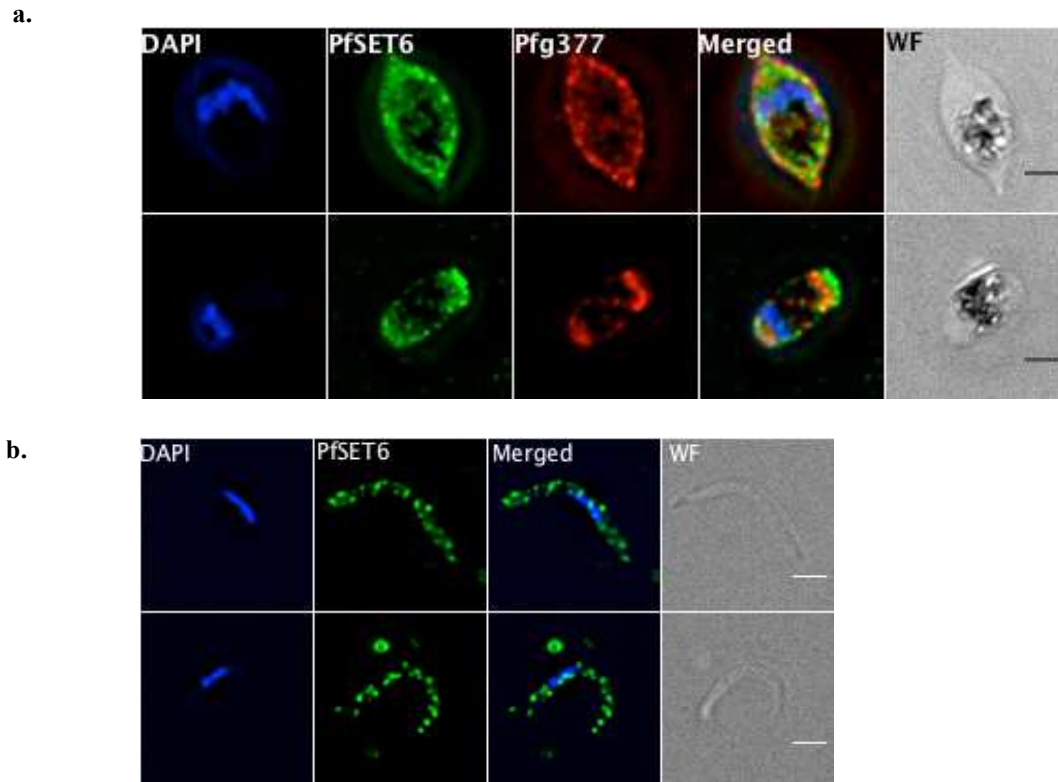
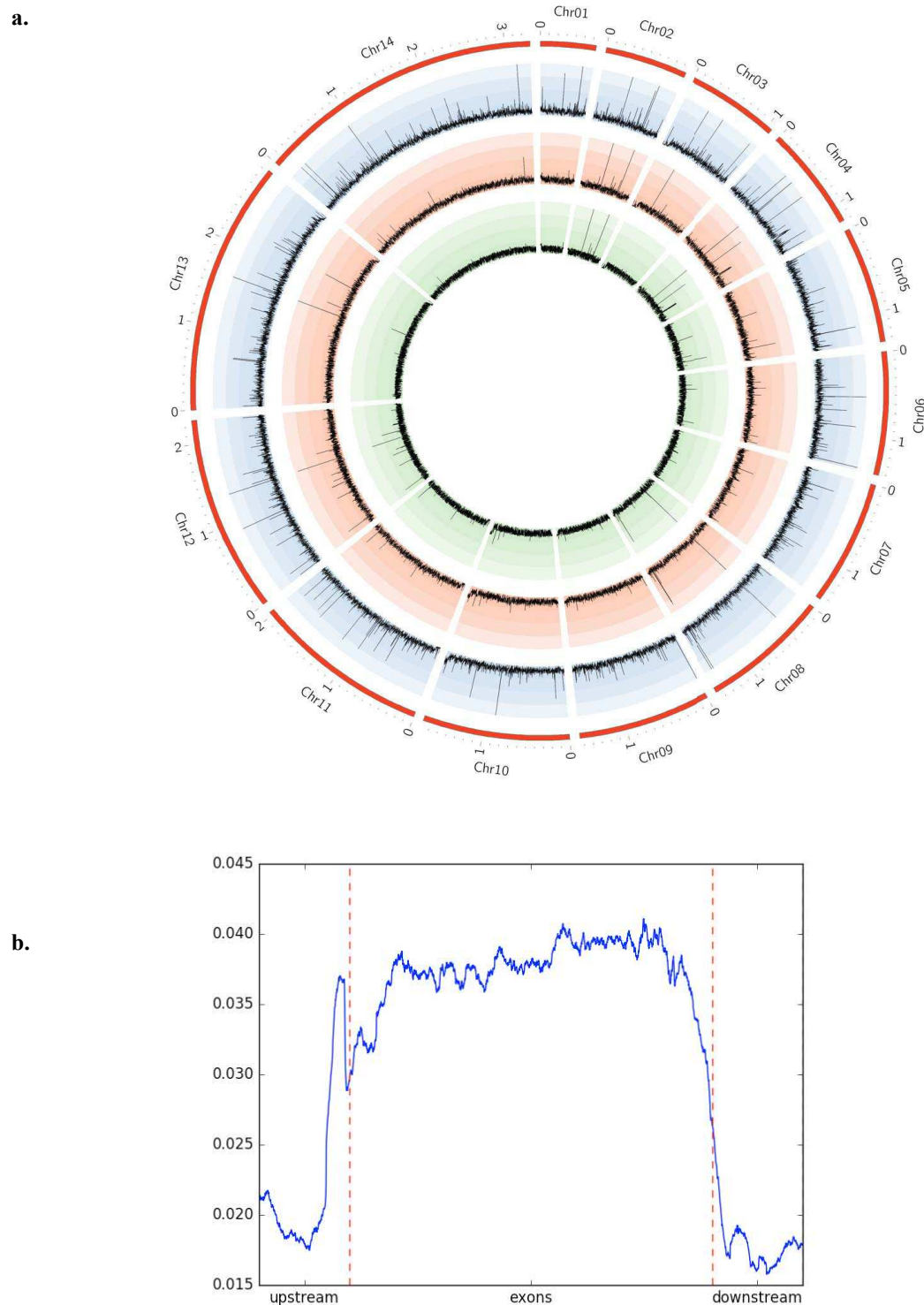


Figure 3 PfSET6 localization is dynamic during asexual blood stage. a. co-IF of schizonts using anti-PfSET6

combined with the nuclear periphery marker PfHP1. b. co-IF of late stage parasites using anti-PfSET6 combined with different markers of cytoplasmic organelles, anti-Bip as an ER marker, anti-ERD2 as a cis-golgi marker, anti-EBA175 as microneme, anti-CLAG as rhoptries. c. co-IF of late stage parasites using anti-PfSET6 combined with markers of mRNP granules including PfAlba1, 2 and 4. The scale bars correspond to 2 $\mu$ m.



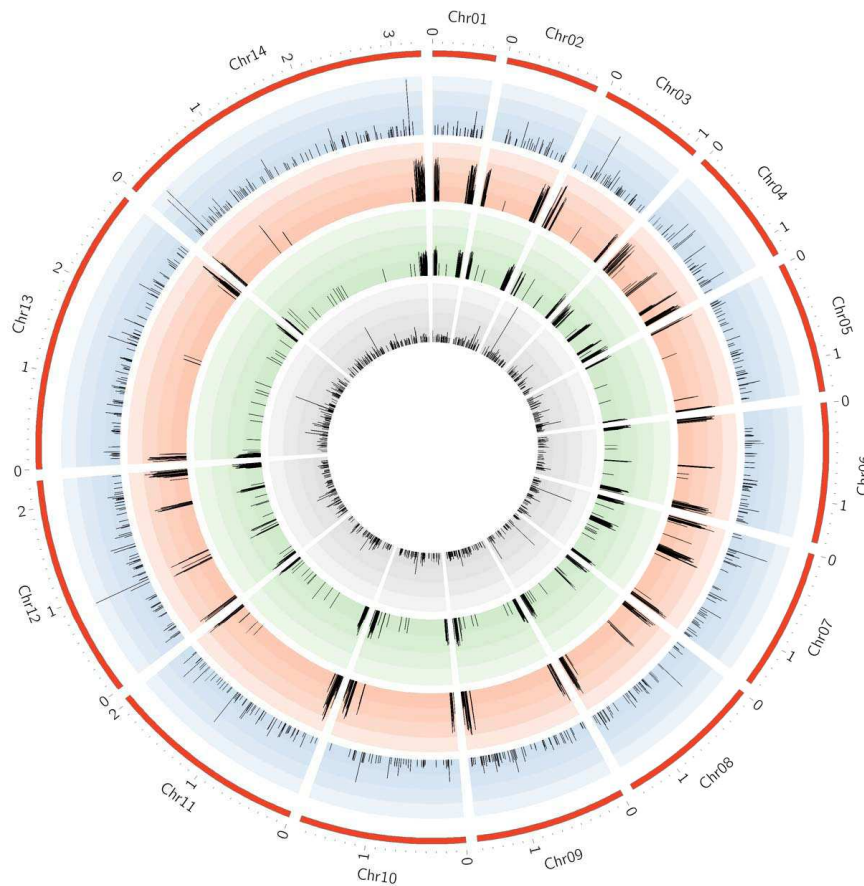
**Figure 4 PfSET6 localizes to discrete foci in the cytoplasm of *P. falciparum* transmission stages.** a. IF of stage IV and V gametocytes using anti-PfSET6 combined with female gametocyte-specific marker anti-Pfg377. The scale bars correspond to 2 $\mu$ m. b. IF localization of PfSET6 in salivary gland sporozoites. The scale bar corresponds to 2  $\mu$ m.



**Figure 5 ChIP-Seq analysis of PfSET6 in ring stage parasites.** a. A circular *P. falciparum* genome with coverage depth plots. Blue circle background represents the signal of PfSET6-IP, red circle background represents mouse IgG mock, and green circle background represents input. The chromosome sizes are indicated

in megabases around the outside of the plot in gray. The position within the genome sequence is indicated at the top. The scale for all three is 0 to 700 RPKM values over bins of 1000 bp/bin. b. Plot of the mean coverage over distance.

a.



b.

Correlation coefficients	PfSET6-IP
PfHP1-IP	0.4780
H3K9me3-IP	0.5431
H3K4me3-IP	0.0707

**Figure 6 PfSET6 genome-wide distribution correlates with the repressive mark histone H3K4me3 and its reader, PfHP1.** a. Circular representation of normalized peak location in PfSET6 (blue), PfHP1 (red), H3K9me3 (green) and H3K4me3 (grey). The height of bar represents the fold-enrichment of the represented state over the respective input data. b. The correlation coefficients between various ChIP datasets.

## SUPPLEMENTARY

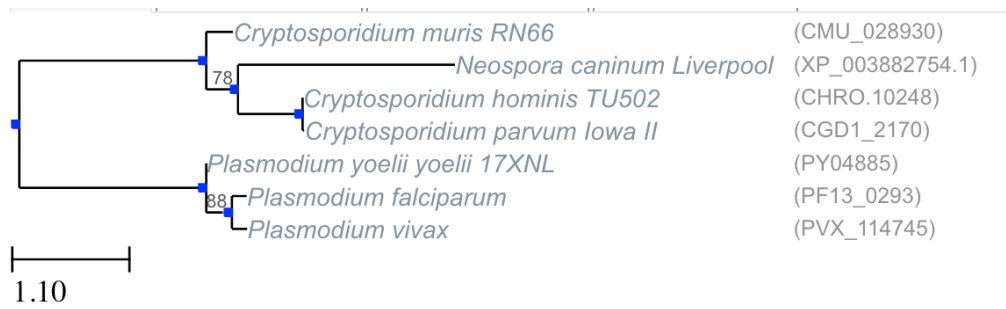


Figure 1 Phylogenetic tree of PfSET6 and Apicomplexa orthologous group.

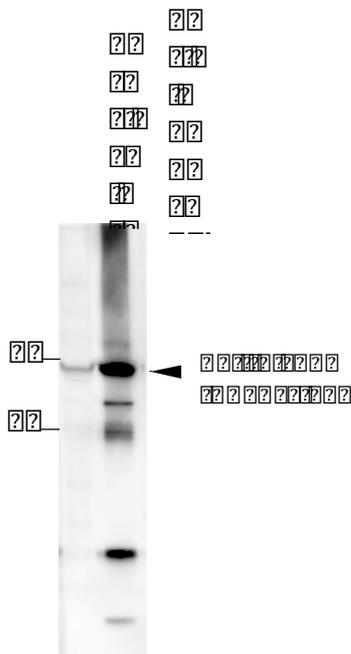


Figure 2 Western blotting of parasite lysates and purified PfSET6 protein using the native anti-PfSET6 antibodies.

**Table 1 List of genes with PfSET6 occupancy as determined by MACS2 peak calling analysis.**

[Gene ID]	[Genomic Location]	[Product Description]
PF3D7_0101100	Pf3D7_01_v3: 69,304 - 70,417 (-)	exported protein family 4 (EPF4)
PF3D7_0101200	Pf3D7_01_v3: 71,624 - 72,426 (+)	exported protein family 3 (EPF3)
PF3D7_0101400	Pf3D7_01_v3: 75,982 - 76,809 (-)	exported protein family 1, pseudogene (EPF1)
PF3D7_0101500	Pf3D7_01_v3: 78,241 - 79,891 (+)	erythrocyte membrane protein 1 (PfEMP1), exon 2, pseudogene (VAR)
PF3D7_0101700	Pf3D7_01_v3: 84,791 - 86,152 (-)	erythrocyte membrane protein 1 (PfEMP1), exon 2, pseudogene (VAR)
PF3D7_0112700	Pf3D7_01_v3: 477,279 - 481,382 (+)	28S ribosomal RNA
PF3D7_0113000	Pf3D7_01_v3: 487,892 - 490,127 (-)	glutamic acid-rich protein (GARP)
PF3D7_0114000	Pf3D7_01_v3: 542,480 - 546,983 (+)	exported protein family 1 (EPF1)
PF3D7_0213800	Pf3D7_02_v3: 558,585 - 560,594 (+)	conserved Plasmodium protein, unknown function
PF3D7_0217500	Pf3D7_02_v3: 720,437 - 722,661 (+)	calcium-dependent protein kinase 1 (CDPK1)
PF3D7_0222000	Pf3D7_02_v3: 876,984 - 877,832 (+)	exported protein family 1 (EPF1)
PF3D7_0222200	Pf3D7_02_v3: 881,469 - 882,267 (-)	exported protein family 3 (EPF3)
PF3D7_0222300	Pf3D7_02_v3: 883,452 - 884,312 (+)	exported protein family 4, pseudogene (EPF4)
PF3D7_0223300	Pf3D7_02_v3: 909,350 - 911,054 (+)	erythrocyte membrane protein 1 (PfEMP1), exon 2
PF3D7_0300300	Pf3D7_03_v3: 49,772 - 51,152 (-)	erythrocyte membrane protein 1 (PfEMP1), exon 2, pseudogene (VAR)
PF3D7_0300600	Pf3D7_03_v3: 58,307 - 58,519 (-)	Plasmodium exported protein, unknown function, fragment
PF3D7_0310200	Pf3D7_03_v3: 427,290 - 440,942 (+)	phd finger protein, putative
PF3D7_0324000	Pf3D7_03_v3: 1,005,952 - 1,006,800 (+)	exported protein family 1 (EPF1)
PF3D7_0324200	Pf3D7_03_v3: 1,010,342 - 1,011,140 (-)	exported protein family 3 (EPF3)
PF3D7_0324300	Pf3D7_03_v3: 1,012,355 - 1,013,464 (+)	exported protein family 4 (EPF4)
PF3D7_0324700	Pf3D7_03_v3: 1,024,030 - 1,025,411 (+)	erythrocyte membrane protein 1 (PfEMP1), exon 2, pseudogene (VAR)
PF3D7_0411800	Pf3D7_04_v3: 519,832 - 525,618 (-)	conserved Plasmodium protein, unknown function
PF3D7_0413100	Pf3D7_04_v3: 591,949 - 599,849 (-)	erythrocyte membrane protein 1, PfEMP1 (VAR)
PF3D7_0420700	Pf3D7_04_v3: 935,031 - 941,875 (-)	erythrocyte membrane protein 1, PfEMP1 (VAR)
PF3D7_0420900	Pf3D7_04_v3: 946,169 - 953,773 (-)	erythrocyte membrane protein 1, PfEMP1 (VAR)
PF3D7_0421000	Pf3D7_04_v3: 956,849 - 956,949 (+)	unspecified product
PF3D7_0421100	Pf3D7_04_v3: 958,067 - 965,611 (-)	erythrocyte membrane protein 1, PfEMP1 (VAR)
PF3D7_0423400	Pf3D7_04_v3: 1,055,665 - 1,056,318 (+)	asparagine-rich protein (AARP)
PF3D7_0500200	Pf3D7_05_v3: 29,233 - 29,304 (-)	erythrocyte membrane protein 1 (PfEMP1), pseudogene
PF3D7_0503400	Pf3D7_05_v3: 140,710 - 141,471 (+)	actin-depolymerizing factor 1 (ADF1)
PF3D7_0504700	Pf3D7_05_v3: 180,421 - 187,470 (+)	centrosomal protein CEP120, putative (CEP120)
PF3D7_0532000	Pf3D7_05_v3: 1,292,410 - 1,296,199 (+)	28S ribosomal RNA
PF3D7_0600400	Pf3D7_06_v3: 18,586 - 22,721 (-)	erythrocyte membrane protein 1, PfEMP1 (VAR)
PF3D7_0600500	Pf3D7_06_v3: 26,557 - 27,830 (+)	rifin (RIF)
PF3D7_0601000	Pf3D7_06_v3: 42,097 - 43,218 (-)	exported protein family 4 (EPF4)
PF3D7_0601100	Pf3D7_06_v3: 44,450 - 45,216 (+)	exported protein family 3 (EPF3)
PF3D7_0601300	Pf3D7_06_v3: 48,874 - 49,722 (-)	exported protein family 1 (EPF1)

PF3D7_0615900	Pf3D7_06_v3: 662,435 - 667,855 (-)	conserved Plasmodium protein, unknown function
PF3D7_0631200	Pf3D7_06_v3: 1,313,708 - 1,315,253 (-)	erythrocyte membrane protein 1 (PfEMP1), pseudogene (VAR)
PF3D7_0631300	Pf3D7_06_v3: 1,316,873 - 1,317,721 (+)	exported protein family 1 (EPF1)
PF3D7_0631500	Pf3D7_06_v3: 1,321,320 - 1,322,094 (-)	exported protein family 3 (EPF3)
PF3D7_0631600	Pf3D7_06_v3: 1,323,294 - 1,324,435 (+)	exported protein family 4 (EPF4)
PF3D7_0631700	Pf3D7_06_v3: 1,326,737 - 1,327,918 (+)	rifin, pseudogene
PF3D7_0701000	Pf3D7_07_v3: 52,086 - 53,636 (+)	erythrocyte membrane protein 1 (PfEMP1), pseudogene
PF3D7_0701300	Pf3D7_07_v3: 62,220 - 63,401 (-)	rifin, pseudogene (RIF)
PF3D7_0701400	Pf3D7_07_v3: 65,718 - 66,854 (-)	exported protein family 4, pseudogene (EPF4)
PF3D7_0701500	Pf3D7_07_v3: 68,066 - 68,840 (+)	exported protein family 3 (EPF3)
PF3D7_0701700	Pf3D7_07_v3: 72,477 - 73,325 (-)	exported protein family 1 (EPF1)
PF3D7_0704600	Pf3D7_07_v3: 216,024 - 229,072 (-)	E3 ubiquitin-protein ligase (UT)
PF3D7_0726000	Pf3D7_07_v3: 1,086,570 - 1,090,357 (+)	28S ribosomal RNA
PF3D7_0732800	Pf3D7_07_v3: 1,410,435 - 1,412,231 (+)	erythrocyte membrane protein 1 (PfEMP1), exon 2
PF3D7_0814200	Pf3D7_08_v3: 687,340 - 688,086 (+)	DNA/RNA-binding protein Alba 1 (ALBA1)
PF3D7_0818200	Pf3D7_08_v3: 830,006 - 831,454 (+)	14-3-3 protein (14-3-3I)
PF3D7_0819700	Pf3D7_08_v3: 888,126 - 890,471 (-)	conserved Plasmodium protein, unknown function
PF3D7_0831800	Pf3D7_08_v3: 1,374,236 - 1,375,299 (-)	histidine-rich protein II (HRPII)
PF3D7_0833200	Pf3D7_08_v3: 1,426,884 - 1,428,135 (+)	rifin (RIF)
PF3D7_0900800	Pf3D7_09_v3: 52,648 - 54,020 (-)	erythrocyte membrane protein 1 (PfEMP1), exon 2, pseudogene (VAR)
PF3D7_0924500	Pf3D7_09_v3: 993,245 - 997,675 (-)	conserved Plasmodium membrane protein, unknown function
PF3D7_1027000	Pf3D7_10_v3: 1,126,523 - 1,131,958 (-)	conserved Plasmodium protein, unknown function
PF3D7_1035200	Pf3D7_10_v3: 1,394,839 - 1,396,596 (+)	S-antigen
PF3D7_1035800	Pf3D7_10_v3: 1,420,533 - 1,422,671 (+)	probable protein, unknown function (M712)
PF3D7_1036400	Pf3D7_10_v3: 1,436,316 - 1,439,804 (+)	liver stage antigen 1 (LSA1)
PF3D7_1038400	Pf3D7_10_v3: 1,519,021 - 1,547,825 (+)	gametocyte-specific protein (Pf11-1)
PF3D7_1039200	Pf3D7_10_v3: 1,576,441 - 1,576,991 (-)	Plasmodium exported protein, unknown function, pseudogene
PF3D7_1039600	Pf3D7_10_v3: 1,590,146 - 1,590,973 (+)	exported protein family 1, pseudogene (EPF1)
PF3D7_1039800	Pf3D7_10_v3: 1,594,503 - 1,595,277 (-)	exported protein family 3 (EPF3)
PF3D7_1039900	Pf3D7_10_v3: 1,596,487 - 1,597,605 (+)	exported protein family 4 (EPF4)
PF3D7_1100900	Pf3D7_11_v3: 60,928 - 61,769 (-)	RESA-like protein, pseudogene
PF3D7_1101400	Pf3D7_11_v3: 76,820 - 78,000 (-)	rifin, pseudogene (RIF)
PF3D7_1101500	Pf3D7_11_v3: 80,306 - 81,424 (-)	exported protein family 4 (EPF4)
PF3D7_1101600	Pf3D7_11_v3: 82,633 - 83,415 (+)	exported protein family 3 (EPF3)
PF3D7_1101800	Pf3D7_11_v3: 87,041 - 87,889 (-)	exported protein family 1 (EPF1)
PF3D7_1102100	Pf3D7_11_v3: 104,300 - 104,852 (+)	Plasmodium exported protein, unknown function, pseudogene
PF3D7_1108100	Pf3D7_11_v3: 356,083 - 360,434 (+)	conserved Plasmodium protein, unknown function
PF3D7_1124000	Pf3D7_11_v3: 948,591 - 950,707 (+)	endoplasmic reticulum oxidoreductin, putative (ERO1)
PF3D7_1148600	Pf3D7_11_v3: 1,925,942 - 1,933,150 (+)	18S ribosomal RNA
PF3D7_1220900	Pf3D7_12_v3: 831,252 - 832,052 (-)	heterochromatin protein 1 (HP1)
PF3D7_1224000	Pf3D7_12_v3: 974,372 - 975,541 (+)	GTP cyclohydrolase I (GCH1)
PF3D7_1228400	Pf3D7_12_v3: 1,153,352 - 1,157,557 (+)	conserved Plasmodium protein, unknown function

PF3D7_1248700	Pf3D7_12_v3: 1,994,775 - 2,000,744 (+)	conserved Plasmodium protein, unknown function
PF3D7_1249700	Pf3D7_12_v3: 2,023,455 - 2,026,181 (-)	conserved Plasmodium protein, unknown function
PF3D7_1254200	Pf3D7_12_v3: 2,207,830 - 2,209,115 (+)	rifin (RIF)
PF3D7_1254300	Pf3D7_12_v3: 2,211,543 - 2,212,554 (+)	stevor
PF3D7_1300400	Pf3D7_13_v3: 47,583 - 48,769 (+)	rifin (RIF)
PF3D7_1300800	Pf3D7_13_v3: 60,097 - 61,172 (-)	erythrocyte membrane protein 1-like (VAR-like)
PF3D7_1302000	Pf3D7_13_v3: 112,792 - 113,815 (-)	EMP1-trafficking protein (PTP6)
PF3D7_1318300	Pf3D7_13_v3: 753,910 - 759,432 (+)	conserved Plasmodium protein, unknown function
PF3D7_1327000	Pf3D7_13_v3: 1,134,070 - 1,138,040 (-)	conserved Plasmodium protein, unknown function
PF3D7_1342400	Pf3D7_13_v3: 1,666,832 - 1,668,153 (-)	casein kinase II beta chain (CK2beta2)
PF3D7_1346300	Pf3D7_13_v3: 1,849,528 - 1,850,517 (+)	DNA/RNA-binding protein Alba 2 (ALBA2)
PF3D7_1371000	Pf3D7_13_v3: 2,800,004 - 2,802,154 (+)	18S ribosomal RNA
PF3D7_1371300	Pf3D7_13_v3: 2,802,945 - 2,807,159 (+)	28S ribosomal RNA
PF3D7_1372900	Pf3D7_13_v3: 2,865,893 - 2,867,226 (+)	erythrocyte membrane protein 1 (PfEMP1), exon 2, pseudogene (VAR)
PF3D7_1400100	Pf3D7_14_v3: 1,393 - 5,343 (+)	erythrocyte membrane protein 1 (PfEMP1), truncated, pseudogene



## ARTICLE 4

### **Analysis of the epigenetic landscape of *Plasmodium falciparum* reveals expression of a clonally variant PfEMP1 member on the surface of sporozoites**

**Zanghì et al, Under review, Nature Microbiology**

Epigenetics play a major role in the regulation of key biological process in *Plasmodium* blood stages cycle, from the monoallelic expression of clonally variant genes to sexual commitment. However, other stages of the *Plasmodium* life cycle have never been investigated. In this project, we aimed to elucidate the epigenetic landscape in *P. falciparum* sporozoites. Genome-wide analysis of H3K9me3, H3K9Ac and PfHP1 occupancy in sporozoites revealed that the sporozoites retain several features observed in asexual blood stages. The major repressive pathway comprised of H3K9me3/PfHP1 is conserved as is nuclear architecture, as evidenced by the formation of PfHP1-containing perinuclear telomeric clusters. A noteworthy difference to the blood stage distribution of these repressive marks was a spreading of PfHP1-containing facultative heterochromatin boundaries to silence genes encoding erythrocyte exported proteins, which are most likely not used by the sporozoite. Strikingly, a single member of the *var* gene family does not retain the repressive epigenetic marks and the corresponding PfEMP1 protein is expressed on the sporozoite surface; in contrast to blood stages, PfEMP1 is now exported to the parasite surface instead of the host membrane. Surface-exposed PfEMP1 may be necessary in the process of homing to the liver *in vivo*, where the sporozoite interacts with different tissues of the mammalian host, or it may play a role in pre-erythrocytic immune evasion. This works sheds light on novel *Plasmodium* biology opening avenues for drug and vaccine development.



**Analysis of the epigenetic landscape of *Plasmodium falciparum* reveals expression of a clonally variant PfEMP1 member on the surface of sporozoites**

Gigliola Zanghì<sup>1</sup>, Shruthi S. Vembar<sup>2,3,4</sup>, Sebastian Baumgarten<sup>2,3,4</sup>, Shuai Ding<sup>2,3,4</sup>, Julien Guizetti<sup>2,3,4</sup>, Jessica M. Bryant<sup>2,3,4</sup>, Denise Mattei<sup>2,3,4</sup>, Anja T.R. Jensen<sup>5</sup>, Jean-François Franetich<sup>1</sup>, Robert Sauerwein<sup>7</sup>, Mallaury Bordessoulles<sup>1</sup>, Olivier Silvie<sup>1</sup>, Olivier Scatton<sup>6</sup>, Dominique Mazier<sup>1\*</sup> & Artur Scherf<sup>2,3,4\*</sup>

<sup>1</sup> Sorbonne Universités, Université Pierre et Marie Curie-Paris 6, UMR S945, Paris, F-75003; Institut National de la Santé et de la Recherche Médicale, U945, F-75013 Paris,; AP-HP, Groupe Hospitalier Pitié-Salpêtrière, Service Parasitologie-Mycologie, Paris, F-75013, France;

<sup>2</sup> Unité Biologie des Interactions Hôte-Parasite, Département de Parasites et Insectes Vecteurs, Institut Pasteur, 75724 Paris 75015, France;

<sup>3</sup> CNRS, ERL 9195, 75724 Paris 75015, France;

<sup>4</sup> INSERM, Unit U1201, 75724 Paris 75015, France;

<sup>5</sup> Centre for Medical Parasitology, Department of Immunology & Microbiology, Faculty of Health and Medical Sciences, University of Copenhagen and Department of Infectious Diseases, Copenhagen University Hospital (Rigshospitalet), Copenhagen, Denmark;

<sup>6</sup> Service de Chirurgie Digestive, Hépatobilio-Pancréatique et Transplantation Hépatique, Hôpital Pitié-Salpêtrière, Paris, France.

<sup>7</sup> Department of Medical Microbiology and Radboud Center for Infectious Diseases, Radboud university medical center, PO Box 9101, 6500 HB, Nijmegen, The Netherlands.

\*To whom correspondence should be addressed: Artur Scherf, Email: [artur.scherf@pasteur.fr](mailto:artur.scherf@pasteur.fr) or Dominique Mazier, Email: [dominique.mazier@upmc.fr](mailto:dominique.mazier@upmc.fr)

### Summary:

Malaria parasites have developed sophisticated strategies during asexual blood stage development that enable chronic infection, pathogenesis and transmission via epigenetically controlled gene expression <sup>1</sup>. In the human parasite *Plasmodium falciparum*, specific epigenetic signatures dictate the transcriptional activation or silencing of immune evasion genes such as the *var* multigene family, which encodes the major virulence factor Erythrocyte Membrane Protein 1 (PfEMP1). However, the epigenetic landscape in other life cycle stages and its impact on host-parasite interaction have not been investigated to date. Here, we map the genome-wide distribution of eu- and heterochromatic features in sporozoites, which migrate through different mosquito and human host cells before infecting a human hepatocyte. Using chromatin immunoprecipitation (ChIP) analysis of Heterochromatin Protein 1 (PfHP1) occupancy and single cell DNA fluorescence *in situ* hybridization (FISH), we found that the genome of sporozoites is organized into heterochromatin-containing gene islands, in particular at chromosome ends, which form 2-4 perinuclear clusters. Importantly, when comparing sporozoites to blood stage parasites, we observed a significant spreading of heterochromatin into gene regions that encode erythrocyte exported proteins. The observed sporozoite PfHP1 signature predicted the expression of a single *var* gene, (*PF3D7\_0809100*), which we confirmed by immunolabeling of the surface of live sporozoites with a specific antibody against the respective PfEMP1 protein. Overall, our work demonstrates that epigenetically controlled variegated gene expression is important in mosquito stages of the *P. falciparum* life cycle. Moreover, the identification of a highly polymorphic sporozoite surface antigen is highly relevant for vaccine development based on attenuated sporozoites.

The most devastating form of human malaria is caused by the protozoan parasite *P. falciparum*, with more than 200 million people infected annually and an estimated 438,000 deaths in 2015 <sup>2</sup>. Malaria is transmitted by the bite of an infected *Anopheles* mosquito, which harbors sporozoites in its salivary glands. From the point of injection into the skin, sporozoites migrate via blood vessels to the liver, cross the sinusoidal cell layer separating the blood and the liver, and finally invade hepatocytes where asexual reproduction leads to the release of thousands of merozoites into the blood stream <sup>3</sup>. These infected red blood cells produce new infective merozoites that initiate a new infective cycle. The persistence and pathogenesis of the human malaria parasite *P. falciparum* during blood stage proliferation relies on the successive expression of variant adhesion molecules termed PfEMP1 encoded

by approximately 60 *var* genes<sup>4</sup>. This immune evasion mechanism called antigenic variation is orchestrated by different layers of epigenetic factors<sup>1</sup>. Monoallelic expression of a single *var* member relies on the default silencing of the rest of the *var* gene family members via facultative heterochromatin. Variegated gene expression is used by the parasite beyond host immune evasion to create phenotypic plasticity in genetically identical parasites during blood stage including sexual commitment of a subset of parasites<sup>5-9</sup>. Although variegated gene expression appears to have evolved as a survival strategy to promote prolonged blood stage infection in humans, it is unknown if it is used by sporozoites, a stage that has been successfully used to provide immune protection to human volunteers<sup>10</sup>.

To fill this important knowledge gap, we developed a robust, low-cell input ChIP assay followed by high throughput sequencing (ChIP-seq) protocol to work with limiting sporozoite numbers. We analyzed the genome-wide distribution of the transcriptionally repressive histone post-translational modification mark (PTM) histone H3-lysine 9-trimethyl (H3K9me3), its reader protein PfHP1, and the transcriptionally activating histone PTMmark H3K9ac. In asexual blood stages, PfHP1 and H3K9me3 regulate transcription of sub-telomeric, clonally variant virulence gene families such as *var* by establishing facultative heterochromatin at promoter regions and gene bodies<sup>5,11,12</sup>. These heterochromatic regions span about hundred kilobases (kb), forming so-called heterochromatin islands. In sporozoites, we observed an enrichment of both H3K9me3 and PfHP1 in sub-telomeric regions of all 14 chromosomes as well as in central chromosome regions of chromosomes 4, 6, 7, 8 and 12 (Fig. 1a and 2a). In contrast, the activating mark H3K9ac is virtually absent from these heterochromatic loci and is dispersed along chromosome regions that contain primarily housekeeping genes (Fig. 1a and 2a). When comparing the genome-wide PfHP1 this pattern to that in asexual blood stage parasites (Fig. 1b and 2a), we observed a general similarity<sup>5</sup>. We noted, however, a significant sporozoite-specific spreading of subtelomeric heterochromatin from nearly all chromosome ends towards central chromosomal regions (Fig. 2a and Fig. 2b). These extended heterochromatic regions of about 50 kb are highly enriched in genes encoding parasite proteins that are typically exported to the host erythrocyte during blood stage development remodeling the erythrocyte to accommodate the parasite's needs<sup>13</sup> (Fig. 2b). Our data suggest for the first time that sporozoites may activate a facultative heterochromatin boundaries remodelling pathway controlled in a stage specific manner and that their extension may function to silence genes that are not expressed in sporozoites to

silence genes encoding exported proteins translocated during intra-erythrocytic development mostly on the surface of the infected erythrocytes (IE).

In blood stage parasites the maintenance of heterochromatin islands are physically linked tethered into several foci at of these regions to the nuclear periphery <sup>5</sup>. To determine if a similar spatial chromosome arrangement is involved/exists in sporozoites, we performed DNA-FISH using a probe corresponding to the conserved subtelomeric repeat TARE6 (Telomere-Associated Repeat 6) <sup>5,9</sup> (Fig. 3a) and indirect immunofluorescence assays (IFAs) with antibodies against PfHP1 (Fig 3b). We observed an average of 2-4 TARE6-containing foci per nucleus, which localized to the nuclear periphery and partially or completely overlapped with PfHP1-containing foci (Fig. 3c). These data indicate a conserved heterochromatin nuclear spatial organization in the nucleus between asexual blood stage parasites and migratory sporozoites.

In asexual stages, only one of the 60 *var* gene members is transcribed at a time to ensure expression of a single erythrocyte surface adhesion protein, implicated in immune evasion and pathogenesis <sup>14,15</sup>. To determine if heterochromatin may control the default silent state of the *var* virulence multigene family in sporozoites as in blood stage parasites we performed bioinformatic analysis of three independent H3K9me3 and PfHP1 ChIP-seq experiments. This analysis revealed that a single member, *Pf3D7\_0809100*, of the *var* gene family showed strongly reduced H3K9me3 and PfHP1 signal in its promoter region and gene body (Fig. 4a), suggesting that *Pf3D7\_0809100* may be expressed in sporozoites. *Pf3D7\_0809100* (here called *var*<sup>SPORO</sup>) is located in the central region of chromosome 8, adjacent to two other *var* genes, which retain higher levels heterochromatin marks (Fig. 4a). Notably, other clonally variant gene families such as *rif*, *Pfmc2TM*, *PfACS* and *clag* families, which are located proximal to subtelomeric *var* genes on 13 of the 14 chromosomes, appear to maintain blood stage-like H3K9me3 and PfHP1 patterns, with only two of 180 *rif* genes, one of 13X *Pfmc2TM* genes and five of 13 *PfACS* genes depleted for these marks in Table 1. In addition, the previously identified master regulator of sexual commitment, AP2-G <sup>7,8</sup> shows a PfHP1 enrichment in sporozoites that is similar to that seen in blood stage parasites (Supplementary Fig S. 2).

As we observed the same pattern of PfHP1 depletion for the single *Pf3D7\_0809100 var* gene in three independent sporozoite preparations, we investigated the possibility that this epigenetic signature was established during the asexual blood stage of the NF54 strain used to generate the sporozoites analyzed in this study. RT-qPCR analysis of all *var* genes in a synchronized bulk culture of NF54 ring stage parasites showed that five different *var* gene transcripts are present at relatively high levels, whereas most other members, including *var*<sup>sporo</sup>, are present at very low levels (Fig. 4b). These data strongly suggest that an epigenetic reset of *var* gene transcription occurs during sexual development, with the specific transcriptional upregulation of *var*<sup>sporo</sup> during the formation of sporozoites in the mosquito.

To determine if *var*<sup>sporo</sup> is indeed expressed in sporozoites, as predicted by H3K9me3 and PfHP1 distribution (Fig. 4a), we performed IFAs on fixed or live sporozoites using either an antibody against the conserved intracellular C-terminal ATS (Acid Terminal Segment) of that reacts with all PfEMP1 proteins<sup>16</sup> or a specific antibody against the extracellular variable CIDR domain (Cysteine-Rich Inter domain region) of *var*<sup>sporo</sup> PfEMP1. Both antibodies reacted with fixed sporozoites and showed a surface membrane-like staining pattern that partially overlapped with Circumsporozoite protein (CSP), the major surface antigen of sporozoites (Fig. 4c top and middle rows). In contrast, no surface staining was observed with antibodies against the extracellular domain of the PfEMP1 encoded by *var2CSA* (*Pf3D7\_1200600*) and a second *var* gene (*Pf3D\_70412700*) (data not shown) that retain H3K9me3/PfHP1 marks, which is predicted to be repressed by the PfHP1 profile (Fig. 4c bottom row and Supplementary S3). When IFA was repeated with live sporozoites which have intact cell membranes, the anti-*var*<sup>sporo</sup> PfEMP1 antibody, but not the anti-ATS antibody, stained the surface of sporozoites (Fig. 4d), again in a pattern that partially overlapped with CSP (Fig. 4c and 4d). Trypsin treatment of live sporozoites (50 µg/ml) abolished antibody surface reactivity confirming that the CIDR domain of *var*<sup>sporo</sup> PfEMP1 is extracellular (data not shown). Together, these results provide the first evidence of a member of the highly polymorphic PfEMP1 protein being expressed on the surface of the sporozoites, with the ATS domain most likely at the cytoplasmic side of the parasite membrane and the CIDR domain exposed to the extracellular milieu. This manner of PfEMP1 expression contrasts with what is observed in blood stage parasites. In intra-erythrocytic parasites, PfEMP1 proteins are exported across the parasite and the parasitophorous vacuolar membrane to the surface of the erythrocyte, where they serve as adhesion molecules that can bind to a variety of endothelial

receptors such as CD36, ICAM, etc., causing malaria pathogenesis by obstructing blood vessels in critical organs such as the brain<sup>4,15</sup>. Given the potential of *var*<sup>sporo</sup> to interact with hepatocytes to contribute to hepatocytes infection, we pre-incubated freshly isolated sporozoites with either the anti-*var*<sup>sporo</sup> antibody directed against the CIDR domain or pre-immune serum before adding them to a primary human hepatocyte culture. The *var*<sup>sporo</sup> antiserum did not reduce infection significantly at 1/50 serum dilution and showed similar level of infection as the corresponding preimmune serum in three independent experiments (Supplementary S4). Anti-CSP antibody confirmed the experimental procedure showing a potent inhibitory effect. Our hepatocyte invasion assay does not support a role for *var*<sup>sporo</sup> PfEMP1 in hepatocyte infection, although better antibodies targeting different regions of this very large protein are needed to further explore its potential interactions with host cell receptors.

This is, to our knowledge, the first genome-wide analysis of important epigenetic signatures in *P. falciparum* sporozoites. Adaptation of ChIP-seq to this stage has uncovered several features that will greatly inform our view of the biology of malaria transmission to humans. Importantly, the transcription of a single *var* gene was predicted by PfHP1 enrichment patterns, and we confirm the corresponding PfEMP1 expression by surface IFA of sporozoites in three independent mosquito infection experiments. Our data strongly suggest that a specific member of the *var* multigene family (~60 members) is selected for expression in sporozoites. This novel concept is further supported by our finding that NF54 blood stage parasites primarily transcribe *var* genes that are distinct from the identified *var*<sup>sporo</sup>. Thus, it is unlikely that *var*<sup>sporo</sup> transcriptional activation is simply maintained in the transition from human blood to mosquito stage. It is currently unclear why a single *var* gene would be specifically expressed in mosquito stage sporozoites. In the future, *var*<sup>sporo</sup> gene knock out experiments are needed to shed light on the biology of *var*<sup>sporo</sup> PfEMP1 during sporozoite development in the mosquito and migration to human hepatocytes. Using *var*<sup>sporo</sup> mutants to infect mosquitos could also reveal if the mechanisms of *var* gene switching are maintained in sporozoites.

In addition, our work adds a new dimension to vaccine development based on live attenuated sporozoites. Successful protection of human volunteers has been reported after challenge with homologous *P. falciparum* parasites. The discovery of a highly polymorphic strain-specific sporozoite surface antigen may indicate that protective immune response targets variant specific antigens. This emphasizes the need to challenge volunteers with heterologous parasite

strains to evaluate the degree of protection due to polymorphic antigens. Future work on *var*<sup>sporo</sup> may shed light on the homing mechanisms of sporozoites to hepatocytes.

### **Acknowledgements**

We thank Benoit Gamain for providing anti-*var*2CSA antibodies. This work was supported by a European Research Council Advanced Grant (PlasmoSilencing 670301), ANR grant HypEpiC (ANR-14-CE16-0013) and the French Parasitology consortium ParaFrap (ANR-11-LABX0024). G.Z. and S.D. are supported by a ParaFrap PhD fellowship, S.S.V. was supported by a fellowship Carnot-Pasteur-Maladies Infectieuse and J.B. by an EMBO fellowship (ALTF 180-2015).

### **Authors' contributions**

G.Z., S.S.V., D.M. and A.S. conceived and designed the experiments; G.Z., S.S.V., S.D. performed ChIP experiments G.Z., S.S.V. and S.B. analyzed the ChiP data; J.B. performed qRT-PCR analysis, D.M. and A.T.R.J. contributed reagents/materials for *var*<sup>sporo</sup> localization experiments, G.Z. and J.G. performed imaging experiments, J.F., M.B., O.S., R.S. and G.Z. contributed to sporozoite preparation and O.S. to primary human hepatocyte infection studies. G.Z. and A.S. wrote the manuscript. All authors read and approved the final manuscript.

### **Competing financial interests :**

The authors declare that they have no competing interests.

### **References**

1. Guizetti, J. & Scherf, A. Silence, activate, poise and switch! Mechanisms of antigenic variation in *Plasmodium falciparum*. *Cell Microbiol* **15**, 718-726 (2013).
2. WHO. Fact Sheet: World Malaria Report 2015. <http://www.who.int/malaria/publications/world-malaria-report-2015/report/en/> (2015).
3. Prudêncio, M., Rodriguez, A. & Mota, M. M. The silent path to thousands of merozoites: the *Plasmodium* liver stage. *Nat Rev Microbiol* **4**, 849-856 (2006).
4. Smith, J. D. The role of PfEMP1 adhesion domain classification in *Plasmodium falciparum* pathogenesis research. *Mol Biochem Parasitol* **195**, 82-87 (2014).

5. Lopez-Rubio, J. J., Mancio-Silva, L. & Scherf, A. Genome-wide analysis of heterochromatin associates clonally variant gene regulation with perinuclear repressive centers in malaria parasites. *Cell Host Microbe* **5**, 179-190 (2009).
6. Rovira-Graells, N. et al. Transcriptional variation in the malaria parasite *Plasmodium falciparum*. *Genome Res* **22**, 925-938 (2012).
7. Sinha, A. et al. A cascade of DNA-binding proteins for sexual commitment and development in *Plasmodium*. *Nature* **507**, 253-257 (2014).
8. Kafsack, B. F. et al. A transcriptional switch underlies commitment to sexual development in malaria parasites. *Nature* **507**, 248-252 (2014).
9. Brancucci, N. M. et al. Heterochromatin protein 1 secures survival and transmission of malaria parasites. *Cell Host Microbe* **16**, 165-176 (2014).
10. Richie, T. L. et al. Progress with *Plasmodium falciparum* sporozoite (PfSPZ)-based malaria vaccines. *Vaccine* **33**, 7452-7461 (2015).
11. Salcedo-Amaya, A. M. et al. Dynamic histone H3 epigenome marking during the intraerythrocytic cycle of *Plasmodium falciparum*. *Proc Natl Acad Sci U S A* **106**, 9655-9660 (2009).
12. Flueck, C. et al. *Plasmodium falciparum* heterochromatin protein 1 marks genomic loci linked to phenotypic variation of exported virulence factors. *PLoS pathogens* **5**, e1000569 (2009).
13. de Koning-Ward, T. F., Dixon, M. W., Tilley, L. & Gilson, P. R. *Plasmodium* species: master renovators of their host cells. *Nat Rev Microbiol* **14**, 494-507 (2016).
14. Scherf, A., Lopez-Rubio, J. J. & Riviere, L. Antigenic variation in *Plasmodium falciparum*. *Annu Rev Microbiol* **62**, 445-470 (2008).
15. Miller, L. H., Ackerman, H. C., Su, X. Z. & Wellems, T. E. Malaria biology and disease pathogenesis: insights for new treatments. *Nat Med* **19**, 156-167 (2013).
16. Nacer, A. et al. Clag9 is not essential for PfEMP1 surface expression in non-cytoadherent *Plasmodium falciparum* parasites with a chromosome 9 deletion. *PLoS One* **6**, e29039 (2011).

## Methods section

### Isolation and purification of *P. falciparum* sporozoites

*P. falciparum* (NF54) sporozoites were obtained from the Department of Medical Microbiology, University Medical Centre, St Radboud, Nijmegen, the Netherlands. Adult *Anopheles stephensi* females were infected with NF54 strain of *P. falciparum*<sup>1</sup>. After 14-21 days from an infective blood meal, the salivary glands were aseptically dissected and purified on 17% Accudenz gradient as previously described<sup>2</sup>.

### Chromatin Immunoprecipitation and Next Generation Sequencing

ChIP was performed as previously described (Lopez-Rubio et al. 2013), using as starting material of  $5 \times 10^6$  parasites for *P. falciparum* sporozoites and  $1 \times 10^9$  parasites of the laboratory-adapted strain 3D7, clone G7, for *P. falciparum* asexual ring stages, using 0.5 ug of anti-H3K9me3, anti-H3K9ac (Millipore) and anti-PfHP1 rabbit polyclonal antibodies<sup>3</sup>. To generate Illumina-compatible sequencing libraries, the immunoprecipitated DNA was processed using the MicroPlex Library Preparation Kit (Diagenode) according to manufacturer's instructions. As controls, DNA corresponding to the ChIP input or DNA immunoprecipitated using rabbit IgG were processed. Pooled, multiplexed libraries were sequenced on an Illumina NextSeq® 500/550 system as a 150 nucleotide single-end run. The resulting data were demultiplexed using bcl2fastq2 (Illumina) to obtain fastq files for downstream analysis. A minimum of two biological replicates was analyzed for each antibody and each parasite stage.

### ChIP-seq Data Analysis

Quality control of fastq files was performed using the FastQC software. Sequencing reads were mapped to the *P. falciparum* genome (v.3, GeneDB) with the Burrows-Wheeler Alignment tool (BWA MEM) using default parameters<sup>4</sup>. Uniquely mapped reads of quality Q20 were considered for peak-calling analysis with the MACS2 software<sup>5</sup> after controlling for a false discovery rate of 5% (default setting of MACS2) using Benjamini and Hochberg's correction method<sup>6</sup>. For the genome-wide representation of HP1, H3K9ac and H3K9m3 from both sporozoites (Fig 1,3 and Fig S1, S2) and blood stage parasites (Fig. 1a,b), the coverages of the respective chromatin marks were calculated as average RPKM (reads per kilobase of genome sequence per one million mapped reads) over bins of 1000bp width using bamCoverage from the package deepTools2 (v2.2.4, PMID: 27079975). Coverage differences between the HP1 ChIP experiment and the input

control (Fig. 3a) were calculated using bamCompare from the same package. Circular and linear coverage plots were generated using circos (v0.69, PMID: 19541911) and the Integrated Genomics Viewer (v2.3.72, PMID: 22517427).

### **Immunofluorescence imaging of sporozoites**

For *var* protein staining  $5 \times 10^4$  sporozoites were placed on poly-L-lysine coated coverslips either live or fixed in 4% PFA for 10 min at room temperature were blocked with 4%BSA/PBS for 30 min, followed by incubation with primary antibody for 1h, three washes with PBS, and detection with Alexa Fluor 488- or 568-conjugated anti-rat IgG, anti-guineapig and anti-rabbit respectively (Life technologies) diluted 1:1000 in PBS/3%BSA. After three final washes in PBS cells were mounted in Vectashield containing DAPI for nuclear staining. Images were captured using a Deltavision Elite imaging system (GE healthcare) with a 60x 1.42 NA objective and a DV Elite CMOS camera. Fiji (<http://fiji.sc>) was used for image analysis of at least two independent replicas.

### **Protein expression and antisera**

The cysteine-rich interdomain region (CIDR)-alpha of PF3D7\_0809100 was cloned into the *Baculovirus* transfer vector pAcGP67-A (BD Biosciences). Recombinant *Baculovirus* were generated by cotransfection of the pAcGP67-A-CIDR construct gene and Bsu36I-linearized Bakpak6 *Baculovirus* DNA (BD Biosciences) into insect Sf9 cells. Recombinant CIDR product was expressed by infection of insect High Five cells with recombinant *Baculovirus*. CIDR protein was purified from culture supernatants on  $\text{Co}^{2+}$  metal chelate agarose columns <sup>7</sup>. Antibodies to *Baculo*-expressed CIDR were raised in Wistar rats by subcutaneous injection as previously described <sup>8</sup>. All experimental animal procedures were approved by The Danish Animal Procedures Committee ("Dyreforsøgstilsynet") as described in permit no. 2008/561-1498 and according to the guidelines described in Danish act LBK 1306 (23/11/2007) and BEK 1273 (12/12/2005). Rabbit anti var2CSA was a gift of Benoit Gamain <sup>9</sup>. The guinea pig antiserum against recombinant PfEMP1 ATS (Acid Terminal Sequence) region was published earlier <sup>10</sup>. Mouse Mab C6 directed against the *P. falciparum* CS protein has been described previously <sup>11</sup>.

### **DNA-FISH and immunofluorescence imaging**

Sporozoites were fixed in suspension with 4% paraformaldehyde in PBS over night at 4°C. Parasites were then deposited on polylysine coated #1.5 cover glasses, permeabilized 15 min with 0.1% Triton-X-100, and subjected to same DNA-FISH labeling conditions as described previously

for blood stage parasites (Mancio-Silva et al. 2008). For sequential immunofluorescence and DNA-FISH parasites were labeled first with rabbit anti-HP1 at 1:2000 in PBS/3%BSA followed by detection with Alexa-Fluor 488-conjugated anti-rabbit IgG (Life technologies). After an additional fixation step we carried out DNA-FISH using a biotinylated LNA probe (Exiqon) labeling all TARE6 telomeric repeat regions 5'-Biotin-+AC+T+AACA+TA+GG+T+CT+T+A-Biotin-3' detected with Streptavidin-Alexa568 (Life Technologies) at 1:2000 in PBS/3%BSA.

### **Trypsin treatment**

Living  $1 \times 10^6$  sporozoites in 200  $\mu$ l Leibovitz's L-15 medium were treated with Trypsin (Gibco) with a final concentration of 50 g/ml for 40 minutes at 25°C to avoid sporozoites activation. Then sporozoites were washed 3 times with Leibovitz's L-15 medium containing serum. The staining and imaging were performed as previously described.

### **Real-Time PCR analysis**

Total RNA was isolated from highly synchronized parasite cultures by sapoin lysis followed by purification with miRNeasy kit (Qiagen). RNA was DNase (Qiagen) treated and reverse transcription was performed using random hexamer primers and SuperScript VILO reverse transcriptase (ThermoFisher Scientific). Quantitative PCR was performed with the resultant cDNA in triplicate on a CFX Real-Time PCR System (BioRad) using Power SYBR Green (Life Technologies) and primers specific for almost all *var* genes, designed in a previous study<sup>12</sup>. Transcript levels were determined using the quantity mean of each triplicate as calculated from a standard curve based on a serial dilution of genomic DNA. *var* gene transcription was normalized to that of a housekeeping gene, seryl tRNA synthetase.

### **Liver stage development inhibition assay**

Primary human hepatocytes were isolated from human liver fragments collected during unrelated surgery after informed consent was obtained from patients undergoing a partial hepatectomy as part of their medical treatment at Service de Chirurgie Digestive, Hepato-Bilio-Pancréatique et Transplantation Hépatique, Hôpital Pitié Salpêtrière, Paris, France. Collection and use of this material for the purposes of the study presented here were undertaken in accordance with French national ethical guidelines under Article L, 1121-1 of the 'Code de la Santé Publique', with approval from the ethics committee of the Centre Hospitalo-Universitaire Pitié-Salpêtrière, Assistance Publique-Hôpitaux de Paris, France. Primary human hepatocyte cultures were prepared from freshly isolated liver fragments as previously described<sup>13</sup>. Cells were seeded at a density of

$8 \times 10^4$  cells per well in 96-well culture plates coated with rat tail collagen I (Becton Dickinson) and cultured at 37 °C, 5% CO<sub>2</sub> in William's Medium E (Life Technologies) supplemented with 10% FCS (Perbio),  $5 \times 10^{-5}$  M hydrocortisone hemisuccinate (Upjohn Laboratories SERB, France), 5 µg per ml insulin (Sigma), 2 mM l-glutamine, 1% penicillin–streptomycin solution (100X, stock solution, GIBCO). After cell adherence (12–24 h), 2% DMSO was added to the culture medium until infection. The different heat-inactivated rat sera of var-sporo and the correspondent pre-immune rat sera were added to the *P. falciparum* sporozoites at a final dilution of 1/50 dilution. A total of  $3 \times 10^4$  sporozoites from the *P. falciparum* NF54 strain in 50 µl of fresh medium were added next to the cells. Plates were centrifuged at 2000 rpm for 10 min at room temperature to facilitate parasite settling onto the cells. Medium changes were carried out at 3, and 48h post addition of sporozoites. Cultures were stopped at day 3 days post infection by fixing with cold methanol. Parasite numbers within hepatocytes were assessed via immunofluorescence using anti-PfHSP70 antibodies as previously described<sup>14</sup>. Quantification was performed by microscopy or using the arrayscan XT<sub>i</sub> imaging system (Thermofisher).

## References

1. Ponnudurai, T. et al. Infectivity of cultured Plasmodium falciparum gametocytes to mosquitoes. *Parasitology* **98 Pt 2**, 165-173 (1989).
2. Kennedy, M. et al. A rapid and scalable density gradient purification method for Plasmodium sporozoites. *Malar J* **11**, 421 (2012).
3. Chen, P. B. et al. Plasmodium falciparum PfSET7: enzymatic characterization and cellular localization of a novel protein methyltransferase in sporozoite, liver and erythrocytic stage parasites. *Sci Rep* **6**, 21802 (2016).
4. Li, H. & Durbin, R. Fast and accurate short read alignment with Burrows-Wheeler transform. *Bioinformatics* **25**, 1754-1760 (2009).
5. Zhang, Y. et al. Model-based analysis of ChIP-Seq (MACS). *Genome Biol* **9**, R137 (2008).
6. Y, B. & Y, H. Controlling false discovery rate: A practical and powerful approach to multiple testing. *Royal statistical society* **57**, 289-300 (1995).
7. Jensen, A. T. et al. Plasmodium falciparum associated with severe childhood malaria preferentially expresses PfEMP1 encoded by group A var genes. *J Exp Med* **199**, 1179-1190 (2004).
8. Bengtsson, A. et al. A novel domain cassette identifies Plasmodium falciparum PfEMP1

- proteins binding ICAM-1 and is a target of cross-reactive, adhesion-inhibitory antibodies. *J Immunol* **190**, 240-249 (2013).
9. Gangnard, S. et al. Structure of the DBL3X-DBL4 $\epsilon$  region of the VAR2CSA placental malaria vaccine candidate: insight into DBL domain interactions. *Sci Rep* **5**, 14868 (2015).
  10. Nacer, A. et al. Clag9 is not essential for PfEMP1 surface expression in non-cytoadherent *Plasmodium falciparum* parasites with a chromosome 9 deletion. *PLoS One* **6**, e29039 (2011).
  11. Okitsu, S. L. et al. Structure-activity-based design of a synthetic malaria peptide eliciting sporozoite inhibitory antibodies in a virosomal formulation. *Chem Biol* **14**, 577-587 (2007).
  12. Salanti, A. et al. Selective upregulation of a single distinctly structured var gene in chondroitin sulphate A-adhering *Plasmodium falciparum* involved in pregnancy-associated malaria. *Mol Microbiol* **49**, 179-191 (2003).
  13. Silvie, O. et al. A role for apical membrane antigen 1 during invasion of hepatocytes by *Plasmodium falciparum* sporozoites. *J Biol Chem* **279**, 9490-9496 (2004).
  14. Rénia, L. et al. A malaria heat-shock-like determinant expressed on the infected hepatocyte surface is the target of antibody-dependent cell-mediated cytotoxic mechanisms by nonparenchymal liver cells. *Eur J Immunol* **20**, 1445-1449 (1990).

**Figures and Figure Legends**

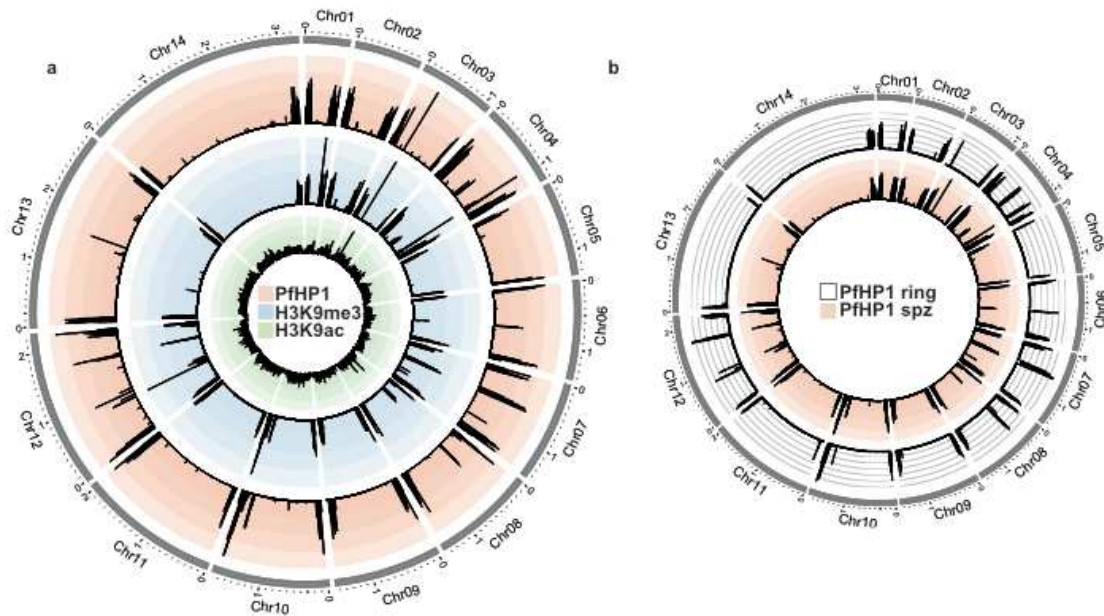


Figure 1

**Figure 1**

**ChIP-seq analysis of transcriptionally repressive and activating chromatin features in *P. falciparum* sporozoites.** Circular representation of ChIP-seq data for all 14 chromosomes. (a) Chromatin enrichment (black) of PfHP1 (red), H3K9me3 (blue) and H3K9ac (green) in sporozoites. (b) Comparison of PfHP1 ChIP data obtained for sporozoites (red) and ring blood stage parasites (black). For both images the chromosome sizes are indicated in megabases around the outside of the plot in gray. The position within the genome sequence is indicated at the top. In all cases, coverage plots are represented as average RPKM values over bins of 1000 bp/bin.

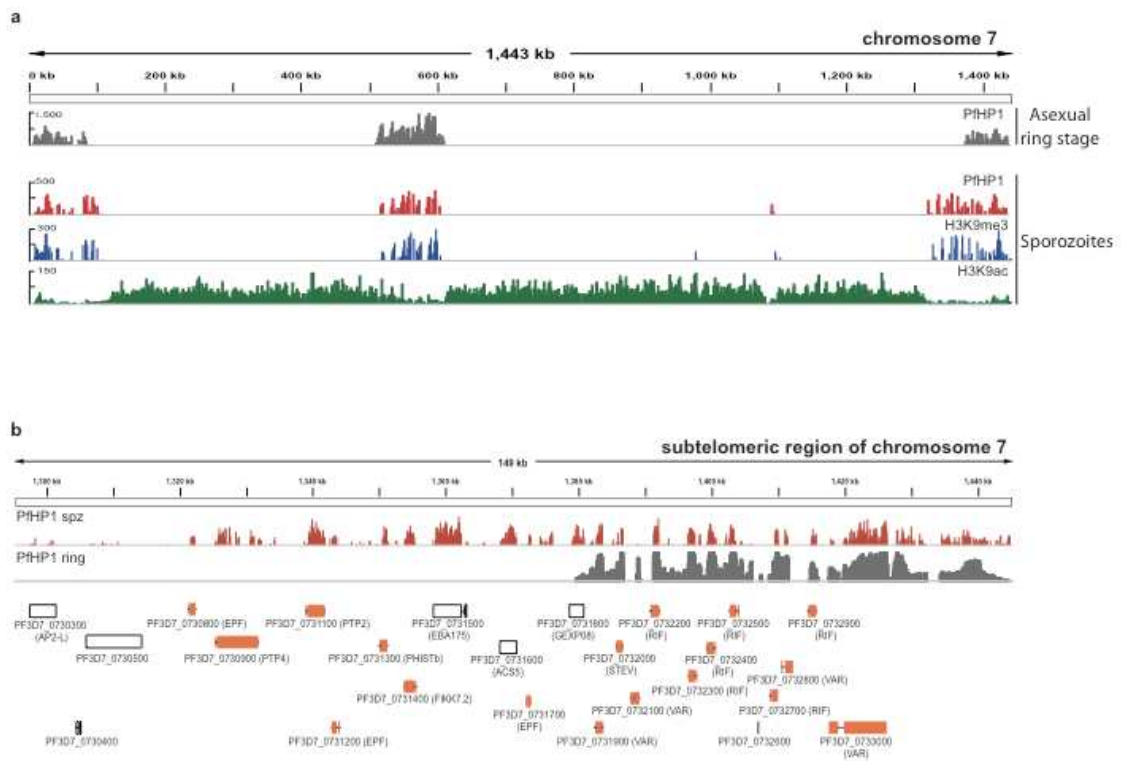


Figure 2

## Figure 2

### Extended heterochromatin islands in subtelomere regions in sporozoites.

(a) Chromosome 7 is shown to illustrate the differences in the PfHP1 distribution at subtelomeric regions between sporozoite (bottom three tracks) and asexual blood stage parasites (top track). (b) Subtelomeric region of chromosome 7 with the telomere at the right, including annotated genes at the bottom. ChIP-seq data show the enrichment of PfHP1 for sporozoites (red) and for the asexual blood stage parasites (black). In sporozoites PfHP1 covers an extra region of 80 kb that is highly enriched in genes encoding exported proteins of infected red blood cells (orange). In (a) coverage plots are represented as average RPKM values over bins of 1000 bp/bin, in (b) coverage plots are represented as an average of 1 single nucleotide/bin. In all cases the position on the genome sequence is indicated at the top.

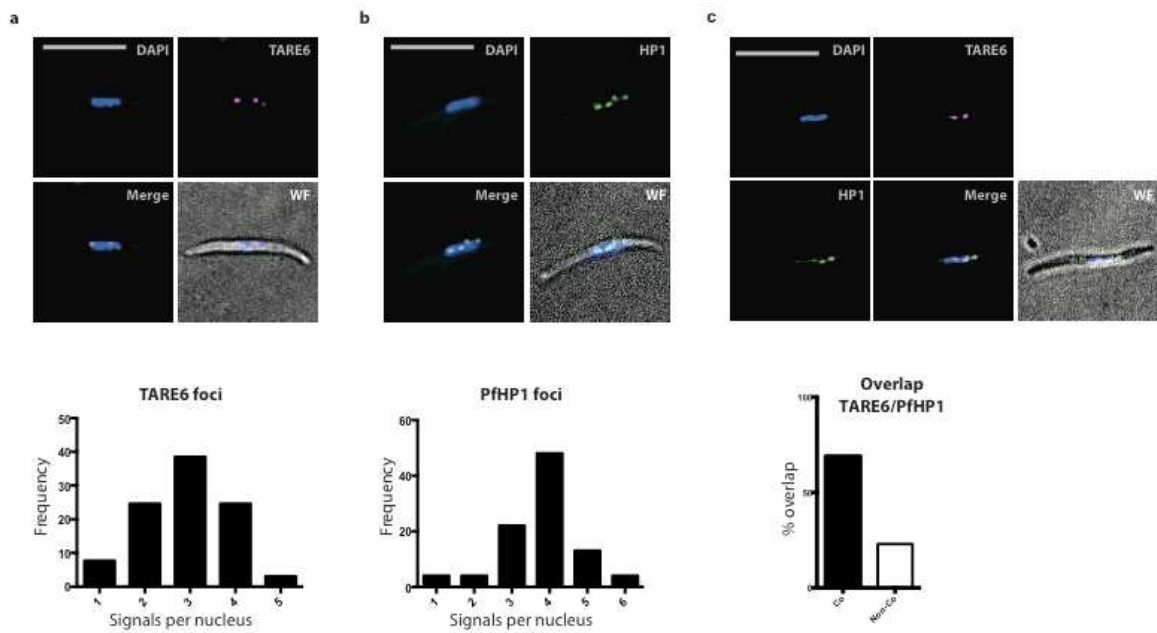


Figure 3

**Figure 3:**

**Frequency and spatial nuclear organization of chromosome ends and heterochromatin islands in sporozoites.** (a) DNA-FISH of telomeres (using a TARE6 probe in magenta) in sporozoites. Frequency distribution of nuclear TARE6 foci with an average of  $3 \pm 1$  foci per nucleus. (b) Immunofluorescence analysis of PfHP1 (green) and its nuclear distribution with an average of  $4 \pm 0.09$  foci per locus. (c) Combined immunofluorescence analysis of PfHP1 (green) and DNA-FISH of telomeres (using a TARE6 probe in magenta) in sporozoites with a percentage of 70% of TARE6 PfHP1 co-localization. DNA was stained with DAPI (blue), indicating the nucleus. Scale bar 5  $\mu$ m. From this experiment, frequency distribution and overlap of TARE6 (telomere clusters) and nuclear PfHP1 foci was established for 50 nuclei for three biological replicates.

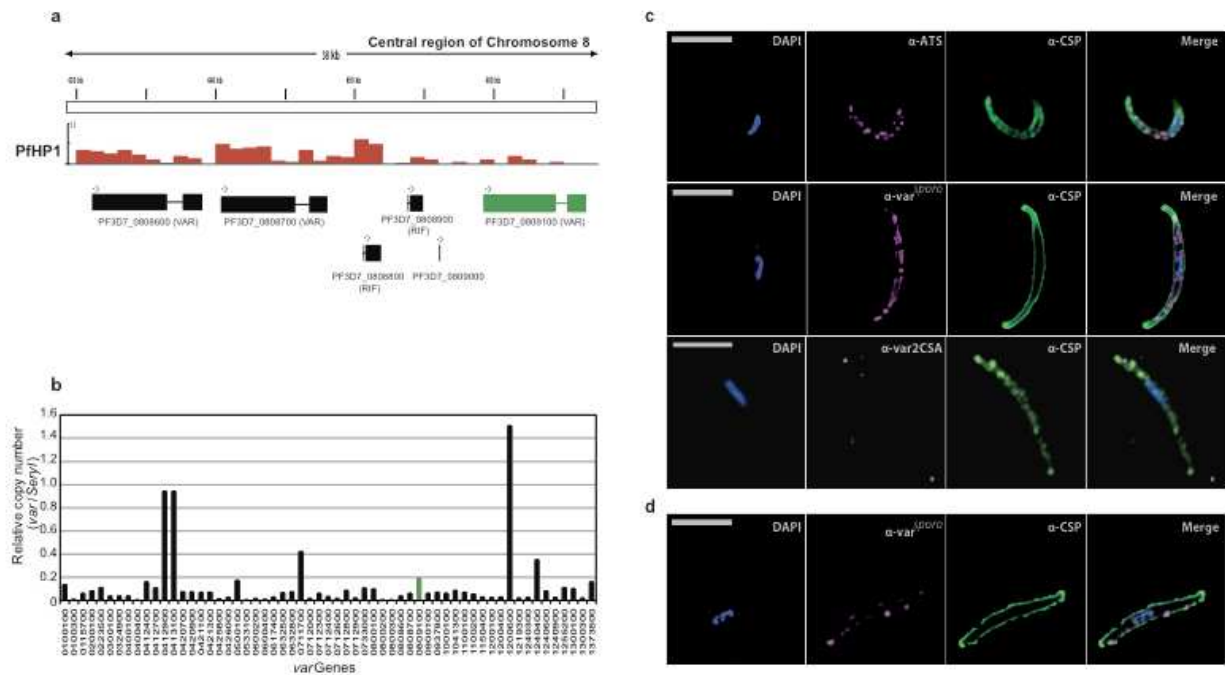


Figure 4

### Figure 4

**Analysis of PfHP1 occupancy reveals sporozoite surface expression of a *var* gene member.** (a) Bioinformatic analysis of ChIP-seq data revealed a single *var* gene - *Pf3D7\_0809100* (*var<sup>sporo</sup>*, highlighted in green) – with extremely low PfHP1 enrichment (indicated on the y-axis) and high enrichment for the neighboring *var* genes (in black) on chromosome 8 (indicated on the x-axis). The position within the genome sequence is indicated at the top. (b) RT-qPCR analysis of all *var* gene RNA transcripts from highly synchronized ring stage parasites 12 hours post infection. *var* gene cDNA levels are normalized to those of seryl tRNA synthetase. The RNA transcript level for *var<sup>sporo</sup>* is highlighted in green. (c) Immunofluorescence analysis of fixed and permeabilized sporozoites using anti-ATS (top row, magenta), anti-*var<sup>sporo</sup>* PfEMP1 (middle row, magenta), anti-*var2CSA* (bottom row, magenta), and anti-CSP (all rows, green) antibodies. (d) Surface immunofluorescence of live sporozoites using anti-CSP (green) and anti-*var<sup>sporo</sup>* (magenta) antibodies. For (c) and (d) DNA was stained with DAPI (blue), indicating the nucleus, and the scale bar is 5  $\mu$ m.

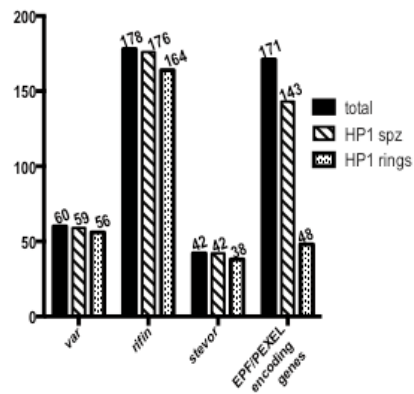


Figure S1

**Supplementary Fig. 1**

**Comparison of PfHP1 enrichment in genes of sporozoites and asexual ring stage parasites.** Bar graph shows clonally variant gene families *var*, *rifin* and *stevor* and genes predicted to be exported into the erythrocyte cytoplasm. Sporozoite show significantly higher PfHP1 coverage for exported proteins. Numbers on top of each bar indicate gene numbers.

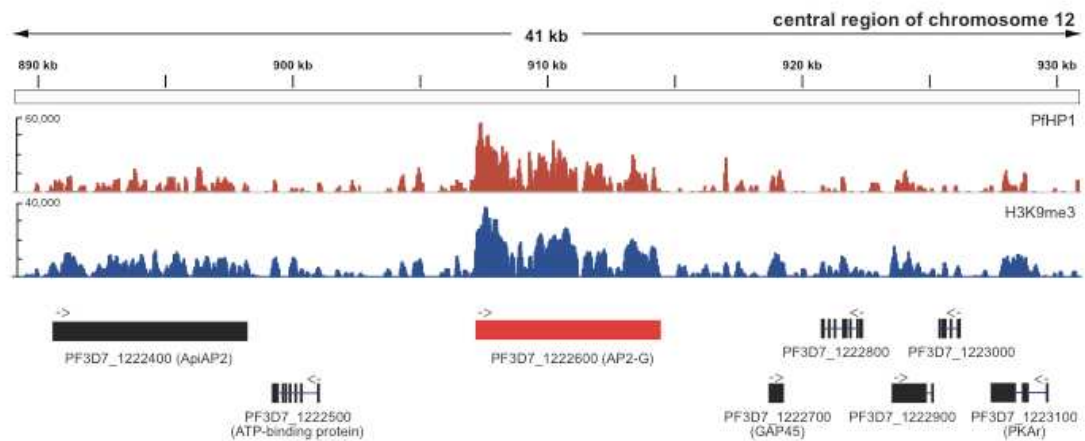


Figure S2

### Supplementary Fig. 2

**H3K9me3 and PfHP1 are enriched at the AP2 gene on chromosome 12 in sporozoites.** ChIP-seq analysis shows the enrichment and colocalization of PfHP1 (red) and H3K9me3 (blue) at the AP2G locus (shown at the bottom). The position on the genome sequence is indicated at the top and coverage plots are represented as an average of 1 single nucleotide/bin.

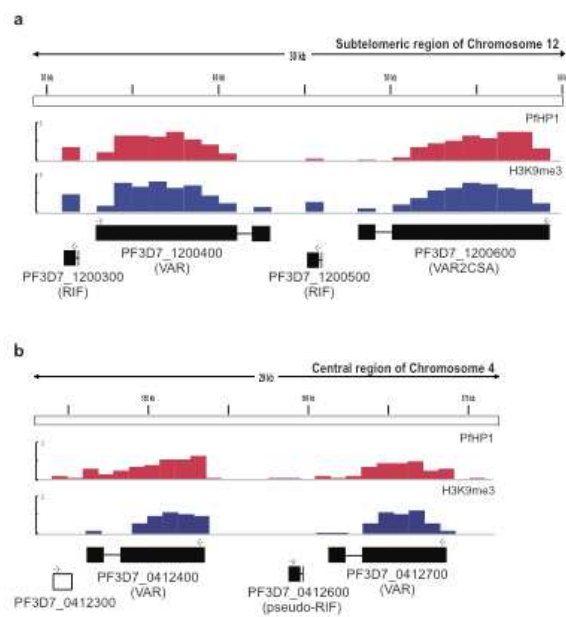


Figure S3

### Supplementary Fig. 3

**Enrichment levels of PfHP1 and H3K9me3 for silent *var* genes used in this study.** (a) ChIP-seq data showing enrichment and colocalization of PfHP1 (red) and H3K9me3 (blue) at the locus of *var2CSA*. (b) PfHP1 (red) and H3K9me3 (blue) enrichment at *var PF3D7\_0412700* locus. In all cases, coverage plots are represented as average of 1000 bp/bin. The position on the genome sequence is indicated at the top.

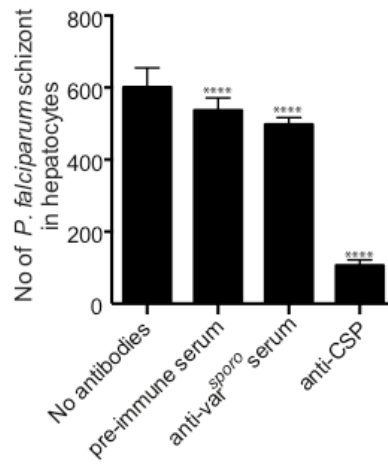


Figure S4

#### Supplementary Fig. 4

**Sporozoite invasion inhibition assay in primary human hepatocytes.** Columns in the graph show the mean of intracellular parasites of three independent biological experiments. Error bars in graph indicate standard deviation. p-value < 0.0001.

**Table1: PfHP1 enrichment in clonally variant gene families**

<b>Name</b>	<b>PfHP1 Enriched</b>	<b>PfHP1 devoid Gene ID</b>	<b>Comments</b>
<i>var</i>	59/60	<i>PF3D7_0809100</i>	Cytoadherence, immune escape, IE surface
<i>rifin</i>	176/178	<i>PF3D7_1219200</i> <i>PF3D7_1240700</i>	IE surface
<i>stevor</i>	42/42	-	IE surface
<i>PfMC-2TM</i>	12/13	<i>PF3D7_0101300</i>	IE surface
<i>PfACS</i>	8/13	<i>PF3D7_0215000</i> <i>PF3D7_0215300</i> <i>PF3D7_0619500</i> <i>PF3D7_1238800</i> <i>PF3D7_0525100</i>	Metabolic proteins
<i>clag</i>			Rhoptry proteins, new IE permeation pathway
<i>clag3.1/ clag3.2</i>	2/2	-	
<i>clag2/clag8/clag9</i>	3/3	-	

IE, infected erythrocyte



# **DISCUSSION**



Epigenetics controls key processes during cellular development in model and non-model organisms. In the case of *P. falciparum*, the study of epigenetic modes of gene regulation came to the forefront only in 2005, with the identification of histone deacetylases as potential regulators of mutually exclusive expression of clonally variant virulence gene families. Since then, the list of processes that are under epigenetic control has expanded rapidly to include the regulation of sexual commitment and the maintenance of hypnozoite dormancy (Dembélé et al., 2014). Simultaneously, epigenetic regulators are being developed as drug targets. We anticipate that shedding light on the role of epigenetics in other stages of the *Plasmodium spp.* life cycle will provide further evidence to develop inhibitors of epigenetic factors as potential antimalarials. Therefore, the main objective of my work was to elucidate the role of epigenetic factors in regulating select biological processes of *P. falciparum* sporozoites that so far has never been investigated.

## **1. Genome-wide ChIP-seq analysis of *P. falciparum* sporozoites**

Chromatin immunoprecipitation (ChIP) studies have previously been used to study the functional role of histone marks, variant histones, and other chromatin factors in gene expression in the human malaria parasite, *P. falciparum* (Lopez-Rubio et al., 2013). To perform the first genome-wide ChIP analysis of *P. falciparum* sporozoites, we needed to develop a robust and reliable ChIP protocol for biological material that is very limited due to the low number of cells that can be recovered from infected mosquito salivary glands. To overcome this challenge, we optimized the ChIP protocol for  $5-8 \times 10^5$  sporozoites in contrast to the standard protocol that uses about  $10^9$  ring stage parasites. Further improvement of this protocol will allow us to adapt ChIP analysis to oocyst or liver stage forms of *Plasmodium*.

## 1.1 *P. falciparum* sporozoites epigenome

The epigenome study of *P. falciparum* sporozoites revealed a number of unexpected results. Given that asexual blood stages establish a chronic infection implicating particular epigenetic mechanisms, it was somewhat unexpected to observe that the distribution of these epigenetic factors is maintained in sporozoites. This includes the major repressive islands H3K9me3/PfHP1 at chromosome ends and some internal chromosome regions (4, 6, 7, 8 and 12). On the other hand the activating histone H3K9ac mark is spread in regions considered as euchromatin. Our FISH studies revealed in addition that these heterochromatin regions form few foci or clusters that are observed at the nuclear periphery, similar to asexual blood stage PERCs. Clearly, the sporozoite epigenetic repression pathway is similar to the one observed in asexual stages in which facultative heterochromatin-based variegated gene silencing acts as the major regulatory mechanism. In the asexual blood stage of *P. falciparum*, PfHP1/H3K9me3 occupancy includes not only clonally variant gene families, but also the majority of *P. falciparum* lineage-specific gene families coding for exported proteins involved in host–parasite interactions. Notably, a subset of genes marked by PfHP1/H3K9me3 code for proteins exported into the host erythrocyte to participate in the processes of host cell remodeling, immune evasion and cytoadherence.

In sporozoites, we noticed an important expansion of facultative heterochromatin within subtelomeric regions of all 14 chromosomes but not within central PfHP1 islands. This redistribution of the heterochromatin landscape correlates with a putative “repression” of almost all the erythrocyte exported proteins that are expressed in IDC (described in Article 4, Figure 2b and S1). Heterochromatin spreading has been observed in humans, where the heterochromatin domains expand to cover developmentally regulated genes during stem cell differentiation, for instance, in turn resulting in large changes to the chromatin landscape (Hawkins et al., 2010). The spreading of heterochromatin into neighborhood regions is mediated by a network of interaction among chromatin proteins and is tightly controlled to maintain stable gene expression patterns.

In the fission yeast *Schizosaccharomyces pombe*, heterochromatin nucleation occurs in the nucleosomal region next to telomeric repeats (Kanoh et al., 2005). In this model, the telomere length regulator Taz1, located in the telomeric and distal portion of TAS, induces the methylation of H3K9me3 by a *S. pombe* HKMT that then recruits the homolog of HP1 (swi6) to form heterochromatin. The same mechanism may be exploited by *P. falciparum* to assemble and spread heterochromatin, establishing stage-specific transcriptional programs

during parasite development. Nevertheless, even in yeast, the mechanism of heterochromatin spreading is not as well understood as the establishment and maintenance of heterochromatin. Similarly, in *P. falciparum*, the *cis*- and *trans*-acting factors involved in the formation of new heterochromatin boundaries are unknown. Fine mapping of these regions may help to identify conserved sequence elements that recruit the enzymatic machinery that sets up heterochromatin and establishes boundaries.

## 1.2 Clonally variant gene regulation

PfHP1 occupation is predictive of the expression of clonally variant gene families in blood stage parasites (Flueck et al., 2009b; Pérez-Toledo et al., 2009). Since epigenetic regulation of the *var* gene family remains unexplored in *P. falciparum* sporozoites, we investigated the distribution of heterochromatin marks for each individual *var* gene member. Surprisingly, in three independent biological replicates of *P. falciparum* sporozoites, we found that the same member of the *var* gene family (PF3D7\_0809100, *var*<sup>sporo</sup>) shows low PfHP1/H3K9me3 occupancy (described in Article 4, Figure 4a). Given this unexpected result, we further investigated the transcription level of *var*<sup>sporo</sup>. Preliminary RNA-seq analysis indicated that the corresponding *var*<sup>sporo</sup> mRNA is not present in mature sporozoites. However, it is possible that the mRNA is transcribed only in early mosquito stages (oocyst or midgut sporozoites) and that *var*<sup>sporo</sup> is maintained in a poised state in mature salivary gland sporozoites, as is observed for the active *var* gene in mature blood stages (see Section 5 of Introduction for more details). Similar to asexual blood stage parasites, where the transcription and protein expression of the *var* gene almost show no overlap (Taylor et al., 2000), the *var*<sup>sporo</sup> PfEMP1 protein is made at a later point than the mRNA and hence detectable in mature sporozoites (described in Article 4, Figure 4b).

We further analysed if the *var*<sup>sporo</sup> is “carried over” by the asexual blood stage parasites that were used for transmission. Analysis of the bulk ring stage culture used to infect mosquitoes revealed several highly transcribed *var* genes but *var*<sup>sporo</sup> mRNA was detected only at very low level, suggesting strongly that *var* genes are reset during sexual stage development. Where this reset takes place remains unknown. Recent studies suggest that *P. falciparum* resets its *var* gene expression during mosquito passage (Bachmann et al., 2016) and our findings support this hypothesis. Step-wise analysis of the epigenome including RNA-seq analysis of the various mosquito stages may allow us to detect when a specific *var*

gene is activated again.

### 1.3 ApiAP2-G regulation in sporozoites

Members of the AP2 DNA-binding protein family such as AP2-O (Ookinete), Api2-Sp (Sporozoites) and AP2-L (Liver stage) identified in *P. berghei*, have been shown to contribute to tight stage-specific gene regulation (Iwanaga et al., 2012; Yuda et al., 2010, 2009). The ApiAP2-G a conserved master regulator of sexual commitment in *P. falciparum* and *P. berghei* (Kafsack et al., 2014; Sinha et al., 2014), is a member of this group of transcription factors in malaria parasites (Balaji et al., 2005). Importantly, it is the only member in asexual blood stage that is silenced via heterochromatin (PfHP1/H3K9me3) (J.-J. Lopez-Rubio et al., 2009). Surprisingly, in *P. falciparum* sporozoites, ApiAP2-G displays characteristics of epigenetically silenced heterochromatin. This is an exciting observation that raises the question: if variegated activation of AP2-G occurs in sporozoites, could this act as the switch to the developmental program needed for liver stage differentiation.

## 2 *var*<sup>sporo</sup> expression in *P. falciparum* sporozoites

By immunofluorescence assays (IFA), we observe *var*<sup>sporo</sup> PfEMP1 on the surface of *P. falciparum* sporozoites. Moreover IFA in living sporozoites for *var*<sup>sporo</sup> PfEMP1 exhibited a punctuate pattern similar to the PfEMP1 staining observed in iRBCs (Contreras et al., 1988). Importantly, virtually all sporozoites were stained with the specific anti-*var*<sup>sporo</sup> PfEMP1 antibodies indicating that they express homogeneously the same *var* member. The presence of a highly polymorphic clonally variant PfEMP1 with cytoadherent and immunogenic properties on the sporozoite surface (Smith et al., 1995), points to a specific function of this adhesion molecule in the vector and/or in the human host.

Earlier proteomic studies of *P. falciparum* NF54 sporozoites, observed some peptides derived from PfEMP1 proteins (Florens et al., 2002; Lasonder et al., 2008). However, these studies did not provide any evidence for expression of the PfEMP1 protein at the surface of sporozoites; ours is the first study to do so. In addition, we found two members of the *rifin* gene family devoid of the PfHP1 repressive marks. However, in the absence of specific antibodies, their expression could not be tested. In another study the expression of STEVOR proteins in sporozoites was observed by IFA (McRobert et al., 2004) although the transcript for *stevor* could not be detected in sporozoite mRNA. Taken together, sporozoites may express several distinct clonally variant proteins on their surface, which may play a role in immune evasion, and host-parasite interaction.

### 2.1 Adhesive properties of sporozoites and PfEMP1

Bioinformatic analysis suggests that CD36 is the cognate receptor for *var*<sup>sporo</sup> PfEMP1 (Lavstsen et al., 2003). This is based on the presence of various CIDR domains in the protein sequence of *var*<sup>sporo</sup> PfEMP1. Considering that CD36 has ubiquitous distribution in host cells, the migratory sporozoites could depend on this receptor during their journey in the mammalian host (Douglas et al., 2015; Mota and Rodriguez, 2004). For instance, CD36-*var*<sup>sporo</sup> PfEMP1 interaction may start in the skin: human skin and dermal microvascular endothelial cells (HDMEC) revealed cell surface expression of CD36 (Swerlick et al., 1992). *var*<sup>sporo</sup> PfEMP1 can interact with the CD36 expressed by HDMEC leading the sporozoites to reach the blood stream. Moreover sporozoites can cross the liver sinusoidal barrier through endothelial cells and/or Kupffer cells using the same proposed *var*<sup>sporo</sup>-CD36 interaction.

Sporozoites are injected from the mosquito proboscis into the skin, then they invade blood vessels to make their way to the liver (Ménard et al., 2013). So far, sporozoite migration and infection of hepatocytes has been correlated to the concerted activity of the gliding actin-myosin motor located beneath the parasite's plasma membrane (Dowse and Soldati, 2004; Kappe et al., 2004) and the released products of secretory organelles (i.e. rhoptries, dense granules and micronemes) (Carruthers and Sibley, 1997). Knockout studies of a membrane component linked to the gliding machinery (thrombospondin related anonymous protein (TRAP) and other TRAP-Like Proteins (TLP)) (Sultan et al., 1997) and incubation with antibodies against CSP (Vanderberg et al., 1969) inhibited cell traversal and subsequent hepatocyte infection (Mishra et al., 2012). Despite these observations, what determines the tropism for the liver remains still unknown. Given that hepatocytes express CD36 on their surface (Greenwalt et al., 1992), and our observations of the expression of an adhesin protein on the sporozoite surface, this may open new avenues to understand parasite homing to the liver. Such studies could also provide an explanation for the controversial role of CSP in sporozoite arrest in the liver (Ménard et al., 2013).

Alternately, depending on the time point at which *var<sup>sporo</sup>* PFEMP1 protein is made in the mosquito vector, it may also play a role in the complex journey of the sporozoites, from the mosquito midgut, crossing different membranes to finally reach the salivary glands. The sporozoites most likely recognize the salivary glands via receptor-ligand interactions and traverse the basal lamina in a transient parasitophorous vacuole that disintegrates during invasion (Rodriguez and Hernández-Hernández, 2004). For maturation in the salivary glands, sporozoites invade the apical membrane of the host epithelial cell, resulting in the release of sporozoites into the gland's central secretory cavity. Once released into the central secretory cavity, free sporozoites associate with each other to form bundles: the mechanism of this aggregation is still unknown (Pimenta et al., 1994). These bundles could result from a PfEMP1-mediated rosetting-like mechanism.

To confirm several of these hypotheses, the function and stage-specific expression of *var<sup>sporo</sup>* PFEMP1 needs to be elucidated. Moreover, a *var<sup>sporo</sup>* knock-out parasite line could shed light on how PfEMP1 impacts sporozoite homing to the liver or migration within mosquitoes. *var<sup>sporo</sup>* knock-out could also reveal if switching to another member of *var* gene can functionally replace *var<sup>sporo</sup>* PFEMP1.

## 2.2 Immunogenic properties

PfEMP1 proteins, beyond their variable cytoadherent characteristics, are immunodominant targets of humoral immunity (Almelli et al., 2014; Portugal et al., 2013; Smith et al., 1995). This protein family is highly polymorphic and switching amongst the different members can fool the immune system that is trying to control malaria infection. In this context, it is important to note that experimental exposure to sporozoites is immune-protective only when individuals are challenged with homologous sporozoites. If *var*<sup>sporo</sup> PfEMP1 (and potentially other PfEMP1 proteins) is part of the protective immune response against sporozoites, it might explain why a heterologous sporozoite challenge protects less than a homologous challenge. It may also explain at a molecular level the difficulty to protect against heterologous challenges in the field, where patients are exposed to a large diversity of *var* genes/PfEMP1 proteins, which change drastically between clinical isolates.

## 3. PfEMP1 protein expression in *P. falciparum* liver stage

Preliminary analysis of PfEMP1 expression in *P. falciparum* liver stage schizonts, using anti-ATS antibodies showed high expression of PfEMP1 proteins (data not shown) with similar localization at the citomere membrane (see Figure 10 in Section 2, Introduction). Indeed, it has been speculated that the merozoite membrane may contain *Plasmodium*-derived adhesion molecules that may bind to the microvascular endothelium. Considering that the pulmonary endothelium expresses CD36, it would explain the high efficiency of merozoite clearance from the blood in the lungs. Furthermore, for the merozoites, the lungs represent the first capillary bed encountered after the liver (Frevort et al., 2014). The significance of *var* gene expression and PfEMP1 production in hepatocytes may have a different, and significant, biological role that needs to be confirmed by more in depth studies.



## CONCLUSION & PERSPECTIVES

This thesis project aimed to unravel the epigenetic regulation in *P. falciparum* pre-erythrocytic stages. This work provides several important advances in sporozoite biology. It shows the first molecular insight into the epigenetic landscape of *P. falciparum* sporozoites stage, which reveals unexpected new biological features that are also relevant for vaccine development using attenuated sporozoites. The major findings can be summarized as follows: We developed a sensitive method that allows working with small parasite samples to obtain reliable genome-wide ChIP data for repressive heterochromatin and active chromatin marks. We discovered an unprecedented mechanism of silencing of genes and multigene families in *Plasmodium* sporozoites. Several hundreds of genes coding for exported blood stage proteins are silenced in sporozoites via heterochromatin formation. The observed repression is based on the expansion of facultative heterochromatin boundaries in sporozoites. Furthermore, we demonstrated that the major repressive pathway H3K9me3/PfHP1 predicts the expression of a specific member of the *var* gene family. The PfEMP1 protein encoded from the selected *var* is expressed at the surface of sporozoites. This points to a specific function of this adhesion molecule during the migration process in mosquitoes and human or the infection process in human hepatocytes.

We provide here the first molecular evidence showing that highly variant genes are expressed on the surface of sporozoites. The expression of a highly polymorphic and strain-specific antigen on the surface of sporozoites may have major implications for vaccine development, supporting the strain-specific components role in the protective immune response against sporozoites. Moreover, this work now highlights new concepts and molecular targets to explore old and new questions surrounding sporozoite biology. Given that *var* genes are not essential in blood stage development during *in vitro* culture, knockout of *var*<sup>sporo</sup> could reveal novel functions of PfEMP1 outside the known immune evasion pathway.

Taken together with our work with humanized mouse models of malaria and the characterization of other epigenetic regulators, i.e., enzymatic machinery involved in the establishing of epigenetic marks, we are now well-positioned to answer several important questions about gene regulation in a variety of parasite life cycle stages and develop new strategies to target these pathways for drug development.



## BIBLIOGRAPHY

- Almelli, T., Ndam, N.T., Ezimegnon, S., Alao, M.J., Ahouansou, C., Sagbo, G., Amoussou, A., Deloron, P., Tahar, R., 2014. Cytoadherence phenotype of *Plasmodium falciparum*-infected erythrocytes is associated with specific pfemp-1 expression in parasites from children with cerebral malaria. *Malar. J.* 13. doi:10.1186/1475-2875-13-333
- Amino, R., Thiberge, S., Martin, B., Celli, S., Shorte, S., Frischknecht, F., Ménard, R., 2006. Quantitative imaging of *Plasmodium* transmission from mosquito to mammal. *Nat. Med.* 12, 220–224. doi:10.1038/nm1350
- Amit-Avraham, I., Pozner, G., Eshar, S., Fastman, Y., Kolevzon, N., Yavin, E., Dzikowski, R., 2015. Antisense long noncoding RNAs regulate var gene activation in the malaria parasite *Plasmodium falciparum*. *Proc. Natl. Acad. Sci. U. S. A.* 112, E982-991. doi:10.1073/pnas.1420855112
- Andrews, K.T., Tran, T.N., Fairlie, D.P., 2012. Towards histone deacetylase inhibitors as new antimalarial drugs. *Curr. Pharm. Des.* 18, 3467–3479.
- Andrews, K.T., Tran, T.N., Lucke, A.J., Kahnberg, P., Le, G.T., Boyle, G.M., Gardiner, D.L., Skinner-Adams, T.S., Fairlie, D.P., 2008. Potent Antimalarial Activity of Histone Deacetylase Inhibitor Analogues. *Antimicrob. Agents Chemother.* 52, 1454–1461. doi:10.1128/AAC.00757-07
- Annoura, T., Ploemen, I.H.J., van Schaijk, B.C.L., Sajid, M., Vos, M.W., van Gemert, G.-J., Chevalley-Maurel, S., Franke-Fayard, B.M.D., Hermsen, C.C., Gego, A., Franetich, J.-F., Mazier, D., Hoffman, S.L., Janse, C.J., Sauerwein, R.W., Khan, S.M., 2012. Assessing the adequacy of attenuation of genetically modified malaria parasite vaccine candidates. *Vaccine* 30, 2662–2670. doi:10.1016/j.vaccine.2012.02.010
- Ashley, E.A., Dhorda, M., Fairhurst, R.M., Amaratunga, C., Lim, P., Suon, S., Sreng, S., Anderson, J.M., Mao, S., Sam, B., Sopha, C., Chuor, C.M., Nguon, C., Sovannaroth, S., Pukrittayakamee, S., Jittamala, P., Chotivanich, K., Chutasmit, K., Suchatsoonthorn, C., Runcharoen, R., Hien, T.T., Thuy-Nhien, N.T., Thanh, N.V., Phu, N.H., Htut, Y., Han, K.-T., Aye, K.H., Mokuolu, O.A., Olaosebikan, R.R., Folaranmi, O.O., Mayxay, M., Khanthavong, M., Hongvanthong, B., Newton, P.N., Onyamboko, M.A., Fanello, C.I., Tshefu, A.K., Mishra, N., Valecha, N., Phyo, A.P., Nosten, F., Yi, P., Tripura, R., Borrmann, S., Bashraheil, M., Peshu, J., Faiz, M.A., Ghose, A., Hossain, M.A., Samad, R., Rahman, M.R., Hasan, M.M., Islam, A., Miotto, O., Amato, R., MacInnis, B., Stalker, J., Kwiatkowski, D.P., Bozdech, Z., Jeeyapant, A., Cheah, P.Y., Sakulthaew, T., Chalk, J., Intharabut, B., Silamut, K., Lee, S.J., Vihokhern, B., Kunasol, C., Imwong, M., Tarning, J., Taylor, W.J., Yeung, S., Woodrow, C.J., Flegg, J.A., Das, D., Smith, J., Venkatesan, M., Plowe, C.V., Stepniewska, K., Guerin, P.J., Dondorp, A.M., Day, N.P., White, N.J., 2014. Spread of Artemisinin Resistance in *Plasmodium falciparum* Malaria. *N. Engl. J. Med.* 371, 411–423. doi:10.1056/NEJMoa1314981
- Bachmann, A., Petter, M., Krumkamp, R., Esen, M., Held, J., Scholz, J.A.M., Li, T., Sim, B.K.L., Hoffman, S.L., Kremsner, P.G., Mordmüller, B., Duffy, M.F., Tannich, E., 2016. Mosquito Passage Dramatically Changes var Gene Expression in Controlled Human *Plasmodium falciparum* Infections. *PLoS Pathog.* 12. doi:10.1371/journal.ppat.1005538

- Baer, K., Klotz, C., Kappe, S.H.I., Schnieder, T., Frevort, U., 2007. Release of Hepatic *Plasmodium yoelii* Merozoites into the Pulmonary Microvasculature. *PLoS Pathog.* 3. doi:10.1371/journal.ppat.0030171
- Balaji, S., Babu, M.M., Iyer, L.M., Aravind, L., 2005. Discovery of the principal specific transcription factors of Apicomplexa and their implication for the evolution of the AP2-integrase DNA binding domains. *Nucleic Acids Res.* 33, 3994–4006. doi:10.1093/nar/gki709
- Baldacci, P., Ménard, R., 2004. The elusive malaria sporozoite in the mammalian host. *Mol. Microbiol.* 54, 298–306. doi:10.1111/j.1365-2958.2004.04275.x
- Balu, B., Maher, S.P., Pance, A., Chauhan, C., Naumov, A.V., Andrews, R.M., Ellis, P.D., Khan, S.M., Lin, J.-W., Janse, C.J., Rayner, J.C., Adams, J.H., 2011. CCR4-associated factor 1 coordinates the expression of *Plasmodium falciparum* egress and invasion proteins. *Eukaryot. Cell* 10, 1257–1263. doi:10.1128/EC.05099-11
- Bannister, A.J., Kouzarides, T., 2011. Regulation of chromatin by histone modifications. *Cell Res.* 21, 381–395. doi:10.1038/cr.2011.22
- Barragan, A., Brossier, F., Sibley, L.D., 2005. Transepithelial migration of *Toxoplasma gondii* involves an interaction of intercellular adhesion molecule 1 (ICAM-1) with the parasite adhesin MIC2. *Cell. Microbiol.* 7, 561–568. doi:10.1111/j.1462-5822.2005.00486.x
- Barry, A.E., Arnott, A., 2014. Strategies for designing and monitoring malaria vaccines targeting diverse antigens. *Microb. Immunol.* 5, 359. doi:10.3389/fimmu.2014.00359
- Baruch, D.I., Gormely, J.A., Ma, C., Howard, R.J., Pasloske, B.L., 1996. *Plasmodium falciparum* erythrocyte membrane protein 1 is a parasitized erythrocyte receptor for adherence to CD36, thrombospondin, and intercellular adhesion molecule 1. *Proc. Natl. Acad. Sci. U. S. A.* 93, 3497–3502.
- Baruch, D.I., Ma, X.C., Singh, H.B., Bi, X., Pasloske, B.L., Howard, R.J., 1997. Identification of a region of PfEMP1 that mediates adherence of *Plasmodium falciparum* infected erythrocytes to CD36: conserved function with variant sequence. *Blood* 90, 3766–3775.
- Baruch, D.I., Pasloske, B.L., Singh, H.B., Bi, X., Ma, X.C., Feldman, M., Taraschi, T.F., Howard, R.J., 1995. Cloning the *P. falciparum* gene encoding PfEMP1, a malarial variant antigen and adherence receptor on the surface of parasitized human erythrocytes. *Cell* 82, 77–87. doi:10.1016/0092-8674(95)90054-3
- Baum, J., Papenfuss, A.T., Mair, G.R., Janse, C.J., Vlachou, D., Waters, A.P., Cowman, A.F., Crabb, B.S., de Koning-Ward, T.F., 2009. Molecular genetics and comparative genomics reveal RNAi is not functional in malaria parasites. *Nucleic Acids Res.* 37, 3788–3798. doi:10.1093/nar/gkp239
- Baum, J., Richard, D., Healer, J., Rug, M., Krnajski, Z., Gilberger, T.-W., Green, J.L., Holder, A.A., Cowman, A.F., 2006. A conserved molecular motor drives cell invasion and gliding motility across malaria life cycle stages and other apicomplexan parasites. *J. Biol. Chem.* 281, 5197–5208. doi:10.1074/jbc.M509807200
- Bengtsson, A., Joergensen, L., Rask, T.S., Olsen, R.W., Andersen, M.A., Turner, L., Theander, T.G., Hviid, L., Higgins, M.K., Craig, A., Brown, A., Jensen, A.T.R., 2013. A novel domain cassette identifies *Plasmodium falciparum* PfEMP1 proteins binding ICAM-1 and is a target of cross-reactive, adhesion-inhibitory antibodies. *J. Immunol. Baltim. Md* 1950 190, 240–249. doi:10.4049/jimmunol.1202578
- Besteiro, S., Dubremetz, J.-F., Lebrun, M., 2011. The moving junction of apicomplexan parasites: a key structure for invasion. *Cell. Microbiol.* 13, 797–805. doi:10.1111/j.1462-5822.2011.01597.x

- Billker, O., Lindo, V., Panico, M., Etienne, A.E., Paxton, T., Dell, A., Rogers, M., Sinden, R.E., Morris, H.R., 1998. Identification of xanthurenic acid as the putative inducer of malaria development in the mosquito. *Nature* 392, 289–292. doi:10.1038/32667
- Bougdour, A., Maubon, D., Baldacci, P., Ortet, P., Bastien, O., Bouillon, A., Barale, J.-C., Pelloux, H., Ménard, R., Hakimi, M.-A., 2009. Drug inhibition of HDAC3 and epigenetic control of differentiation in Apicomplexa parasites. *J. Exp. Med.* 206, 953–966. doi:10.1084/jem.20082826
- Bozdech, Z., Llin??s, M., Pulliam, B.L., Wong, E.D., Zhu, J., DeRisi, J.L., 2003. The transcriptome of the intraerythrocytic developmental cycle of *Plasmodium falciparum*. *PLoS Biol.* 1, 85–100. doi:10.1371/journal.pbio.0000005
- Brancucci, N.M.B., Bertschi, N.L., Zhu, L., Niederwieser, I., Chin, W.H., Wampfler, R., Freymond, C., Rottmann, M., Felger, I., Bozdech, Z., Voss, T.S., 2014. Heterochromatin Protein 1 Secures Survival and Transmission of Malaria Parasites. *Cell Host Microbe* 16, 165–176. doi:10.1016/j.chom.2014.07.004
- Bull, P.C., Abdi, A.I., 2016. The role of PfEMP1 as targets of naturally acquired immunity to childhood malaria: prospects for a vaccine. *Parasitology* 143, 171–186. doi:10.1017/S0031182015001274
- Bunnik, E.M., Le Roch, K.G., 2015. PfAlba1: master regulator of translation in the malaria parasite. *Genome Biol.* 16, 221. doi:10.1186/s13059-015-0795-x
- Carlson, J., Helmbj, H., Hill, A.V., Brewster, D., Greenwood, B.M., Wahlgren, M., 1990. Human cerebral malaria: association with erythrocyte rosetting and lack of anti-rosetting antibodies. *Lancet Lond. Engl.* 336, 1457–1460.
- Carman, C.V., Springer, T.A., 2004. A transmigratory cup in leukocyte diapedesis both through individual vascular endothelial cells and between them. *J. Cell Biol.* 167, 377–388. doi:10.1083/jcb.200404129
- Carruthers, V.B., Sibley, L.D., 1997. Sequential protein secretion from three distinct organelles of *Toxoplasma gondii* accompanies invasion of human fibroblasts. *Eur. J. Cell Biol.* 73, 114–123.
- Cary, C., Lamont, D., Dalton, J.P., Doerig, C., 1994. *Plasmodium falciparum* chromatin: nucleosomal organisation and histone-like proteins. *Parasitol. Res.* 80, 255–258.
- Chaal, B.K., Gupta, A.P., Wastuwidyaningtyas, B.D., Luah, Y.-H., Bozdech, Z., 2010. Histone Deacetylases Play a Major Role in the Transcriptional Regulation of the *Plasmodium falciparum* Life Cycle. *PLOS Pathog* 6, e1000737. doi:10.1371/journal.ppat.1000737
- Chen, P.B., Ding, S., Zanghì, G., Soulard, V., DiMaggio, P.A., Fuchter, M.J., Mecheri, S., Mazier, D., Scherf, A., Malmquist, N.A., 2016. *Plasmodium falciparum* PfSET7: enzymatic characterization and cellular localization of a novel protein methyltransferase in sporozoite, liver and erythrocytic stage parasites. *Sci. Rep.* 6, 21802. doi:10.1038/srep21802
- Chen, Q., Barragan, A., Fernandez, V., Sundström, A., Schlichtherle, M., Sahlén, A., Carlson, J., Datta, S., Wahlgren, M., 1998. Identification of *Plasmodium falciparum* erythrocyte membrane protein 1 (PfEMP1) as the rosetting ligand of the malaria parasite *P. falciparum*. *J. Exp. Med.* 187, 15–23.
- Chen, Q., Heddini, A., Barragan, A., Fernandez, V., Pearce, S.F., Wahlgren, M., 2000. The semiconserved head structure of *Plasmodium falciparum* erythrocyte membrane protein 1 mediates binding to multiple independent host receptors. *J. Exp. Med.* 192, 1–10.
- Chêne, A., Vembar, S.S., Rivière, L., Lopez-Rubio, J.J., Claes, A., Siegel, T.N., Sakamoto, H., Scheidig-Benatar, C., Hernandez-Rivas, R., Scherf, A., 2012. PfAlbas constitute a

- new eukaryotic DNA/RNA-binding protein family in malaria parasites. *Nucleic Acids Res.* 40, 3066–3077. doi:10.1093/nar/gkr1215
- Chitnis, C.E., Sharma, A., 2008. Targeting the *Plasmodium vivax* Duffy-binding protein. *Trends Parasitol.* 24, 29–34. doi:10.1016/j.pt.2007.10.004
- Chookajorn, T., Dzikowski, R., Frank, M., Li, F., Jiwani, A.Z., Hartl, D.L., Deitsch, K.W., 2007. Epigenetic memory at malaria virulence genes. *Proc. Natl. Acad. Sci. U. S. A.* 104, 899–902. doi:10.1073/pnas.0609084103
- Clyde, D.F., 1990. Immunity to falciparum and vivax malaria induced by irradiated sporozoites: a review of the University of Maryland studies, 1971-75. *Bull. World Health Organ.* 68 Suppl, 9–12.
- Cogswell, F.B., 1992. The hypnozoite and relapse in primate malaria. *Clin. Microbiol. Rev.* 5, 26–35.
- Contreras, C.E., Santiago, J.I., Jensen, J.B., Udeinya, I.J., Bayoumi, R., Kennedy, D.D., Druilhe, P., 1988. RESA-IFA assay in *Plasmodium falciparum* malaria, observations on relationship between serum antibody titers, immunity, and antigenic diversity. *J. Parasitol.* 74, 129–134.
- Cottrell, G., Musset, L., Hubert, V., Le Bras, J., Clain, J., 2014. Emergence of Resistance to Atovaquone-Proguanil in Malaria Parasites: Insights from Computational Modeling and Clinical Case Reports. *Antimicrob. Agents Chemother.* 58, 4504–4514. doi:10.1128/AAC.02550-13
- Counihan, N.A., Kalanon, M., Coppel, R.L., de Koning-Ward, T.F., 2013. *Plasmodium* rhoptry proteins: why order is important. *Trends Parasitol.* 29, 228–236. doi:10.1016/j.pt.2013.03.003
- Cowman, A.F., Crabb, B.S., 2006. Invasion of red blood cells by malaria parasites. *Cell* 124, 755–766. doi:10.1016/j.cell.2006.02.006
- Cui, L., Miao, J., 2010. Chromatin-Mediated Epigenetic Regulation in the Malaria Parasite *Plasmodium falciparum*. *Eukaryot. Cell* 9, 1138–1149. doi:10.1128/EC.00036-10
- Cui, L., Miao, J., Furuya, T., Li, X., Su, X., Cui, L., 2007. PfGCN5-Mediated Histone H3 Acetylation Plays a Key Role in Gene Expression in *Plasmodium falciparum*. *Eukaryot. Cell* 6, 1219–1227. doi:10.1128/EC.00062-07
- Cui, L.L., Fan, Q., Cui, L.L., Miao, J., 2008. Histone lysine methyltransferases and demethylases in *Plasmodium falciparum*. *Int. J. Parasitol.* 38, 1083–1097. doi:10.1016/j.ijpara.2008.01.002
- da Silva, H.B., Caetano, S.S., Monteiro, I., Gómez-Conde, I., Hanson, K., Penha-Gonçalves, C., Olivieri, D.N., Mota, M.M., Marinho, C.R., D’Imperio Lima, M.R., Tadokoro, C.E., 2012. Early skin immunological disturbance after *Plasmodium*-infected mosquito bites. *Cell. Immunol.* 277, 22–32. doi:10.1016/j.cellimm.2012.06.003
- Darkin-Rattray, S.J., Gurnett, A.M., Myers, R.W., Dulski, P.M., Crumley, T.M., Allocco, J.J., Cannova, C., Meinke, P.T., Colletti, S.L., Bednarek, M.A., Singh, S.B., Goetz, M.A., Dombrowski, A.W., Polishook, J.D., Schmatz, D.M., 1996. Apicidin: A novel antiprotozoal agent that inhibits parasite histone deacetylase. *Proc. Natl. Acad. Sci. U. S. A.* 93, 13143–13147.
- Dastidar, E.G., Dayer, G., Holland, Z.M., Dorin-Semblat, D., Claes, A., Chene, A., Sharma, A., Hamelin, R., Moniatte, M., Lopez-Rubio, J.-J., Scherf, A., Doerig, C., 2012. Involvement of *Plasmodium falciparum* protein kinase CK2 in the chromatin assembly pathway. *BMC Biol.* 10, 5. doi:10.1186/1741-7007-10-5
- Demb, L., Franetich, P., Lorthiois, A., Gego, A., Zeeman, A.-M., M Kocken, C.H., Le Grand, R., Dereuddre-Bosquet, N., van Gemert, G.-J., Sauerwein, R., Vaillant, J.-C., Hannoun, L., Fuchter, M.J., Diagana, T.T., Malmquist, N.A., Scherf, A., Snounou, G.,

- Mazier, D., 2014. Persistence and activation of malaria hypnozoites in long-term primary hepatocyte cultures. doi:10.1038/nm.3461
- Dembélé, L., Franetich, J.-F., Lorthiois, A., Gego, A., Zeeman, A.-M., Kocken, C.H.M., Le Grand, R., Dereuddre-Bosquet, N., van Gemert, G.-J., Sauerwein, R., Vaillant, J.-C., Hannoun, L., Fuchter, M.J., Diagana, T.T., Malmquist, N.A., Scherf, A., Snounou, G., Mazier, D., 2014. Persistence and activation of malaria hypnozoites in long-term primary hepatocyte cultures. *Nat. Med.* 20, 307–312. doi:10.1038/nm.3461
- Doerig, C., Rayner, J.C., Scherf, A., Tobin, A.B., 2015a. Post-translational protein modifications in malaria parasites. *Nat. Rev. Microbiol.* 13, 160–172. doi:10.1038/nrmicro3402
- Doerig, C., Rayner, J.C., Scherf, A., Tobin, A.B., 2015b. Post-translational protein modifications in malaria parasites. *Nat. Rev. Microbiol.* 13, 160–172. doi:10.1038/nrmicro3402
- Douglas, A.D., Williams, A.R., Illingworth, J.J., Kamuyu, G., Biswas, S., Goodman, A.L., Wyllie, D.H., Crosnier, C., Miura, K., Wright, G.J., Long, C.A., Osier, F.H., Marsh, K., Turner, A.V., Hill, A.V.S., Draper, S.J., 2011. The Blood-Stage Malaria Antigen PfRH5 is Susceptible to Vaccine-Inducible Cross-Strain Neutralizing Antibody. *Nat. Commun.* 2, 601. doi:10.1038/ncomms1615
- Douglas, R.G., Amino, R., Sinnis, P., Frischknecht, F., 2015. Active migration and passive transport of malaria parasites. *Trends Parasitol.* 31, 357–362. doi:10.1016/j.pt.2015.04.010
- Dowse, T., Soldati, D., 2004. Host cell invasion by the apicomplexans: the significance of microneme protein proteolysis. *Curr. Opin. Microbiol.* 7, 388–396. doi:10.1016/j.mib.2004.06.013
- Drew, D.R., Beeson, J.G., 2015. PfRH5 as a candidate vaccine for *Plasmodium falciparum* malaria. *Trends Parasitol.* 31, 87–88. doi:10.1016/j.pt.2015.02.001
- Dudareva, M., Andrews, L., Gilbert, S.C., Bejon, P., Marsh, K., Mwacharo, J., Kai, O., Nicosia, A., Hill, A.V.S., 2009. Prevalence of serum neutralizing antibodies against chimpanzee adenovirus 63 and human adenovirus 5 in Kenyan Children, in the context of vaccine vector efficacy. *Vaccine* 27, 3501–3504. doi:10.1016/j.vaccine.2009.03.080
- Ewer, K.J., O’Hara, G.A., Duncan, C.J.A., Collins, K.A., Sheehy, S.H., Reyes-Sandoval, A., Goodman, A.L., Edwards, N.J., Elias, S.C., Halstead, F.D., Longley, R.J., Rowland, R., Poulton, I.D., Draper, S.J., Blagborough, A.M., Berrie, E., Moyle, S., Williams, N., Siani, L., Folgori, A., Colloca, S., Sinden, R.E., Lawrie, A.M., Cortese, R., Gilbert, S.C., Nicosia, A., Hill, A.V.S., 2013. Protective CD8+ T-cell immunity to human malaria induced by chimpanzee adenovirus-MVA immunisation. *Nat. Commun.* 4. doi:10.1038/ncomms3836
- Fairhurst, R.M., 2015. Understanding artemisinin-resistant malaria: what a difference a year makes. *Curr. Opin. Infect. Dis.* 28, 417–425. doi:10.1097/QCO.0000000000000199
- Fan, Q., Miao, J., Cui, L., Cui, L., 2009. Characterization of PRMT1 from *Plasmodium falciparum*. *Biochem. J.* 421, 107–118. doi:10.1042/BJ20090185
- Figueiredo, L.M., Pirrit, L.A., Scherf, A., Pirritt, L.A., 2000. Genomic organisation and chromatin structure of *Plasmodium falciparum* chromosome ends. *Mol. Biochem. Parasitol.* 106, 169–174.
- Florens, L., Washburn, M.P., Raine, J.D., Anthony, R.M., Grainger, M., Haynes, J.D., Moch, J.K., Muster, N., Sacci, J.B., Tabb, D.L., Witney, A.A., Wolters, D., Wu, Y., Gardner, M.J., Holder, A.A., Sinden, R.E., Yates, J.R., Carucci, D.J., 2002. A proteomic view of the *Plasmodium falciparum* life cycle. *Nature* 419, 520–526. doi:10.1038/nature01107

- Flueck, C., Bartfai, R., Volz, J., Niederwieser, I., Salcedo-Amaya, A.M., Alako, B.T.F., Ehlgén, F., Ralph, S.A., Cowman, A.F., Bozdech, Z., Stunnenberg, H.G., Voss, T.S., 2009a. Plasmodium falciparum Heterochromatin Protein 1 Marks Genomic Loci Linked to Phenotypic Variation of Exported Virulence Factors. *PLoS Pathog.* 5. doi:10.1371/journal.ppat.1000569
- Flueck, C., Bartfai, R., Volz, J., Niederwieser, I., Salcedo-Amaya, A.M., Alako, B.T.F., Ehlgén, F., Ralph, S.A., Cowman, A.F., Bozdech, Z., Stunnenberg, H.G., Voss, T.S., 2009b. Plasmodium falciparum heterochromatin protein 1 marks genomic loci linked to phenotypic variation of exported virulence factors. *PLoS Pathog.* 5, e1000569. doi:10.1371/journal.ppat.1000569
- Foth, B.J., Zhang, N., Chahal, B.K., Sze, S.K., Preiser, P.R., Bozdech, Z., 2011. Quantitative time-course profiling of parasite and host cell proteins in the human malaria parasite Plasmodium falciparum. *Mol. Cell. Proteomics MCP* 10, M110.006411. doi:10.1074/mcp.M110.006411
- Freitas-Junior, L.H., Hernandez-Rivas, R., Ralph, S.A., Montiel-Condado, D., Ruvalcaba-Salazar, O.K., Rojas-Meza, A.P., Mâncio-Silva, L., Leal-Silvestre, R.J., Gontijo, A.M., Shorte, S., Scherf, A., 2005. Telomeric Heterochromatin Propagation and Histone Acetylation Control Mutually Exclusive Expression of Antigenic Variation Genes in Malaria Parasites. *Cell* 121, 25–36. doi:10.1016/j.cell.2005.01.037
- Frevort, U., 2004. Sneaking in through the back entrance: the biology of malaria liver stages. *Trends Parasitol.* 20, 417–424. doi:10.1016/j.pt.2004.07.007
- Frevort, U., Engelmann, S., Zougbedé, S., Stange, J., Ng, B., Matuschewski, K., Liebes, L., Yee, H., 2005. Intravital Observation of Plasmodium berghei Sporozoite Infection of the Liver. *PLoS Biol.* 3. doi:10.1371/journal.pbio.0030192
- Frevort, U., Nacer, A., Cabrera, M., Movila, A., Leberl, M., 2014. Imaging Plasmodium Immunobiology in Liver, Brain, and Lung. *Parasitol. Int.* 63. doi:10.1016/j.parint.2013.09.013
- Frevort, U., Sinnis, P., Cerami, C., Shreffler, W., Takacs, B., Nussenzweig, V., 1993. Malaria circumsporozoite protein binds to heparan sulfate proteoglycans associated with the surface membrane of hepatocytes. *J. Exp. Med.* 177, 1287–1298.
- Fried, M., Duffy, P.E., 1996. Adherence of Plasmodium falciparum to chondroitin sulfate A in the human placenta. *Science* 272, 1502–1504.
- Frischknecht, F., Baldacci, P., Martin, B., Zimmer, C., Thiberge, S., Olivo-Marin, J.-C., Shorte, S.L., Ménard, R., 2004. Imaging movement of malaria parasites during transmission by Anopheles mosquitoes. *Cell. Microbiol.* 6, 687–694. doi:10.1111/j.1462-5822.2004.00395.x
- García-Martínez, J., Aranda, A., Pérez-Ortín, J.E., 2004. Genomic run-on evaluates transcription rates for all yeast genes and identifies gene regulatory mechanisms. *Mol. Cell* 15, 303–313. doi:10.1016/j.molcel.2004.06.004
- Gardner, M.J., Hall, N., Fung, E., White, O., Berriman, M., Hyman, R.W., Carlton, J.M., Pain, A., Nelson, K.E., Bowman, S., Paulsen, I.T., James, K., Eisen, J.A., Rutherford, K., Salzberg, S.L., Craig, A., Kyes, S., Chan, M.-S., Nene, V., Shallom, S.J., Suh, B., Peterson, J., Angiuoli, S., Pertea, M., Allen, J., Selengut, J., Haft, D., Mather, M.W., Vaidya, A.B., Martin, D.M.A., Fairlamb, A.H., Fraunholz, M.J., Roos, D.S., Ralph, S.A., McFadden, G.I., Cummings, L.M., Subramanian, G.M., Mungall, C., Venter, J.C., Carucci, D.J., Hoffman, S.L., Newbold, C., Davis, R.W., Fraser, C.M., Barrell, B., 2002a. Genome sequence of the human malaria parasite Plasmodium falciparum. *Nature* 419. doi:10.1038/nature01097
- Gardner, M.J., Hall, N., Fung, E., White, O., Berriman, M., Hyman, R.W., Carlton, J.M., Pain, A., Nelson, K.E., Bowman, S., Paulsen, I.T., James, K., Eisen, J.A., Rutherford,

- K., Salzberg, S.L., Craig, A., Kyes, S., Chan, M.-S., Nene, V., Shallom, S.J., Suh, B., Peterson, J., Angiuoli, S., Pertea, M., Allen, J., Selengut, J., Haft, D., Mather, M.W., Vaidya, A.B., Martin, D.M.A., Fairlamb, A.H., Fraunholz, M.J., Roos, D.S., Ralph, S.A., McFadden, G.I., Cummings, L.M., Subramanian, G.M., Mungall, C., Venter, J.C., Carucci, D.J., Hoffman, S.L., Newbold, C., Davis, R.W., Fraser, C.M., Barrell, B., 2002b. Genome sequence of the human malaria parasite *Plasmodium falciparum*. *Nature* 419. doi:10.1038/nature01097
- Garnham, P.C., Bird, R.G., Baker, J.R., 1963. Electron microscope studies of motile stages of malaria parasites. IV. The fine structure of the sporozoites of four species of *Plasmodium*. *Trans. R. Soc. Trop. Med. Hyg.* 57, 27–31.
- Garver, L.S., Dong, Y., Dimopoulos, G., 2009. Caspar Controls Resistance to *Plasmodium falciparum* in Diverse Anopheline Species. *PLoS Pathog.* 5. doi:10.1371/journal.ppat.1000335
- Goel, S., Palmkvist, M., Moll, K., Joannin, N., Lara, P., Akhouri, R.R., Moradi, N., Öjemalm, K., Westman, M., Angeletti, D., Kjellin, H., Lehtiö, J., Blixt, O., Idestrom, L., Gahmberg, C.G., Storry, J.R., Hult, A.K., Olsson, M.L., von Heijne, G., Nilsson, I., Wahlgren, M., 2015. RIFINs are adhesins implicated in severe *Plasmodium falciparum* malaria. *Nat. Med.* 21, 314–317. doi:10.1038/nm.3812
- Gottlieb, P.D., Pierce, S. a, Sims, R.J., Yamagishi, H., Weihe, E.K., Harriss, J. V, Maika, S.D., Kuziel, W. a, King, H.L., Olson, E.N., Nakagawa, O., Srivastava, D., 2002. Bop encodes a muscle-restricted protein containing MYND and SET domains and is essential for cardiac differentiation and morphogenesis. *Nat. Genet.* 31, 25–32. doi:10.1038/ng866
- Graewe, S., Stanway, R.R., Rennenberg, A., Heussler, V.T., 2012. Chronicle of a death foretold: *Plasmodium* liver stage parasites decide on the fate of the host cell. *FEMS Microbiol. Rev.* 36, 111–130. doi:10.1111/j.1574-6976.2011.00297.x
- Greenwalt, D.E., Lipsky, R.H., Ockenhouse, C.F., Ikeda, H., Tandon, N.N., Jamieson, G.A., 1992. Membrane glycoprotein CD36: a review of its roles in adherence, signal transduction, and transfusion medicine. *Blood* 80, 1105–1115.
- Gueirard, P., Tavares, J., Thiberge, S., Bernex, F., Ishino, T., Milon, G., Franke-Fayard, B., Janse, C.J., Ménard, R., Amino, R., 2010. Development of the malaria parasite in the skin of the mammalian host. *Proc. Natl. Acad. Sci. U. S. A.* 107, 18640–18645. doi:10.1073/pnas.1009346107
- Guizetti, J., Barcons-Simon, A., Scherf, A., 2016. Trans-acting GC-rich non-coding RNA at var expression site modulates gene counting in malaria parasite. *Nucleic Acids Res.* gkw664. doi:10.1093/nar/gkw664
- Guizetti, J., Scherf, A., 2013. Silence, activate, poise and switch! Mechanisms of antigenic variation in *Plasmodium falciparum*. *Cell. Microbiol.* doi:10.1111/cmi.12115
- Hafalla, J.C.R., Cockburn, I.A., Zavala, F., 2006. Protective and pathogenic roles of CD8+ T cells during malaria infection. *Parasite Immunol.* 28, 15–24. doi:10.1111/j.1365-3024.2006.00777.x
- Hamamoto, R., Furukawa, Y., Morita, M., Iimura, Y., Silva, F.P., Li, M., Yagyu, R., Nakamura, Y., 2004. SMYD3 encodes a histone methyltransferase involved in the proliferation of cancer cells. *Nat. Cell Biol.* 6, 731–740. doi:10.1038/ncb1151
- Hawkins, R.D., Hon, G.C., Lee, L.K., Ngo, Q., Lister, R., Pelizzola, M., Edsall, L.E., Kuan, S., Luu, Y., Klugman, S., Antosiewicz-Bourget, J., Ye, Z., Espinoza, C., Agarwahl, S., Shen, L., Ruotti, V., Wang, W., Stewart, R., Thomson, J.A., Ecker, J.R., Ren, B., 2010. Distinct Epigenomic Landscapes of Pluripotent and Lineage-Committed Human Cells. *Cell Stem Cell* 6, 479–491. doi:10.1016/j.stem.2010.03.018

- Hemmer, C.J., Holst, F.G.E., Kern, P., Chiwakata, C.B., Dietrich, M., Reisinger, E.C., 2006. Stronger host response per parasitized erythrocyte in *Plasmodium vivax* or *ovale* than in *Plasmodium falciparum* malaria. *Trop. Med. Int. Health* 11, 817–823. doi:10.1111/j.1365-3156.2006.01635.x
- Hernandez-Rivas, R., Pérez-Toledo, K., Herrera Solorio, A.-M., Delgadillo, D.M., Vargas, M., 2010. Telomeric Heterochromatin in *Plasmodium falciparum*. *J. Biomed. Biotechnol.* 2010. doi:10.1155/2010/290501
- Hoffman, S.L., Subramanian, G.M., Collins, F.H., Venter, J.C., 2002. *Plasmodium*, human and *Anopheles* genomics and malaria. *Nature* 415, 702–709. doi:10.1038/415702a
- Holder, A.A., 2009. The carboxy-terminus of merozoite surface protein 1: structure, specific antibodies and immunity to malaria. *Parasitology* 136, 1445–1456. doi:10.1017/S0031182009990515
- Howard, R.J., Barnwell, J.W., Rock, E.P., Neequaye, J., Ofori-Adjei, D., Maloy, W.L., Lyon, J.A., Saul, A., 1988. Two approximately 300 kilodalton *Plasmodium falciparum* proteins at the surface membrane of infected erythrocytes. *Mol. Biochem. Parasitol.* 27, 207–223.
- Huang, B., Deng, C., Yang, T., Xue, L., Wang, Q., Huang, S., Su, X., Liu, Y., Zheng, S., Guan, Y., Xu, Q., Zhou, J., Yuan, J., Bacar, A., Abdallah, K.S., Attoumane, R., Mliva, A.M.S.A., Zhong, Y., Lu, F., Song, J., 2015. Polymorphisms of the artemisinin resistant marker (K13) in *Plasmodium falciparum* parasite populations of Grande Comore Island 10 years after artemisinin combination therapy. *Parasit. Vectors* 8. doi:10.1186/s13071-015-1253-z
- Hviid, L., Jensen, A.T.R., 2015. Chapter Two - PfEMP1 – A Parasite Protein Family of Key Importance in *Plasmodium falciparum* Malaria Immunity and Pathogenesis, in: Stothard, D.R. and J.R. (Ed.), *Advances in Parasitology*. Academic Press, pp. 51–84.
- Ishino, T., Chinzei, Y., Yuda, M., 2005. A *Plasmodium* sporozoite protein with a membrane attack complex domain is required for breaching the liver sinusoidal cell layer prior to hepatocyte infection. *Cell. Microbiol.* 7, 199–208. doi:10.1111/j.1462-5822.2004.00447.x
- Iwanaga, S., Kaneko, I., Kato, T., Yuda, M., 2012. Identification of an AP2-family Protein That Is Critical for Malaria Liver Stage Development. *PLOS ONE* 7, e47557. doi:10.1371/journal.pone.0047557
- Jiang, L., Mu, J., Zhang, Q., Ni, T., Srinivasan, P., Rayavara, K., Yang, W., Turner, L., Lavstsen, T., Theander, T.G., Peng, W., Wei, G., Jing, Q., Wakabayashi, Y., Bansal, A., Luo, Y., Ribeiro, J.M.C., Scherf, A., Aravind, L., Zhu, J., Zhao, K., Miller, L.H., 2013. PfSETvs methylation of histone H3K36 represses virulence genes in *Plasmodium falciparum*. *Nature* 499. doi:10.1038/nature12361
- Jones, D.O., Mattei, M.G., Horsley, D., Cowell, I.G., Singh, P.B., 2001. The gene and pseudogenes of *Cbx3/mHP1 gamma*. *DNA Seq. J. DNA Seq. Mapp.* 12, 147–160.
- Josling, G.A., Petter, M., Oehring, S.C., Gupta, A.P., Dietz, O., Wilson, D.W., Schubert, T., Längst, G., Gilson, P.R., Crabb, B.S., Moes, S., Jenoe, P., Lim, S.W., Brown, G.V., Bozdech, Z., Voss, T.S., Duffy, M.F., 2015. A *Plasmodium Falciparum* Bromodomain Protein Regulates Invasion Gene Expression. *Cell Host Microbe* 17, 741–751. doi:10.1016/j.chom.2015.05.009
- Josling, G.A., Selvarajah, S.A., Petter, M., Duffy, M.F., 2012. The Role of Bromodomain Proteins in Regulating Gene Expression. *Genes* 3, 320–343. doi:10.3390/genes3020320
- Kafsack, B.F.C., Rovira-Graells, N., Clark, T.G., Bancells, C., Crowley, V.M., Campino, S.G., Williams, A.E., Drought, L.G., Kwiatkowski, D.P., Baker, D.A., Cortés, A., Llinás, M., 2014. A transcriptional switch underlies commitment to sexual

- development in human malaria parasites. *Nature* 507, 248–252.  
doi:10.1038/nature12920
- Kaiser, K., Camargo, N., Kappe, S.H.I., 2003. Transformation of Sporozoites into Early Exoerythrocytic Malaria Parasites Does Not Require Host Cells. *J. Exp. Med.* 197, 1045–1050. doi:10.1084/jem.20022100
- Kanoh, J., Sadaie, M., Urano, T., Ishikawa, F., 2005. Telomere Binding Protein Taz1 Establishes Swi6 Heterochromatin Independently of RNAi at Telomeres. *Curr. Biol.* 15, 1808–1819. doi:10.1016/j.cub.2005.09.041
- Kappe, S.H.I., Buscaglia, C.A., Nussenzweig, V., 2004. Plasmodium Sporozoite Molecular Cell Biology. *Annu. Rev. Cell Dev. Biol.* 20, 29–59.  
doi:10.1146/annurev.cellbio.20.011603.150935
- Kariu, T., Ishino, T., Yano, K., Chinzei, Y., Yuda, M., 2006. CelTOS, a novel malarial protein that mediates transmission to mosquito and vertebrate hosts. *Mol. Microbiol.* 59, 1369–1379. doi:10.1111/j.1365-2958.2005.05024.x
- Keeley, A., Soldati, D., 2004. The glideosome: a molecular machine powering motility and host-cell invasion by Apicomplexa. *Trends Cell Biol.* 14, 528–532.  
doi:10.1016/j.tcb.2004.08.002
- Kimani, D., Jagne, Y.J., Cox, M., Kimani, E., Bliss, C.M., Gitau, E., Ogwang, C., Afolabi, M.O., Bowyer, G., Collins, K.A., Edwards, N., Hodgson, S.H., Duncan, C.J.A., Spencer, A.J., Knight, M.G., Drammeh, A., Anagnostou, N.A., Berrie, E., Moyle, S., Gilbert, S.C., Soipei, P., Okebe, J., Colloca, S., Cortese, R., Viebig, N.K., Roberts, R., Lawrie, A.M., Nicosia, A., Imoukhuede, E.B., Bejon, P., Chilengi, R., Bojang, K., Flanagan, K.L., Hill, A.V.S., Urban, B.C., Ewer, K.J., 2014. Translating the Immunogenicity of Prime-boost Immunization With ChAd63 and MVA ME-TRAP From Malaria Naive to Malaria-endemic Populations. *Mol. Ther.* 22, 1992–2003.  
doi:10.1038/mt.2014.109
- Kirchner, S., Power, B.J., Waters, A.P., 2016a. Recent advances in malaria genomics and epigenomics. *Genome Med.* 8. doi:10.1186/s13073-016-0343-7
- Kirchner, S., Power, B.J., Waters, A.P., 2016b. Recent advances in malaria genomics and epigenomics. *Genome Med.* 8. doi:10.1186/s13073-016-0343-7
- Kouzarides, T., 2007. SnapShot: Histone-modifying enzymes. *Cell* 131, 822.  
doi:10.1016/j.cell.2007.11.005
- Kun, J.F., Schmidt-Ott, R.J., Lehman, L.G., Lell, B., Luckner, D., Greve, B., Matousek, P., Kremsner, P.G., 1998. Merozoite surface antigen 1 and 2 genotypes and rosetting of Plasmodium falciparum in severe and mild malaria in Lambaréné, Gabon. *Trans. R. Soc. Trop. Med. Hyg.* 92, 110–114.
- Langreth, S.G., Reese, R.T., Motyl, M.R., Trager, W., 1979. Plasmodium falciparum: loss of knobs on the infected erythrocyte surface after long-term cultivation. *Exp. Parasitol.* 48, 213–219.
- Lasonder, E., Janse, C.J., van Gemert, G.-J., Mair, G.R., Vermunt, A.M.W., Douradinha, B.G., van Noort, V., Huynen, M.A., Luty, A.J.F., Kroeze, H., Khan, S.M., Sauerwein, R.W., Waters, A.P., Mann, M., Stunnenberg, H.G., 2008. Proteomic profiling of Plasmodium sporozoite maturation identifies new proteins essential for parasite development and infectivity. *PLoS Pathog.* 4, e1000195.  
doi:10.1371/journal.ppat.1000195
- Lavstsen, T., Salanti, A., Jensen, A.T., Arnot, D.E., Theander, T.G., 2003. Sub-grouping of Plasmodium falciparum 3D7 var genes based on sequence analysis of coding and non-coding regions. *Malar. J.* 2, 27. doi:10.1186/1475-2875-2-27
- Lavstsen, T., Turner, L., Saguti, F., Magistrado, P., Rask, T.S., Jespersen, J.S., Wang, C.W., Berger, S.S., Baraka, V., Marquard, A.M., Seguin-Orlando, A., Willerslev, E., Gilbert,

- M.T.P., Lusingu, J., Theander, T.G., 2012. Plasmodium falciparum erythrocyte membrane protein 1 domain cassettes 8 and 13 are associated with severe malaria in children. *Proc. Natl. Acad. Sci. U. S. A.* 109, E1791-1800. doi:10.1073/pnas.1120455109
- Le Roch, K.G., Zhou, Y., Blair, P.L., Grainger, M., Moch, J.K., Haynes, J.D., De La Vega, P., Holder, A.A., Batalov, S., Carucci, D.J., Winzeler, E.A., 2003. Discovery of gene function by expression profiling of the malaria parasite life cycle. *Science* 301, 1503–1508. doi:10.1126/science.1087025
- Leech, J.H., Barnwell, J.W., Miller, L.H., Howard, R.J., 1984. Identification of a strain-specific malarial antigen exposed on the surface of Plasmodium falciparum-infected erythrocytes. *J. Exp. Med.* 159, 1567–1575.
- Lopez-Rubio, J.J., Gontijo, A.M., Nunes, M.C., Issar, N., Hernandez Rivas, R., Scherf, A., 2007. 5' Flanking Region of Var Genes Nucleate Histone Modification Patterns Linked To Phenotypic Inheritance of Virulence Traits in Malaria Parasites. *Mol. Microbiol.* 66, 1296–1305. doi:10.1111/j.1365-2958.2007.06009.x
- Lopez-Rubio, J.J., Mancio-Silva, L., Scherf, A., 2009. Genome-wide Analysis of Heterochromatin Associates Clonally Variant Gene Regulation with Perinuclear Repressive Centers in Malaria Parasites. *Cell Host Microbe* 5, 179–190. doi:10.1016/j.chom.2008.12.012
- Lopez-Rubio, J.-J., Mancio-Silva, L., Scherf, A., 2009. Genome-wide Analysis of Heterochromatin Associates Clonally Variant Gene Regulation with Perinuclear Repressive Centers in Malaria Parasites. *Cell Host Microbe* 5, 179–190. doi:10.1016/j.chom.2008.12.012
- Lopez-Rubio, J.-J., Siegel, T.N., Scherf, A., 2013. Genome-wide chromatin immunoprecipitation-sequencing in Plasmodium. *Methods Mol. Biol. Clifton NJ* 923, 321–333. doi:10.1007/978-1-62703-026-7\_23
- Maier, A.G., Cooke, B.M., Cowman, A.F., Tilley, L., 2009. Malaria parasite proteins that remodel the host erythrocyte. *Nat. Rev. Microbiol.* 7, 341–354. doi:10.1038/nrmicro2110
- Malmquist, N.A., Moss, T.A., Mecheri, S., Scherf, A., Fuchter, M.J., 2012. Small-molecule histone methyltransferase inhibitors display rapid antimalarial activity against all blood stage forms in Plasmodium falciparum. *Proc. Natl. Acad. Sci.* 109, 16708–16713. doi:10.1073/pnas.1205414109
- Malmquist, N.A., Sundriyal, S., Caron, J., Chen, P., Witkowski, B., Menard, D., Suwanarusk, R., Renia, L., Nosten, F., Jimenez-Diaz, M.B., Angulo-Barturen, I., Martinez, M.S., Ferrer, S., Sanz, L.M., Gamo, F.J., Wittlin, S., Duffy, S., Avery, V.M., Ruecker, A., Delves, M.J., Sinden, R.E., Fuchter, M.J., Scherf, A., 2015. Histone methyltransferase inhibitors are orally bioavailable, fast-acting molecules with activity against different species causing malaria in humans. *Antimicrob. Agents Chemother.* doi:10.1128/AAC.04419-14
- Matuschewski, K., Nunes, A.C., Nussenzweig, V., Ménard, R., 2002a. Plasmodium sporozoite invasion into insect and mammalian cells is directed by the same dual binding system. *EMBO J.* 21, 1597–1606. doi:10.1093/emboj/21.7.1597
- Matuschewski, K., Ross, J., Brown, S.M., Kaiser, K., Nussenzweig, V., Kappe, S.H.I., 2002b. Infectivity-associated changes in the transcriptional repertoire of the malaria parasite sporozoite stage. *J. Biol. Chem.* 277, 41948–41953. doi:10.1074/jbc.M207315200
- Mazur, P.K., Gozani, O., Sage, J., Reynold, N., 2016. Novel insights into the oncogenic function of the SMYD3 lysine methyltransferase. *Transl. Cancer Res.* 5, 330–333. doi:10.21037/tcr.2016.06.26

- McRobert, L., Preiser, P., Sharp, S., Jarra, W., Kaviratne, M., Taylor, M.C., Renia, L., Sutherland, C.J., 2004. Distinct Trafficking and Localization of STEVOR Proteins in Three Stages of the *Plasmodium falciparum* Life Cycle. *Infect. Immun.* 72, 6597–6602. doi:10.1128/IAI.72.11.6597-6602.2004
- Medana, I.M., Turner, G.D.H., 2006. Human cerebral malaria and the blood–brain barrier. *Int. J. Parasitol., Blood-brain Barrier in Parasitic Disease* 36, 555–568. doi:10.1016/j.ijpara.2006.02.004
- Ménard, R., Tavares, J., Cockburn, I., Markus, M., Zavala, F., Amino, R., 2013. Looking under the skin: the first steps in malarial infection and immunity. *Nat. Rev. Microbiol.* 11, 701–712. doi:10.1038/nrmicro3111
- Merrick, C.J., Duraisingh, M.T., 2007. *Plasmodium falciparum* Sir2: an Unusual Sirtuin with Dual Histone Deacetylase and ADP-Ribosyltransferase Activity. *Eukaryot. Cell* 6, 2081–2091. doi:10.1128/EC.00114-07
- Miao, J., Fan, Q., Cui, L., Li, J., Li, J., Cui, L., 2006. The malaria parasite *Plasmodium falciparum* histones: organization, expression, and acetylation. *Gene* 369, 53–65. doi:10.1016/j.gene.2005.10.022
- Miao, J., Fan, Q., Parker, D., Li, X., Li, J., Cui, L., 2013. Puf mediates translation repression of transmission-blocking vaccine candidates in malaria parasites. *PLoS Pathog.* 9, e1003268. doi:10.1371/journal.ppat.1003268
- Miao, J., Li, J., Fan, Q., Li, X., Li, X., Cui, L., 2010. The Puf-family RNA-binding protein PfPuf2 regulates sexual development and sex differentiation in the malaria parasite *Plasmodium falciparum*. *J. Cell Sci.* 123, 1039–1049. doi:10.1242/jcs.059824
- Miller, L.H., 1969. Distribution of mature trophozoites and schizonts of *Plasmodium falciparum* in the organs of *Aotus trivirgatus*, the night monkey. *Am. J. Trop. Med. Hyg.* 18, 860–865.
- Mishra, S., Nussenzweig, R.S., Nussenzweig, V., 2012. Antibodies to *Plasmodium* circumsporozoite protein (CSP) inhibit sporozoite’s cell traversal activity. *J. Immunol. Methods* 377, 47. doi:10.1016/j.jim.2012.01.009
- Morrisette, N.S., Sibley, L.D., 2002. Cytoskeleton of apicomplexan parasites. *Microbiol. Mol. Biol. Rev. MMBR* 66, 21–38; table of contents.
- Mota, M.M., Rodriguez, A., 2004. Migration through host cells: the first steps of *Plasmodium* sporozoites in the mammalian host. *Cell. Microbiol.* 6, 1113–1118. doi:10.1111/j.1462-5822.2004.00460.x
- Mota, M.M., Rodriguez, A., 2001. Migration through host cells by apicomplexan parasites. *Microbes Infect.* 3, 1123–1128.
- Mueller, A.-K., Camargo, N., Kaiser, K., Andorfer, C., Frevert, U., Matuschewski, K., Kappe, S.H.I., 2005a. *Plasmodium* liver stage developmental arrest by depletion of a protein at the parasite–host interface. *Proc. Natl. Acad. Sci. U. S. A.* 102, 3022–3027. doi:10.1073/pnas.0408442102
- Mueller, A.-K., Labaied, M., Kappe, S.H.I., Matuschewski, K., 2005b. Genetically modified *Plasmodium* parasites as a protective experimental malaria vaccine. *Nature* 433, 164–167. doi:10.1038/nature03188
- Niang, M., Bei, A.K., Madnani, K.G., Pelly, S., Dankwa, S., Kanjee, U., Gunalan, K., Amaladoss, A., Yeo, K.P., Bob, N.S., Malleret, B., Duraisingh, M.T., Preiser, P.R., 2014. STEVOR is a *Plasmodium falciparum* erythrocyte binding protein that mediates merozoite invasion and rosetting. *Cell Host Microbe* 16, 81–93. doi:10.1016/j.chom.2014.06.004
- Nussenzweig, R.S., Vanderberg, J., Most, H., Orton, C., 1967. Protective immunity produced by the injection of x-irradiated sporozoites of *plasmodium berghei*. *Nature* 216, 160–162.

- Offeddu, V., Thathy, V., Marsh, K., Matuschewski, K., 2012. Naturally acquired immune responses against *Plasmodium falciparum* sporozoites and liver infection. *Int. J. Parasitol., Molecular Approaches to Malaria 2012 (MAM 2012)* 42, 535–548. doi:10.1016/j.ijpara.2012.03.011
- Ogwang, C., Afolabi, M., Kimani, D., Jagne, Y.J., Sheehy, S.H., Bliss, C.M., Duncan, C.J.A., Collins, K.A., Garcia Knight, M.A., Kimani, E., Anagnostou, N.A., Berrie, E., Moyle, S., Gilbert, S.C., Spencer, A.J., Soipei, P., Mueller, J., Okebe, J., Colloca, S., Cortese, R., Viebig, N.K., Roberts, R., Gantlett, K., Lawrie, A.M., Nicosia, A., Imoukhuede, E.B., Bejon, P., Urban, B.C., Flanagan, K.L., Ewer, K.J., Chilengi, R., Hill, A.V.S., Bojang, K., 2013. Safety and Immunogenicity of Heterologous Prime-Boost Immunisation with *Plasmodium falciparum* Malaria Candidate Vaccines, ChAd63 ME-TRAP and MVA ME-TRAP, in Healthy Gambian and Kenyan Adults. *PLoS ONE* 8. doi:10.1371/journal.pone.0057726
- Painter, H.J., Campbell, T.L., Llinás, M., 2011. The Apicomplexan AP2 family: Integral factors regulating *Plasmodium* development. *Mol. Biochem. Parasitol.* 176, 1–7. doi:10.1016/j.molbiopara.2010.11.014
- Patel, V., Mazitschek, R., Coleman, B., Nguyen, C., Uргаonkar, S., Cortese, J., Barker, R.H., Greenberg, E., Tang, W., Bradner, J.E., Schreiber, S.L., Duraisingh, M.T., Wirth, D.F., Clardy, J., 2009. Identification and Characterization of Small Molecule Inhibitors of a Class I Histone Deacetylase from *Plasmodium falciparum*. *J. Med. Chem.* 52, 2185–2187. doi:10.1021/jm801654y
- Peccarelli, M., Kebaara, B.W., 2014. Regulation of natural mRNAs by the nonsense-mediated mRNA decay pathway. *Eukaryot. Cell* 13, 1126–1135. doi:10.1128/EC.00090-14
- Peeters, E., Driessen, R.P.C., Werner, F., Dame, R.T., 2015. The interplay between nucleoid organization and transcription in archaeal genomes. *Nat. Rev. Microbiol.* 13, 333–341. doi:10.1038/nrmicro3467
- Pérez-Toledo, K., Rojas-Meza, A.P., Mancio-Silva, L., Hernández-Cuevas, N.A., Delgadillo, D.M., Vargas, M., Martínez-Calvillo, S., Scherf, A., Hernandez-Rivas, R., 2009. *Plasmodium falciparum* heterochromatin protein 1 binds to tri-methylated histone 3 lysine 9 and is linked to mutually exclusive expression of var genes. *Nucleic Acids Res.* 37, 2596–2606. doi:10.1093/nar/gkp115
- Pimenta, P.F., Touray, M., Miller, L., 1994. The Journey of Malaria Sporozoites in the Mosquito Salivary Gland. *J. Eukaryot. Microbiol.* 41, 608–624. doi:10.1111/j.1550-7408.1994.tb01523.x
- Ponnudurai, T., Lensen, A.H., van Gemert, G.J., Bolmer, M.G., Meuwissen, J.H., 1991. Feeding behaviour and sporozoite ejection by infected *Anopheles stephensi*. *Trans. R. Soc. Trop. Med. Hyg.* 85, 175–180.
- Portugal, S., Pierce, S.K., Crompton, P.D., 2013. Young Lives Lost as B Cells Falter: What We Are Learning About Antibody Responses in Malaria. *J. Immunol.* 190, 3039–3046. doi:10.4049/jimmunol.1203067
- Pradel, G., Garapaty, S., Frevet, U., 2002. Proteoglycans mediate malaria sporozoite targeting to the liver. *Mol. Microbiol.* 45, 637–651.
- Prudêncio, M., Mota, M.M., 2007. To Migrate or to Invade: Those Are the Options. *Cell Host Microbe* 2, 286–288. doi:10.1016/j.chom.2007.10.008
- Prusty, D., Mehra, P., Srivastava, S., Shivange, A.V., Gupta, A., Roy, N., Dhar, S.K., 2008. Nicotinamide inhibits *Plasmodium falciparum* Sir2 activity in vitro and parasite growth. *FEMS Microbiol. Lett.* 282, 266–272. doi:10.1111/j.1574-6968.2008.01135.x
- Quakyi, I.A., Carter, R., Rener, J., Kumar, N., Good, M.F., Miller, L.H., 1987. The 230-kDa gamete surface protein of *Plasmodium falciparum* is also a target for transmission-blocking antibodies. *J. Immunol.* 139, 4213–4217.

- Ralph, S.A., Scherf, A., 2005. The epigenetic control of antigenic variation in *Plasmodium falciparum*. *Curr. Opin. Microbiol.* 8, 434–440. doi:10.1016/j.mib.2005.06.007
- Rask, T.S., Hansen, D.A., Theander, T.G., Gorm Pedersen, A., Lavstsen, T., 2010. *Plasmodium falciparum* erythrocyte membrane protein 1 diversity in seven genomes--divide and conquer. *PLoS Comput. Biol.* 6. doi:10.1371/journal.pcbi.1000933
- Remarque, E.J., Faber, B.W., Kocken, C.H.M., Thomas, A.W., 2008. Apical membrane antigen 1: a malaria vaccine candidate in review. *Trends Parasitol.* 24, 74–84. doi:10.1016/j.pt.2007.12.002
- Renner, J., Graves, P.M., Carter, R., Williams, J.L., Burkot, T.R., 1983. Target antigens of transmission-blocking immunity on gametes of *Plasmodium falciparum*. *J. Exp. Med.* 158, 976–981. doi:10.1084/jem.158.3.976
- Rieger, H., Yoshikawa, H.Y., Quadt, K., Nielsen, M.A., Sanchez, C.P., Salanti, A., Tanaka, M., Lanzer, M., 2015. Cytoadhesion of *Plasmodium falciparum*-infected erythrocytes to chondroitin-4-sulfate is cooperative and shear enhanced. *Blood* 125, 383–391. doi:10.1182/blood-2014-03-561019
- Roch, K.G.L., Johnson, J.R., Florens, L., Zhou, Y., Santosyan, A., Grainger, M., Yan, S.F., Williamson, K.C., Holder, A.A., Carucci, D.J., Yates, J.R., Winzeler, E.A., 2004. Global analysis of transcript and protein levels across the *Plasmodium falciparum* life cycle. *Genome Res.* 14, 2308–2318. doi:10.1101/gr.2523904
- Rodriguez, M.H., Hernández-Hernández, F. de la C., 2004. Insect–malaria parasites interactions: the salivary gland. *Insect Biochem. Mol. Biol., Molecular and population biology of mosquitoes* 34, 615–624. doi:10.1016/j.ibmb.2004.03.014
- Roestenberg, M., McCall, M., Hopman, J., Wiersma, J., Luty, A.J.F., van Gemert, G.J., van de Vegte-Bolmer, M., van Schaijk, B., Teelen, K., Arens, T., Spaarman, L., de Mast, Q., Roeffen, W., Snounou, G., Rénia, L., van der Ven, A., Hermsen, C.C., Sauerwein, R., 2009. Protection against a malaria challenge by sporozoite inoculation. *N. Engl. J. Med.* 361, 468–477. doi:10.1056/NEJMoa0805832
- Rosenberg, R., Wirtz, R.A., Schneider, I., Burge, R., 1990. An estimation of the number of malaria sporozoites ejected by a feeding mosquito. *Trans. R. Soc. Trop. Med. Hyg.* 84, 209–212.
- Rowe, A., Obeiro, J., Newbold, C.I., Marsh, K., 1995. *Plasmodium falciparum* rosetting is associated with malaria severity in Kenya. *Infect. Immun.* 63, 2323–2326.
- Rowe, J.A., Moulds, J.M., Newbold, C.I., Miller, L.H., 1997. *P. falciparum* rosetting mediated by a parasite-variant erythrocyte membrane protein and complement-receptor 1. *Nature* 388, 292–295. doi:10.1038/40888
- Salanti, A., Dahlbäck, M., Turner, L., Nielsen, M.A., Barfod, L., Magistrado, P., Jensen, A.T.R., Lavstsen, T., Ofori, M.F., Marsh, K., Hviid, L., Theander, T.G., 2004. Evidence for the involvement of VAR2CSA in pregnancy-associated malaria. *J. Exp. Med.* 200, 1197–1203. doi:10.1084/jem.20041579
- Salanti, A., Staalsoe, T., Lavstsen, T., Jensen, A.T.R., Sowa, M.P.K., Arnot, D.E., Hviid, L., Theander, T.G., 2003. Selective upregulation of a single distinctly structured var gene in chondroitin sulphate A-adhering *Plasmodium falciparum* involved in pregnancy-associated malaria. *Mol. Microbiol.* 49, 179–191.
- Salcedo-Amaya, A.M., van Driel, M.A., Alako, B.T., Trelle, M.B., van den Elzen, A.M.G., Cohen, A.M., Janssen-Megens, E.M., van de Vegte-Bolmer, M., Selzer, R.R., Iniguez, A.L., Green, R.D., Sauerwein, R.W., Jensen, O.N., Stunnenberg, H.G., 2009. Dynamic histone H3 epigenome marking during the intraerythrocytic cycle of *Plasmodium falciparum*. *Proc. Natl. Acad. Sci. U. S. A.* 106, 9655–60. doi:10.1073/pnas.0902515106

- Sannella, A.R., Olivieri, A., Bertuccini, L., Ferrè, F., Severini, C., Pace, T., Alano, P., 2012. Specific tagging of the egress-related osmiophilic bodies in the gametocytes of *Plasmodium falciparum*. *Malar. J.* 11, 88. doi:10.1186/1475-2875-11-88
- Santos, J.M., Lebrun, M., Daher, W., Soldati, D., Dubremetz, J.-F., 2009. Apicomplexan cytoskeleton and motors: key regulators in morphogenesis, cell division, transport and motility. *Int. J. Parasitol.* 39, 153–162. doi:10.1016/j.ijpara.2008.10.007
- Saraf, A., Cervantes, S., Bunnik, E.M., Ponts, N., Sardu, M.E., Chung, D.-W.D., Prudhomme, J., Varberg, J.M., Wen, Z., Washburn, M.P., Florens, L., Le Roch, K.G., 2016a. Dynamic and Combinatorial Landscape of Histone Modifications during the Intraerythrocytic Developmental Cycle of the Malaria Parasite. *J. Proteome Res.* 15, 2787–2801. doi:10.1021/acs.jproteome.6b00366
- Saraf, A., Cervantes, S., Bunnik, E.M., Ponts, N.P., Sardu, M.E., Chung, D.-W.D., Prudhomme, J., Varberg, J., Wen, Z., Washburn, M.P., Florens, L.A., Le Roch, K.G., 2016b. Dynamic and combinatorial landscape of histone modifications during the intra-erythrocytic developmental cycle of the malaria parasite. *J. Proteome Res.* acs.jproteome.6b00366. doi:10.1021/acs.jproteome.6b00366
- Sauerwein, R.W., Bousema, T., 2015. Transmission blocking malaria vaccines: Assays and candidates in clinical development. *Vaccine, Malaria Vaccines 2015* 33, 7476–7482. doi:10.1016/j.vaccine.2015.08.073
- Scherf, A., Figueiredo, L.M., Freitas-Junior, L.H., 2001. *Plasmodium* telomeres: a pathogen's perspective. *Curr. Opin. Microbiol.* 4, 409–414. doi:10.1016/S1369-5274(00)00227-7
- Scherf, A., Lopez-Rubio, J.J., Riviere, L., 2008a. Antigenic variation in *Plasmodium falciparum*. *Annu. Rev. Microbiol.* 62, 445–470. doi:10.1146/annurev.micro.61.080706.093134
- Scherf, A., Rivière, L., Lopez-Rubio, J.J., 2008b. SnapShot: var Gene Expression in the Malaria Parasite. *Cell* 134, 190–190.e1. doi:10.1016/j.cell.2008.06.042
- Seder, R.A., Chang, L.-J., Enama, M.E., Zephir, K.L., Sarwar, U.N., Gordon, I.J., Holman, L.A., James, E.R., Billingsley, P.F., Gunasekera, A., Richman, A., Chakravarty, S., Manoj, A., Velmurugan, S., Li, M., Ruben, A.J., Li, T., Eappen, A.G., Stafford, R.E., Plummer, S.H., Hendel, C.S., Novik, L., Costner, P.J.M., Mendoza, F.H., Saunders, J.G., Nason, M.C., Richardson, J.H., Murphy, J., Davidson, S.A., Richie, T.L., Sedegah, M., Sutamihardja, A., Fahle, G.A., Lyke, K.E., Laurens, M.B., Roederer, M., Tewari, K., Epstein, J.E., Sim, B.K.L., Ledgerwood, J.E., Graham, B.S., Hoffman, S.L., VRC 312 Study Team, 2013. Protection against malaria by intravenous immunization with a nonreplicating sporozoite vaccine. *Science* 341, 1359–1365. doi:10.1126/science.1241800
- Shimp, R.L., Rowe, C., Reiter, K., Chen, B., Nguyen, V., Aebig, J., Rausch, K.M., Kumar, K., Wu, Y., Jin, A.J., Jones, D.S., Narum, D.L., 2013. Development of a Pfs25-EPA malaria transmission blocking vaccine as a chemically conjugated nanoparticle. *Vaccine* 31, 2954–2962. doi:10.1016/j.vaccine.2013.04.034
- Sidjanski, S., Vanderberg, J.P., 1997. Delayed migration of *Plasmodium* sporozoites from the mosquito bite site to the blood. *Am. J. Trop. Med. Hyg.* 57, 426–429.
- Silva, F.P., Hamamoto, R., Kunizaki, M., Tsuge, M., Nakamura, Y., Furukawa, Y., 2008. Enhanced methyltransferase activity of SMYD3 by the cleavage of its N-terminal region in human cancer cells. *Oncogene* 27, 2686–92. doi:10.1038/sj.onc.1210929
- Silvie, O., Semblat, J.P., Franetich, J.F., Hannoun, L., Eling, W., Mazier, D., 2002. Effects of irradiation on *Plasmodium falciparum* sporozoite hepatic development: implications for the design of pre-erythrocytic malaria vaccines. *Parasite Immunol.* 24, 221–223.
- Sinha, A., Hughes, K.R., Modrzynska, K.K., Otto, T.D., Pfander, C., Dickens, N.J., Religa, A.A., Bushell, E., Graham, A.L., Cameron, R., Kafsack, B.F.C., Williams, A.E.,

- Llinás, M., Berriman, M., Billker, O., Waters, A.P., 2014. A cascade of DNA-binding proteins for sexual commitment and development in *Plasmodium*. *Nature* 507, 253–257. doi:10.1038/nature12970
- Smith, J.D., Chitnis, C.E., Craig, A.G., Roberts, D.J., Hudson-Taylor, D.E., Peterson, D.S., Pinches, R., Newbold, C.I., Miller, L.H., 1995. Switches in expression of *Plasmodium falciparum* var genes correlate with changes in antigenic and cytoadherent phenotypes of infected erythrocytes. *Cell* 82, 101–110. doi:10.1016/0092-8674(95)90056-X
- Spring, M., Murphy, J., Nielsen, R., Dowler, M., Bennett, J.W., Zarling, S., Williams, J., de la Vega, P., Ware, L., Komisar, J., Polhemus, M., Richie, T.L., Epstein, J., Tamminga, C., Chuang, I., Richie, N., O’Neil, M., Heppner, D.G., Healer, J., O’Neill, M., Smithers, H., Finney, O.C., Mikolajczak, S.A., Wang, R., Cowman, A., Ockenhouse, C., Krzych, U., Kappe, S.H.I., 2013. First-in-human evaluation of genetically attenuated *Plasmodium falciparum* sporozoites administered by bite of *Anopheles* mosquitoes to adult volunteers. *Vaccine* 31, 4975–4983. doi:10.1016/j.vaccine.2013.08.007
- Strahl, B.D., Allis, C.D., 2000. The language of covalent histone modifications. *Nature* 403, 41–45. doi:10.1038/47412
- Su, X., Heatwole, V.M., Wertheimer, S.P., Guinet, F., Herrfeldt, J.A., Peterson, D.S., Ravetch, J.A., Wellems, T.E., 1995. The large diverse gene family var encodes proteins involved in cytoadherence and antigenic variation of *Plasmodium falciparum*-infected erythrocytes. *Cell* 82, 89–100. doi:10.1016/0092-8674(95)90055-1
- Sultan, A.A., Thathy, V., Frevert, U., Robson, K.J.H., Crisanti, A., Nussenzweig, V., Nussenzweig, R.S., Ménard, R., 1997. TRAP Is Necessary for Gliding Motility and Infectivity of *Plasmodium* Sporozoites. *Cell* 90, 511–522. doi:10.1016/S0092-8674(00)80511-5
- Sundriyal, S., Malmquist, N. a, Caron, J., Blundell, S., Liu, F., Chen, X., Srimongkolpithak, N., Jin, J., Charman, S. a, Scherf, A., Fuchter, M.J., 2014. Development of Diaminoquinazoline Histone Lysine Methyltransferase Inhibitors as Potent Blood-Stage Antimalarial Compounds. *ChemMedChem* 9, 2360–2373. doi:10.1002/cmde.201402098
- Swerlick, R.A., Lee, K.H., Wick, T.M., Lawley, T.J., 1992. Human dermal microvascular endothelial but not human umbilical vein endothelial cells express CD36 in vivo and in vitro. *J. Immunol.* 148, 78–83.
- Takala, S.L., Plowe, C.V., 2009. Genetic diversity and malaria vaccine design, testing, and efficacy: Preventing and overcoming “vaccine resistant malaria.” *Parasite Immunol.* 31, 560–573. doi:10.1111/j.1365-3024.2009.01138.x
- Tamminga, C., Sedegah, M., Maiolatesi, S., Fedders, C., Reyes, S., Reyes, A., Vasquez, C., Alcorta, Y., Chuang, I., Spring, M., Kavanaugh, M., Ganeshan, H., Huang, J., Belmonte, M., Abot, E., Belmonte, A., Banania, J., Farooq, F., Murphy, J., Komisar, J., Richie, N.O., Bennett, J., Limbach, K., Patterson, N.B., Bruder, J.T., Shi, M., Miller, E., Dutta, S., Diggs, C., Soisson, L.A., Hollingdale, M.R., Epstein, J.E., Richie, T.L., 2013. Human adenovirus 5-vectored *Plasmodium falciparum* NMRC-M3V-Ad-PfCA vaccine encoding CSP and AMA1 is safe, well-tolerated and immunogenic but does not protect against controlled human malaria infection. *Hum. Vaccines Immunother.* 9, 2165–2177. doi:10.4161/hv.24941
- Tavares, J., Formaglio, P., Thiberge, S., Mordelet, E., Van Rooijen, N., Medvinsky, A., Ménard, R., Amino, R., 2013. Role of host cell traversal by the malaria sporozoite during liver infection. *J. Exp. Med.* 210, 905–915. doi:10.1084/jem.20121130

- Taylor, H.M., Kyes, S.A., Newbold, C.I., 2000. Var gene diversity in *Plasmodium falciparum* is generated by frequent recombination events. *Mol. Biochem. Parasitol.* 110, 391–397. doi:10.1016/S0166-6851(00)00286-3
- Tonkin, C.J., Carret, C.K., Duraisingh, M.T., Voss, T.S., Ralph, S.A., Hommel, M., Duffy, M.F., Silva, L.M. da, Scherf, A., Ivens, A., Speed, T.P., Beeson, J.G., Cowman, A.F., 2009. Sir2 paralogues cooperate to regulate virulence genes and antigenic variation in *Plasmodium falciparum*. *PLoS Biol.* 7, e84. doi:10.1371/journal.pbio.1000084
- Trelle, M.B., Salcedo-Amaya, A.M., Cohen, A.M., Stunnenberg, H.G., Jensen, O.N., 2009. Global histone analysis by mass spectrometry reveals a high content of acetylated lysine residues in the malaria parasite *Plasmodium falciparum*. *J. Proteome Res.* 8, 3439–50. doi:10.1021/pr9000898
- Treutiger, C.J., Hedlund, I., Helmbj, H., Carlson, J., Jepson, A., Twumasi, P., Kwiatkowski, D., Greenwood, B.M., Wahlgren, M., 1992. Rosette formation in *Plasmodium falciparum* isolates and anti-rosette activity of sera from Gambians with cerebral or uncomplicated malaria. *Am. J. Trop. Med. Hyg.* 46, 503–510.
- Turner, L., Lavstsen, T., Berger, S.S., Wang, C.W., Petersen, J.E.V., Avril, M., Brazier, A.J., Freeth, J., Jespersen, J.S., Nielsen, M.A., Magistrado, P., Lusingu, J., Smith, J.D., Higgins, M.K., Theander, T.G., 2013. Severe malaria is associated with parasite binding to endothelial protein C receptor. *Nature* 498, 502–505. doi:10.1038/nature12216
- van Dijk, M.R., Douradinha, B., Franke-Fayard, B., Heussler, V., van Dooren, M.W., van Schaijk, B., van Gemert, G.-J., Sauerwein, R.W., Mota, M.M., Waters, A.P., Janse, C.J., 2005. Genetically attenuated, P36p-deficient malarial sporozoites induce protective immunity and apoptosis of infected liver cells. *Proc. Natl. Acad. Sci. U. S. A.* 102, 12194–12199. doi:10.1073/pnas.0500925102
- Vanderberg, J., Nussenzweig, R., Most, H., 1969. Protective immunity produced by the injection of x-irradiated sporozoites of *Plasmodium berghei*. V. In vitro effects of immune serum on sporozoites. *Mil. Med.* 134, 1183–1190.
- Vembar, S.S., Droll, D., Scherf, A., 2016. Translational regulation in blood stages of the malaria parasite *Plasmodium* spp.: systems-wide studies pave the way. *Wiley Interdiscip. Rev. RNA* 7, 772–792. doi:10.1002/wrna.1365
- Vembar, S.S., Macpherson, C.R., Sismeiro, O., Coppée, J.-Y., Scherf, A., 2015. The PfAlba1 RNA-binding protein is an important regulator of translational timing in *Plasmodium falciparum* blood stages. *Genome Biol.* 16, 212. doi:10.1186/s13059-015-0771-5
- Vembar, S.S., Scherf, A., Siegel, T.N., 2014. Noncoding RNAs as emerging regulators of *Plasmodium falciparum* virulence gene expression. *Curr. Opin. Microbiol.* 20, 153–161. doi:10.1016/j.mib.2014.06.013
- Vermeulen, A.N., Ponnudurai, T., Beckers, P.J., Verhave, J.P., Smits, M.A., Meuwissen, J.H., 1985. Sequential expression of antigens on sexual stages of *Plasmodium falciparum* accessible to transmission-blocking antibodies in the mosquito. *J. Exp. Med.* 162, 1460–1476.
- Vlachou, D., Schlegelmilch, T., Runn, E., Mendes, A., Kafatos, F.C., 2006. The developmental migration of *Plasmodium* in mosquitoes. *Curr. Opin. Genet. Dev.*, Pattern formation and developmental mechanisms 16, 384–391. doi:10.1016/j.gde.2006.06.012
- Volz, J., Carvalho, T.G., Ralph, S.A., Gilson, P., Thompson, J., Tonkin, C.J., Langer, C., Crabb, B.S., Cowman, A.F., 2010. Potential epigenetic regulatory proteins localise to distinct nuclear sub-compartments in *Plasmodium falciparum*. *Int. J. Parasitol.* doi:10.1016/j.ijpara.2009.09.002

- Volz, J.C., Bártfai, R., Petter, M., Langer, C., Josling, G.A., Tsuboi, T., Schwach, F., Baum, J., Rayner, J.C., Stunnenberg, H.G., Duffy, M.F., Cowman, A.F., 2012. PfSET10, a Plasmodium falciparum Methyltransferase, Maintains the Active var Gene in a Poised State during Parasite Division. *Cell Host Microbe* 11, 7–18. doi:10.1016/j.chom.2011.11.011
- Volz, J.C., Bártfai, R., Petter, M., Langer, C., Josling, G.A., Tsuboi, T., Schwach, F., Baum, J., Rayner, J.C., Stunnenberg, H.G., Duffy, M.F., Cowman, A.F., 2012. PfSET10, a Plasmodium falciparum Methyltransferase, Maintains the Active var Gene in a Poised State during Parasite Division. *Cell Host Microbe*. doi:10.1016/j.chom.2011.11.011
- Wang, Q., Fujioka, H., Nussenzweig, V., 2005. Exit of Plasmodium sporozoites from oocysts is an active process that involves the circumsporozoite protein. *PLoS Pathog.* 1, e9. doi:10.1371/journal.ppat.0010009
- Warren, A., Bertolino, P., Benseler, V., Fraser, R., McCaughan, G.W., Le Couteur, D.G., 2007. Marked changes of the hepatic sinusoid in a transgenic mouse model of acute immune-mediated hepatitis. *J. Hepatol.* 46, 239–246. doi:10.1016/j.jhep.2006.08.022
- Wassmer, S.C., Combes, V., Candal, F.J., Juhan-Vague, I., Grau, G.E., 2006. Platelets Potentiate Brain Endothelial Alterations Induced by Plasmodium falciparum. *Infect. Immun.* 74, 645–653. doi:10.1128/IAI.74.1.645-653.2006
- Wertheimer, S.P., Barnwell, J.W., 1989. Plasmodium vivax interaction with the human Duffy blood group glycoprotein: identification of a parasite receptor-like protein. *Exp. Parasitol.* 69, 340–350.
- WHO, 2015. World Malaria Report 2015. Who.
- Wisse, E., De Zanger, R.B., Charels, K., Van Der Smissen, P., McCuskey, R.S., 1985. The liver sieve: considerations concerning the structure and function of endothelial fenestrae, the sinusoidal wall and the space of Disse. *Hepatol. Baltim. Md* 5, 683–692.
- Yadava, A., Hall, C.E., Sullivan, J.S., Nace, D., Williams, T., Collins, W.E., Ockenhouse, C.F., Barnwell, J.W., 2014. Protective Efficacy of a Plasmodium vivax Circumsporozoite Protein-Based Vaccine in Aotus nancymae Is Associated with Antibodies to the Repeat Region. *PLoS Negl. Trop. Dis.* 8. doi:10.1371/journal.pntd.0003268
- Yamauchi, L.M., Coppi, A., Snounou, G., Sinnis, P., 2007. Plasmodium sporozoites trickle out of the injection site. *Cell. Microbiol.* 9, 1215–1222. doi:10.1111/j.1462-5822.2006.00861.x
- Yayon, A., Vande Waa, J.A., Yayon, M., Geary, T.G., Jensen, J.B., 1983. Stage-dependent effects of chloroquine on Plasmodium falciparum in vitro. *J. Protozool.* 30, 642–647.
- Yuda, M., Iwanaga, S., Shigenobu, S., Kato, T., Kaneko, I., 2010. Transcription factor AP2-Sp and its target genes in malarial sporozoites. *Mol. Microbiol.* 75, 854–863. doi:10.1111/j.1365-2958.2009.07005.x
- Yuda, M., Iwanaga, S., Shigenobu, S., Mair, G.R., Janse, C.J., Waters, A.P., Kato, T., Kaneko, I., 2009. Identification of a transcription factor in the mosquito-invasive stage of malaria parasites. *Mol. Microbiol.* 71, 1402–1414. doi:10.1111/j.1365-2958.2009.06609.x
- Zhang, M., Fennell, C., Ranford-Cartwright, L., Sakthivel, R., Gueirard, P., Meister, S., Caspi, A., Doerig, C., Nussenzweig, R.S., Tuteja, R., Sullivan, W.J., Roos, D.S., Fontoura, B.M.A., Ménard, R., Winzeler, E.A., Nussenzweig, V., 2010. The Plasmodium eukaryotic initiation factor-2alpha kinase IK2 controls the latency of sporozoites in the mosquito salivary glands. *J. Exp. Med.* 207, 1465–1474. doi:10.1084/jem.20091975
- Zhang, Q., Huang, Y., Zhang, Y., Fang, X., Claes, A., Duchateau, M., Namane, A., Lopez-Rubio, J.-J., Pan, W., Scherf, A., 2011. A critical role of perinuclear filamentous actin

in spatial repositioning and mutually exclusive expression of virulence genes in malaria parasites. *Cell Host Microbe* 10, 451–463. doi:10.1016/j.chom.2011.09.013

Zhang, Q., Siegel, T.N., Martins, R.M., Wang, F., Cao, J., Gao, Q., Cheng, X., Jiang, L., Hon, C.-C., Scheidig-Benatar, C., Sakamoto, H., Turner, L., Jensen, A.T.R., Claes, A., Guizetti, J., Malmquist, N.A., Scherf, A., 2014. Exonuclease-mediated degradation of nascent RNA silences genes linked to severe malaria. *Nature* 513, 431–435. doi:10.1038/nature13468

# ANNEXES



## ARTICLE 5

### **In Vitro Analysis of the Interaction between Atovaquone and Proguanil against Liver Stage Malaria Parasites**

Barata, Houzé, Boutbibe, Zanghì, et al, *Antimicrob Agents Chemotherapy*, 2016

Atovaquone-Proguanil is an antimalarial drug combination of used both as prophylaxis, for its action on the liver stage, and as a treatment against the blood stage. It has been shown that Proguanil has a synergic effect on Atovaquone against infected red blood cells, in vitro. . However, the interaction in the malaria liver stage has never been investigated.

Apart from its own antimalarial action, Proguanil has another stronger one when metabolized to Cycloguanil through cytochrome P450. In this study, the interaction between Atovaquone and Proguanil was evaluated through a fixed-ratio isobologram method, in both primary human hepatocytes and HepG2-CD81. These latter lack cytochrome P450 and, consequently, are unable to metabolize Proguanil into Cycloguanil, allowing a sharper insight into the synergistic effect of Proguanil on Atovaquone.

Our results show that the atovaquone-proguanil combination synergistically inhibits Plasmodium liver stage, providing a pharmacological basis for these drugs mechanism of action in malaria prophylaxis.

**In this work I collaborated in the isolation of human hepatocytes from patients that undergo partial hepatectomy. I have also performed an important experiment on the dose-dependent toxicity of DMSO (an essential compound for the dilution of Atovaquone) against hepatocytes, which allowed to corroborate the veracity of the results.**



# In Vitro Analysis of the Interaction between Atovaquone and Proguanil against Liver Stage Malaria Parasites

Lidia Barata,<sup>a,b,c</sup> Pascal Houzé,<sup>d</sup> Khadija Boutbibe,<sup>d</sup> Gigliola Zanghi,<sup>a</sup> Jean-François Franetich,<sup>a</sup> Dominique Mazier,<sup>a,e,f</sup> Jérôme Clain<sup>b,c,g</sup>

Sorbonne Universités, Université Pierre et Marie Curie, INSERM U1135, CNRS ERL 8255, Centre d'Immunologie et des Maladies Infectieuses (CIMI-Paris), Paris, France<sup>a</sup>; UMR 216, Faculté de Pharmacie, Université Paris Descartes, Université Sorbonne Paris Cité, Paris, France<sup>b</sup>; UMR 216, Institut de Recherche pour le Développement, Paris, France<sup>c</sup>; Laboratoire de Biochimie, Secteur Chromatographie, Hôpital Saint Louis, AP-HP, Paris, France<sup>d</sup>; Centre National de Référence du Paludisme, Hôpital Pitié-Salpêtrière, AP-HP, Paris, France<sup>e</sup>; AP-HP, Groupe Hospitalier La Pitié-Salpêtrière, Service de Parasitologie Mycologie, Paris, France<sup>f</sup>; Centre National de Référence du Paludisme, Hôpital Bichat-Claude Bernard, AP-HP, Paris, France<sup>g</sup>

**The interaction between atovaquone and proguanil has never been studied against liver stage malaria, which is the main target of this drug combination when used for chemoprevention. Using human hepatocytes lacking cytochrome P450 activity, and thus avoiding proguanil metabolizing into potent cycloguanil, we show *in vitro* that the atovaquone-proguanil combination synergistically inhibits the growth of rodent *Plasmodium yoelii* parasites. These results provide a pharmacological basis for the high efficacy of atovaquone-proguanil used as malaria chemoprevention.**

The drug combination atovaquone-proguanil (AP) is an efficient drug for malaria chemoprevention and treatment. The rationale for combining these two drugs originated from the observation that they produce a synergistic inhibitory effect against replicating blood stage parasites *in vitro* (1–3). In the context of malaria chemoprevention, however, AP exerts its protective effect primarily during the hepatic phase of the parasite infection (4, 5), and whether the AP synergy is operating during this preerythrocytic phase has not been explored.

To test this directly, we sought to evaluate *in vitro* the interaction between atovaquone and proguanil against liver stage *Plasmodium* infection through a fixed-ratio isobologram method. In hepatocytes, proguanil is partially metabolized by host cytochrome P450 enzymes into cycloguanil (6), which potently inhibits the development of liver stage *Plasmodium* infection (7). To address this confounding factor, we used HepG2-CD81 human hepatoma cells that retain many liver-specific properties and can be infected by some *Plasmodium* species (8) while displaying impaired cytochrome P450 activity (9).

To confirm the lack of or very minimal proguanil metabolism, HepG2-CD81 cells were incubated in the presence of 100  $\mu$ M proguanil for 2 days, and cell culture supernatants were collected at 24 and 48 h after treatment to quantify drug levels. Proguanil and its metabolite cycloguanil were separated and quantified on a liquid chromatography mass detection mass spectrometer (TSQ Quantum Ultra; Thermo Fisher, France) using an Atlantis dC<sub>18</sub> column (100 by 2.1 mm, 3  $\mu$ m; Waters, France) and a calibration curve. Cycloguanil was not detected in any of the collected samples from the 24- and 48-h time points ( $n = 8$  values) at the 0.04  $\mu$ M limit of our assay (proguanil was detected as expected). In contrast, cycloguanil was detected in the corresponding samples of primary human hepatocytes used as positive controls (median, 0.32  $\mu$ M; minimum, 0.21  $\mu$ M; maximum, 0.97  $\mu$ M;  $n = 8$  values;  $P < 0.001$ , Mann-Whitney test). The same observations regarding cycloguanil production in the two cell types were made when using 20  $\mu$ M instead of 100  $\mu$ M proguanil ( $P < 0.001$ , Mann-Whitney test).

Subsequently, *Plasmodium*-infected hepatocytes were treated

with single agents, and then combination treatments were performed to assess drug interaction. Primary human hepatocytes were isolated as previously described (8). HepG2 cells were derived from the liver tissue of a 15-year-old boy with differentiated hepatocellular carcinoma (10) and modified to induce CD81 expression (11). *Plasmodium yoelii* sporozoites (BY265 strain) were obtained from infected salivary glands of *Anopheles stephensi* 14 to 21 days after an infective blood meal on a parasite-infected Swiss-Webster mouse. Using a 96-well plate, 15,000 sporozoites were added per well, containing an average of 80,000 HepG2-CD81 or primary human hepatocyte cells in a monolayer at a density of 250,000 cells/cm<sup>2</sup>. Drugs at various concentrations along with no-drug (solvent-only) controls were added together with sporozoites.

The drug-containing cell culture media were replaced 2 and 24 h after infection, and the development of liver stage parasites was stopped 48 h after infection by fixation with methanol. Liver stage parasites were stained with a polyclonal antibody specific for *Plasmodium* HSP70 (12), and host and parasite nuclei were stained with DAPI (4',6-diamidino-2-phenylindole). Fluorescent labeling was visualized using a fluorescence microscope with  $\times 400$  magnification (Leica DMI4000 B), and parasites were counted visually. We measured the drug effects on parasite maturation into liver stage schizonts as a proxy for parasite growth. Only small parasites with a single nucleus were considered to display arrested maturation and thus were not counted as schizonts (Fig. 1A). We

Received 15 July 2015 Returned for modification 20 October 2015

Accepted 26 February 2016

Accepted manuscript posted online 29 February 2016

Citation Barata L, Houzé P, Boutbibe K, Zanghi G, Franetich J-F, Mazier D, Clain J. 2016. *In vitro* analysis of the interaction between atovaquone and proguanil against liver stage malaria parasites. *Antimicrob Agents Chemother* 60:4333–4335. doi:10.1128/AAC.01685-15.

Address correspondence to Dominique Mazier, dominique.mazier@upmc.fr, or Jérôme Clain, jerome.clain@parisdescartes.fr.

Copyright © 2016, American Society for Microbiology. All Rights Reserved.

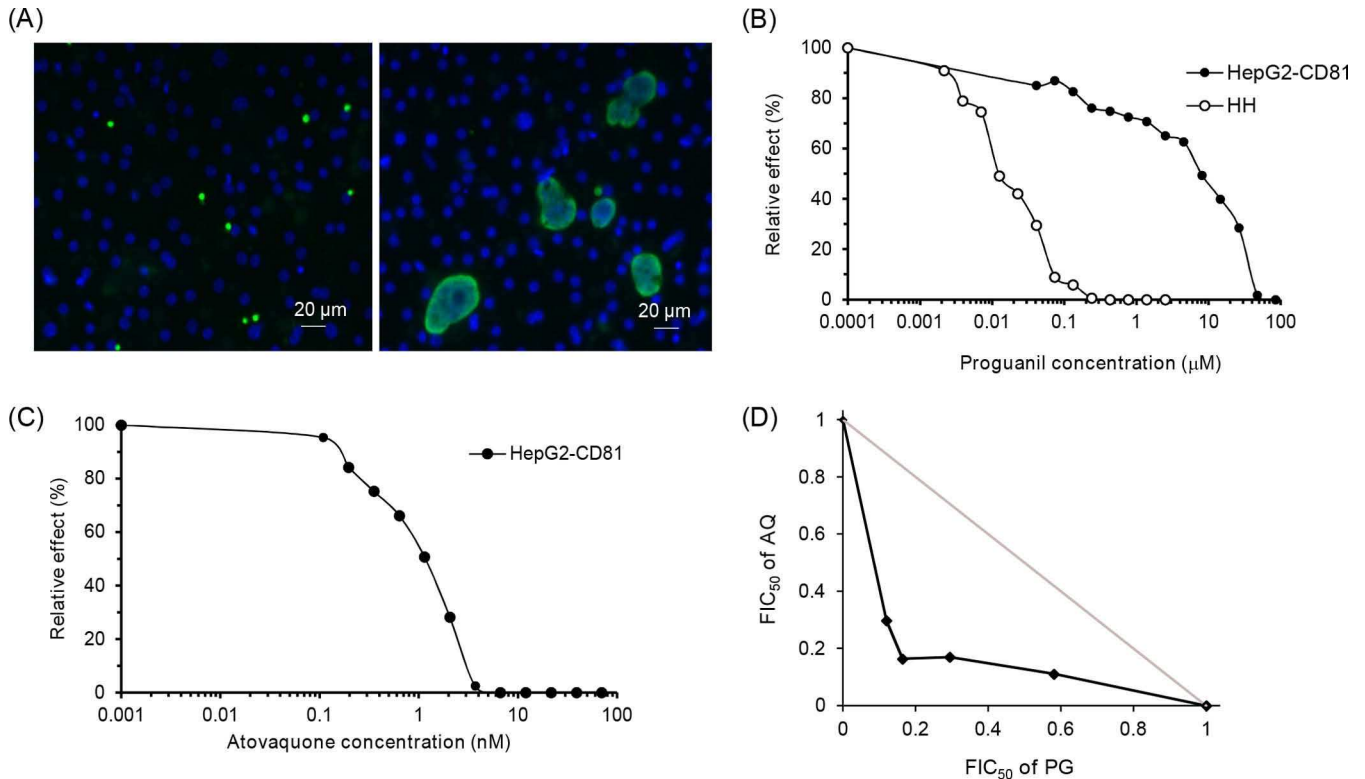


**FIG 1** Inhibitory effect of atovaquone and proguanil on the development of liver stage rodent *Plasmodium* infection. *P. yoelii* sporozoites were added to HepG2-CD81 cell monolayers together with different drug concentrations. The drug-containing cell culture media were replaced 2 and 24 h after infection, and the development of liver stage parasites was stopped 48 h after infection by fixation with methanol. Liver stage parasites were stained with a polyclonal antibody specific for *Plasmodium* HSP70 (green), while host and parasite nuclei were stained with DAPI (blue). The numbers of arrested and nonarrested parasites were evaluated by microscopic examination. (A) Representative image of *P. yoelii* parasites 48 h after infection. Small arrested parasitic forms (<7 μM) with a single nucleus are shown in the left panel, and fully developed schizonts are displayed in the right panel. (B) Dose-response curves for proguanil against *P. yoelii* in HepG2-CD81 and primary human hepatocytes (HH). Data are representative of those from three independent assays. (C) Dose-response curve for atovaquone against *P. yoelii* in HepG2-CD81 cells. Data are representative of those from three independent assays. (D) Isobologram showing the interaction between atovaquone and proguanil against *P. yoelii* infecting HepG2-CD81 cells. Drug interactions are represented by the normalized FIC<sub>50</sub>s for atovaquone and proguanil plotted against each other. Data are representative of those from three independent assays. The gray line is the line of additivity.

estimated the 50% inhibitory concentration (IC<sub>50</sub>) by plotting the relative reduction in the number of schizonts per well on the y axis against drug concentration on the x axis (13). Experiments were repeated at least three times with different sporozoite and hepatocyte batches. No hepatocyte toxicity was observed at any of the highest atovaquone and proguanil concentrations used in the study (0.039 and 154 μM, respectively). Two or three wells per drug concentration were used to analyze parasite counts in the IC<sub>50</sub> and synergy experiments, respectively. The median numbers of schizonts per well in drug-free controls were 100 (minimum, 53; maximum, 319) and 505 (minimum, 311; maximum, 527) for the IC<sub>50</sub> and synergy experiments, respectively.

We first compared the IC<sub>50</sub>s for proguanil against *P. yoelii* parasites obtained from HepG2-CD81 and human primary hepatocytes. The IC<sub>50</sub>s were about 100-fold higher in HepG2-CD81 (IC<sub>50</sub>s, 2.2, 3.2, and 18.4 μM; median, 3.2 μM) than in primary human hepatocytes (IC<sub>50</sub>s, 0.02, 0.03, and 0.04 μM; median, 0.03 μM) (Fig. 1B). Altogether, the drug dosage and IC<sub>50</sub> measurements indicated a deficiency in proguanil metabolism in HepG2-CD81 cells. Regarding atovaquone, the median IC<sub>50</sub> in HepG2-CD81 cells was 0.92 nM (IC<sub>50</sub>s, 0.76, 0.92, and 1.1 nM) (Fig. 1C). The proguanil and atovaquone IC<sub>50</sub> values in HepG2-CD81 cells were consistent with those in a previous report (7).

Because we had evidence that cycloguanil production is dramatically reduced or prevented in HepG2-CD81 cells, we explored the effect of the AP combination against *P. yoelii* infection through a fixed-ratio isobologram method, as previously described (14). Briefly, six starting solutions containing six fixed atovaquone/proguanil molar ratios were prepared and then serially diluted 2-fold seven times. The starting solutions 1 to 6 were prepared at atovaquone/proguanil nanomolar concentrations of 6:0, 4.8:4,000, 3.6:8,000, 2.4:12,000, 1.2:16,000, and 0:20,000, respectively. The fractional inhibitory concentration (FIC) was calculated for each drug in each combination according to the following equation:

$$\text{FIC}_{50} = \frac{\text{IC}_{50} \text{ of drug in combination}}{\text{IC}_{50} \text{ of drug alone}}$$

The isobologram curve was generated by plotting the FIC<sub>50</sub> of atovaquone against the FIC<sub>50</sub> of proguanil. The mean FIC<sub>50</sub> index was calculated according to the following equation:

$$\text{FIC}_{50 \text{ index}} = \text{average FIC}_{50} (\text{atovaquone}) + \text{average FIC}_{50} (\text{proguanil})$$

The median isobologram (of 3 independent experiments) for the interaction between atovaquone and proguanil is shown in

Fig. 1D. The  $FIC_{50}$  index had a median value of 0.64 (0.62, 0.64, and 0.69), which together with the isobolograms indicated that the interaction between the two drugs is synergistic.

In conclusion, we report here the first *in vitro* study, to our knowledge, that formally investigated the effect of a drug combination on liver stages of malaria. We showed that the synergism between atovaquone and proguanil against rodent malaria parasites *in vitro* is conserved across liver and blood stages, which provides a pharmacological basis for the high efficacy of AP when used as malaria chemoprevention.

#### ACKNOWLEDGMENTS

We thank Jacques Le Bras, Gilles Cottrell, and Michel Cot for helpful discussions and suggestions and Sophie Adjalley and Rich Eastman for critical reading of the manuscript.

L.B. was supported by a DIM Malinf Fellowship. This work was supported by DIM Malinf Région Ile de France (to L.B., D.M., J.-F.F., and J.C.), the Fondation pour la Recherche Médicale (to D.M. and J.C.), and the Assistance Publique des Hôpitaux de Paris (P.H.).

#### FUNDING INFORMATION

This work, including the efforts of Lídia Barata, Jean-François Franetich, Dominique Mazier, and Jérôme Clain, was funded by DIM Malinf (dim120048). This work, including the efforts of Lídia Barata, Dominique Mazier, and Jérôme Clain, was funded by Fondation pour la Recherche Médicale (DPM20121125558).

Neither funder had a role in study design, data analysis, data interpretation, or data reporting.

#### REFERENCES

- Canfield CJ, Pudney M, Gutteridge WE. 1995. Interactions of atovaquone with other antimalarial drugs against *Plasmodium falciparum* *in vitro*. *Exp Parasitol* 80(3):373–381. <http://dx.doi.org/10.1006/expr.1995.1049>.
- Jones K, Ward SA. 2002. Biguanide-atovaquone synergy against *Plasmodium falciparum* *in vitro*. *Antimicrob Agents Chemother* 46(8):2700–2703. <http://dx.doi.org/10.1128/AAC.46.8.2700-2703.2002>.
- Srivastava IK, Vaidya AB. 1999. A mechanism for the synergistic antimalarial action of atovaquone and proguanil. *Antimicrob Agents Chemother* 43(6):1334–1339.
- Berman JD, Nielsen R, Chulay JD, Dowler M, Kain KC, Kester KE, Williams J, Whelen AC, Shmuklarsky MJ. 2001. Causal prophylactic efficacy of atovaquone-proguanil (Malarone) in a human challenge model. *Trans R Soc Trop Med Hyg* 95(4):429–432. [http://dx.doi.org/10.1016/S0035-9203\(01\)90206-8](http://dx.doi.org/10.1016/S0035-9203(01)90206-8).
- Deye GA, Miller RS, Miller L, Salas CJ, Tosh D, Macareo L, Smith BL, Fracisco S, Clemens EG, Murphy J, Sousa JC, Dumler JS, Magill AJ. 2012. Prolonged protection provided by a single dose of atovaquone-proguanil for the chemoprophylaxis of *Plasmodium falciparum* malaria in a human challenge model. *Clin Infect Dis* 54(2):232–239. <http://dx.doi.org/10.1093/cid/cir770>.
- Lu AH, Shu Y, Huang SL, Wang W, Ou-Yang DS, Zhou HH. 2000. *In vitro* proguanil activation to cycloguanil is mediated by CYP2C19 and CYP3A4 in adult Chinese liver microsomes. *Acta Pharmacol Sin* 21(8):747–752.
- Delves M, Plouffe D, Scheurer C, Meister S, Wittlin S, Winzeler EA, Sinden RE, Leroy D. 2012. The activities of current antimalarial drugs on the life cycle stages of *Plasmodium*: a comparative study with human and rodent parasites. *PLoS Med* 9(2):e1001169. <http://dx.doi.org/10.1371/journal.pmed.1001169>.
- Silvie O, Rubinstein E, Franetich JF, Prenant M, Belnoue E, Renia L, Hannoun L, Eling W, Levy S, Boucheix C, Mazier D. 2003. Hepatocyte CD81 is required for *Plasmodium falciparum* and *Plasmodium yoelii* sporozoite infectivity. *Nat Med* 9(1):93–96. <http://dx.doi.org/10.1038/nm808>.
- Donato MT, Lahoz A, Castell JV, Gomez-Lechon MJ. 2008. Cell lines: a tool for *in vitro* drug metabolism studies. *Curr Drug Metab* 9(1):1–11. <http://dx.doi.org/10.2174/138920008783331086>.
- Knowles BB, Howe CC, Aden DP. 1980. Human hepatocellular carcinoma cell lines secrete the major plasma proteins and hepatitis B surface antigen. *Science* 209(4455):497–499. <http://dx.doi.org/10.1126/science.6248960>.
- Yalaoui S, Zougbede S, Charrin S, Silvie O, Arduise C, Farhati K, Boucheix C, Mazier D, Rubinstein E, Froissard P. 2008. Hepatocyte permissiveness to *Plasmodium* infection is conveyed by a short and structurally conserved region of the CD81 large extracellular domain. *PLoS Pathog* 4(2):e1000010. <http://dx.doi.org/10.1371/journal.ppat.1000010>.
- Mahmoudi N, Ciceron L, Franetich JF, Farhati K, Silvie O, Eling W, Sauerwein R, Danis M, Mazier D, Derouin F. 2003. *In vitro* activities of 25 quinolones and fluoroquinolones against liver and blood stage *Plasmodium* spp. *Antimicrob Agents Chemother* 47(8):2636–9. <http://dx.doi.org/10.1128/AAC.47.8.2636-2639.2003>.
- Le Nagard H, Vincent C, Mentre F, Le Bras J. 2011. Online analysis of *in vitro* resistance to antimalarial drugs through nonlinear regression. *Comput Methods Programs Biomed* 104(1):10–18. <http://dx.doi.org/10.1016/j.cmpb.2010.08.003>.
- Fivelman QL, Adagu IS, Warhurst DC. 2004. Modified fixed-ratio isobologram method for studying *in vitro* interactions between atovaquone and proguanil or dihydroartemisinin against drug-resistant strains of *Plasmodium falciparum*. *Antimicrob Agents Chemother* 48(11):4097–4102. <http://dx.doi.org/10.1128/AAC.48.11.4097-4102.2004>.

## Epigenetic studies of *Plasmodium falciparum* pre-erythrocytic stages

**Abstract:** Epigenetic mechanisms control key processes during *Plasmodium falciparum* blood stage development such as antigenic variation, malaria pathogenesis and sexual commitment. In addition, in some *Plasmodium* species, dormant malaria liver stages appear to be influenced by epigenetic components. However, the epigenetic landscape has not been reported for the pre-erythrocytic sporozoite and liver stages. To characterize epigenetic regulation in sporozoites, we tested the major epigenetic regulators *P. falciparum* Heterochromatin Protein 1 (PfHP1) and the histone lysine methyltransferases (PfSET6 and PfSET7) in *P. falciparum* sporozoites. Given the difficulty to obtain sufficient material from infected mosquitoes, I first developed a chromatin immunoprecipitation (ChIP) method that allows working with low parasite numbers. This technique allowed me to obtain reliable genome-wide occupancy data for repressive heterochromatin and active euchromatin marks. Notably, I discovered an unprecedented mechanism of silencing in sporozoites, where in a stage specific manner, several hundreds of genes encoding parasite proteins that are exported to the surface are transcriptionally repressed. This is based on an expansion of facultative heterochromatin boundaries in sporozoites. Moreover, I demonstrate that a single member of the polymorphic *var* gene family, which encodes the blood stage virulence factor PfEMP1 (called *var*<sup>sporo</sup> PfEMP1 in this study), is expressed at the surface of sporozoites. This is in contrast to blood stages where PfEMP1 is transported to the erythrocyte surface and participates in cytoadhesion. Overall, my findings give rise to new and important biological questions including what are the factors that regulate heterochromatin boundaries and what is the function of an important virulence-associated surface antigen in pre-erythrocytic stages. Given that the mechanism of sporozoite homing to the liver remains unknown, my findings point to a putative function of this adhesion molecule during sporozoite migration in mosquitoes and humans. Moreover, the expression of a highly polymorphic and strain-specific antigen on the surface of sporozoites might provide a molecular explanation for the observation that the protective immune response induced by attenuated sporozoites used for vaccine development is strain-specific.

Keywords : Epigenetics, *Plasmodium*, Sporozoites, Heterochromatin Protein 1, *var* gene, PfEMP1.

## Etudes épigénétiques des stades pré-érythrocytaires de *Plasmodium falciparum*

**Résumé:** L'épigénétique joue un rôle majeur au cours de processus clés du développement érythrocytaire de *Plasmodium falciparum*, processus tels que variation antigénique, pathogenèse, différenciation sexuée. De plus, le phénomène de quiescence des formes hépatiques observé avec certaines espèces de *Plasmodium* semble être influencé par des éléments de régulation épigénétiques. Cependant, ces éléments n'ont jusqu'à présent jamais été décrits chez les sporozoïtes ou les stades hépatiques. Pour caractériser la régulation épigénétique au niveau des sporozoïtes, nous avons étudié les principaux régulateurs épigénétiques PfHP1 (*P. falciparum* hétérochromatine Protein 1) ainsi que PfSET6 et PfSET7 (méthyltransférases histone lysine) dans des sporozoïtes de *P. falciparum*. Compte tenu de la difficulté d'obtenir des quantités importantes de moustiques infectés, j'ai développé une méthode d'immunoprécipitation de la chromatine (ChIP) qui permet de travailler avec un faible nombre de parasites. Cette technique m'a permis d'établir une cartographie au niveau du génome entier des marques épigénétiques répressives associées à l'hétérochromatine, et actives associées à l'euchromatine. J'ai notamment identifié un nouveau mécanisme de contrôle de l'expression génique chez les sporozoïtes, où d'une manière stade-spécifique, plusieurs centaines de gènes codant pour des protéines exportées sont transcriptionnellement réprimés. Ce mécanisme repose sur une expansion des portions d'hétérochromatine facultative chez les sporozoïtes. De plus, je démontre qu'un seul membre de la famille des gènes *var* polymorphes, qui code pour le facteur de virulence PfEMP1 des stades sanguins (appelé *var*<sup>sporo</sup> PfEMP1 dans cette étude), est exprimé à la surface des sporozoïtes. Cette localisation contraste avec les stades sanguins, où PfEMP1 est transporté à la surface des érythrocytes infectés et participe à cytoadhérence. L'ensemble de ces résultats donnent lieu à de nouvelles et importantes questions biologiques, telles que : quels sont les facteurs qui régulent la formation d'hétérochromatine chez les sporozoïtes ? Quelle est la fonction d'un antigène associé à la virulence quand il est exprimé en surface d'un sporozoïte ? Étant donné que le mécanisme de « homing » des sporozoïtes vers le foie reste inconnu, mes conclusions indiquent une fonction putative de cette molécule d'adhérence lors de la migration des sporozoïtes chez le moustique et chez l'homme infectés. En outre, l'expression, à la surface du sporozoïte, d'un antigène hautement polymorphique et spécifique de souche pourrait fournir une explication moléculaire de l'observation selon laquelle la réponse immunitaire protectrice induite par les sporozoïtes atténués utilisés pour le développement d'un vaccin est spécifique de la souche.

Mots clés : Épigénétique, *Plasmodium*, sporozoïtes, hétérochromatine Protein 1, gènes *var*, PfEMP1.